UNIVERSIDADE DE TAUBATÉ
PROGRAMA DE PÓS-GRADUAÇÃO EM CIÊNCIAS AMBIENTAIS
Revista Ambiente & Água
An Interdisciplinary Journal of Applied Science

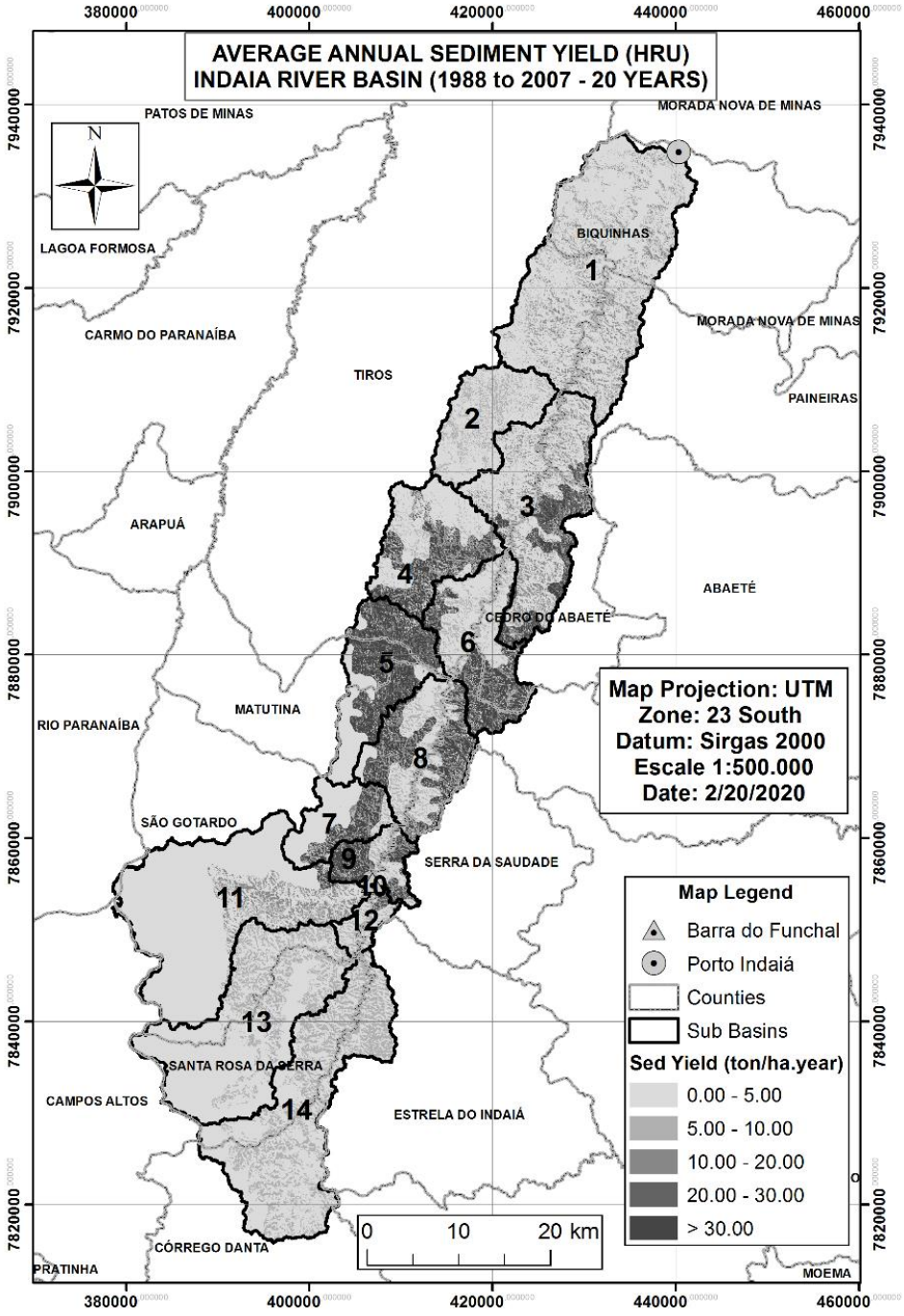

ISSN = 1980-993X (Online)
http://www.ambi-agua.net

EDITORIAL BOARD

Editors

Getulio Teixeira Batista (Emeritus Editor) Universidade de Taubaté - UNITAU, BR

Nelson Wellausen Dias (Editor-in-Chief), Fundação Instituto Brasileiro de Geografia e Estatística - IBGE, BR

Associate Editors

Ana Aparecida da Silva Almeida	Universidade de Taubaté (UNITAU), BR
Marcelo dos Santos Targa	Universidade de Taubaté (UNITAU), BR

Editorial Commission

Andrea Giuseppe Capodaglio	University of Pavia, ITALY
Arianna Callegari	Università degli Studi di Pavia, ITALY
Antonio Teixeira de Matos	Universidade Federal de Minas Gerais (UFMG), BR
Apostol Tiberiu	University Politechnica of Bucharest, Romênia
Claudia M. dos S. Cordovil	Centro de estudos de Engenharia Rural (CEER), Lisboa, Portugal
Dar Roberts	University of California, Santa Barbara, United States
Giordano Urbini	University of Insubria, Varese, Italy
Gustaf Olsson	Lund University, Lund, Sweden
Hélio Nobile Diniz	Inst. Geológico, Sec. do Meio Amb. do Est. de SP (IG/SMA), BR
Ignacio Morell Evangelista	University Jaume I- Pesticides and Water Research Institute, Spain
János Fehér	Debrecen University, Hungary
Julio Cesar Pascale Palhares	Embrapa Pecuária Sudeste, CPPSE, São Carlos, SP, BR
Luis Antonio Merino	Institute of Regional Medicine, National University of the Northeast, Corrientes, Argentina
Maria Cristina Collivignarelli	University of Pavia, Depart. of Civil Engineering and Architecture, Italy
Massimo Raboni	LIUC - University "Cattaneo", School of Industrial Engineering, Italy
Petr Hlavínek	Brno University of Technology República Tcheca
Richarde Marques da Silva	Universidade Federal da Paraíba (UFPB), BR
Stefan Stanko	Slovak Technical University in Bratislava Slovak, Eslováquia
Teresa Maria Reyna	Universidad Nacional de Córdoba, Argentina
Yosio Edemir Shimabukuro	Instituto Nacional de Pesquisas Espaciais (INPE), BR
Zhongliang Liu Beijing	University of Technology, China

Text Editor	Theodore D`Alessio, **FL, USA,** Maria Cristina Bean, **FL, USA**
Reference Editor	Liliane Castro, **Bibliotecária** - CRB/8-6748**, Taubaté, BR**
Peer-Reviewing Process	Marcelo Siqueira Targa, **UNITAU, BR**
System Analyst	Tiago dos Santos Agostinho, **UNITAU, BR**
Secretary and Communication	Luciana Gomes de Oliveira, **UNITAU, BR**

Library catalog entry by Liliane Castro CRB/8-6748

Revista Ambiente & Água - An Interdisciplinary Journal of Applied Science / Instituto de Pesquisas Ambientais em Bacias Hidrográficas. Taubaté. v. 16, n.3 (2006) - Taubaté: IPABHi, 2021.
Quadrimestral (2006 – 2013), Trimestral (2014 – 2016), Bimestral (2017), Publicação Contínua a partir de Janeiro de 2018.

Resumo em português e inglês.
ISSN 1980-993X

1. Ciências ambientais. 2. Recursos hídricos. I. Instituto de Pesquisas Ambientais em Bacias Hidrográficas.

CDD - 333.705
CDU - (03)556.18

TABLE OF CONTENTS

COVER:

The map shows the average annual sediment yield map (ton/ha.year) of the Indaia river basin in Minas Gerais, Brazil. This research analyzed the sediment yield generated by water erosion in this basin from 1988 to 2017, applying the SWAT hydrological model. The results provided insights into identifying areas that contribute most to the sediment yield in the basin, that is, the source areas. Source: SIMÕES, K. et al. Application of the SWAT hydrological model in flow and solid discharge simulation as a management tool of the Indaia River Basin, Alto São Francisco, Minas Gerais. **Rev. Ambient. Água, Taubaté, vol. 16 n. 3, p. 1-18, 2021.** ***doi:10.4136/ambi-agua.2694***

ARTICLES

01	**Water balance for determination of excess water in soybean cultivated in lowland soils** ***doi:10.4136/ambi-agua.2614*** Mateus Possebon Bortoluzzi, Paulo Ivonir Gubiani, Arno Bernardo Heldwein, Roberto Trentin, Jocélia Rosa da Silva, Astor Henrique Nied, Alencar Junior Zanon	1-12
02	**Low-cost flow photoreactor for degradation of Reactive Black 5 dye by UV/H_2O_2, Fenton and photo-Fenton processes: a performance comparison** ***doi:10.4136/ambi-agua.2687*** Andrea Maria da Silva, Tainá Natália dos Santos, Raiane dos Santos, Thiago Sabino Pessoa, Luiz Carlos Araújo dos Anjos, Nelson Alves da Silva Sobrinho, Paula Barone da Paz Sales	1-17
03	**Removal of nutrients due to biomass harvest of *Eucalyptus urograndis* in different soils: macronutrients** ***doi:10.4136/ambi-agua.2671*** Simone Martini Salvador, Aline Aparecida Ludvichak, Dione Richer Momolli, Kristiana Fiorentin dos Santos, Catarine Barcellos Consensa, Mauro Valdir Schumacher, James Stahl	1-14
04	**Dynamics of natural regeneration after disturbance in a remnant of Mixed Ombrophilous Forest in southern Brazil** ***doi:10.4136/ambi-agua.2679*** Alyne Regina Ruggiero, Lauri Amândio Schorn, Kristiana Fiorentin dos Santos, Tatiele Anete Bergamo Fenilli	1-14
05	**Freshwater mollusks as proxies for assessing agrochemicals hazards in Volta Grande Reservoir, Brazil** ***doi:10.4136/ambi-agua.2681*** Andressa Mendes Sene, Daniel Melo Rosa, Silvia Maria Millan Gutierre, Paulo Santos Pompeu	1-13
06	**Evaluation of the environmental life cycle of an STP that employs a low-rate trickling filter as post-treatment of a UASB reactor and different sludge-management alternatives** ***doi:10.4136/ambi-agua.2648*** Karina Guedes Cubas do Amaral, Julio Cezar Rietow, Miguel Mansur Aisse	1-14
07	**Evaluation of anaerobic and anoxic reactors installed in serial to treat fish tank effluent** ***doi:10.4136/ambi-agua.2678*** Maria Lidia Carra, Vitória Teodoro Gonçalves, Tiago Palladino Delforno, Valéria Maia de Oliveira, Ariovaldo José da Silva	1-16
08	**Machine-learning methods for hydrological imputation data: analysis of the goodness of fit of the model in hydrographic systems of the Pacific – Ecuador** ***doi:10.4136/ambi-agua.2708*** Diego Heras, Carlos Matovelle	1-12
09	**Analysis of microbial community biodiversity in activated sludge from a petrochemical plant**	1-22

	doi:10.4136/ambi-agua.2655 Themis Collares Antunes; Leticia Marconatto; Luiz Gustavo dos Anjos Borges; Adriana Giongo; Sueli Teresinha Van Der Sand	
10	**Statistical study of growth kinetics and lipid content of microalgae grown in brackish waters for bioenergetic purposes** *doi:10.4136/ambi-agua.2649* Bruna da Silveira Guimarães; Kepler Borges França	1-14
11	**Surveillance of public water supply fluoridation and municipal indicators: an analysis in the state of Espirito Santo, Brazil** *doi:10.4136/ambi-agua.2693* Ariane Mendonça; Katrini Guidolini Martinelli; Carolina Dutra Degli Esposti; Lorrayne Belotti; Karina Tonini dos Santos Pacheco	1-15
12	**Application of the SWAT hydrological model in flow and solid discharge simulation as a management tool of the Indaia River Basin, Alto São Francisco, Minas Gerais** *doi:10.4136/ambi-agua.2694* Kauem Simões; Rita de Cássia Cerqueira Condé; Henrique Llacer Roig; Rejane Ennes Cicerelli	1-18
13	**Use of natural mucilage extracted from the Stenocereus griseus (Cardón Guajiro) plant as a coagulant in the treatment of domestic wastewater** *doi:10.4136/ambi-agua.2705* Arnulfo Antonio Tarón Dunoyer; Rafael Emilio González Cuello; Fredy Colpas Castillo	1-10
14	**Analysis of fire risk in the Amazon: a systematic review** *doi:10.4136/ambi-agua.2706* Natasha Sousa Araujo Lemos; José Mauricio Cunha	1-16

Ambiente & Água - An Interdisciplinary Journal of Applied Science
ISSN 1980-993X – doi:10.4136/1980-993X
www.ambi-agua.net
E-mail: ambi.agua@gmail.com

Water balance for determination of excess water in soybean cultivated in lowland soils

ARTICLES doi:10.4136/ambi-agua.2614

Received: 01 Jul. 2020; Accepted: 25 Jan. 2021

Mateus Possebon Bortoluzzi[1*]; Paulo Ivonir Gubiani[2]; Arno Bernardo Heldwein[3]; Roberto Trentin[4]; Jocélia Rosa da Silva[3]; Astor Henrique Nied[3]; Alencar Junior Zanon[3]

[1]Faculdade de Agronomia e Medicina Veterinária. Universidade de Passo Fundo (UPF), Rodovia BR 285, km 292, CEP: 99052-900, Passo Fundo, RS, Brazil.
[2]Departamento de Solos. Universidade Federal de Santa Maria (UFSM), Avenida Roraima, n° 1000, CEP: 97105-900, Santa Maria, RS, Brazil. E-mail: paulogubiani@gmail.com
[3]Departamento de Fitotecnia. Universidade Federal de Santa Maria (UFSM), Avenida Roraima, n° 1000, CEP: 97105-900, Santa Maria, RS, Brazil. E-mail: arno.heldwein@ufsm.br, jocelia.s@gmail.com, astor.nied@ufsm.br, alencarzanon@hotmail.com
[4]Departamento de Fitotecnia. Universidade Federal de Pelotas (UFPel), Campus Universitário Capão do Leão, s/n, CEP: 96010-610, Capão do Leão, RS, Brazil. E-mail: roberto.trentin@ufpel.edu.br
[*]Corresponding author. E-mail: mateusbortoluzzi@upf.br

ABSTRACT

The aim of this study was to derive a methodology for calculating a sequential water balance that accurately estimates the occurrence of excess water in soybeans cultivated in lowlands. We tested four calculation strategies of water balance associated with the simulation of soybean development, which differed on the calculation of rainfall and time of water drainage from the soil macropores. Data of volumetric moisture monitored in three soil layers throughout the soybean cycle in the 2014/15 agricultural year were used as a reference. Microporosity was used as a lower limit for the occurrence of excess water in the area. Excess water was considered to be whenever the daily volumetric soil moisture in the 0-100 mm layer was greater than 0.39 mm^3 mm^{-3}. Over the 111 days of measurement, soil moisture indicated the presence of excess water in 38 days. The traditional calculation strategy of water balance underestimated the occurrence of excess water, as well as the other strategies that considered effective precipitation in their formulas. The calculation strategy that considers that all the rainfall infiltrates in the soil and that the water from macropores is removed only by crop evapotranspiration exhibited good performance and indicated 35 days of excess water, being the most appropriate and recommended for determining excess water in lowland soybeans.

Keywords: compute model, effective rainfall, *Glycine max*, hypoxia.

Balanço hídrico para a determinação do excesso hídrico na soja em terras baixas

RESUMO

O objetivo deste trabalho foi obter uma metodologia de cálculo do balanço hídrico sequencial que estime com acurácia a ocorrência de excesso hídrico na soja em terras baixas. Foram testadas quatro estratégias de cálculo do balanço hídrico associadas à simulação do

This is an Open Access article distributed under the terms of the Creative Commons Attribution License, which permits unrestricted use, distribution, and reproduction in any medium, provided the original work is properly cited.

desenvolvimento da soja, as quais se diferenciaram em função da forma de cômputo da chuva e do tempo de drenagem da água dos macroporos do solo. Como referência foram utilizados os dados de umidade volumétrica monitorada em três camadas de solo ao longo do ciclo da soja no ano agrícola 2014/15. A microporosidade foi utilizada como limite inferior da ocorrência de excesso hídrico na área. Assim, o excesso hídrico foi considerado sempre que a umidade volumétrica diária do solo na camada 0-100 mm foi maior que 0,39 mm^3 mm^{-3}. Ao longo dos 111 dias de medição, a umidade do solo indicou a presença de excesso hídrico em 38 dias. A estratégia de cálculo tradicional do balanço hídrico subestimou a ocorrência de excesso hídrico, assim como as demais estratégias que consideraram a precipitação efetiva na sua metodologia. A estratégia de cálculo que considera que toda a chuva infiltra no solo e que a água dos macroporos é removida somente pela evapotranspiração da cultura apresentou bom desempenho e indicou 35 dias de excesso hídrico, sendo a mais adequada e recomendada para a determinação do excesso hídrico na soja em terras baixas.

Palavras-chave: *Glycine max*, hipóxia, modelo de cômputo, precipitação efetiva.

1. INTRODUCTION

High demand for vegetable protein and favorable economic condition enables the expansion of soybean cultivation in areas that were not traditionally cultivated, i.e., the lowland areas in southern Brazil (Rocha *et al.*, 2017; Sartori *et al.*, 2016), entailing 1/3 of the area traditionally sown with irrigated rice (IRGA, 2019). In addition, crop rotation is an alternative to control weed infestations (Scherner *et al.*, 2018; Fraga *et al.*, 2019), break pest and disease cycles, improve soil conditions for plant development and increase the sustainability of the system (Goulart *et al*., 2020)

Imperfectly drained soils (Planosols) predominate in these areas due to the water table being close to the surface (Streck *et al.*, 2008). In areas cultivated with irrigated rice, the superficial layers undergo disruption and compaction due to mechanized operations used for rice cultivation, which usually take place under soaked soil conditions and reduce the water infiltration rate (Sartori *et al.*, 2016).

Excess water is one of the main risk factors for soybean grown in lowland areas (Bortoluzzi *et al.*, 2017; Gubiani *et al.*, 2018). The assessment of excess water can be performed by measuring the soil water content or aeration condition. However, prediction of risks due to excess water requires modeling the water balance throughout the crop cycle. Bortoluzzi *et al.* (2017) carried out a risk analysis of excess water for soybean cultivation in lowlands in the central region of Rio Grande do Sul (RS) by adapting the calculation of the daily sequential water balance (SWB) of Thornthwaite and Mather (1955). The authors also considered the effective precipitation (EP) of the U.S. Soil Conservation Service as infiltration as described by Frizzone and Andrade Júnior (2005) and applied the crop development model proposed by Trentin *et al.* (2013). Excess water was considered to be whenever the soil water content was above the field capacity. Another assumption was that after soil saturation two days of drainage were required for water content to decrease to field capacity.

One of the improvements required in the SWB carried out by Bortoluzzi *et al.* (2017) is the adjustment of the effective root depth. The authors considered that the roots explored a 0-400 mm layer, based on the effective depth used in the SWB calculation performed by Fietz and Rangel (2008) for soybeans grown in well-drained soils (Latosol or Rhodic Hapludox). However, lowland studies have shown that soybean roots are concentrated in superficial layers, which requires redefinition of the layer utilized for the soil available water capacity (AWC) calculation. For example, there are reports that the taproot reached a maximum depth of 230 mm (Marchesan *et al.*, 2013) and between 130 mm and 300 mm (Rocha *et al.*, 2017).

The deepening of roots is often restricted in lowland areas because the water table level is often close to the surface. Gubiani *et al.* (2018) found that soil moisture was close to the saturation moisture during practically the entire soybean crop cycle in the 300-400 mm layer. In this case, there is a strong impediment to root penetration, considering that soil saturation can cause the death of the soybean taproot and increase the growth of lateral and adventitious roots (Pires *et al.*, 2002).

Flat relief hinders runoff and favors the accumulation of water on the lowland soil surface (Streck *et al.*, 2008). Moreover, the use of effective precipitation (EP) from the U.S. Soil Conservation Service tends to underestimate infiltration and overestimate the runoff in these areas. Therefore, calculation adjustments for infiltration and runoff in the SWB carried out by Bortoluzzi *et al.* (2017) are also required to improve the model for predicting the risk of water excess for lowland soybeans.

Field capacity (θ_{fc}) also deserves consideration to establish the upper limit of AWC. In soils with drainage limitations such as lowland soils, the concept of field capacity based on negligible drainage criteria is difficult to detect in the field. In addition, the time for soil water content to decrease to θ_{fc} in lowland soils is greater than in well-drained soils (Gubiani *et al.* 2018). This increased time can result in a significant portion of water available to plants while the water content in the soil is above θ_{fc} (de Jong van Lier, 2017). In order to compute this additional available water, a strategy would be to replace θ_{fc} with the θ corresponding to the microporosity in the AWC calculation, since the value of the second (θ at the 0.6 m pressure head) is slightly higher than the estimates of the first (θ at the 1 m pressure head).

For lowland areas with slow drainage, a water balance calculation that immediately removes the water content from the soil between the upper AWC limit and soil saturation can underestimate the soil water content. If deep drainage from the macropores is very slow, the decrease in water content down to the AWC upper limit is predominantly dependent on the daily crop evapotranspiration. Furthermore, this adaptation can be included in SWB calculations to account for deep drainage limitations in lowland areas in determining excess water in soybeans.

Significant parts of the soybean process-based models were developed to estimate growth and productivity in the potential condition, without considering soil restrictions (Setiyono *et al.*, 2010). Likewise, the CROPGRO model (Boote *et al.*, 1998) allows the simulation of SWB and is one of the most used worldwide (Cera *et al.*, 2017), but has weaknesses in the estimates of excess water simulations in lowlands (Fensterseifer *et al.*, 2017).

This study aimed to explore whether the change in the parameterization of the upper limit of the AWC along with the inclusion of the calculation of macropore drainage time allows the SWB to better estimate the occurrence of excess water for lowland soybean cultivation.

2. MATERIALS AND METHODS

The study was carried out by comparing the excess water data obtained from four strategies of calculating the daily sequential water balance (SWB) with water excess data measured in a soybean field. The calculation and parameterization strategies, meteorological data and model calibration are described below.

TM_{1955}: traditional methodology proposed by Thornthwaite and Mather (1955) and described by Pereira *et al.* (1997). In this strategy, the entire precipitation infiltrates in the soil, but only the amount of water held between an upper and a lower limit is considered for computing the AWC. Surplus water from precipitation is immediately drained and excess water is considered to be whenever the soil water storage exceeds the AWC upper limit.

The AWC calculation was performed by Equation 1:

$$AWC_1 = (\theta_{mic} - \theta_{pwp})Z_1 \quad (1)$$

Where AWC_1 is the available water capacity (mm), θ_{mic} is the volumetric water content corresponding to the microporosity ($mm^3\ mm^{-3}$), which was set as the upper limit; θ_{pwp} is the volumetric water content at the permanent wilting point ($mm^3\ mm^{-3}$); and Z1 is the root system depth over the crop cycle (mm).

Up to the first trifoliate leaf (V2), we considered Z_1 = 100 mm, which resulted in an AWC_1 of 22 mm. For the subperiod between V2 and the beginning of flowering (R1), the AWC_1 ranged from 22 mm at Z_1 = 100 mm to 66 mm at Z_1 = 300 mm. The deepening of the roots was simulated with a sigmoidal growth curve of the root system (Dourado Neto *et al.*, 1999) as a function of the development rate (DR) calculated by a non-linear model of response to air temperature and photoperiod (Sinclair *et al.*, 1991), according to Equation 2. The maximum depth of 300 mm was defined considering the root depth verified by Gubiani *et al.* (2018) in the study area. After R1, AWC_1 was maintained at 66 mm. The θ_{mic} and θ_{pwp} values were, respectively, 0.39 $mm^3\ mm^{-3}$ and 0.17 $mm^3\ mm^{-3}$ (Gubiani *et al.*, 2018).

$$AWC_n = AWC_{V2} + \frac{(AWC_{R1} - AWC_{V2})}{2} \times [1 - cos\ cos\ (\pi \times DR)\ ] \quad (2)$$

Where AWC_n is the AWC stored in the day "n" (mm), AWC_{V2} is the AWC stored up to V2 stage (mm), AWC_{R1} is the AWC stored after R1 stage (mm); and DR is the development rate, variable from 0 to 1. MAC_{PM}: new methodology proposed in this study, where the total AWC was composed of a portion of the AWC stored in the micropores and another in the macropores (Figure 1). The AWC stored in the micropores is the AWC_1 calculated in the TM_{1995} strategy.

The AWC stored in the macropores was calculated using Equation 3:

$$AWC_2 = (\theta_{sat} - \theta_{mic})Z_2 \quad (3)$$

Where AWC_2 is the AWC stored in the macropores (mm), θ_{sat} is the volumetric water content at saturation ($mm^3\ mm^{-3}$); and Z_2 is the root system depth up to which the effect of the water table level in the absence of flooding can be considered of little importance throughout the cycle (mm). AWC_2 is computed only in a surficial layer (Figure 1) where the macropores will be occupied with water only in periods of complete saturation of the soil profile, generally coinciding with the flooding event. Based on the monitoring of θ by Gubiani *et al.* (2018) in the study area, Z_2 was considered 100 mm (Figure 1), and the θ_{sat} value was 0.45 $mm^3\ mm^{-3}$.

The total AWC (AWC_{tot}, mm) was calculated using Equation (4):

$$AWC_{tot} = AWC_1 + AWC_2 \quad (4)$$

We also considered that all measured rainfall infiltrates the soil and that the maximum soil water storage is equal to AWC_{tot}. Excess water is considered to be whenever $AWC > AWC_1$, a condition that can occur due to excess precipitation and also due to the drainage time of the AWC portion occupying AWC_2 after the end of the precipitation event. In situations where $AWC_1 \leq AWC \leq AWC_{tot}$ after the end of precipitation, the portion of AWC occupying AWC_2 (AWC_{tot} - AWC_1) is daily reduced by crop evapotranspiration. Consequently, there is a gradual reduction of water storage in the soil until reaching the upper limit of AWC_1. The duration of this period depends on the condition of atmosphere evaporative demand and the crop development stage. During this period, the fraction of air-filled/water-filled macropores

gradually increases and water excess due oxygen restriction gradually reduces. Usually, a value of 0.10 mm^3 mm^{-3} of air-filled porosity is considered an empirical non-limiting threshold for aeration (Gubiani *et al.*, 2018). We considered that the plants were subjected to oxygen deficiency while the soil macropores were not totally drained, because their capacity of store air (θ_{sat} - θ_{mic} = 0.06 mm^{-3} mm^{-3}) is less than the non-limiting threshold for aeration (0.10 mm^3 mm^{-3}).

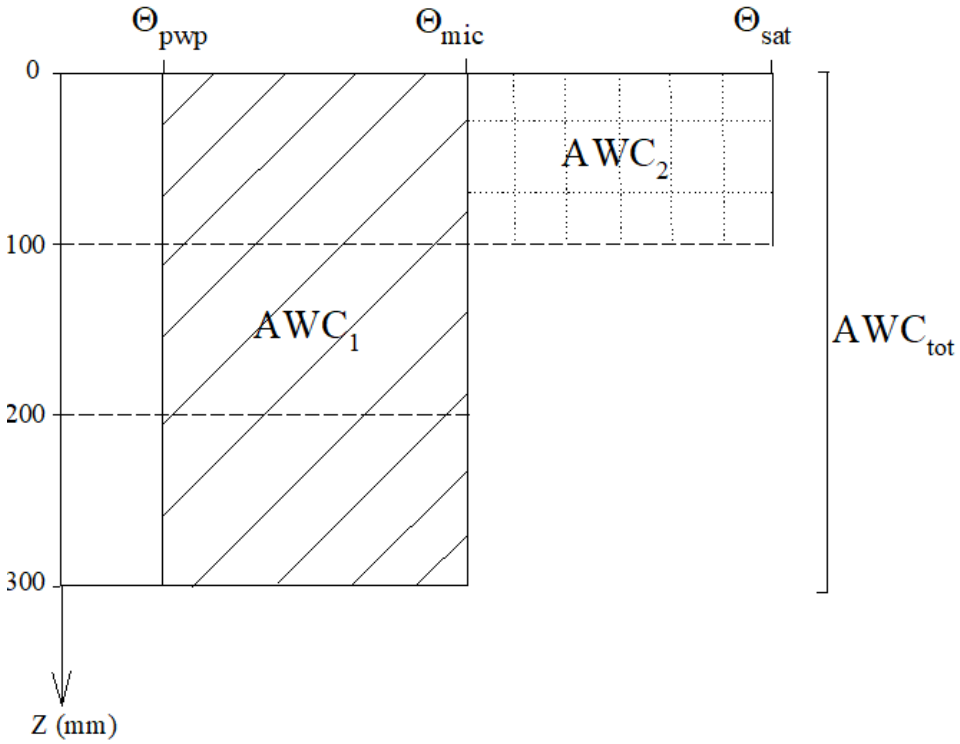

Figure 1. Scheme representation of the limits of soil water content referring to the methodologies that consider the drainage time of the macropores (MAC_{PM} and MAC_{PE}). They are represented by the soil water content between saturation (θ_{sat}) and microporosity (θ_{mic}) (AWC_2) until 100 mm depth; AWC_1 is the water content between θ_{mic} and permanent wilting point (θ_{pwp}) up to 300 mm depth (Z) and AWC_{tot} is the sum of AWC_2 e AWC_1.

MAC_{PE}: this strategy is similar to MAC_{PM}, with the only difference being the consideration of the effective precipitation (EP) of the U.S. Soil Conservation Service as the water infiltrated into the soil, as described by Frizzone and Andrade Júnior (2005). The value of the curve number (CN) used was 91 as the soil in the field area has more than half of the granulometric composition of silt and clay (Gubiani *et al.*, 2018), and a loss of 25% of initial precipitation was assumed due to interception. Therefore, we were able to assess whether there is an important difference in the estimate of excess water due to the method of rain computation.

$BORT_{2017}$: this strategy is the same used by Bortoluzzi *et al.* (2017) with a slight change in the AWC upper limit, replacing the volumetric water content in the field capacity (θ_{fc}, mm^3 mm^{-3}) by θ_{mic}, which establishes the maximum water storage in the soil. Infiltration is considered to be EP (Frizzone and Andrade Júnior, 2005) and in the event of excess water from precipitation, a drainage time of two days is required for the soil to reach θ_{mic}. Excess water is defined when water storage in the soil exceeds the AWC upper limit.

The four SWB calculation strategies use crop evapotranspiration (ETc) calculated as the product of reference evapotranspiration (ET_o) by the crop coefficient (Kc). ET_o was estimated by means of the Penman-Monteith method (Allen *et al.*, 1998). The FAO-recommended Kc values of 0.40, 1.15 and 0.50 for soybeans were considered constant respectively for the

subperiods between sowing (S) and first trifoliolate leaf (V2); beginning of flowering (R1) to beginning of seed filling (R5) and from the beginning of maturation (R7) to full maturation (R8) (Allen *et al.*, 1998). In the V2-R1 subperiod, the daily Kc was calculated respectively as a function of the variation in the relative development rate (SD) (Sinclair *et al.*, 1991) and in the R5-R7 subperiod as a function of the thermal sum (Martorano *et al.*, 2012), according to Equations 5 and 6:

$$Kc = 1.087 \cdot SD + 0.063 \quad (5)$$

$$Kc = -0.0012 \cdot TS_{R5-R7} + 1.1512 \quad (6)$$

Where Kc is the crop coefficient, SD is the relative development rate and $TS_{R5\text{-}R7}$ is the accumulated thermal sum between the R5- R7 subperiod.

All the daily meteorological data required to operationalize the four SWB calculation strategies were collected at the Main Weather Station of Santa Maria, RS, Brazil. The simulation period was from November 14, 2014 to March 26, 2015, which coincides with the period between soybean sowing and physiological maturity (Gubiani *et al.*, 2018) in a lowland area at 800 m from the weather station. The daily water excess determined during the soybean cycle was used to evaluate the efficiency of the SWB calculation strategies.

The soybean was grown after a fallow season of a field previously cultivated with irrigated rice, with straw turnover after harvest. The field was leveled with a 'remaplan' blade and kept fallow during the winter season, with pre-emergent weed control. During the soybean crop, the volumetric water content in the soil (θ) was monitored with TDR100 sensors at 30 minute intervals in three soil layers from December 6, 2014 until the end of the cycle (111 days of monitoring). The calculation of excess water was performed through the θ daily mean measured at four monitoring points in the 0-100 mm depth layer, where most of the soybean roots were concentrated. Condition of excess water was considered whenever θ was greater than the volumetric water content corresponding to the microporosity (θ_{mic}) for this soil layer (0.39 mm^3 mm^{-3}).

Details of soybean cultivation, θ monitoring and microporosity determination are described in Gubiani *et al.* (2018). Lastly, the TM_{1955}, MAC_{PE}, MAC_{PM} and $BORT_{2017}$ strategies were compared with each other and with the excess water measured in field conditions.

3. RESULTS AND DISCUSSION

The soil water content recorded by the TDR sensors in the 0-100 mm layer was greater than the microporosity (θ_{mic} = 0.39 mm^3 mm^{-3}) in 38 days of the 111 days of measurement period (Table 1). These 38 days of excess water (EXC) were due to the total rainfall of 551 mm, distributed during the period from December 6, 2014 until March 26, 2015. The SWB modeling strategy that estimated the number of EXC days closest to the number of EXC days observed in the field (38 days) was MAC_{PM}, with 35 days of EXC (Table 1). Additional strategies were not very efficient, indicating respectively 17, 16 and 13 days of EXC with MAC_{PE}, $BORT_{2017}$ and TM_{1955} (Table 1).

The MAC_{PE} and $BORT_{2017}$ strategies presented similar EXC days to field-observed values only until the beginning of January (Table 1). After that period, the strategies that used effective precipitation (EP) calculated by the U.S. Soil Conservation Service methodology as an estimate of soil water infiltration underestimated the number of days with EXC. However, Lucas *et al.* (2015) deployed a similar strategy to $BORT_{2017}$, with satisfactory performance for sunflower cultivation in different types of highland soils, where the use of PE is more appropriate.

Table 1. Measured daily volumetric soil moisture (Mv), measured precipitation (MP) and days with excess water (EXC) estimated by different water balance calculation strategies (*), over the soybean cycle in a Haplic Planosol during the 2014/15 agricultural year in Santa Maria, RS.

Date	Mv* ($mm^3\ mm^{-3}$)	MP (mm)	MAC_{PM}	MAC_{PE}	$BORT_{2017}$	TM_{1995}
09/12/2014	-	12.6	EXC	-		
10/12/2014	0.427	22.6	EXC	EXC	EXC	EXC
11/12/2014	0.409	0	EXC	EXC	EXC	-
12/12/2014	0.395	0	EXC	EXC	EXC	-
13/12/2014	-	0	EXC	EXC	-	-
16/12/2014	0.401	0.5	-	-	-	-
17/12/2014	0.437	29.1	EXC	EXC	EXC	EXC
18/12/2014	0.429	0	EXC	EXC	EXC	-
19/12/2014	0.397	0	-	-	EXC	-
21/12/2014	0.438	71.6	EXC	EXC	EXC	EXC
22/12/2014	0.428	21.2	EXC	EXC	EXC	EXC
23/12/2014	0.403	0	EXC	EXC	EXC	-
24/12/2014	-	0	-	-	EXC	-
27/12/2014	0.433	101.1	EXC	EXC	EXC	EXC
28/12/2014	0.427	0.7	EXC	EXC	EXC	-
29/12/2014	0.430	3.5	EXC	EXC	EXC	-
30/12/2014	0.418	0	EXC	-	-	-
31/12/2014	0.405	0	-	-	-	-
01/01/2015	0.406	0	-	-	-	-
02/01/2015	0.444	23.8	EXC	EXC	EXC	EXC
03/01/2015	0.427	0	EXC	EXC	EXC	-
04/01/2015	0.403	0	-	-	EXC	-
09/01/2015	0.421	18.6	-	-	-	-
10/01/2015	0.432	14.7	EXC	-	-	EXC
11/01/2015	0.432	13	EXC	EXC	-	EXC
12/01/2015	0.429	0.1	-	-	-	-
14/01/2015	0.417	19.8	EXC	EXC	-	EXC
15/01/2015	0.441	8.8	EXC	-	-	EXC
16/01/2015	0.430	0	EXC	-	-	-
17/01/2015	0.436	10.5	EXC	EXC	-	EXC
18/01/2015	0.428	0	EXC	-	-	-
29/01/2015	0.448	33.8	EXC	-	-	EXC
30/01/2015	0.433	3.4	EXC	-	-	-
31/01/2015	0.394	0	-	-	-	-
11/02/2015	0.405	31.4	-	-		-
20/02/2015	0.425	29.4	-	-	-	-
21/02/2015	0.395	0.1	-	-	-	-
26/02/2015	0.427	16.8	EXC	-	-	-
27/02/2015	0.416	4.6	EXC	-	-	-
02/03/2015	0.397	15.8	EXC	-	-	EXC
03/03/2015	-	0	EXC	-	-	-
04/03/2015	-	0	EXC	-	-	-
05/03/2015	0.398	5.9	EXC	-	-	-
06/03/2015	-	0	EXC	-	-	-
07/03/2015	-	0	EXC	-	-	-
11/03/2015	-	9	EXC	-	-	-
12/03/2015	-	0	EXC	-	-	-

(*) Soil moisture determined from data measured by Gubiani *et al.* (2018) in the 0-100 mm layer; (-) days without occurrence of water excess. AWC_{PM} and MAC_{PE} are strategies that respectively consider the measured precipitation (MP) and the effective precipitation (EP) as the time required to drain the macropores and use as infiltration; $BORT_{2017}$ is the methodology proposed by Bortoluzzi *et al.* (2017); TM_{1955} is the Thornthwaite and Mather (1955) methodology.

In contrast, the MAC_{PM} strategy was efficient throughout the entire period because it considered that all precipitation infiltrates into the soil and that the water in the macropores is temporarily stored. The TM_{1955} strategy differs from MAC_{PM} by not considering that water in the macropores is temporarily stored. Poor performance of TM_{1955} showed that water retention in the macropores is an important conditioning factor for EXC and should be included in WB models for accurate prediction of EXC.

The TM_{1955} strategy was able to indicate only one third of the days when there was water excess, evidencing considerable underestimation of EXC in lowlands. The low accuracy occurred because the TM_{1955} strategy does not consider that longer drainage time is necessary in lowlands (Mundstock *et al.*, 2017). Mainly, whenever there was enough rain to saturate the soil, TM_{1955} was able to indicate the presence of excess water. However, when the rain stopped or if there was less rain than the crop evapotranspiration after the day of EXC, the model removed water from the soil, making the current AWC less than AWC_1 (Equation 1), which represents a condition without EXC. For instance, there was an accumulated rainfall of 111 mm on December 27, 2014, but the TM_{1955} strategy did not indicate EXC in the following day (Table 1). On the contrary, the MAC_{PM} model indicated EXC in the following three days, precisely because it considers the delay in draining macropores (Table 1).

The MAC_{PM} strategy indicated eight days of EXC without them having been detected by measurements of volumetric soil moisture (Table 1). However, this inconsistency occurred mainly at the end of the crop cycle, when this condition was verified six times. Until the end of February, the MAC_{PM} strategy indicated precisely the days when the water content measured by the TDR probe in the 0-100 mm layer was above the θ_{mic} (0.39 mm^3 mm^{-3}) of that layer (Figure 2A). The lower accuracy of the MAC_{PM} strategy at the end of the soybean cycle is due to the small crop evapotranspiration (mean of 2 mm day^{-1}), being insufficient to reduce AWC_{tot} up to the upper limit of AWC_1. For example, the crop evapotranspiration of 2 mm day^{-1} was insufficient for the total drainage of the macropores ($AWC_2 = 0$) from the 5^{th} to the 7^{th} of March, indicating the presence of EXC. Nevertheless, the volumetric water content of the 0-100 mm layer decreased from 0.39 to 0.32 mm^3 mm^{-3} (7 mm of storage difference) in the same period (Figure 2A), characterizing the absence of EXC.

Measurements made with TDR showed that the water content in the 100-200 mm (Figure 2B) and 200-300 mm (Figure 2C) layers was also slightly less than the θ_{mic} of each layer at the end of the crop cycle. This indicates that there was participation of deep and/or lateral drainage in the extraction of water from the evaluated soil, but it was only relevant to affect the EXC estimates of the MAC_{PM} strategy when there was low crop evapotranspiration.

Analyzing the concept of the MAC_{PM} strategy, the likelihood of overestimating the EXC decreases with the increase in the ratio (crop evapotranspiration)/(deep and/or lateral drainage). Soybean crop evapotranspiration is lower in the initial and final growth stages, increasing the likelihood that deep and/or lateral drainage is not negligible for calculating EXC with the MAC_{PM} strategy. However, these stages growth have less relative importance in reducing the productivity in comparison to the soybean vegetative and reproductive phases (Beutler *et al.*, 2014; Rhine *et al.*, 2010; Scott *et al.*, 1989). For this reason, the use of the MAC_{PM} strategy is appropriate for soils where deep and/or lateral drainage can be considered negligible in relation to crop evapotranspiration.

The MAC_{PM} strategy was more efficient and accurate than the other strategies for predicting EXC in almost the entire soybean development cycle. The EXC indication was mostly consistent with the high volumetric water content in the soil measured in the field (Figure 2). In just 16 days in the 100-200 mm layer (Figure 2B) and 10 days in the 200-300 mm layer (Figure 2C) the water content in the soil was below θ_{mic}. In this area, the water table was close to the surface for a considerable period due to the occurrence of high rainfall (Gubiani *et al.*, 2018). This demonstrates that the field scenario was of water excess and that the MAC_{PM}

strategy was efficient in indicating the EXC on most days of its actual occurrence. Overall, the improvement of the excess water estimate through the SWB calculation contributes to the performance of risk analysis using historical series of meteorological data and future inclusion in soybean process-based models. Moreover, accurate estimates assist in the decision-making of management practices and in the reduction of the yield gap.

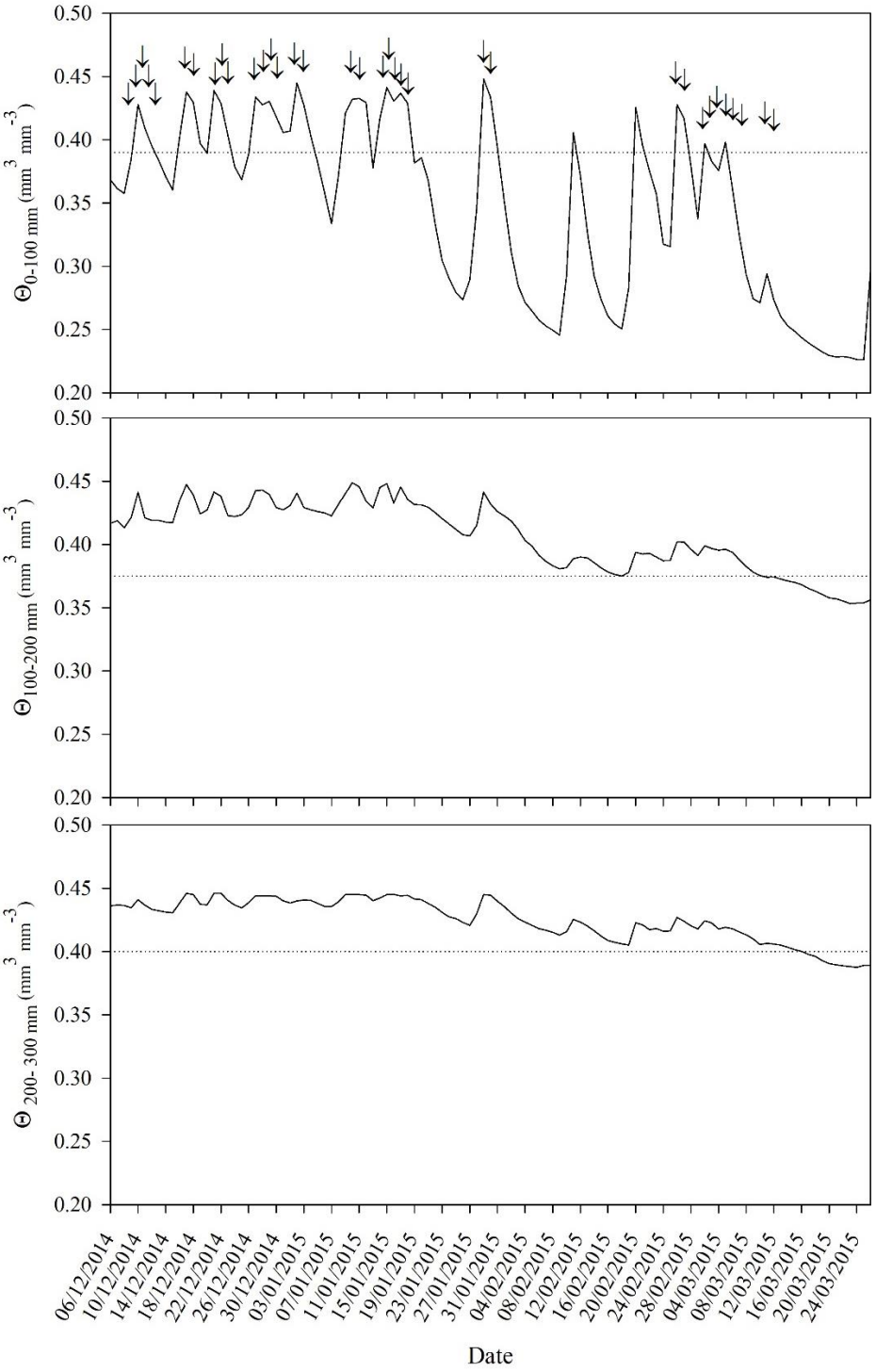

Figure 2. Volumetric water content in the soil (θ) throughout the soybean cycle in Planosol Haplic in the 0-100 mm (A), 100-200 mm (B) and 200-300 mm (C) layers. The horizontal dashed line represents the microporosity (θ_{mic}) and the arrows indicate the days of water excess obtained by the MAC_{PM} methodology for calculating the sequential water balance.

4. CONCLUSIONS

The traditional calculation strategy of water balance TM_{1955} underestimates the occurrence of water excess for lowland soybean cultivation.

The use of effective precipitation in water balance calculations also underestimates the occurrence of excess water in lowland field conditions.

The MAC_{PM} calculation strategy considers that all precipitation infiltrates into the soil and delays the drainage time of the macropores; it is efficient and can be recommended for predicting excess water in soybeans cultivated in lowlands.

5. ACKNOWLEDGEMENTS

This work was performed with the financial support from the National Council for Scientific and Technological Development (CNPq) and the Coordination for the Improvement of Higher Education Personnel (CAPES).

6. REFERENCES

ALLEN, R. G. *et al*. **Crop evapotranspiration-Guidelines for computing crop water requirements**. Rome: Fao, 1998. (FAO Irrigation and drainage paper, 56).

BEUTLER, A. N.; GIACOMELI, R.; ALBERTO, C. M.; SILVA, V. N.; NETO, G. F. S.; MACHADO, G. A.; SANTO, A. T. L. Soil hydric excess and soybean yield and development in Brazil. **Australian Journal of Crop Science**. v. 8, n. 10, p. 1461-1466, 2014.

BOOTE, K. J.; JONES, J. W.; HOOGENBOOM, G. Simulation of crop growth: CROPGRO model. *In*: PEART, R. M.; CURRY, R. B. (Eds.). **Agricultural Systems Modeling and Simulation**. New York: Marcel Dekker, 1998. p. 651–692.

BORTOLUZZI, M. P.; HELDWEIN, A. B.; TRENTIN, R.; LUCAS, D. D. P.; RIGHI, E. Z.; LEONARDI, M. Risk of water surplus in soybean crop on haplic planosol soil in the Central Depression of Rio Grande do Sul State, Brazil. **Ciência Rural**, v. 47, n. 2, 2017. http://dx.doi.org/10.1590/0103-8478cr20160170

CERA, J. C.; STRECK, N. A.; YANG, H.; ZANON, A. J.; DE PAULA, G. M.; LAGO, I. Extending the evaluation of the SoySim model to soybean cultivars with high maturation groups. **Field Crops Research**, v. 201, p. 162-174, 2017. https://doi.org/10.1016/j.fcr.2016.11.006

DE JONG VAN LIER, Q. Field capacity, a valid upper limit of crop available water? **Agricultural Water Management**, v. 193, p. 214–220, 2017. https://doi.org/10.1016/j.agwat.2017.08.017

DOURADO NETO, D.; GARCÍA, G. A.; FANCELLI, A. L.; FRIZZONE, J. A.; REICHARDT, K. Balance hídrico cíclico y secuencial: estimación de almacenamiento de agua en el suelo. **Scientia Agrícola**, v. 56, n. 3, p. 537-546, 1999. http://dx.doi.org/10.1590/S0103-90161999000300005

FENSTERSEIFER, C. A.; STRECK, N. A.; BAIGORRIA, G. A.; TIMILSINA, A. P.; ZANON, A. J.; CERA, J. C.; ROCHA, T. S.M. On the number of experiments required to calibrate a cultivar in a crop model: The case of CROPGRO-soybean. **Field Crops Research.** v. 204, p. 146–152, 2017. http://dx.doi.org/10.1016/j.fcr.2017.01.007

FIETZ, C. R.; RANGEL, M. A. S. Época de semeadura da soja para a região de Dourados - MS, com base na deficiência hídrica e no fotoperíodo. **Engenharia Agrícola**, v. 28, n. 4, p. 666-672, 2008. http://dx.doi.org/10.1590/S0100-69162008000400006

FRAGA, D. S.; AGOSTINETTO, D.; LANGARO, A. C.; OLIVEIRA, C.; ULGUIM, A. R.; SILVA, J. D. G. Morphological and Metabolic Changes in Soybean Plants Cultivated in Irrigated Rice Rotation and as Affected by Imazapyr and Imazapic Herbicides Carryover. **Planta daninha**, v. 37, 2019. http://dx.doi.org/10.1590/s0100-83582019370100023

FRIZZONE, J. A.; ANDRADE JÚNIOR, A. S. **Planejamento de irrigação**: Análise de decisão de investimentos. Brasília: Embrapa Informação Tecnológica, 2005. 627p.

GOULART, R. Z.; REICHERT, J. M.; RODRIGUES, M. F. Cropping poorly-drained lowland soils: alternative to rice monoculture, their challenges and management strategies. **Agricultural Systems**, v. 177, 2020. https://doi.org/10.1016/j.agsy.2019.102715

GUBIANI, P. I.; MÜLLER, E. A.; SOMAVILLA, A.; ZWIRTES, A. L.; MULAZZANI, R. P.; MARCHESAN, E. Transpiration reduction factor and soybean yield in lowland soil with ridge and chiseling. **Revista Brasileira de Ciência do Solo**, v. 42, p. 1-14, 2018. https://dx.doi.org/10.1590/18069657rbcs20170282

INSTITUTO RIOGRANDENSE DO ARROZ. **Boletim de resultados da lavoura** - safra 2018/19 – arroz irrigado e soja em rotação. 2019. Available at: https://irga.rs.gov.br/irga-divulga-boletim-de-resultados-da-safra-2018-2019. Access: 07 dez. 2019.

LUCAS, D. D. P.; HELDWEIN, A. B.; MALDANER, I. C.; TRENTIN, R.; HINNAH, F. D.; SILVA, J. R. Excedente hídrico em diferentes solos e épocas de semeadura do girassol no Rio Grande do Sul. **Pesquisa Agropecuária Brasileira,** v. 50, n. 6, p. 431-440, 2015. http://dx.doi.org/10.1590/S0100-204X2015000600001

MARCHESAN, E.; ARAMBURU, B. B.; VIZZOTTO, V. R.; OLIVEIRA, M. L.; CASTRO, I. A.; TONETTO, F.; GIACOMELI, R. Sistema de implantação e seus efeitos na resistência mecânica do solo à penetração de raízes e na produtividade de soja em área de várzea. *In*: CONGRESSO BRASILEIRO DE ARROZ IRRIGADO, 8., 12-15 de agosto 2013, Santa Maria. **Anais[...].** Santa Maria: Epagri, 2013. v. 2. p. 120-123. Available at: http://cbai2013.web2265.uni5.net/cdonline/docs/trab-5979-535.pdf. Access: 15 jan. 2020.

MARTORANO, L. G.; BERGAMASCHI, H.; FARIA, R. T.; DALMAGO, G. D. Decision Strategies for Soil Water Estimations in Soybean Crops Subjected to No-Tillage and Conventional Systems, in Brazil. *In*: KUMAR, M. (Org.). **Problems, Perspectives and Challenges of Agricultural Water Management.** Rijeka: InTech, 2012, p. 439-453.

MUNDSTOCK, C. M.; SCHOENFELD, R.; ALMEIDA, D.; UHRY JUNIOR, D. F. ; CARLOS, F. S.; ZANON, A. J.; ULGUIM, A. R.; OGOSHI, C.; MARCOLIN, E.; MORAES, F. A.; BADINELLI, P. G.; SILVA, P. R. F.; ANGHINONI, I. **Soja 6.000 Manejo para alta produtividade em terras Baixas.** 1. ed. Porto Alegre: IRGA, 2017. 68 p.

PEREIRA, A. R.; VILLA NOVA, N. A.; SEDIYAMA, G. C. **Evapo(transpi)ração.** Piracicaba: FEALQ, 1997. 183p.

PIRES, J. L. F.; SOPRANO, E.; CASSOL, B. Adaptações morfofisiológicas da soja em solo inundado. **Pesquisa Agropecuária Brasileira**, v. 37, n. 1, p. 41-50, 2002. http://dx.doi.org/10.1590/S0100-204X2002000100006

RHINE, M. D.; STEVENS, G.; SHANNON, G.; WRATHER, A.; SLEPER, D. Yield and nutritional responses to waterlogging of soybean cultivars. **Irrigation Science**, v. 28, n. 2, p.135-142, 2010.http://dx.doi.org/10.1007/s00271-009-0168-x

ROCHA, T. S. M.; STRECK, N. A.; ZANON, A. J.; PETRY, M. T.; TAGLIAPIETRA, E. L.; BALEST, D.; BEXAIRA, K. P.; MARCOLIN, E. Performance of soybean in hydromorphic and non hydromorphic soil under irrigated or rainfed conditions. **Pesquisa Agropecuaria Brasileira**, v. 52, n. 5, p. 293-302, 2017.https://doi.org/10.1590/s0100-204x2017000500002

SARTORI, G. M. S.; MARCHESAN, E.; DAVID, R.; DONATO, G.; COELHO, L. L.; AIRES, N. P.; ARAMBURU, B. B. Soil tillage systems and seeding on grain yield of soybean in lowland area. **Ciência Rural**, v. 46, n. 3, p. 492-498, 2016. http://dx.doi.org/10.1590/0103-8478cr20150676

SCOTT, H. D.; DEANGULO, J.; DANIELS, M. B.; WOOD, L. S. Flood duration effects on soybean growth and yield. **Agronomy Journal**, v. 81, n. 4, p. 631-636, 1989. http://dx.doi.org/10.2134/agronj1989.00021962008100040016x

SCHERNER, A.; SCHREIBER, F.; ANDRES, A.; CONCENÇO, G.; MARTINS, M. B.; PITOL, A. Rice crop rotation: a solution for weed management. *In*: SHAH, F.; KHAN, Z. H.; IQBAL, A. (eds.). **Rice crop t current developments**. London: IntechOpen, 2018. https://dx.doi.org/10.5772/intechopen.75884

SETIYONO, T. D.; CASSMAN, K. G.; SPECHT, J. E.; DOBERMANN, A.; WEISS, A.; YANG, H.; CONLEY, S. P.; ROBINSON, A. P.; PEDERSEN, P.; DE BRUIN, J. L. Simulation of soybean growth and yield in near-optimal growth conditions. **Field Crops Research,** v. 119, p. 161–174, 2010. http://dx.doi.org/10.1016/j.fcr.2010.07.007

SINCLAIR, T. R.; KITANI, S.; KITANI, S.; HINSON, K.; BRUNIARD, J.; HORIE, T. Soybean flowering date: linear and logistic models based on temperature and photoperiod. **Crop Science**, v. 31, n. 3, p. 786–790, 1991. http://dx.doi.org/10.2135/cropsci1991.0011183X003100030049x

STRECK, E. V. *et al.* **Solos do Rio Grande do Sul**. 2. ed. Porto Alegre: EMATER/RS-ASCAR, 2008. 222 p.

THORNTHWAITE, C. W.; MATHER, J. R. **The water balance**. Centerton: Drexel institute of technology, 1955. (Publications in Climatology).

TRENTIN, R.; HELDWEIN, A. B.; STRECK, N. A.; TRENTIN, G.; SILVA, J. C. Subperíodos fenológicos e ciclo da soja conforme grupos de maturidade e datas de semeadura. **Pesquisa Agropecuária Brasileira**, v. 48, n. 7, p. 703-713, 2013. http://dx.doi.org/10.1590/S0100-204X2013000700002

Ambiente & Água - An Interdisciplinary Journal of Applied Science
ISSN 1980-993X – doi:10.4136/1980-993X
www.ambi-agua.net
E-mail: ambi.agua@gmail.com

Low-cost flow photoreactor for degradation of Reactive Black 5 dye by UV/H_2O_2, Fenton and photo-Fenton processes: a performance comparison

ARTICLES doi:10.4136/ambi-agua.2687

Received: 15 Dec. 2020; Accepted: 12 Apr. 2021

Andrea Maria da Silva[1]; Tainá Natália dos Santos[1]; Raiane dos Santos[1]; Thiago Sabino Pessoa[1]; Luiz Carlos Araújo dos Anjos[1*]; Nelson Alves da Silva Sobrinho[1]; Paula Barone da Paz Sales[2]

[1]Departamento de Química. Instituto Federal de Educação, Ciência e Tecnologia de Pernambuco (IFPE), Rodovia PE-60, km 14, CEP: 55590-000, Ipojuca, PE, Brazil.
E-mail: andrea.mary51@gmail.com, tnatalia710@gmail.com, raianesantos@ipojuca.ifpe.edu.br, thiagosabino@ipojuca.ifpe.edu.br, nelsonalves@ipojuca.ifpe.edu.br
[2]Coordenação de Petroquímica. Instituto Federal de Educação, Ciência e Tecnologia de Pernambuco (IFPE), Rodovia PE-60, km 14, CEP: 55590-000, Ipojuca, PE, Brazil. E-mail: paulabarone@ipojuca.ifpe.edu.br
[*]Corresponding author. E-mail: luizaraujo@ipojuca.ifpe.edu.br

ABSTRACT

In this work, a flow photoreactor was designed and set up using low-cost and recyclable parts to develop chemical treatments based on advanced oxidation processes (AOP) of highly colored textile wastewater. To evaluate this sustainable system´s efficiency, we investigated and compared the performance of three types of destructive methods (UV/H_2O_2, Fenton, and photo-Fenton) on the decolorization of aqueous solutions of Reactive Black 5 dye (RB5). We also analyzed the effect of the oxidant and dye concentrations on the rate of color removal in each one of the three methods. The results showed that, regardless of the initial operating conditions, the photo-Fenton process achieved the highest degradation rates, particularly when the highest ratio between the oxidant and dye concentrations was used ([H_2O_2]: [RB5] = 24.5 mg L^{-1}: 25 mg L^{-1}), leading to complete color removal within only 10 minutes of reaction. With the same initial condition, the Fenton and UV/H_2O_2 processes were also capable of removing the color entirely, even though they demanded more extended runs of 25 min. and 45 min., respectively. The effect of pH on the decolorization by the photo-Fenton process was also investigated, showing the same high performance at pHs 3 and 4. The degradation profile achieved by the photo-Fenton treatment was appropriately fitted by a pseudo-first-order kinetic. The non-expensive photoreactor proved to be quite useful for the degradation of the RB5, mainly when this azo dye underwent the photo-Fenton process.

Keywords: advanced oxidation process, color removal, Reactive Black 5 dye, textile pollutants.

Fotorreator contínuo de baixo custo para degradação do corante Reactive Black 5 pelos processos UV/H_2O_2, Fenton e foto-Fenton: uma comparação de performances

RESUMO

Neste trabalho, um fotorreator contínuo foi projetado e montado, usando peças recicláveis

This is an Open Access article distributed under the terms of the Creative Commons Attribution License, which permits unrestricted use, distribution, and reproduction in any medium, provided the original work is properly cited.

e de baixo custo, para desenvolver tratamentos químicos, baseados em processos oxidativos avançados (AOP), de efluentes têxteis altamente coloridos por azo-compostos. A fim de avaliar a eficiência deste sistema reacional sustentável, foi investigada a performance de três tratamentos destrutivos (UV/H_2O_2, Fenton e foto-Fenton) sobre a remoção de cor de soluções aquosas do corante denominado Reactive Black 5 (RB5). O efeito da concentração de oxidante (H_2O_2) e da carga inicial de corante sobre a taxa de remoção de cor foi também analisado. Os resultados mostraram que, independentemente das condições operacionais iniciais, o processo foto-Fenton alcançou as taxas mais elevadas de degradação, especialmente quando a maior razão entre as concentrações do oxidante e do corante foi empregada ([H_2O_2]: [RB5] = 24.5 mg L^{-1}: 25 mg L^{-1}), com a completa remoção de cor em apenas 10 minutos de experimento. Usando-se as mesmas condições iniciais, os processos Fenton e UV/H_2O_2 foram também capazes de descolorir completamente o poluente têxtil, entretanto precisando de 25 minutos e 45 minutos de reação, respectivamente. O efeito do pH sobre a descoloração pelo processo foto-Fenton foi também investigado, mostrando a mesma elevada performance nos pHs 3 e 4. O perfil de degradação obtido no tratamento foto-Fenton foi devidamente modelado pela cinética de pseudo-primeira ordem. O fotorreator contínuo de baixo custo mostrou-se bastante útil na degradação do corante RB5, principalmente quando o processo foto-Fenton foi empregado.

Palavras-chave: corante Reactive Black 5, poluentes têxteis, processos oxidativos avançados, remoção de cor.

1. INTRODUCTION

The textile industry is one of the essential socio-economic activities in Brazil. According to the Brazilian Association of the Textile Industry and Confection (ABIT), this type of sector accounts for more than 1 million tons of fabric annually, making this industrial segment stand out as the second-most important in respect of job generation nationwide.

Although this activity significantly contributes to wealth creation and social inclusion, inevitably, environmental impacts may be caused, especially when there is inappropriate disposal of the effluents from the fabric dyeing process. These effluents typically have a high organic load of synthetic dyes, particularly azo dyes, which combine high toxicity with low biodegradability (Bali and Karagözoglu, 2007; Liu *et al.*, 2011; Silva *et al.*, 2009). Azo dyes are molecules bearing the functional group diazenyl (R – N = N – R´), where R and R´ usually are aromatic groups, which makes them a highly conjugated and stable system. Figure 1 shows the structure of azo dye Reactive Black 5 (RB5 dye) studied in the present work.

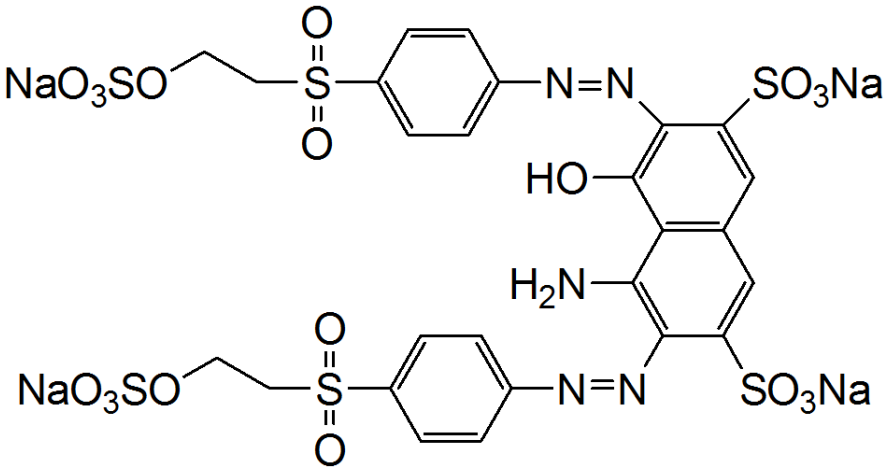

Figure 1. Structural formula of the Reactive Black 5 dye (RB5).

Therefore, to reduce potential impacts in the environment, the development and application of efficient techniques are crucial for removal or degradation of that type of dye from textile industry effluents.

Countless published studies have demonstrated promising aspects of advanced oxidation processes (AOP) for the degradation of organics pollutants (Fragoso *et al.,* 2009; Guimarães *et al.*, 2012; Vedrenne *et al.*, 2012; Basturk *et al.*, 2015; Abhilasha *et al.*, 2016; Leite *et al.*, 2016; Starling *et al.,* 2017; Manaa *et al.,* 2019; Mittersteiner *et al.,* 2020). In that technique, the organic molecule undergoes successive oxidative breakings through a chain reaction initiated with highly reactive radicals, particularly the hydroxyl (·OH) and hydroperoxyl (·OOH). These radicals are promoted by the direct action of solar light or artificial source of UV radiation on the hydrogen peroxide (H_2O_2), a process known as UV-induced peroxidation (UV/H_2O_2). Another way to induce those radicals is to use iron ions (Fe^{2+}, Fe^{3+}) as initiating species, a process, in this case, known as Fenton. The following equations describe an overview of the reactions mentioned (Hsueh *et al.*, 2005; Ioannou *et al.*, 2015; Mofrad *et al.*, 2015; Pouran *et al.*, 2015; Gutierrez-Mata *et al.*, 2017; Vorontsov, 2019).

H_2O_2 photolysis (Equation 1):

$$H_2O_2 + h\nu \rightarrow \cdot OH + \cdot OH \quad (1)$$

Fenton Equations 2 and 3:

$$Fe^{2+} + H_2O_2 \rightarrow Fe^{3+} + OH^- + \cdot OH \qquad k_1 = 76\ Ms^{-1} \quad (2)$$

$$Fe^{3+} + H_2O_2 \rightarrow Fe^{2+} + \cdot OOH + H^+ \qquad k_2 = 0.001 - 0.01\ Ms^{-1} \quad (3)$$

Upon comparing the reaction rate constants (k_1, k_2), it becomes evident that the Fe^{2+} ion is remarkably more active than the Fe^{3+} ion, as a radical promoter of the oxidation process, a fact that unexpectedly brings about a technical drawback. As can be seen in Equation 3, the Fe^{2+} ion is regenerated from the reduction of Fe^{3+} ion. Unfortunately, since $k_2 << k_1$, the regeneration of the most active iron ion is much slower than its consumption rate, leading to a gradual reduction in the Fenton process efficiency over time. Additionally, the pH increase (Equation 2), along with the Fe^{3+} accumulation, might lead to coagulated ferric complexes (Neyens and Baeyens, 2003), which requires na extra solid-liquid separation step or a pH adjustment to the efluente treatment process.

Combination of UV irradiation and the Fenton process (photo-Fenton) is considered a promising alternative to the drawbacks aforementioned, since the radiation allows the direct photolysis of the H_2O_2, as well as na increase in the Fe^{2+} regeneration rates, according to Equation 4, enhancing the overall production rate of hydroxyl radicals.

$$Fe^{3+} + H_2O + h\nu \rightarrow Fe^{2+} + \cdot OH + H^+ \quad (4)$$

The high reactivity of the radicals from H_2O_2, especially the hydroxyl (·OH), turn them into non-selective and strong oxidants (Gligorovski *et al.*, 2015; Miao *et al.*, 2018), which considerably broadens the application spectrum of the Fenton process and photo-Fenton process. Thus, they are capable of efficiently degrading countless types of organic pollutants, such as pharmaceutical residues (Trovó *et al.*, 2012; Dúran *et al.,* 2013; Ahmed and Chiron, 2014), agricultural defensives (Farré *et al.*, 2006; Zhang and Pagilla, 2010; Monteagudo *et al.*, 2011) and the azo dyes themselves (Barka *et al.*, 2010; Sun *et al.*, 2013; Yu *et al.*, 2010; Mehrdad *et al.*, 2011; Khataee *et al.*, 2016; Leite *et al.*, 2016; Guo *et al.*, 2018; Rubeena *et al.*, 2018). Several of those applications highlight the photo-Fenton capability to obtain high mineralization rates of pollutants, according to Equation 5 (Sun *et al.*, 2009; Idel-aouad *et al.*, 2011; Guimarães *et al.*, 2012; Monteagudo *et al.*, 2014). This vital outcome significantly reduces the environmental impacts from the effluents with a high organic load.

$$R-H\,(org.) + \cdot OH \rightarrow H_2O + \cdot R \rightarrow \text{further oxidation} \rightarrow CO_2 + H_2O + \text{mineralization products} \quad (5)$$

As the Fenton process is usually performed in mild conditions and needs simple and low-cost chemicals, it can lead to economically feasible industrial applications. According to the work of Starling *et al.* (2017), the processing cost is estimated somewhere between US$ 0.90 and 2.20 per cubic meter of treated effluent, including the energy costs.

However, it is essential to consider the usually high initial costs with the project and assembly of the reactor. In a global scenario of financial limitations, the first step to achieving an industrial system of effluent treatment that is technically and economically feasible consists of building a versatile and low-cost lab-scale apparatus to research the operating conditions that optimize the pollutant degradation.

In most reported studies, the AOP experiments have been developed in batch systems, usually by adapting glass beakers or Erlenmeyer flasks as reactors (Farré *et al.*, 2006; Bali *et al.*, 2007; Fragoso *et al.*, 2009; Silva *et al.*, 2009; Guimarães *et al.*, 2012; Módenes *et al.*, 2012; Khataee *et al.*, 2016; Starling *et al.*, 2017; Guo *et al.*, 2018; Rubeena *et al.*, 2018; Manaa *et al.*, 2019; Mittersteiner *et al.*, 2020;). Although this alternative is capable of providing essential data for the optimization of operating conditions, the batch reactor is rare when it comes to industrial applications, where processes with flowing streams are much more common. Thus, the advantage of employing a flow photo-reactor in lab experiments is undeniable, even with refluxing streams, since it allows not only an assessment on variables that directly affect the reaction rates but also the hydrodynamic conditions, which can speed up an industrial scale-up.

Hence, primarily focusing on a sustainable and cost-effective approach, the present study had as a first step the design and setup of a continuous annular photo-reactor, employing recyclable materials and adapting low-cost parts, available on the local market. With this reactional apparatus, experiments with three types of advanced oxidation process (UV/H_2O_2, Fenton and photo-Fenton) were carried out in order to compare their effectiveness of decolorizing RB5 dye solutions. Additionally, the chemical kinetics was studied, assessing the effect of the oxidant dosage and dye concentration on degradation rates.

2. MATERIAL AND METHODS

2.1. Chemicals

Reactive Black 5 (RB5, color index 20505, CAS number 17095-24-8) was used in this study as the model of azo textile dye without any further purification process. Its molecular formula is $C_{26}H_{21}O_{19}N_5S_6Na_4$, a molecular weight of 991,82 g mol^{-1}, maximum absorbance wavelength of 597 nm, and water solubility of 200 g L^{-1} at 20°C.

To make the Fenton´s reagent, hydrogen peroxide (H_2O_2, 30% m/m) was used as oxidant agent, purchased from Êxodo Científica (Brazil), and, as the source of ferrous ions (Fe^{2+}), ferrous sulfate heptahydrate ($FeSO_4.7H_2O$, purity 99%) was acquired from Vetec (Brazil). For any pH adjustments, sulfuric acid (H_2SO_4) and sodium hydroxide (NaOH) was used as needed.

2.2. Photoreactor Setup

The experimental apparatus was almost entirely designed and constructed in our lab and basically consisted of an annular flow photoreactor (Figure 2, left). This reactor was set up by mounting a UV-C germicidal Hg-lamp (power 30 W) in the center of a cylindrical glass tube 1 m long, a configuration that left a total working volume of 334 mL. The glass tube was externally wrapped with an aluminum foil to prevent the technicians from being exposed to the harmful UV irradiation.

The bottom of two recyclable PET bottles (volume of 2 L each) was transversally cut off to turn them into reservoirs (Figure 2, right), one for the aqueous dye solution and the other one

for cooling water. The cooling system is composed of two Liebig condensers with a series connection, working as heat exchangers to maintain temperature during the reaction.

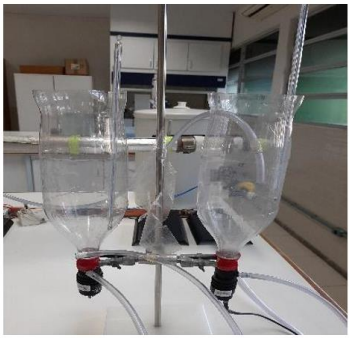

Figure 2. Annular flow photoreactor with the aluminum foil (left) and reservoirs for the dye solution and cooling water (right).

Two windshield washer pumps were purchased from a local auto parts store and adapted to the reservoir outlets to pump the dye solution through the photoreactor and the cooling water through the heat exchangers. A digital power supply (MedTec, Model PS-4000) was used to set the voltage and current appropriately to operate the pumps at a constant volumetric flow rate of 1.5 10^{-5} m^3 s^{-1}.

2.3. Advanced oxidation experiments: efficiency analysis

Before the AOP experiments themselves, various standard RB5 solutions (2 ,4, 10, 20, 50, 80, 100 and 150 mg L^{-1}) were prepared to build the calibration curve that depicts the relationship between the dye concentration and maximum absorbance of its chromophore group, which occurs at the wavelength of 547 nm. A UV-visible spectrophotometer (THERMOSCIENTIFIC, Model EVO 60) was used to measure the absorbances.

To evaluate the effectiveness of the photoreactor towards the color removal of the azo dye RB5, several assays of three types of homogeneous advanced oxidation process were performed: UV-induced peroxidation, Fenton and photo-Fenton process. Photolysis experiments without any oxidant agent were carried out as well.

For all the assays aforementioned, dye solutions 50 mg L^{-1} were prepared by dissolving the RB5 in distilled water. The effect on the color removal of two different concentrations of the hydrogen peroxide (2.45 mg L^{-1} and 24.50 mg L^{-1}) was analyzed. For the Fenton and photo-Fenton experiments, the ferrous sulfate heptahydrate 15.00 mg L^{-1} was dissolved in the dye samples. Their pH was adjusted to 3, by using a solution of H_2SO_4 0.50 mol L^{-1} previously prepared, in order to avoid the coagulation of ferric ions (Fe^{3+}) with the hydroxyl ions (Pignatello *et al.*, 2006).

The UV-induced peroxidation (UV/H_2O_2) was performed at neutral pH. Each one of AOP runs was performed in the photoreactor, keeping the volumetric flow rate at 1.50 10^{-5} m^3 s^{-1}, with the UV-C lamp turned on, except for the Fenton process. Afterwards, all the samples were taken to the UV-visible spectrophotometer to read the absorbance at the characteristic wavelength (547 nm), then the final concentrations were obtained by using the calibration curve.

The efficiency of each treatment on color removal was calculated as follows (Equation 6), where C_0 and C denote, respectively, the initial azo dye concentration and its concentration at a given time.

$$Efficiency\ (\%) = \frac{(C_0 - C)}{C_0}\ x\ 100 \qquad (6)$$

The AOP at the highest ratio [oxidant]:[RB5] that led to the most efficient color removal was chosen to investigate the residual hydrogen peroxide, by using permanganate titration in acidic medium (Tzanov *et al*., 2002). Moreover, the acidity effect on the dye degradation profile was evaluated at two different pHs, one slightly lower (pH=2) and the other higher (pH=4) than the value set for all experiments.

2.4. Kinetics analysis of AOPs

The kinetic profiles of the color removal were obtained for the Fenton, photo-Fenton, and UV/H_2O_2 processes, performing experiments with the following initial azo dye concentrations: 25, 50 and 100 mg L^{-1}.

For each run, the effluent reservoir was loaded with 1 L of the dye solution and enough oxidant solution to provide 24.5 mg of H_2O_2 ([H_2O_2] = 0.720 mM). Moreover, 15 mg $FeSO_4.7H_2O$ was dissolved for the Fenton and photo-Fenton assays, corresponding to a concentration of 0.054 mM for the ferrous ion (Fe^{2+}). The UV lamp and pumps were turned on simultaneously, allowing the dye solution to be exposed to the UV irradiation, except for the Fenton process, which takes place in a completely dark environment. During the reaction, effluent aliquots were collected from the reservoir, at predefined time intervals, then their absorbances were immediately measured by the UV-vis spectrophotometer.

The pseudo-first-order and pseudo-second-order kinetic models (Equations 7 and 8) were employed to check, through linear regression, which one better fits the actual degradation profiles of the dye over the reaction time. In Equations 7 and 8, C_0, C and k denote the initial concentration of the dye, its concentration at a given time t, and the apparent rate constant, respectively.

$$Ln\left(\frac{C_0}{C}\right) = kt \qquad (pseudo - first - order\ model) \tag{7}$$

$$\frac{1}{C} - \frac{1}{C_0} = kt \qquad (pseudo - second - order\ model) \tag{8}$$

3. RESULTS AND DISCUSSIONS

In this study, a low-cost annular photoreactor was built to develop and study several degradation processes of the RB5 azo dye. The efficiencies of four techniques were investigated (UV photolysis, UV/H_2O_2, Fenton, and photo-Fenton), using three initial concentrations of dye (25, 50, 100 mg L^{-1}). Two different dosages of H_2O_2 were used (2.45 mg L^{-1} and 24.5 mg L^{-1}) to investigate the oxidant effect on the advanced oxidation processes. The kinetic modeling of the RB5 decolorization by Fenton and photo-Fenton treatments was also studied and reported.

3.1. Efficiency comparison between UV/H_2O_2 and photolysis

First, to bring up an overview on the role played by the presence of the oxidant on the degradation of the dye, the efficiency of the lone action of the UV irradiation (photolysis) was compared to the combination of UV with H_2O_2 (UV-induced peroxidation), performing the experiments with a specific set of initial concentrations ([RB5] = 50 mg L^{-1}, [H_2O_2] = 24.5 mg L^{-1}) at neutral pH.

As can be seen in Figure 3, after a long 90-min. run, the dye degradation by photolysis was quite low, roughly 22%, an expected result (Lizama *et al.*, 2002; Elmorsi *et al.*, 2010), since no oxidant nor catalyst was employed. The degradation rate notably improves with the H_2O_2, as this oxidant generates highly reactive radicals (·OH) under the action of UV photons. As a result, those species promote fast successive bond breakings, generating other intermediate radicals through a complex mechanism that can lead to the mineralization of most organic

fragments (Shu and Chang, 2005; Elmorsi *et al.*, 2010). Figure 3 shows the complete removal of the dye color by the UV/H_2O_2 process after the same 90-min. run. Although this time interval seems long, it is important to highlight that the UV/H_2O_2 process required approximately 30 min. to bleach more than 90% of the dye.

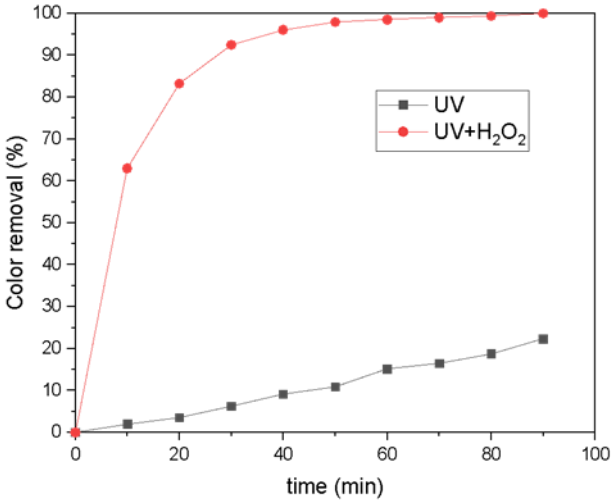

Figure 3. Color removal of the RB5 dye by the UV photolysis and UV/H_2O_2. Initial concentrations: [RB5] = 50 mg L^{-1}, [H_2O_2] = 24.5 mg L^{-1}.

3.2. Efficiency of the advanced oxidation processes

The results of the three advanced oxidation processes on the decolorization of RB5 are depicted in Figure 4. The effect of the initial concentrations of dye and oxidant dosages on the degradation profile can also be analyzed. Upon a quick comparison between the three processes, it becomes evident, as expected, that the photo-Fenton turns out to be the most efficient and fastest on the color removal of RB5 in all initial operating conditions employed in this study.

The lowest oxidant dosage (2.45 mg L^{-1}) appears inadequate to bleach the dye dissolved completely in the studied solutions (25, 50, 100 mg L^{-1}). In this case, naturally, the best result occurs with the highest ratio [H_2O_2]:[RB5], where a maximum degradation of 79% is reached by the Fenton and photo-Fenton treatments, and 63% by UV/H_2O_2 process (Figure 4 (a)).

By observing all the graphics in Figure 4, the slope of the curves clearly demonstrates that the higher [H_2O_2]:[RB5] ratio, the higher degradation rate of the azo dye, regardless of the type of treatment used. The best scenario for the dye degradation emerges, as shown in Figure 5 (b), when the highest oxidant dosage (24.5 mg L^{-1}) and lowest dye concentration (25 mg L^{-1}) are used. With this initial set of concentrations, the most efficient treatment, photo-Fenton, was capable of a complete color removal after only 10 min. The dark Fenton and UV/H_2O_2 treatments were less efficient, requiring approximately 25-min. and 45-min. run, respectively, to bleach the solution entirely. Furthermore, higher dye loads make its degradation even lower, an outcome that can be explained by the shallow penetration of the UV photons into the solution with high intense color (Behnajady *et al.*, 2004).

In each one of the graphics (Figure 4), a comparison between the three treatments demonstrated that the degradation promoted by the UV/H_2O_2 is clearly slower than the one achieved by the Fenton and photo-Fenton processes, which suggests that the ferrous ions play an essential role in the generation of H_2O_2-derived radicals. As expected, the highest degradation rate of the azo dye occurs when the ferrous ions are combined with the UV irradiation, since it increases the generation of those radicals (Neamtu *et al.*, 2003).

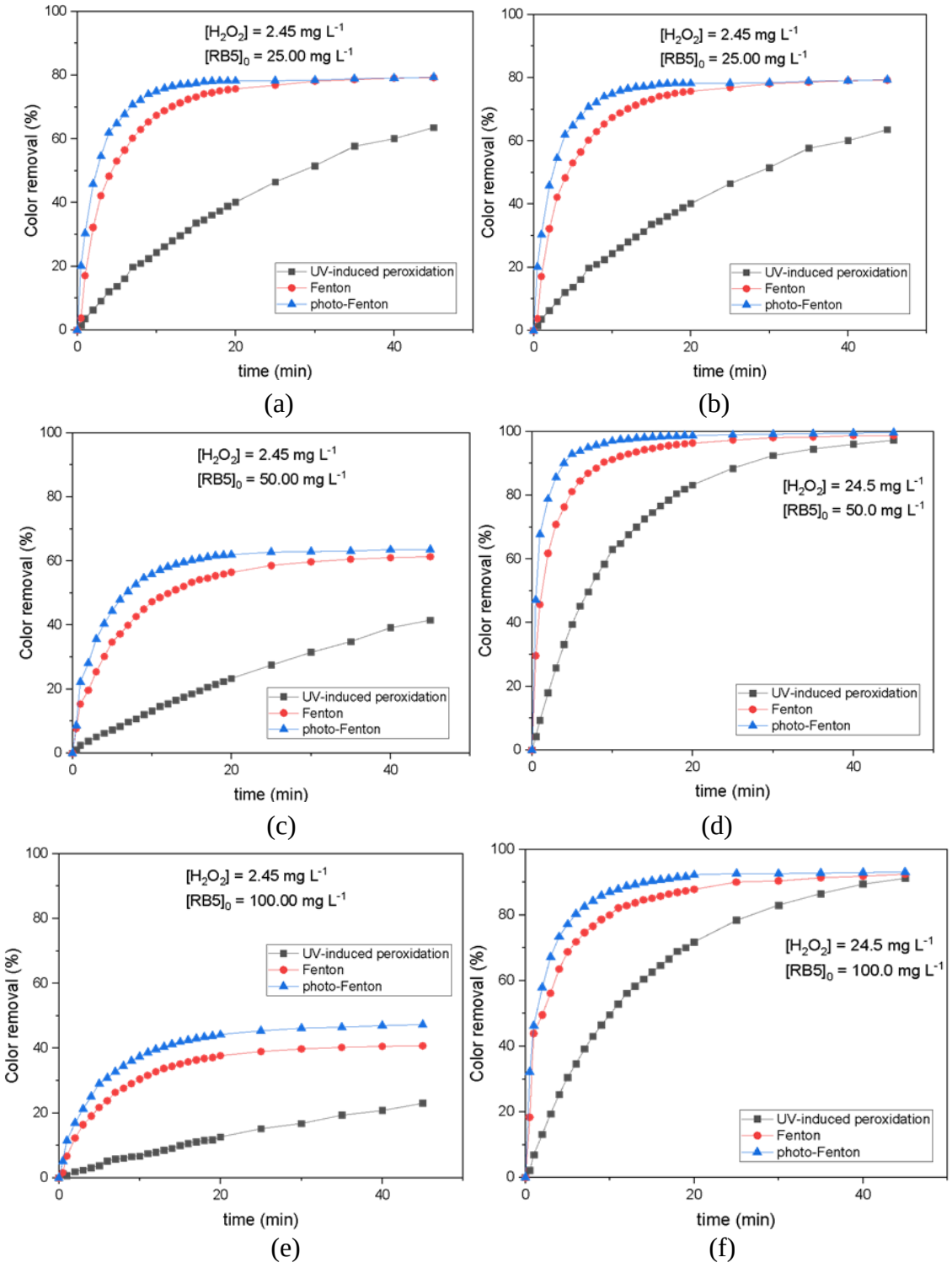

Figure 4. Decolorization profile of the RB5 dye by UV/H_2O_2, Fenton and photo-Fenton treatments with respect to initial dye concentration and oxidant dosage.

For comparison purposes, Table 1 presents an overview of the AOP performances on the dye color removal at some reaction times, using the highest oxidant dosage ([H_2O_2] = 24.5 mg L^{-1}).

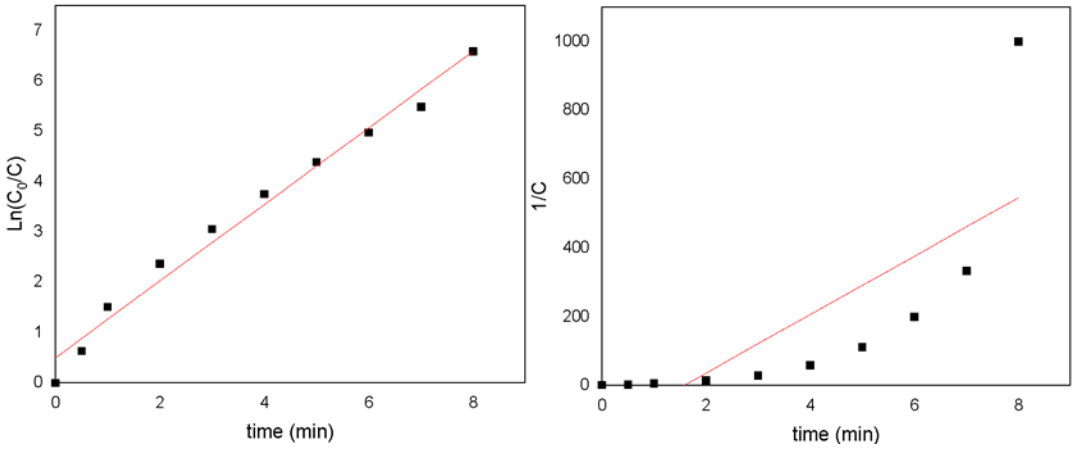

Figure 5. Kinetic profile of the RB5 degradation by the photo-Fenton treatment ([H_2O_2] = 24.5 mg L^{-1}, [RB5] = 25 mg L^{-1}). Pseudo-first-order fitting (left) and Pseudo-second-order fitting (right).

Table 1. RB5 color removal by the UV/H_2O_2, Fenton and photo-Fenton processes using the initial oxidant dosage of 24.5 mg L^{-1}.

[RB5] (mg L^{-1})	Dye color removal (%)			
	Reaction time (min)	UV/H_2O_2	Fenton process	Photo-Fenton process
25	5	47.2	92.2	98.7
	10	76.6	97.8	100
	30	98.8	99.8	100
50	5	39.4	81.1	92.4
	10	63.0	91.2	
	30	92.5	98.0	99.2
100	5	30.5	68.8	77.2
	10	49.6	79.9	87.0
	30	83.0	90.4	92.7

The results described in some similar previous studies found in the literature can corroborate the promising aspects of the continuous photo-reactor developed in the presented work. For instance, Silva *et al.* (2009) carried out several photo-Fenton experiments to degrade the RB5 in a batch reactor, testing out, among other operational conditions, three different reaction times (40 min., 50 min., 60 min.). In the shortest run (40 min.), complete dye removal was only reached when the concentration ratio was [H_2O_2]:[RB5] = 150 mg L^{-1}:100 mg L^{-1}, slightly higher than the best concentration set used in our work ([H_2O_2]:[RB5] = 24.5 mg L^{-1}:25 mg L^{-1}). In another AOP work, now using a flow photo-reactor, Leite *et al.* (2016) developed studies of degradation of the dispersed red 1 (DR1) dye, also by the UV-Fenton process. In this work, a 45-min. run was required to reduce the dye concentration from 23 mg L^{-1} to 0.4 mg L^{-1} (98.2% removal) with a high oxidant concentration of 170 mg L^{-1}. In the Miao *et al*. (2018) study, a heterogeneous photo-Fenton system, with α-FeOOH as the catalyst, was used to study Orange II dye color removal. With the initial concentrations of the oxidant and dye set at 340 mg L^{-1} and 70 mg L^{-1}, respectively, color removal of 99.7% was obtained in 30-min. reaction. In comparison to the instances above and other previous works (Barka *et al*., 2010; Belayachi *et al.*, 2019), the results presented in Table 1 demonstrate more rapid dye degradation rates, particularly by the photo-Fenton process, despite using a lower ratio [oxidant]:[dye] than the ones set in those works. This comparison suggests that the continuous photo-reactor, set-up and used in our work, notably allowed an improvement in

color removal efficiency and, thus, this low-cost apparatus can be considered as a promising alternative towards a feasible treatment of textile pollutants.

The results of the residual hydrogen peroxide for the best treatment (photo-Fenton) and ratio $[H_2O_2]$:[RB5] = 24.5 mg L^{-1}:25 mg L^{-1} are presented in Table 2.

Table 2. Residual hydrogen peroxide for the photo-Fenton process with ratio $[H_2O_2]$:[RB5] = 24.5 mg L^{-1}:25 mg L^{-1}.

Reaction time (min.)	$[H_2O_2]$ (mg L^{-1})	Residual percentage
0	24.5	100.0
45	3.4	13.9
90	2.0	8.2

The residual concentration of hydrogen peroxide, higher than 10%, even after 45 min. of photo-Fenton reaction, indicates that a much lower oxidant dosage would have been needed if the only goal of the treatment was the RB5 color removal. Actually, it is well known that the color of a dye emerges from a structure based on the resonance of highly conjugated π-electrons, and, therefore, a simple cleavage of the azo bonds (- N = N -), turning the RB5 into smaller fragments, would cease this extended resonance and accomplish the effluent decolorization. However, besides the color removal, other issues are likewise crucial for appropriate effluent treatment, such as the aromatic chemicals´ degradation. The slight drop of the hydrogen peroxide concentration, from 3.4 mg L^{-1} to 2.0 mg L^{-1}, between 45 min. and 90 min. of reaction, significantly later than the complete color removal (10 min.), demonstrates few oxidable organic compounds remained in the system after 45 min. However, further analysis should be essential to corroborate this outcome, such as total organic chemical (TOC) analysis.

3.3. Kinetic modelling

Graphics of - $ln(C_0/C)$ and $1/C$ versus time were plotted, and their linearization coefficients (R^2) were calculated to compare the ability of pseudo-first-order and pseudo-second-order kinetic models in fitting the experimental results of dye degradation. The most efficient operating condition, which was the photo-Fenton process with the highest ratio $[H_2O_2]$/[RB5] ($[H_2O_2]$ = 24.5 mg L^{-1}; [RB5] = 25 mg L^{-1}), was chosen to analyze the kinetic modelling of the degradation profile. The temperature was kept constant at 20ºC.

As shown in Figure 5, the pseudo-first-order kinetic fits the RB5 degradation appropriately, which can be confirmed by its high linearization coefficient (R^2 = 0.98). The rate constant and half-life are shown in the Table 3 for this pseudo-first-order degradation. The same conclusion is reported by several other studies in the literature (Shuai *et al.*, 2018; Manaa *et al.*, 2019). On the other hand, the pseudo-second-order kinetic is remarkably inadequate to fit the experimental results (R^2 = 0.54).

Table 3. Kinetic parameters of the pseudo-first-order modelling for the dye degradation by the photo-Fenton treatment ($[H_2O_2]$ = 24.5 mg L^{-1}; [RB5] = 25 mg L^{-1}).

Parameter	Value
Rate constant (k)	0.76 min^{-1}
Half-life ($t_{1/2}$)	0.91 min

3.4. Effect of the initial pH

Three different acidic pHs (2, 3, and 4) were chosen to investigate its effect on color removal of the photo-Fenton treatment. Higher pHs can bring about the complexation of insoluble ferric hydroxides, which hinders the crucial reaction between ferrous ions (Fe^{2+}) and H_2O_2. As a result, the concentration of hydroxyl radicals is reduced (Sun *et al.*, 2009). Furthermore, this coagulation is likely to clog the pumps, which decreases the flow rate and eventually damages them. Figure 6 depicts the decolorization efficiency at 3 min., 5 min., and 10 min. of reaction for the three chosen pHs. All the experiments were carried out with the highest ratio [oxidant]:[RB5].

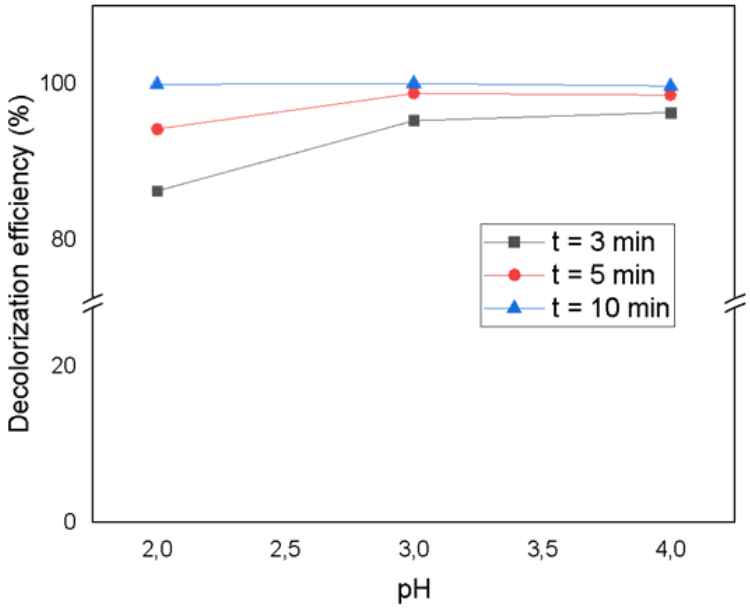

Figure 6. Effect of initial pH on the color removal of RB5 by photo-Fenton process. [H_2O_2]:[RB5] = 24.5 mg L^{-1}: 25 mg L^{-1}.

The results showed that pH had an insignificant effect on the time required for complete color removal of RB5, which was nearly 10 min. of reaction in the three acidic conditions. The only notable effect of the pH on the decolorization arose within the first 3-min. reaction when the most acidic condition (pH=2) led to 86% efficiency. In contrast, the pHs of 3 and 4 led to higher decolorization degrees, 95% and 96%, respectively. After 5-min. reaction, the decolorization efficiency reached 94% in the most acidic condition, in this case slightly closer to the results at the other studied pHs (99%). Based on similar reported studies (Sun *et al.*, 2009; Elmorsi *et al.*, 2010; Liu *et al.*, 2011), the pH that maximizes the degradation rates ranges between 3 and 4. Moreover, those studies demonstrated the dye degradation appears to slow at very low pHs. According to Xu *et al.* (2004), pH < 2.5 increases the concentration of the ferrous hexaaqua complex, $[Fe(H_2O)_6]^{2+}$, which is less active than the $[Fe(OH)(H_2O)_5]^{+}$ complex towards the hydroxyl radicals generation. Therefore, the overall oxidation is retarded.

3.5. EE/O analysis

In order to estimate the cost-effectiveness with electricity of our oxidative system towards RB5 color removal, the electrical energy per order (EE/O) was calculated for the UV/H_2O_2 and photo-Fenton processes, and the results are presented in Table 4. EE/O is defined as the electric energy required to degrade one order of magnitude of the textile pollutant in one cubic meter of effluent, and it can be calculated according to the following Equation 9 (Nikravesh *et al.*, 2020).

$$\frac{EE}{O} = \frac{P.t.1000}{60.V.log\left(\frac{C_0}{C}\right)} \quad (9)$$

Where P is the power (kW) of UV lamp, V is the volume (L) of effluent, t is reaction time (min), C_0 and C are initial and final concentrations of RB5.

Table 4. EE/O for RB5 color removal by the UV/H_2O_2 and photo-Fenton processes ([H_2O_2] = 24.5 mg L^{-1}).

	EE/O (kWh m^{-3} $order^{-1}$)	
[RB5] (mg L^{-1})	UV/H_2O_2	Photo-Fenton
25	7.5	1.0
50	13.5	2.0
100	21.0	7.5

As expected, the photo-Fenton process with the highest ratio [oxidant]:[RB5] stands out as the most effective treatment in the matter of energy cost, with the lowest EE/O of 1.0 kWh m^{-3} $order^{-1}$. Additionally, Table 4 corroborates the crucial role played by ferrous ions on the degradation rates, since without them, in the UV/H_2O_2 treatment, the cost with electricity might be 7.5 times higher to achieve the same degradation degree, depending on the initial concentrations.

The EE/O was not reported for the experiments with the lowest oxidant dosage ([H_2O_2] = 2.45 mg L^{-1}), because with this initial condition, the processes were unable to reach 90% color removal within the total reaction time, as can be observed in Figure 4.

4. CONCLUSIONS

The presented work aimed to design and build a sustainable experimental apparatus for performing advanced oxidation processes (AOPs), adapting low-cost parts and recyclable materials. Several experiments were performed with this annular flow photo-reactor for color removal of dye RB5, using three types of AOP, namely UV-induced peroxidation, Fenton, and photo-Fenton process. The effect of the dye load and oxidant (H_2O_2) concentration on the degradation efficiency was evaluated. As expected, the combination of Fe^{2+} ions and UV photons to generate more hydroxyl radicals made the photo-Fenton process the most effective treatment, regardless of the set of initial concentrations. For instance, for the highest ratio [H_2O_2]:[RB5] (24.5 mg L^{-1}: 25 mg L^{-1}), the photo-Fenton was capable of bleaching entirely the dye solution within only 10 minutes, whereas the Fenton and UV/H_2O_2 processes required 25 min. and 45 min., respectively.

The pH study showed that the high decolorization efficiency by the photo-Fenton process was not impacted by switching the pH from 3 to 4. The most acidic condition (pH=2) slightly slowed down the degradation rate, although it can be considered high, with 86% of color removal achieved within only a 3 min. reaction. Naturally, from a cost-wise point of view, the pH of 4 should be chosen for further studies with photo-Fenton treatment, since closer pHs to neutral conditions allows lower acid-base consumption for appropriate treatment and disposal of the effluent.

It is crucial to point out that the lower the ratio [H_2O_2]:[RB5], the lower the degradation efficiency in all types of AOPs evaluated in this work. For the lowest ratio ([H_2O_2]:[RB5] = 2.45 mg L^{-1}: 100 mg L^{-1}), none of the treatments were capable of complete color removal. Even the photo-Fenton process only led to a degradation of roughly 47% after 45 minutes.

As long as the adequate oxidant concentration is set for a given pollutant load, those results demonstrated that the non-expensive photo-reactor, built in this work, proved to be a propitious system for textile effluent treatments. Especially when the photo-Fenton process is employed, notable decolorization rates were accomplished.

5. ACKNOWLEDGEMENTS

The authors would like to thank the Federal Institute for Education, Science and Technology (IFPE), Brazil, for financial support of this research.

6. REFERENCES

ABHILASHA, J.; ASHMA, A.; MARAZBAN, K. A greener approach for the degradation of dye methylene blue by organic additive catalyzed photo-Fenton process. **Journal of the Chilean Chemical Society**, v. 61, p. 3043-3048, 2016. http://dx.doi.org/10.4067/S0717-97072016000300007

AHMED, M. M.; CHIRON, S. Solar photo-Fenton like using persulphate for carbamazepine removal from domestic wastewater. **Water Research**, v. 48, p. 229-236, 2014. https://doi.org/10.1016/j.watres.2013.09.033

BALI, U.; KARAGÖZOGLU, B. Performance comparison of Fenton process, ferric coagulation and H_2O_2/pyridine/Cu(II) system for decolorization of Remazol Turquoise Blue G-133. **Dyes and Pigments**, v. 74, p. 73-80, 2007. https://doi.org/10.1016/j.dyepig.2006.01.013

BARKA, N.; QOURZAL, S.; ASSABBANE, A.; NOUNAH, A.; AIT-ICHOU, Y. Photocatalytic degradation of an azo reactive dye, Reactive Yellow 84, in water using an industrial titanium dioxide coated media. **Arabian Journal of Chemistry**, v. 3, p. 279-283, 2010. https://doi.org/10.1016/j.arabjc.2010.06.016

BASTURK, E.; KARATAS, M. Decolorization of antraquinone dye Reactive Blue 181 solution by UV/H_2O_2 process. **Journal of Photochemistry and Photobiology A: Chemistry**, v. 299, p. 67-72, 2015. https://doi.org/10.1016/j.jphotochem.2014.11.003

BEHNAJADY, M. A.; MODIRSHAHLA, N.; SHOKRI, M. Photodestruction of Acid Orange 7 (AO7) in aqueous solutions by UV/H_2O_2: influence of operational parameters. **Chemosphere**, v. 55, p. 129-134, 2004. https://doi.org/10.1016/j.chemosphere.2003.10.054

BELAYACHI, H.; BESTANI, B.; BENDERDOUCHE, N.; BELHAKEM, M. The use of TiO_2 immobilized into grape marc-based activated carbon for RB-5 Azo dye photocatalytic degradation. **Arabian Journal of Chemistry**, v. 12, p. 3018-3027, 2019. https://doi.org/10.1016/j.arabjc.2015.06.040

DÚRAN, A.; MONTEAGUDO, J. M.; SANMARTÍN, I.; CARRASCO, A. Solar photo-Fenton mineralization of antipyrine in aqueous solution. **Journal of Environmental Management**, v. 130, p. 64-71, 2013. https://doi.org/10.1016/j.jenvman.2013.08.043

ELMORSI, T. M.; RIYAD, Y. M.; MOHAMED, Z. H.; ABD EL BARY, M. H. Decolorization of Mordant red 73 azo dye using H_2O_2/UV and photo-Fenton treatment. **Journal of Hazardous Materials**, v. 174, p. 352-358, 2010. https://doi.org/10.1016/j.jhazmat.2009.09.057

FARRÉ, M. J.; DOMÉNECH, X.; PERAL, J. Assessment of photo-Fenton and biological treatment coupling for Diuron and Linuron removal from water. **Water Research**, v. 40, p. 2533-2540, 2006. https://doi.org/10.1016/j.watres.2006.04.034

FRAGOSO, C. T.; BATTISTI, R.; MIRANDA, C.; JESUS, P. C. Kinetic of the degradation of C.I. Food Yellow 3 and C.I. Food Yellow 4 azo dyes by the oxidation with hydrogen peroxide. **Journal of Molecular Catalysis A: Chemical,** v. 301, p. 93-97, 2009. https://doi.org/10.1016/j.molcata.2008.11.014

GLIGOROVSKI, S.; STREKOWSKI, R.; BARBATI, S.; VIONE, D. Environmental Implications of Hydroxyl Radicals (•OH). **Chemical Reviews**, v. 115, p. 13051-13092, 2015. https://doi.org/10.1021/cr500310b

GUIMARÃES, J. R.; MANIERO, M. G.; ARAÚJO, R. N. A comparative study on the degradation of RB-19 dye in an aqueous medium by advanced oxidation processes. **Journal of Environmental Management**, v. 110, p. 33-39, 2012. https://doi.org/10.1016/j.jenvman.2012.05.020

GUO, S.; YANG, Z.; WEN, Z.; FIDA, H.; ZHANG, G.; CHEN, J. Reutilization of iron sludge as heterogeneous Fenton catalyst for the degradation of rhodamine B: Role of sulfur and mesoporous structure. **Journal of Colloid Interface Science**, v. 532, p. 441-448, 2018. https://doi.org/10.1016/j.jcis.2018.08.005

GUTIERREZ-MATA, A. G.; VELAZQUEZ-MARTÍNEZ, S.; ÁLVAREZ-GALLEGOS, A.; AHMADI, M.; HERNÁNDEZ-PÉREZ, J. A.; GHANBARI, F.; SILVA-MARTÍNEZ, S. Recent overview of Solar Photocatalysis and Solar Photo-Fenton processes for wastewater treatment. **International Journal of Photoenergy**, p. 1-27, 2017. https://doi.org/10.1155/2017/8528063

HSUEH, C. L.; HUANG, Y. H.; WANG, C. C.; CHEN, C.Y. Degradation of azo dyes using low iron concentration of Fenton and Fenton-like system. **Chemosphere**, v. 58, p. 1409-1414, 2005. https://doi.org/10.1016/j.chemosphere.2004.09.091

IDEL-AOUAD, R.; VALIENTE, M.; YAACOUBI, A.; TANOUTTI, B.; LÓPEZ-MESAS, M. Rapid decolourization and mineralization of the azo dye C.I. Acid Red 14 by heterogeneous Fenton reaction. **Journal of Hazardous Materials**, v. 186, p. 745-750, 2011. https://doi.org/10.1016/j.jhazmat.2010.11.056

IOANNOU, L. A.; PUMA, G. L.; FATTA-KASSINOS, D. Treatment of winery wastewater by physicochemical, biological and advanced processes: A review. **Journal of Hazardous Materials**, v. 286, p. 343-368, 2015. https://doi.org/10.1016/j.jhazmat.2014.12.043

KHATAEE, A.; GHOLAMI, P.; SHEYDAEI, M. Heterogeneous Fenton process by natural pyrite for removal of a textile dye from water: Effect of parameters and intermediate identification. **Journal of Taiwan Institute of Chemical Engineers**, v. 58, p. 366-373, 2016. https://doi.org/10.1016/j.jtice.2015.06.015

LEITE, L. S.; MASELLI, B. S.; UMBUZEIRO, G. A.; NOGUEIRA, R. F. P. Monitoring ecotoxicity of dispersed red 1 dye during photo-Fenton degradation. **Chemosphere**, v. 148, p. 511-517, 2016. https://doi.org/10.1016/j.chemosphere.2016.01.053

LIU, X.; QIU, M.; HUANG, C. Degradation of the Reactive Black 5 by Fenton and Fenton-like system. **Procedia Engineering**, v. 15, p. 4835-4840, 2011. https://doi.org/10.1016/j.proeng.2011.08.902

LIZAMA, C.; FREER, J.; BAEZA, J.; MANSILLA, H. D. Optimized photodegradation of Reactive Blue 19 on TiO_2 and ZnO suspensions. **Catalysis Today**, v. 76, p. 235-246, 2002. https://doi.org/10.1016/S0920-5861(02)00222-5

MANAA, Z.; CHEBLI, D.; BOUGUETTOUCHA, A.; ATOUT, H.; AMRANE, A. Low-cost Photo-Fenton-Like Process for the Removal of Synthetic Dye in Aqueous Solution at Circumneutral pH. **Arabian Journal for Science and Engineering**, v. 44, p. 9859-9867, 2019. https://doi.org/10.1007/s13369-019-04101-4

MEHRDAD, A.; MASSOUMI, B.; HASHEMZADEH, R. Kinetic study of degradation of Rhodamine B in the presence of hydrogen peroxide and some metal oxide. **Chemical Engineering Journal**, v. 168, p. 1073-1078, 2011. https://doi.org/10.1016/j.cej.2011.01.087

MIAO, X.; DAI, H.; CHEN, J.; ZHU, J. The enhanced method of hydroxyl radical generation in the heterogeneous UV-Fenton system with α-FeOOH as catalyst. **Separation and Purification Technology**, v. 200, p. 36-43, 2018. https://doi.org/10.1016/j.seppur.2018.02.012

MITTERSTEINER, M.; BARBIERI, M. R.; COLZANI, J.; SCHARF, D. R.; JESUS, P. C.: Relationship between structure and catalyst effect in the degradation kinetics of reactive dyes with hydrogen peroxide: UV-light versus sodium hydroxide. **Journal of Molecular Liquids**, v. 299, p. 1-9, 2020. https://doi.org/10.1016/j.molliq.2019.112171

MÓDENES, A. N.; ESPINOZA-QUIÑONES, F. R.; MANENTI, D. R.; BORBA, F. H.; PALÁCIO, S. M.; COLOMBO, A. Performance evaluation of a photo-Fenton process applied to pollutant removal from textile effluents in a batch system. **Journal of Environmental Management**, v. 104, p. 1-8, 2012. https://doi.org/10.1016/j.jenvman.2012.03.032

MOFRAD, M. R.; NEZHAD, M. E.; AKBARI, H.; ATHARIZADE, M.; MIRANZADEH, M. B. Evaluation of Efficacy of Advanced Oxidation Processes Fenton, Fenton-like and Photo-Fenton Removal of Phenol from Aqueous Solutions. **Journal of the Chemical Society of Pakistan**, v. 37, 2015.

MONTEAGUDO, J. M.; DURÁN, A.; MARTÍN, I. S. Mineralization of wastewater from the pharmaceutical industry containing chloride ions by UV photolysis of H_2O_2/Fe(II) and ultrasonic irradiation. **Journal of Environmental Management**, v. 141, p. 61-69, 2014. https://doi.org/10.1016/j.jenvman.2014.03.020

MONTEAGUDO, J. M.; DURÁN, A.; SAN MARTÍN, I. Optimization of the mineralization of a mixture of phenolic pollutants under a ferroxialate-induced solar photo-Fenton process. **Journal of Hazardous Materials**, v. 185, p. 131-139, 2011. https://doi.org/10.1016/j.jhazmat.2010.09.007

NEAMTU, M.; YEDILER, A.; SIMINICEANU, I.; KETTRUP, A. Oxidation of commercial reactive azo dye aqueous solutions by the photo-Fenton and Fenton-like processes. **Journal of Photochemistry and Photobiology A: Chemistry**, v. 161, p. 87-93, 2003. https://doi.org/10.1016/S1010-6030(03)00270-3

NEYENS, E.; BAEYENS, J. A review of classic Fenton´s peroxidation as an advanced oxidation technique. **Journal of Hazardous Materials**, v. 98, p. 33-50, 2003. https://doi.org/10.1016/S0304-3894(02)00282-0

NIKRAVESH, B.; SHOMALNASAB, A.; NAYYER, A.; AGHABABAEI, N. UV/Chlorine process for dye degradation in aqueous solution: Mechanism, affecting factors and toxicity evaluation for textile wastewater. **Journal Environmental Chemical Engineering,** v. 8, p. 1-10, 2020. https://doi.org/10.1016/j.jece.2020.104244

PIGNATELLO, J. J.; OLIVEROS, E.; MACKAY, A. Advanced Oxidation Processes for Organic Contaminant Destruction Based on the Fenton Reaction and Related Chemistry. **Critical Reviews in Environmental Science and Technology**, v. 36, p. 1-84, 2006. https://doi.org/10.1080/10643380500326564

POURAN, S. R.; AZIZ, A. R. A.; DAUD, W. M. A. W. Review on the main advances in photo-Fenton oxidation system for recalcitrant wastewaters. **Journal of Industrial and Engineering Chemistry**, v. 21, p. 53-69, 2015. https://doi.org/10.1016/j.jiec.2014.05.005

RUBEENA, K. K.; REDDY, H. P.; LAIJU, A. R.; NIDHEESH, P. V. Iron impregnated biochars as heterogeneous Fenton catalyst for the degradation of acid red 1 dye. **Journal of Environmental Management,** v. 226, p. 320-328, 2018. https://doi.org/10.1016/j.jenvman.2018.08.055

SHU, H.; CHANG, M. Decolorization and mineralization of a phthalocyanine dye C.I. Direct Blue 199 using UV/H_2O_2 process. J**ournal of Hazardous Materials B,** v. 125, p. 96-101, 2005. https://doi.org/10.1016/j.jhazmat.2005.05.016

SHUAI, W.; LIU, C.; WANG, Y.; ZHU, F.; ZHOU, D.; GAO, J. (Fe^{3+})-UVC-(aliphatic/phenolic carboxyl acids) systems for diethyl phthalate ester degradation: A density functional theory (DFT) and experimental study. **Applied Catalysis A, General**, v. 567, p. 20-27, 2018. https://doi.org/10.1016/j.apcata.2018.09.007

SILVA, L. C.; NETO, B. B.; SILVA, V. L. Homogeneous degradation of the Remazol Black B dye by Fenton and photo-Fenton processes in aqueous medium. **Afinidad LXVI**, v. 541, p. 232-237 2009.

STARLING, M. C. V. M.; CASTRO, L. A. S.; MARCELINO, R. B. P.; LEÃO, M. M. D.; AMORIM, C. C. Optimized treatment conditions for textile wastewater reuse using photocatalytic processes under UV and visible light sources. **Environmental Science and Pollution Research,** v. 24, p. 6222-6232, 2017. https://doi.org/10.1007/s11356-016-6157-8

SUN, J.; SHI, S.; LEE, Y.; SUN, S. Fenton oxidative decolorization of the azo dye Direct Blue 15 in aqueous solution. **Chemical Engineering Journal**, v. 155, p. 680-683, 2009. https://doi.org/10.1016/j.cej.2009.08.027

SUN, J.; YAN, X.; LV, K.; SUN, S.; DENG, K.; DU, D. Photocatalytic degradation pathway for azo dye in TiO_2/UV/O_3 system: Hydroxyl radical versus hole. **Journal of Molecular Catalysis A: Chemical**, v. 367, p. 31-37, 2013. https://doi.org/10.1016/j.molcata.2012.10.020

TROVÓ, A. G.; NOGUEIRA, R. F. P.; AGÜERA, A.; FERNANDEZ-ALBA, A. R.; MALATO, S. Paracetamol degradation intermediates and toxicity during photo-Fenton treatment using different iron species. **Water Research**, v. 46, p. 5374-5380, 2012. https://doi.org/10.1016/j.watres.2012.07.015

TZANOV, T.; COSTA, S. A.; GÜBITZ, G. M.; CAVACO-PAULO, A. Hydrogen peroxide Generation with immobilized glucose oxidase for textile bleaching. **Journal of Biotechnology**, v. 93, p. 87-94, 2002. https://doi.org/10.1016/S0168-1656(01)00386-8

VEDRENNE, M.; VASQUEZ-MEDRANO, R.; PRATO-GARCIA, D.; FRONTANA-URIBE, B. A.; HERNANDEZ-ESPARZA, M.; ANDRÉS, J. M. A ferrous oxalate mediated photo-Fenton system: Toward an increased biodegradability of indigo dyed wastewaters. **Journal of Hazardous Materials,** v. 243, p. 292-301, 2012. https://doi.org/10.1016/j.jhazmat.2012.10.032

VORONTSOV, A. V. Advancing Fenton and photo-Fenton water treatment through the catalyst design. **Journal of Hazardous Materials**, v. 372, p. 103-112, 2019. https://doi.org/10.1016/j.jhazmat.2018.04.033

XU, X. R.; ZHAO, Z. Y.; LI, X. Y., GU, J. D. Chemical oxidative degradation of methyl tert-butyl ether in aqueous solution by Fenton´s reagent. **Chemosphere,** v.55, p. 73-79, 2004. https://doi.org/10.1016/j.chemosphere.2003.11.017

YU, C.; WU, C.; HO, T.; HONG, P. K. A. Decolorization of C.I. Reactive Black 5 in UV/TiO_2, UV/oxidant and UV/TiO_2/oxidant systems: A comparative study. **Chemical Engineering Journal**, v. 158, p. 578-583, 2010. https://doi.org/10.1016/j.cej.2010.02.001

ZHANG, Y.; PAGILLA, K. Treatment of malathion pesticide wastewater with nanofiltration and photo-Fenton oxidation. **Desalination**, v. 263, p. 36-44, 2010. https://doi.org/10.1016/j.desal.2010.06.031

Ambiente & Água - An Interdisciplinary Journal of Applied Science
ISSN 1980-993X – doi:10.4136/1980-993X
www.ambi-agua.net
E-mail: ambi.agua@gmail.com

Removal of nutrients due to biomass harvest of *Eucalyptus urograndis* in different soils: macronutrients

ARTICLES doi:10.4136/ambi-agua.2671

Received: 09 Nov. 2020; Accepted: 12 Apr. 2021

Simone Martini Salvador[1]; Aline Aparecida Ludvichak[1]; Dione Richer Momolli[1]; Kristiana Fiorentin dos Santos[2*]; Catarine Barcellos Consensa[1]; Mauro Valdir Schumacher[1]; James Stahl[3]

[1]Departamento de Engenharia Florestal. Universidade Federal de Santa Maria (UFSM), Avenida Roraima, n° 1000, CEP: 97105-900, Santa Maria, RS, Brazil. E-mail: simone.ufsm@gmail.com, aline_lud@yahoo.com.br, dionemomolli@gmail.com, catarineconsensa@gmail.com, mauro.schumacher@ufsm.br
[2]Departamento de Engenharia Florestal. Universidade Regional de Blumenau (FURB), Rua São Paulo, n° 3250, CEP: 89030-000, Blumenau, SC, Brazil.
[3]Klabin S. A., Unidade de Monte Alegre, Avenida Brasil, n° 26, CEP: 84275-000, Telêmaco Borba, PR, Brazil. E-mail: jstahl@klabin.com.br
[*]Corresponding author. E-mail: kristianafiorentin@gmail.com

ABSTRACT

Intensive management of forest stands can increase biomass production, as well as increase the removal of nutrients from the site. This study therefore sought to simulate different harvest intensities and to calculate the nutrient-use efficiency of *Eucalyptus urograndis* in different types of soil. The study was carried out in a plantation of seven-year-old hybrid *E. urograndis* in the city of Telêmaco Borba, Paraná, Brazil. The study site included two sub areas with sandy soil and clayey soil (Cambisols Inceptisol and Ferralsols Oxisols, respectively). Using biomass and nutrients stock data, nutrient removal was simulated under five different harvest scenarios. Nutrient-use efficiency was obtained from the relation between the amount of biomass and nutrients of each tree component. Harvesting the whole tree resulted in the removal of approximately 61% of the nutrients from the site in sandy soil, while in clayey soil 57% of the nutrients were removed. With harvesting of only the commercial stemwood, only 22% of the nutrients were removed from the sandy soil, and 21% from the clayey soil. Stemwood was the component that had the highest nutrient-use efficiency values for all the analyzed nutrients. In conclusion, to achieve nutritional sustainability of *E. urograndis* stands, the best harvesting system involves the removal of only commercial stemwood. For the production of stemwood, sandy soils have a greater biological efficiency of calcium and magnesium when compared to clayey soil.

Keywords: clayey soil, forest nutrition, harvest intensity, nutrient use efficiency, sandy soil.

Remoção de nutrientes pela colheita de biomassa de *Eucalyptus urograndis* em diferentes tipos solos: macronutrientes

RESUMO

O manejo intensivo de povoamentos florestais pode aumentar a produção de biomassa, bem como aumentar a remoção de nutrientes do local. Assim, o objetivo deste estudo foi simular

This is an Open Access article distributed under the terms of the Creative Commons Attribution License, which permits unrestricted use, distribution, and reproduction in any medium, provided the original work is properly cited.

diferentes intensidades de colheita e calcular a eficiência de utilização de nutrientes para Euc*alyptus urograndis* em diferentes tipos de solo. O estudo foi realizado em um plantio do híbrido *E. urograndis* de sete anos de idade, no município de Telêmaco Borba, Paraná, Brasil. O local de estudo incluiu duas subáreas com solo arenoso e solo argiloso (Cambissolo Háplico e Latossolo Vermelho, respectivamente). Com os dados de estoque de biomassa e nutrientes foi simulada a remoção de nutrientes em cinco cenários de colheita diferentes. A eficiência de utilização de nutrientes foi obtida a partir da relação entre a quantidade de biomassa e os nutrientes de cada componente da árvore. A colheita da árvore inteira resultou na retirada de aproximadamente 61% dos nutrientes do local em solo arenoso, enquanto em solo argiloso, 57% dos nutrientes foram removidos. Com a colheita apenas da madeira do fuste comercial, apenas 22% dos nutrientes foram retirados do solo arenoso e 21% do solo argiloso. A madeira do caule foi o componente que apresentou os maiores valores da eficiência de utilização de nutrientes para todos os nutrientes analisados. Para alcançar a sustentabilidade nutricional dos povoamentos de *E. urograndis*, o melhor sistema de colheita envolve a remoção apenas da madeira do tronco comercial. Para a produção de madeira, os solos arenosos apresentam maior eficiência biológica de cálcio e magnésio quando comparados aos solos argilosos.

Palavras-chave: eficiência de utilização de nutrientes, intensidade de colheita, nutrição florestal, solo arenoso, solo argiloso.

1. INTRODUCTION

Use of renewable energy was boosted by the oil crisis in the 1970s, increasing the demand for energy biomass, which led to the search for available waste after forest harvesting operations (Egnell, 2017). However, intensively managed forest stands can increase biomass production, but may also increase the removal of nutrients from the site (Viera *et al*., 2011).

In the case of energetic biomass, the adopted management can involve harvesting all parts of the tree, including the roots, and, in extreme cases, the removal of accumulated litter and understory (Viera *et al*., 2015). Viera *et al*., (2013) emphasize that intensively managed plantations with the use of short rotations, without predicting a minimum period required for nutrient replacement, have been found to be the main reason for the chemical exhaustion of soils. However, for long-term forest management, knowledge of the relationships between the amount of nutrients removed by harvests and the bioavailability of nutrients at the site is imperative in order to achieve sustainable energy standards under various rotations (Santana *et al*., 2008).

New plantations have been implanted into different types of soils and climatic and management conditions (Kumaraswamy *et al*., 2015). There are differences between plantations and natural ecosystems, which are self-sustainable. Natural ecosystems are able to maintain their productivity and nutrient dynamics. However, forest plantations are a diversified form of land use, and in order to develop plantations that do not have significant negative impacts on the ecosystem, plantations need to be in harmony with the ecological properties of their environment.

In this context, knowledge about the growth and nutrient allocation to the different biomass components of trees is essential for crop optimization and the nutritional management of plantations (Schumacher *et al.*, 2011; Yan *et al*., 2017), because the removal of nutrients in the harvest depends on the productivity of the stands and the concentrations of nutrients in the components of biomass (Silva *et al*., 2013).

The effects of harvesting for forest management are mainly related to the collection system adopted; but other factors, such as climate, soil type, and topography, may also be important (Olsson *et al*., 2017). The research hypothesis is that the removal of nutrients will occur more

intensely in the site with sandy soil and this will result in a reduced number of rotations when compared to clayey soil. With the development of new hybrids and genotypes, it is essential to assess their performance under different edaphoclimatic conditions. The region of the present study does not have a historical silvicultural tradition. Considering this aspect, few studies evaluating the removal of nutrients in different scenarios of harvest and soil texture have been published. The objective of this study was to estimate the removal of macronutrients simulating different harvest intensities and to calculate the nutrient-use efficiency of nutrients in hybrid eucalyptus stands on different soil types.

2. MATERIAL AND METHODS

2.1. Characterization of the experimental area

The study was carried out in stands of seven-year-old hybrid *Eucalyptus urograndis* (*Eucalyptus grandis* Hill ex Maiden x *Eucalyptus urophylla* S.T. Blake) at Farm Monte Alegre in the municipality of Telêmaco Borba, Paraná, Brazil. The climate of the region is characterized as Cfa, according to the climatic classification of Köppen. The average annual temperature is approximately 18.6°C and the average annual precipitation reaches 1,443 mm (Alvares *et al.*, 2013).

Within this study site, subareas with two distinct soil types were chosen. The first subarea had soil with a sandy texture (Cambisols Inceptisols), and the second had soil with a clayey texture (Ferralsols Oxisols). The determination of the physical and chemical attributes of the soil were carried out with the collection of 3 samples in each plot, totaling 12 samples per soil type, in the depths of 0 - 20 cm, 20 - 40 cm and 40 - 60 cm (Table 1).

In each soil type, four sample plots of 2,550 m^2 were plotted, with tree spacing of 3.0 m x 2.5 m, composed of 340 plants. The planting was done manually, with a spacing of 3.0 m x 2.5 m and an initial density of 1,333 plants per hectare. For the planting, a soil subsoiling was carried out in the planting line, with a depth of 45 cm, where a dosage of 200 kg ha^{-1} of natural rock phosphate was incorporated. After the planting, two other fertilizations were carried out; the first was basic fertilization with 15 kg ha^{-1} of nitrogen, 35 kg ha^{-1} of phosphor, 15 kg ha^{-1} of potassium, and the second was cover fertilization with 40 kg ha^{-1} of nitrogen, 5 kg ha^{-1} of phosphor, 65 kg ha^{-1} of potassium + 1,5 kg ha^{-1} of boron.

2.2. Biomass and nutrients

Based on the diameter at breast-height (DBH) survey of all the trees present in the plots, 12 trees were selected in each plot for the determination of the above-ground biomass (leaves, branches, stembark and stemwood) through the destructive method, thus totaling in each type of soil. The biomass of the roots was analyzed from the selection of four medium DBH trees in each soil type. The root system (stump, fine roots < 2 mm, medium roots of 2.1 to 10 mm, and large roots > 10 mm) was extracted using a backhoe and manual excavation (shovels and spades), in an area of 7.5 m^2 surrounding the tree (according to spacing) to the depth of 1 m.

In order to evaluate the understory (all naturally occurring vegetation, native or exotic) were collected all the biomass contained within the useful area (7 m^2) of each sectioned tree for the sampling of the tree biomass, thus totaling 12 samples in each soil type, from which the average diameter tree minus a standard deviation, the average diameter tree and the average diameter tree plus one were selected. standard deviation. The evaluation of litter on the soil was carried out through the collection of 10 samples in an area of 30 cm x 30 cm distributed randomly within each plot, totaling 40 samples in each soil type.

The selected trees were sectioned at ground level and divided into the following components: leaves, branches, stembark, stemwood and roots. The amount of green biomass in these components of the tree was determined by means of weighing with a hook scale in the field.

Table 1. Chemical and physical attributes of distinct soils planted with *E. urograndis* in the region of Telêmaco Borba, Paraná, Brazil.

Attribute	Sandy			Clayey		
	0-20 cm	20-40 cm	40-60 cm	0-20 cm	20-40 cm	40-60 cm
Organic matter (%)	1.79 (0.14)	1.32 (0.22)	1.42 (0.43)	3.39 (0.12)	2.45 (0.15)	1.72 (0.05)
pH (H_2O)	3.97 (0.07)	3.97 (0.10)	3.95 (0.02)	3.98 (0.04)	4.19 (0.04)	4.41 (0.01)
P* (mg dm^{-3})	1.61 (0.18)	1.12 (0.13)	0.89 (0.31)	0.86 (0.20)	0.68 (0.20)	0.68 (0.04)
K* (mg dm^{-3})	30.92 (1.48)	20.08 (1.73)	35.11 (7.71)	45.04 (1.16)	32.59 (1.28)	27.63 (0.26)
S (mg dm^{-3})	9.08 (1.58)	10.28 (2.04)	13.03 (2.02)	26.13 (2.33)	23.36 (2.41)	11.26 (3.90)
B (mg dm^{-3})	0.55 (0.03)	0.63 (0.06)	0.67 (0.05)	0.61 (0.07)	0.61 (0.08)	0.56 (0.08)
Cu (mg dm^{-3})	1.25 (0.27)	1.22 (0.29)	1.19 (0.23)	2.65 (0.14)	2.06 (0.20)	1.40 (0.09)
Zn (mg dm^{-3})	0.54 (0.07)	0.48 (0.11)	0.43 (0.09)	0.58 (0.12)	0.25 (0.01)	0.19 (0.02)
Ca ($cmol_c$ dm^{-3})	0.09 (0.02)	0.06 (0.01)	0.06 (0.01)	0.18 (0.05)	0.05 (0.01)	0.03 (0.01)
Mg ($cmol_c$ dm^{-3})	0.07 (0.01)	0.05 (0.01)	0.05 (0.01)	0.45 (0.06)	0.11 (0.02)	0.03 (0.01)
Effective cation exchange capacity ($cmol_c$ dm^{-3})	2.30 (0.33)	2.41 (0.16)	2.47 (0.15)	3.72 (0.17)	2.85 (0.18)	2.29 (0.07)
Saturation per exchangeable base (%)	2.54 (0.59)	1.53 (0.40)	2.68 (0.55)	2.89 (0.40)	1.00 (0.08)	0.75 (0.10)
Exchangeable aluminum saturation (%)	89.92 (2.79)	96.19 (0.87)	93.36 (1.52)	80.02 (1.99)	91.76 (0.37)	94.25 (0.77)
Coarse sand: 2.0 - 0.2 mm (%)	39.89 (6.41)	40.33 (4.07)	40.72 (3.88)	14.68 (2.77)	16.51 (0.59)	16.18 (0.97)
Fine sand: 2.0 - 0.05 mm (%)	40.36 (7.24)	40.50 (3.83)	37.05 (4.96)	6.87 (2.24)	5.79 (1.80)	6.73 (0.66)
Silt: 0.05 - 0.002 mm (%)	4.19 (0.27)	2.11 (0.63)	3.67 (0.81)	28.23 (1.94)	31.48 (2.78)	26.87 (1.09)
Clay: < 0.002 mm (%)	15.56 (1.29)	17.06 (1.26)	18.56 (1.41)	50.22 (1.50)	46.22 (1.26)	50.22 (0.96)

*Determination of nutrients using the Mehlich^{-1} extractor (HCI + H_2SO_4). P: Phosphorus determined by atomic absorption spectrophotometry (660 nm); K: Potassium determined by flame photometry; S: Sulfur extracted with Ca $(H_2PO_4)_2$ and determined by turbidimetry (440 nm); B: Boron extracted with curcumin and determined by spectrophotometry (460 nm); Cu: Copper and Zn: Zinc extracted with HCL (0.1 mol L^{-1}) and determined by spectrophotometry atomic absorption (324.75 and 213.86 nm, respectively); Ca: Calcium and Mg: Magnesium, extracted with KCL (1.0 mol L^{-1}) and determined by spectrophotometry atomic absorption (422.70 and 285.20 nm, respectively); ECEC= Effective Cation Exchange Capacity. Values in parentheses represent the standard errors.

Representative samples were collected of each component of the biomass of trees, with the exception of stembark and stemwood, which were obtained by 4-cm-thick wooden discs (bark and wood) in the following positions depending on commercial height: base, 25%, 50%, 75%, 100% and tree tops, being considered the fraction of 100% (minimum diameter of 8 cm).

After being weighed in the field, the samples were sent to the laboratory to be dried in an air-circulating oven at 70ºC for 72 hours. Dried samples were subsequently milled in a Wiley-type mill, followed by chemical analysis to determine the macronutrients according to Tedesco *et al*. (1995) and Miyazawa *et al.* (2009). Sulfuric digestion (H_2SO_4 + H_2O_2) was used for the determination of nitrogen through the Kjeldahl method, nitric-perchloric digestion (HNO_3 + $HClO_4$ - [3:1]) for determination Ca (422.67 nm), Mg (285.21nm), with atomic absorption spectrophotometry, K with flame photometry, P (660.00 nm) with spectrophotometry and S (420.00 nm) by turbidimetry.

The total tree biomass per hectare was determined based on the dry weight of each sample multiplied by the total wet biomass of each component of the tree, which was extrapolated based on the number of trees in one hectare. In the case of the understory and litter, the estimate was made by extrapolation of the sample area. For the estimation of the total amount of macronutrient, we computed the product between the nutrient content and the dry biomass for each component. A detailed description of the methodology adopted for biomass determination can also be found in Salvador *et al.* (2015).

2.3. Simulation of harvest intensities

Estimation of nutrient removal was calculated considering the accumulated amount in the biomass and the outputs under five simulations of harvest intensities, with the commercial stemwood being considered with a minimum diameter of 8 cm, as follows:

1st simulation - Whole tree = harvest of whole biomass tree (stemwood with stembark, tree tops, leaves, branches and roots, leaving understory and litter);

2nd simulation - Full tree = harvest aboveground biomass (stemwood with stembark, tree tops, leaves and branches, leaving roots, understory and litter);

3rd simulation - Harvest of the stemwood with stembark and tree tops (leaving leaves, branches, roots, understory and litter);

4th simulation - Harvest of the commercial stemwood with stembark (leaving tree tops, leaves, branches, roots, understory and litter);

5th simulation - Harvest of the commercial stemwood (leaving stembark, leaves, branches, tree tops, roots, understory and litter).

2.4. Potential number of rotations and rate of nutrient removal

The calculation of the potential number of rotation (PNR) for seven-year-old *E. urograndis* was performed using the ratio of the amount of nutrients remaining at the site (kg) to the amount of nutrients removed from the site (kg) according to the different harvest intensities for both types of soil (Equation 1).

$$PNR = \frac{(Amount\ of\ nutrient\ remaining\ after\ harvest\ in\ kg\ ha^{-1})}{(Amount\ of\ nutrient\ harvested\ in\ kg\ ha^{-1})} \quad (1)$$

The nutrient removal rate (NRR) was obtained by the ratio between the amount of nutrients (kg) removed with the harvest and the amount of biomass harvested (Mg) for each harvest intensity in the two types of soil (Equation 2).

$$NRR = \frac{(Amount\ of\ nutrient\ harvested\ in\ kg\ ha^{-1})}{(Biomass\ harvested\ in\ Mg\ ha^{-1})} \quad (2)$$

2.5. Nutrient-use efficiency

The nutrient-use efficiency was obtained according to a calculation proposed by Barros

et al. (1986) using the relation between the amount of biomass and the amount of nutrients of each component, both with the same unit (Equation 3).

$$NRR = \frac{(Amount\ of\ biomass\ in\ Mg\ ha^{-1})}{(Amount\ of\ nutrient\ in\ Mg\ ha^{-1})} \quad (3)$$

2.6. Statistical analysis

The data were plotted in box plots for the identification and exclusion of outliers. After, Shapiro-Wilk (to prove the normality of the data) were applied as assumptions to the use of analysis of variance. Results that did not meet the assumptions were transformed by applying the natural logarithm or Box Cox. The amount of nutrients and nutrient-use efficiency were subjected to analysis of variance (ANOVA) for comparison of means, between the same components, in different soil types ($P < 0.05$).

3. RESULTS AND DISCUSSION

3.1. Harvest simulation based on different harvesting intensities

Quantification of the nutrients in different soil types is essential to be able to establish sustainable harvest systems. Sandy soil had greater amounts of nutrients in the treetop wood when compared to clayey soil, with the exception of calcium and sulfur, which were not significant (Table 2). However, the clayey soil had a higher biomass and amount of nutrients than the sandy soil, except for sulfur. Harvesting tree tops in sandy soils can significantly increase nutrient exports when compared to harvesting this component in clayey soils.

Table 2. Amounts of nutrients available in biomass and soil in stands of seven-year-old *E. urograndis* in sandy and clayey soils in the region of Telêmaco Borba, Paraná, Brazil.

Solo	Component	Biomass	N	P	K	Ca	Mg	S
		Mg ha^{-1}	kg ha^{-1}					
Sandy	Leaves	2.61^{ns*}	52.73^{ns}	2.90^{ns}	28.15^{ns}	11.06^{b}	6.20^{ns}	2.40^{ns}
	Branches	6.95^{ns}	19.81^{b}	1.81^{ns}	33.65^{ns}	18.57^{b}	5.16^{ns}	2.64^{ns}
	Tree tops bark	1.42^{ns}	5.99^{ns}	1.04^{ns}	8.92^{ns}	12.06^{a}	4.12^{ns}	0.33^{ns}
	Tree tops wood	12.42^{ns}	27.56^{a}	2.44^{a}	42.28^{a}	6.07^{ns}	4.89^{a}	3.84^{ns}
	Stembark	12.07^{ns}	46.23^{ns}	6.44^{ns}	115.19^{ns}	100.67^{ns}	28.31^{ns}	4.84^{ns}
	Stemwood	180.26^{ns}	186.18^{ns}	12.02^{ns}	169.22^{ns}	87.37^{ns}	22.44^{ns}	40.45^{ns}
	Roots	43.05^{ns}	166.39^{ns}	7.78^{ns}	63.57^{b}	57.30^{b}	24.11^{b}	17.98^{a}
	Understore	1.08^{ns}	8.17^{ns}	0.72^{ns}	10.19^{ns}	2.61^{ns}	1.55^{ns}	0.92^{ns}
	Litter	17.35^{b}	142.29^{b}	5.59^{b}	23.09^{b}	96.52^{b}	28.77^{b}	11.89^{a}
	Soil	--	222.96^{ns}	7.24^{ns}	172.22^{ns}	84.17^{ns}	41.34^{ns}	64.78^{ns}
Clayey	Leaves	4.01^{ns}	88.98^{ns}	4.82^{ns}	46.44^{ns}	25.07^{a}	11.08^{ns}	4.18^{ns}
	Branches	11.44^{ns}	41.35^{a}	4.05^{ns}	42.30^{ns}	98.25^{a}	12.04^{ns}	2.87^{ns}
	Tree tops bark	1.28^{ns}	5.55^{ns}	1.21^{ns}	7.35^{ns}	9.28^{b}	5.91^{ns}	0.38^{ns}
	Tree tops wood	12.52^{ns}	16.86^{b}	1.44^{b}	19.07^{b}	8.25^{ns}	2.99^{b}	3.06^{ns}
	Stembark	12.58^{ns}	46.96^{ns}	5.98^{ns}	90.60^{ns}	157.94^{ns}	37.61^{ns}	3.49^{ns}
	Stemwood	211.21^{ns}	213.66^{ns}	13.30^{ns}	218.63^{ns}	132.86^{ns}	39.27^{ns}	52.50^{ns}
	Roots	36.95^{ns}	137.57^{ns}	8.64^{ns}	149.60^{a}	87.59^{a}	40.32^{a}	9.63^{b}
	Understore	0.65^{ns}	10.68^{ns}	0.60^{ns}	6.37^{ns}	2.42^{ns}	1.50^{ns}	1.48^{ns}
	Litter	20.93^{a}	169.12^{a}	6.42^{a}	29.31^{a}	165.11^{a}	41.61^{a}	9.70^{b}
	Soil	--	377.89^{ns}	4.44^{ns}	210.52^{ns}	104.21^{ns}	143.44^{ns}	121.50^{ns}

[*]Mean of each component in the different soil types followed by ns, did not differ significantly at the level of 5% error.
Source: Salvador *et al.* (2019).

Each element should be analyzed based on the nutrients of the amount in the different components and as amount removed at harvest for reposition. Such importance is evident when observing that the leaves, in spite of presenting low biomass production, have high amounts of nutrients, mainly nitrogen, and the same analysis is valid for calcium in the stembark.

The harvesting only of stem (third simulation), a system adopted by large companies to exploit the stembark and tree tops (wood and bark) as an energy source and stemwood for cellulose production, resulted in the removal of more than 43-50% of the total phosphor, calcium and potassium in sandy soil. However, in clayey soil, this harvesting system resulted in the removal of 39-43% of phosphorus, potassium and calcium (Figure 1). Not harvesting the stembark can mitigate the effects of biomass harvest on soil fertility. Corroborating this result, Achat *et al*. (2015), after studying different biomass harvesting systems, found that harvesting only the stemwood was able to reduce the loss of calcium by 56%. Santos *et al*. (2020), evaluating the estimation the of nutrient export in different eucalypts genotypes in southern Brazil, observed that the harvesting only the stemwood maintained Ca in the other biomass components, which varied from 71 to 82% (*E. dunnii* and *E. benthamii* (P1)). In contrast, considering the harvest of the wood with the stem bark, the permanence of the same nutrient in the area reduces to 26 to 37% (*E. benthamii* (P2) and *E. uro globulus*). Therefore, when removing the trunk, debarking of the trees in the stands should be carried out to reduce the export of Ca. In this way, soils with lower concentrations of this nutrient could have their productivity preserved for a longer period (Santos *et al*., 2019a).

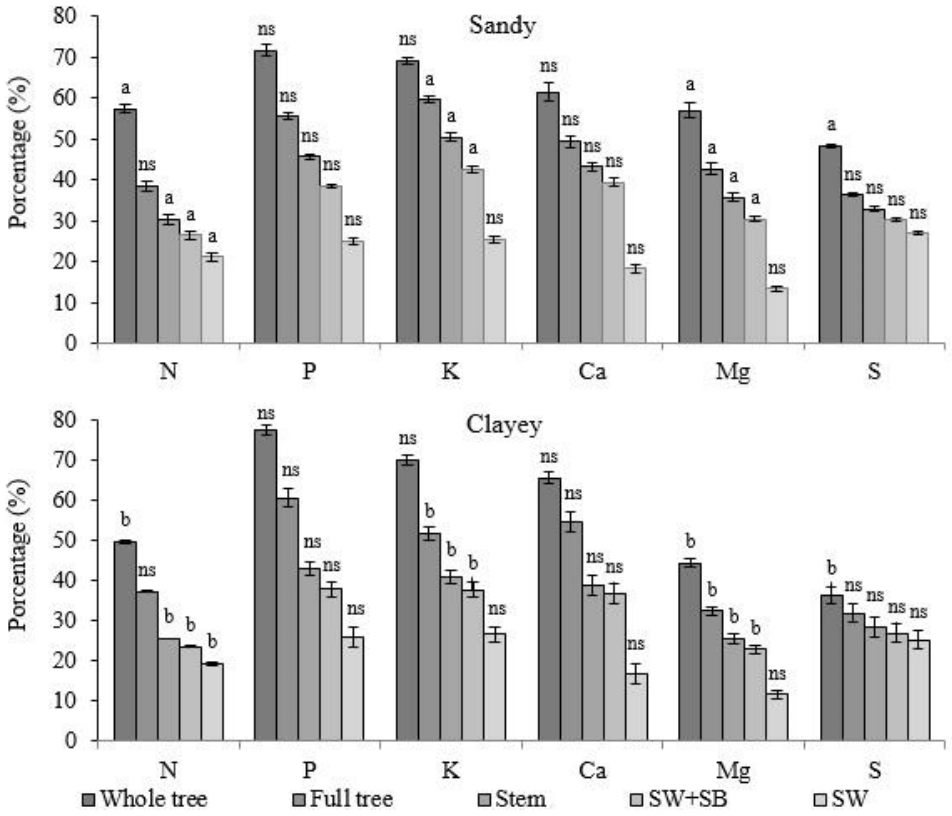

Figure 1. Removal of nutrients at different harvest intensities of seven-year-old *E. urograndis* in sandy and clayey soils in the region of Telêmaco Borba, Paraná, Brazil.

Whole tree: harvest of whole biomass tree; Full tree: harvest above ground biomass; Stem: harvest of stemwood with stembark; SW+SB: commercial stemwood with stembark; SW: commercial stemwood. *Mean of each harvest's intensities in the different soil types, followed by ns, did not differ significantly at the level of 5% error.

Considering the fourth harvesting system (SW+SB without tree tops, leaves, branches, roots, understory and litter) in sandy site, nutrient removal reached 43% for potassium, 39% for calcium and 38% for phosphor, resulting in a decrease in nutrient loss of 26, 23 and 34%, respectively, compared to the first harvesting system. For the clayey soil, this harvesting system resulted in a higher phosphor, potassium and calcium removal (38%, 38% and 37%, respectively), and a lower removal of magnesium (23%) (Figure 1).

In a study on nutrient removal rates under different harvesting intensities of the biomass of *E. urophylla* x *E. globulus*, Viera *et al*. (2015) observed that harvesting the stembark resulted in a removal of more than 47% of the total aboveground accumulated biomass for all macronutrients, with less than 35% of the stemwood being harvested. As such, it was observed that a biomass harvest of the whole tree resulted in greater removal of nutrients from the site.

In the fifth harvesting system (SW), considering only the removal of commercial stemwood, nutrient exports in the sandy soil would not exceed 27% for s sulfur and lower than that for the other macronutrients. However, for clayey soil, the maximum nutrient removal was found to be 27% for potassium and the minimum was found to be 12% for magnesium (Figure 1).

Under the first harvesting system, 48-72% and 36-77% of the nutrients were removed for sandy and clayey soils, respectively. Under the second harvesting system, this was 36-60% for the sandy soil and 32-61% for the clayey soil. Under the fifth harvesting system, nutrient removal was limited to 27% in sandy soils (sulfur) and 27% (potassium) in clayey soils, on average 39% and 36% less than under the first harvesting system, respectively. As such, we recommend using the third harvest system, which includes the only removal of the stemwood, as this is the most sustainable for the site, and will result in the best nutritional conditions for subsequent rotations.

A study by Witschoreck (2008) reported that some of the lost nutrients can be replenished through the application of fertilizers, but the nutrients that can be replenished are usually limited to the triad of elements nitrogen, phosphorus and potassium. Given the distribution of biomass and nutrients in each component of the trees, it is possible to evaluate these during the development of the stand and crop, as this information can be useful for the future maintenance of the site.

In general, for all harvesting systems, the sandy soil presented a higher percentage of removal of nitrogen, potassium and magnesium and sulfur (on average 35%, 49%, 36% and 35%, respectively). The clayey soil has greater phosphorus removal, an average of 49% among all harvesting systems. This result confirms our hypothesis that sandy soils would present the greatest removal of nutrients by the eucalyptus harvest. Sandy soils naturally present a low capacity for cation exchange, thus presenting the largest stock of nutrients in the eucalyptus biomass in this system. With the harvest, the nutritional impact on this soil is greater than on clay soils.

3.2. Potential number of rotations and rate of nutrient removal

Considering an average of all the macronutrients for commercial stemwood harvesting (SW) results in an increase in the number of rotations 5.8 times greater than the whole tree harvest for the sandy soil and 4.8 times for the clayey soil (Table 3). Comparing the number of rotations between SW + SB and SE, the calcium increases by 2.9 times the number of rotations in the SW for both types of soil (Table 3).

The first harvesting system (whole tree) allows one more rotation only for sulfur, while the clay soil, in this harvesting system, would support another rotation for nitrogen, magnesium and sulfur. Considering only the stemwood harvest (SW), phosphor, potassium and sulfur are the ones that most limit the growth of the next rotations (Table 3).

Table 3. Estimation of the potential number of rotations based on the amount of nutrients in the biomass and available in the soil, and the nutrient removal rates according to the harvest intensity of *E. urograndis* biomass, at seven years old in sandy and clayey soils in the region of Telêmaco Borba, Paraná, Brazil.

Harvest intensities	Sandy						Clayey					
	N	P	K	Ca	Mg	S	N	P	K	Ca	Mg	S
Whole tree	0.74^{b*}	0.39^{ns}	0.45^{ns}	0.63^{ns}	0.75^{b}	1.07^{b}	1.01^{a}	0.29^{ns}	0.43^{ns}	0.52^{ns}	1.25^{a}	1.74^{a}
Full tree	1.59^{ns}	0.80^{ns}	0.68^{b}	0.90^{ns}	1.30^{b}	1.75^{ns}	1.68^{ns}	0.65^{ns}	0.93^{a}	0.83^{ns}	2.08^{a}	2.14^{ns}
Stem	2.30^{b}	1.19^{ns}	0.99^{b}	1.31^{ns}	1.79^{b}	2.03^{ns}	2.92^{a}	1.32^{ns}	1.44^{a}	1.57^{ns}	2.91^{a}	2.51^{ns}
SW+SB	2.78^{b}	1.60^{ns}	1.34^{b}	1.53^{ns}	2.29^{b}	2.31^{ns}	3.25^{a}	1.64^{ns}	1.65^{a}	1.72^{ns}	3.37^{a}	2.73^{ns}
SW	3.72^{b}	2.99^{ns}	2.94^{ns}	4.45^{ns}	6.44^{ns}	2.71^{ns}	4.19^{a}	2.83^{ns}	2.75^{ns}	4.95^{ns}	7.55^{ns}	2.98^{ns}

Whole tree: harvest of whole biomass tree. Full tree: harvest above-ground biomass; Stem: harvest of stemwood with stembark; SW+SB: commercial stemwood with stembark; SW: commercial stemwood. *Mean of each harvest intensities, in the different soil types, followed by ^{ns} did not differ significantly at the level of 5% error.

The results of the present study indicate that harvest intensity planning should be adopted locally, and should be based on the nutrient removal of each tree section harvested and the type of soil, as the clayey soil was suitable for a higher number of rotations of seven-year-old *E. urograndis*, in commercial harvesting systems of the stemwood. Viera *et al*. (2015) verified that in *E. urophylla* x *E. globulus* stands, phosphorus and calcium were the main nutrients to become limiting in subsequent rotations under a harvest system in which the stemwood and stembark were harvested.

Considering the harvest of stemwood only, the limiting nutrients for both soil types were phosphorus, potassium and sulfur, with numbers less than three rotations in this harvesting system. If you consider harvesting stemwood + stembark, the limiting nutrients are phosphorus, potassium and calcium, with less than two rotations. Magnesium is the least limiting growth nutrient, with a potential of six rotations for sandy soil and seven rotations for clay soil.

In the harvest of stemwood + stembark, a very common system by companies in the cellulose sector, the sandy soil has the lowest number of rotations for all the analyzed nutrients. This shows the fragility of this soil and the attention given to fertilizing the plantations implanted in this type of soil to guarantee the sustainability of the system.

Just as the estimated number of rotations varies according to the biomass harvest intensity, the rate of nutrient removal also depends on which components will be harvested (Table 4). The SW harvest system has the lowest nutrient removal rate, as it has the lowest amount of nutrients per biomass.

The lowest rates of nutrient removal were observed with the harvesting of commercial stemwood, independent on the soil type, due to the high amount of biomass and the low amount of nutrients of this component when compared to the others. When comparing the two types of soil, we found that the removal rate is analogous to the harvesting of the commercial stemwood without the stembark, since the harvest of the stembark with tree tops resulted in higher rates of nutrient removal in the clayey soil, which was possibly related to higher biomass production of this soil.

Studies on the removal of nutrients through biomass harvesting provide a basis for the understanding of nutritional dynamics in stands, and are vital for sustainable production, as such studies enable us to predict situations that are critical to both productivity and chemical characteristics of the soil (Viera *et al*., 2015).

Nitrogen, potassium and calcium are the nutrients that present the greatest reduction in the rate of removal of nutrients according to the harvest intensity for both types of soil. There is a 50% reduction in the rate of calcium removal if the harvesting system leaves the bark in place and removes only the stemwood. Regardless of the harvesting system, the rate of sulfur removal

in the clayey soil is practically unchanged, since the largest amount of this element is found in the soil followed by stemwood, a component that is removed in all harvesting systems. As in the sandy soil, the sulfur stock in the soil is lower than in the clayey soil, thus it presents a decrease in the removal rate according to the harvest intensity.

Table 4. Nutrient removal rate based on nutrient and biomass removed, according to harvest intensity of *E. urograndis* biomass at seven years old in sandy and clayey soils in the region of Telêmaco Borba, Paraná, Brazil.

Harvest intensities	Sandy						Clayey					
	N	P	K	Ca	Mg	S	N	P	K	Ca	Mg	S
Whole tree	1.96^{ns*}	0.13^{ns}	1.79^{b}	1.14^{b}	0.37^{b}	0.28^{ns}	1.83^{ns}	0.13^{ns}	1.91^{a}	1.72^{a}	0.50^{a}	0.25^{ns}
Full tree	1.57^{ns}	0.12^{ns}	1.82^{ns}	1.10^{b}	0.33^{b}	0.25^{ns}	1.56^{ns}	0.12^{ns}	1.67^{ns}	1.63^{a}	0.41^{a}	0.25^{ns}
Stem	1.29^{ns}	0.11^{ns}	1.63^{ns}	1.00^{b}	0.29^{b}	0.24^{ns}	1.14^{ns}	0.09^{ns}	1.35^{ns}	1.24^{a}	0.34^{a}	0.24^{ns}
SW+SB	1.21^{ns}	0.10^{ns}	1.48^{ns}	0.98^{b}	0.26^{b}	0.24^{ns}	1.11^{ns}	0.08^{ns}	1.32^{ns}	1.24^{a}	0.33^{a}	0.24^{ns}
SW	1.03^{ns}	0.07^{ns}	0.94^{ns}	0.48^{ns}	0.12^{b}	0.22^{ns}	1.01^{ns}	0.06^{ns}	1.04^{ns}	0.63^{ns}	0.19^{a}	0.25^{ns}

Whole tree: harvest of whole biomass tree. Full tree: harvest above ground biomass; Stem: harvest of stemwood with stembark; SW+SB: commercial stemwood with stembark; SW: commercial stemwood. *Mean of each harvest intensities in the different soil types followed by ^{ns} did not differ significantly at the level of 5% error.

3.3. Nutrient-use efficiency

The nutrient-use efficiency (NUE) corresponds to the rate of conversion of nutrients into biomass. This value demonstrates how many units of biomass are formed per unit of nutrient, and the higher the value, the more efficient the conversion of nutrients into biomass. By improving the NUE, stemwood productivity can be increased. The NUE is one of the fundamental parameters for the definition of the best management techniques, and consequently for the maintenance of the productive capacity of forest stands (Santana *et al*., 2002).

Analyzing the NUE between the different components of the biomass, we found that the stemwood was the component that had the highest values of NUE for all nutrients analyzed, both in sandy and clayey soil, and the inverse was observed in the leaves for nitrogen, phosphorus, potassium, and sulfur. The stembark presented the lowest NUE for calcium, independent of the soil type (Table 5). The high NUE of wood indicates that the xylem used the lowest quantity of nutrients for each unit of biomass produced (Medeiros *et al*., 2020).

NUE decreased in the following order: phosphorus > magnesium > sulfur > calcium > nitrogen > potassium for sandy and clayey soil. This result is similar to the order found by Santos *et al.* (2017), for *E. urograndis* in Rio de Janeiro, Brazil, where the authors observed NUE magnitudes in the order of phosphorus > magnesium> calcium > nitrogen > potassium. However, Schumacher *et al*. (2019), found inverse values for *Eucalyptus* spp. in Rio Grande do Sul, Brazil, and reported NUE based on total biomass in the following order: phosphorus > sulfur > magnesium> potassium > nitrogen > calcium.

For the production of all components of the biomass, the elements phosphorus, magnesium and sulfur were the macronutrients most efficiently used in both types of soil analyzed (Table 5). However, considering only the stemwood component of the trees, since this is the component of main commercial interest in the stands, the NUE decreased in the following order: phosphor > magnesium > sulfur > calcium > nitrogen > potassium for sandy and clayey soil. Similar results, although with inversion in the distribution of some nutrients, were reported by Santos *et al.* (2019b) studying the nutritional efficiency of different eucalyptus genotypes in Southern Brazil (P > S > Mg > Ca > N > K).

Table 5. Nutrient-use efficiency for a plantation of seven-year-old *E. urograndis* on sandy and clayey soils, in the region of Telêmaco Borba, Paraná, Brazil.

Soil	Component	N	P	K	Ca	Mg	S
Sandy	Leaves	48^{ns*}	852^{ns}	88^{ns}	233^{a}	407^{a}	1069^{ns}
	Branches	334^{a}	298^{ns}	195^{ns}	377^{a}	1045^{a}	2575^{b}
	Tree tops bark	219^{ns}	1575^{ns}	152^{ns}	109^{b}	321^{a}	4136^{ns}
	Tree tops wood	466^{b}	5180^{b}	297^{b}	2157^{a}	2828^{b}	3116^{b}
	Stembark	258^{ns}	1831^{ns}	101^{b}	125^{a}	439^{a}	2462^{b}
	Stemwood	979^{ns}	14765^{ns}	1089^{ns}	221^{a}	8354^{a}	4323^{ns}
	Roots	255^{ns}	5385^{ns}	671^{a}	806^{ns}	1778^{a}	2374^{b}
Clayey	Leaves	45^{ns}	834^{ns}	84^{ns}	154^{b}	348^{b}	951^{ns}
	Branches	227^{b}	2952^{ns}	238^{ns}	12 ^{b}	575^{b}	3799^{a}
	Tree tops bark	235^{ns}	1321^{ns}	180^{ns}	137^{a}	268^{b}	3713^{ns}
	Tree tops wood	731^{a}	8885^{a}	666^{a}	1966^{b}	4232^{a}	4642^{a}
	Stembark	254^{ns}	2017^{ns}	133^{a}	83^{b}	362^{b}	3464^{a}
	Stemwood	984^{ns}	16888^{ns}	1015^{ns}	1640^{b}	5851^{b}	4217^{ns}
	Roots	269^{ns}	4275^{ns}	247^{b}	437^{ns}	930^{b}	3831^{a}

*Mean of each component, in the different soil types, followed by ^{ns}, did not differ significantly at the level of 5% error.

The sandy soil has better NUE for calcium and magnesium for the SW harvest system when compared to the clay soil, possibly explained by a luxury consumption, since the clay soil had higher concentrations of these elements in the soil. Considering only the stemwood, the sandy soil showed a higher NUE for calcium and magnesium when compared to clayey soil. The use of fertilization in forest stands is based on the quantification of the nutrients exported from the site by the harvested biomass, and the relation between the biomass production and the nutrients contained in each component (Lafetá *et al*., 2018). In addition, Santana *et al.* (2002) point out that nutrient utilization efficiency may be related to the characteristics of each species and to water availability, and nutritional non-equilibrium in the soil-plant system may cause a limitation or excess of one or more available nutrients.

Sandy soil had a higher biological efficiency of calcium and magnesium for the production of stemwood when compared to clayey soil. Magnesium was not a growth-limiting nutrient as observed in the simulation of the number of rotations. However, if the stemwood + stembark harvest is considered, calcium was a limiting nutrient to growth. In sandy soils, *E. urograndis* showed a higher nutrient-use efficiency than clayey soil for both stemwood and stembark, showing the luxury consumption of the species, since the clay soil had higher concentrations of this element in the soil. This study demonstrated the adaptation of eucalyptus to the different types of soils in Brazil, showing the main limiting nutrients for each type of soil in different harvesting systems. Therefore, the NUE is a parameter of great utility in the selection of species to be used in reforestation, especially in nutrient poor soils (Silva *et al*., 1983).

4. CONCLUSIONS

The best harvesting system considers the removal of only commercial stemwood, as this will reduce the removal of nutrients and result in a better nutritional balance of the sites, independently of the soil type.

Clay soils had a higher biological efficiency of calcium and magnesium for the production of stemwood when compared to clayey soil, possibly explained by a luxury consumption, since the clay soil had higher concentrations of these elements in the soil.

5. ACKNOWLEDGEMENTS

We thank the Klabin Company, and the Monte Alegre farm, for their support during the development of this project, for allowing us to conduct our research in the study area, and for their logistical and financial support. The fourth and fifth authors thank the Coordination for the Improvement of Higher Education Personnel (CAPES) for the scholarship.

6. REFERENCES

ACHAT, D. L.; DELEUZE, C.; LANDMANN, G.; POUSSE, N.; RANGER, J.; AUGUSTO L. Quantifying consequences of removing harvesting residues on forest soils and tree growth – A meta-analysis. **Forest Ecology and Management**, v. 348, n. 15, p. 124-141, 2015. https://doi.org/10.1016/j.foreco.2015.03.042

ALVARES, C. A.; STAPE, J. L.; SENTELHAS, P. C.; GONÇALVES, J. L. M.; SPAROVEK, G. Köppen's climate classification map for Brazil. **Meteorologische Zeitschrift**, v. 22, n. 6, p. 1-18, 2013. https://doi.org/10.1127/0941-2948/2013/0507

BARROS, N. F.; NOVAIS, R. F.; CARMO, D. N.; NEVES, J. C. L. Classificação nutricional de sítios florestais – descrição de uma metodologia. **Revista Árvore**, v. 10, p. 112-120, 1986.

EGNELL, G. A review of Nordic trials studying effects of biomass harvest intensity on subsequent forest production. **Forest Ecology and Management**, v. 383, n. 1, p. 27-36, 2017. https://doi.org/10.1016/j.foreco.2016.09.019

KUMARASWAMY, S.; MENDHAM, D. S.; GROVE, T. S.; O'CONNELL, A. M.; SANKARAN, K. V.; RANCE, S. J. Harvest residue effects on soil organic matter, nutrients and microbial biomass in eucalypt plantations in Kerala, India. **Forest Ecology and Management**, v. 328, n. 15, p. 140-149, 2015. https://doi.org/10.1016/j.foreco.2014.05.021

LAFETÁ, B. O.; SANTANA, R. C.; NOGUEIRA, G. S.; NEVES, J. C. L.; PENIDO, T. M. A. Eficiência de utilização de macronutrientes em eucalipto por método não destrutivo estimados por redes neurais artificiais. **Ciência Florestal**, v. 28, n. 2, p. 613-623, 2018. https://doi.org/10.1016/j.foreco.2014.05.021

MEDEIROS, P. L.; SILVA, G. G. C.; OLIVEIRA, E. M. M.; RIBEIRO, C. O.; SILVA, J. M. S.; PIMENTA, A. S. Efficiency of nutrient use for biomass production of a *Eucalyptus* clone as a function of planting density in short-rotation cropping. **Australian forestry**, v. 83, n. 2, p. 66-74, 2020. https://doi.org/10.1080/00049158.2020.1774958

MIYAZAWA, M.; PAVAN, M. A.; MURAOKA, T.; CARMO, C. A. F. S.; MELO, W. J. Análises químicas de tecido vegetal. *In*: SILVA, F. C. da (ed.). **Manual de análises químicas de solos, plantas e fertilizantes**. Rio de Janeiro: Embrapa, 2009. p. 190-233.

OLSSON, B. A.; ÅKERBLOM, S.; BISHOP, K.; EKLÖF, K.; RING, E. Does the harvest of logging residues and wood ash application affect the mobilization and bioavailability of trace metals? **Forest Ecology and Management**, v. 383, n. 1, p. 61-72, 2017. https://doi.org/10.1016/j.foreco.2016.09.017

SALVADOR, S. M.; SCHUMACHER, M. V.; STAHL, J.; SANTOS, J. C. Biomassa arbórea e de subbosque e da serapilheira acumulada em povoamentos de *Eucalyptus urophylla* x *Eucalyptus grandis*. **Ecologia e Nutrição Florestal**, v. 3, n. 3, p. 82-93, 2015. https://doi.org/10.5902/2316980X19414

SALVADOR, S. M.; SCHUMACHER, M. V.; STHAL, J.; LUDVICHAK, A. A.; MOMOLLI, D. R.; CONSENSA, C. B. Effects of soil type in nutrient amount in eucalyptus urograndis: Macronutrients. **Journal of Experimental Agriculture International**, v. 35, n. 3, p. 1-9, 2019. https://doi.org/10.9734/jeai/2019/v35i330204

SANTANA, R. C.; BARROS, N. F.; NEVES, J. C. L. Eficiência de utilização de nutrientes e sustentabilidade da produção em procedências de *Eucalyptus grandis* e *Eucalyptus saligna* em sítios florestais do estado de São Paulo. **Revista Árvore**, v. 26, n. 4, p. 447-457, 2002. https://doi.org/10.1590/S0100-67622002000400007

SANTANA, R. C.; BARROS, N. F.; NOVAIS, R. F.; LEITE, H. G.; COMERFORD, N. B. Alocação de nutrientes em plantios de eucalipto no Brasil. **Revista Brasileira de Ciência do Solo**, v. 32, n. spe, p. 2723-2733, 2008. https://doi.org/10.1590/S0100-06832008000700016

SANTOS, F. M.; CHAER, M.; DINIZ, A. R.; BALIEIRO, F. C. Nutrient cycling over five years of mixed-species plantations of *Eucalyptus* and *Acacia* on a sandy tropical soil. **Forest Ecology and Management**, v. 384, n. 1, p. 110-121, 2017. https://doi.org/10.1016/j.foreco.2016.10.041

SANTOS, K. F.; LUDVICHAK, A. A.; QUEIROZ, T. B.; SCHUMACHER, M. V.; ARAÚJO, E. F. Biomass production and nutrient content in different *Eucalyptus* genotypes in Pampa Gaúcho, Brazil. **Revista Brasileira de Ciências Agrárias**, v. 14, n. 4, e6575, 2019a. https://doi.org/10.5039/agraria.v14i4a6575

SANTOS, K. F.; SCHUMACHER, M. V.; LUDVICHAK, A. A.; ARAÚJO, E. F. Biomass and stock of nutrients in different genotypes of eucalypts in Southern Brazil. **Journal of Experimental Agriculture International**, v. 34, n. 4, p. 1-12, 2019b. https://doi.org/10.9734/jeai/2019/v34i430178

SANTOS, K. F.; LUDVICHAK, A. A.; QUEIROZ, T. B.; SCHUMACHER, M. V.; ARAÚJO, E. F.; MOMOLLI, D. R. Estimation of nutrient export in eucalyptus genotypes under different harvest intensities in southern Brazil. **Idesia**, v. 38, n. 1, p. 33-38, 2020. http://dx.doi.org/10.4067/S0718-34292020000100033

SCHUMACHER, M. V.; WITSCHORECK, R.; CALIL, F. N.; LOPES, V. G.; VIERA, M. Produção de biomassa no corte raso em plantio de *Araucaria angustifolia* (Bertol.) Kuntze de 27 anos de idade em Quedas Do Iguaçu, PR. **Ciência Florestal**, v. 21, n. 1, p. 53-62, 2011. https://doi.org/10.5902/198050982747

SCHUMACHER, M. V.; WITSCHORECK, R.; CALIL, F. N.; LOPES, V. G. Manejo da biomassa e sustentabilidade nutricional em povoamentos de Eucalyptus spp. em pequenas propriedades rurais. **Ciência Florestal**, v. 29, n. 1, p. 144-156, 2019. http://dx.doi.org/10.5902/198050985135

SILVA, H. D.; POGGIANI, F.; COELHO, L. C. Eficiência de utilização de nutrientes em cinco espécies de *Eucalyptus*. **Boletim de Pesquisa Florestal**, n. 6/7, p.1-8, 1983.

SILVA, P. H. M.; POGGIANI, F.; LIBARDI, P. L.; GONÇALVES, N. A. Fertilizer management of eucalypt plantations on sandy soil in Brazil: Initial growth and nutrient cycling. **Forest Ecology and Management**, v. 301, n. 1, p. 67-78, 2013. https://doi.org/10.1016/j.foreco.2012.10.033

TEDESCO, M. J.; GINELLO, C.; BISSANI, C. A.; BOHNEN, H.; VOLKWEISS, S. J. **Análise de solo, plantas e outros materiais**. Porto Alegre: UFRGS, 1995. 174 p.

VIERA, M.; SCHUMACHER, M. V.; BONACINA, D. M. Biomassa e nutrientes removidos no primeiro desbaste de um povoamento de *Pinus taeda* L. em Cambará do Sul, RS. **Revista Árvore**, v. 35, n. 3, p. 371-379, 2011. https://doi.org/10.1590/S0100-67622011000300001

VIERA, M.; SCHUMACHER, M. V.; KLEINPAUL, I. S. Estoque de nutrientes em consórcios de *Eucalyptus urograndis*, *Acacia mearnsii* e *Zea mays*. **Ciência Florestal**, v. 23, n. 3, p. 317-327, 2013. https://doi.org/10.5902/1980509810543

VIERA, M.; SCHUMACHER, M. V.; TRÜBY, P.; ARAÚJO, E. F. Implicações nutricionais com base em diferentes intensidades de colheita da biomassa de *Eucalyptus urophylla* x *Eucalyptus globulus*. **Ciência Rural**, v. 45, n. 3, p. 432-439, 2015. https://doi.org/10.1590/0103-8478cr20120367

WITSCHORECK, R. **Biomassa e nutrientes no corte raso de um povoamento de *Pinus taeda L.* de 17 anos de idade no município de Cambará do Sul-RS.** 2008. 80f. Dissertação (Mestrado em Engenharia Florestal) - Universidade Federal de Santa Maria, Santa Maria, 2008.

YAN, T.; ZHU, J.; YANG, K.; YU, L.; ZHANG, J. Nutrient removal under different harvesting scenarios for larch plantations in northeast China: Implications for nutrient conservation and management. **Forest Ecology and Management**, v. 400, n. 15, p. 150-158, 2017. https://doi.org/10.1016/j.foreco.2017.06.004

Ambiente & Água - An Interdisciplinary Journal of Applied Science
ISSN 1980-993X – doi:10.4136/1980-993X
www.ambi-agua.net
E-mail: ambi.agua@gmail.com

Dynamics of natural regeneration after disturbance in a remnant of Mixed Ombrophilous Forest in southern Brazil

ARTICLES doi:10.4136/ambi-agua.2679

Received: 18 Nov. 2020; Accepted: 19 Apr. 2021

Alyne Regina Ruggiero; Lauri Amândio Schorn; Kristiana Fiorentin dos Santos*; Tatiele Anete Bergamo Fenilli

Departamento de Engenharia Florestal. Universidade Regional de Blumenau (FURB), Rua São Paulo, n° 3250, CEP: 89030-080, Blumenau, SC, Brazil.
E-mail: alyne.cena@gmail.com, lschorn@furb.br, tfenilli@furb.br
*Corresponding author. E-mail: kristianafiorentin@gmail.com

ABSTRACT

This study evaluated changes in the structure for remnant Mixed Ombrophilous Forest recovering from logging, which ceased over 40 years ago. Regarding the dynamics of the floristic composition of natural regeneration, 18 species remained (23.38% of the total) and 27 new species entered (35.06% of the total). The greatest increases were observed for *Allophylus edulis*, *Myrsine umbellata*, and *Miconia cinerascens*. When analyzing the dynamics of regeneration in ecological groups, it was observed that pioneer species had a similar value in both surveys (29.4% and 29.6%); secondary species decreased from 56.6% to 52.8%, and late-successional species increased from 0.2% to 6.0%. Therefore, the forest fragment studied is in a healing phase after disturbance, characterized by the increased regeneration of pioneer species as a result of sufficient light entering the interior of the forest.

Keywords: horizontal structure, ingress, mortality, succession stages.

Dinâmica da regeneração natural após distúrbio em uma remanescente de Floresta Ombrófila Mista no Sul do Brasil

RESUMO

O presente estudo teve como objetivo avaliar as alterações ocorridas, no período de 2012 a 2016, na estrutura da regeneração natural de um remanescente de Floresta Ombrófila Mista, sem intervenções há mais de 40 anos. Em relação a dinâmica da composição florística da regeneração natural, houve a saída de 18 espécies (23,38% do total) e a entrada de 27 novas espécies (35,06% do total). Os maiores acréscimos foram observados para *Allophylus edulis*, *Myrsine umbellata e Miconia cinerascens*. Analisando a dinâmica da regeneração em grupos ecológicos, observou-se que as espécies pioneiras tiveram um valor similar em ambos os levantamentos (29,4 a 29,6%). As espécies secundárias decresceram de 56,6% para 52,8%. E as espécies de sucessão tardia aumentaram de 0,2 a 6,0%. Logo, o remanescente estudado encontra-se em fase de cicatrização de distúrbio, caracterizada pelo aumento da regeneração de espécies pioneiras, uma vez que há quantidade suficiente de luminosidade incidindo no interior da floresta.

Palavras-chave: estágios de sucessão, estrutura horizontal, ingresso, mortalidade.

This is an Open Access article distributed under the terms of the Creative Commons Attribution License, which permits unrestricted use, distribution, and reproduction in any medium, provided the original work is properly cited.

1. INTRODUCTION

Mixed Ombrophilous Forest (MOF), also known as Araucaria forest, is one of the main forest types of southern Brazil (Higuchi *et al.*, 2012a). Its geographical distribution occurs predominantly in the southern plateau region and is associated with places of high altitude and low average annual temperatures (Higuchi *et al.*, 2012a). This forest formation consists mainly of *Araucaria angustifolia* (Bertol.) Kuntze, in association with *Ocotea porosa* (Nees & Mart.) Barroso, *Ilex paraguariensis* A. St.-Hil., *Mimosa scabrella* Benth., *Cedrella fissilis* Vell., *Roupala brasiliensis* Klotzsch, in addition to numerous species belonging to the Myrtaceae family (Higuchi *et al.*, 2012a, 2012b, 2015; Dalla Rosa *et al.*, 2016).

However, the MOF has been intensely altered by strong deforestation because of logging, the expansion of agriculture and livestock, the homogeneous reforestation of exotic species, and the advancement of urban areas, and is thus considered one of the most threatened forest types in Brazil (Ribeiro *et al.*, 2009; Vibrans *et al.*, 2013; Souza *et al.*, 2014; Aguiar *et al.*, 2017). In fact, only 12.6% of the original MOF extension remains (Ribeiro *et al.*, 2009). A lack of knowledge regarding native MOF management has contributed to the reduction in area and low diversity of natural remnants (Hess *et al.*, 2010). Currently, in the State of Santa Catarina, only 24.4% of the original MOF remains, with forest areas distributed in fragmented remnants not exceeding 50 ha (Vibrans *et al.*, 2013). However, even with the disturbances that have occurred, the remaining fragments can be maintained through natural ecological processes, as evidenced by the natural regeneration of tree species (Santos *et al.*, 2018).

Therefore, because of the great environmental and social importance of the MOF, the conservation and restoration of its remnant fragments is a primary objective of MOF management (Higuchi *et al.*, 2012a). In this context, studies of natural regeneration are extremely important because they generate results that enable a better understanding of the behavior of tree communities (Aguiar *et al.*, 2017). With regard to this, a greater understanding of the plant succession process in areas with different disturbance histories is essential, as it can generate data that detect the need to facilitate natural regeneration actions, as well as forest management incentives that facilitate recovery of other similar areas (Larsen *et al.*, 2019). Thus, these studies can support the conservation and recovery plans of forest ecosystems by enabling the identification of limiting environmental factors and inferring the future dynamics of forests (Aguiar *et al.*, 2017; Dalla Rosa *et al.*, 2016).

In this light, this study evaluated the changes that occurred from 2012 to 2016 in the structure of the natural regeneration of a remnant of Mixed Ombrophilous Forest that has remained without intervention for more than 40 years, in the state of Santa Catarina, Brazil.

2. MATERIAL AND METHODS

2.1. Characterization of the study area

The studied forest remnant is located in Fazenda Guamirim Gateados and is part of the "Emílio Einsfeld Filho" Private Reserve of Natural Heritage (PNHR), located in the municipalities of Campo Belo do Sul and Capão Alto, Santa Catarina, Brazil. The experimental area has a total of 3,365 ha, with approximately 72% forest cover, characterized by several succession stages of Mixed Ombrophilous Forest. Sampling was conducted within a radius of up to 500 m from the coordinate point 28°02'55.00" S and 50°45' 59.56" W.

Much of the vegetation in the study area has been subjected to selective logging, which targeted high commercial value woods (Zeller, 2010). According to the Köppen climate classification, the climate of the region is characterized as humid subtropical mesothermal (Cfb), with cool summers, no defined dry season, and frequent severe frosts. The average annual temperature is approximately 15.8°C, varying from 11.4°C in the coldest month to 20.3°C in

the hottest month. The average annual precipitation is 1,742 mm (Alvares *et al.*, 2013). The region that encompasses the municipality of Campo Belo do Sul is located in the southern plateau, which in the State of Santa Catarina is bordered to the east by dense ombrophilous forest in addition to deciduous forest along the banks of the Uruguay River (Vibrans *et al.*, 2013).

2.2. Data collection

In February 2012, 20 permanent circular plots were established in a random design in the experimental area. Each plot was 5 m in diameter, and the total sample area was 392.5 m² (Figure 1). In 2016, the same sample units were remeasured. Between the two survey occasions, a gale occurred in the study area, eliminating part of the upper tree layer in four sample units. The collected data corresponded to the number, height, and identification of the regenerating individuals in the sample units. Individuals with a minimum height of 0.50 m and a diameter breast height of less than 15 cm were considered to be regenerating.

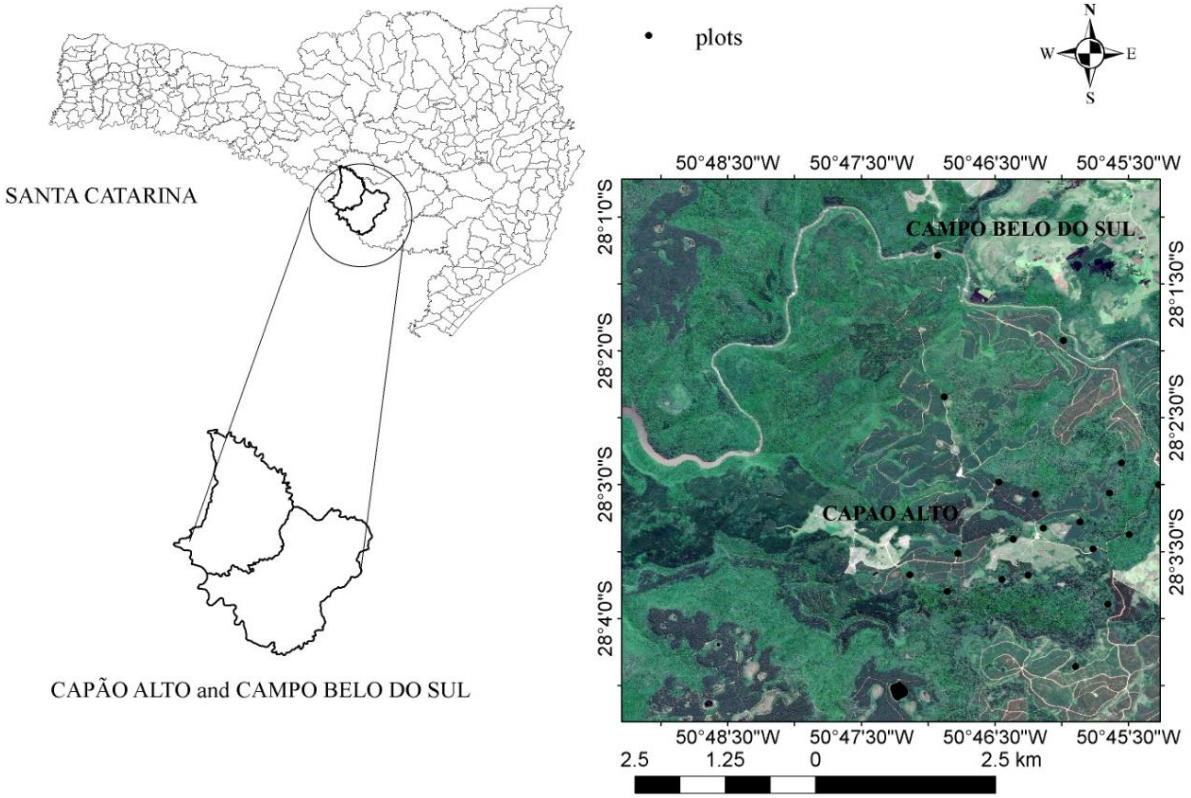

Figure 1. Geographic location of the plots in a remnant of Mixed Ombrophilous Forest in Santa Catarina, Brazil.

2.3. Data analysis

Using data collected in the permanent plots from 2012 and 2016, the floristic and phytosociological parameters of natural regeneration were estimated. For this, the species found in the plots were identified by visual analysis in the field or in the expert opinions and specialized literature. For the ecological classification of species, in addition to observations in the field, the methodology described by Vibrans *et al.* (2013) was followed. This system considers the following categories: pioneer species (P), secondary species (SE), and late-successional species (LS).

The dynamics of regeneration were evaluated by changing the values of diversity and structure of species between the two periods surveyed. The parameters used to estimate the regeneration structure were density and frequency, based on Mueller-Dombois and Ellenberg

(1974), and the category of size and value of the regeneration based on Finol (1971). Species diversity was calculated using the Shannon's Diversity Index (H′), Simpson's diversity index (D), and Pielou's equability index (J′) (Brower and Zar, 1984). All analyses were done by the PAST® statistical software, Version 2.17c, according to the methodology described by Felfili and Rezende (2003) and Magurran (2004).

The regeneration-size category parameter (absolute and relative) refers to the distribution of regenerating individuals in height classes by determining the phytosociological values of natural regeneration. The regeneration value, in absolute and relative terms, in turn expresses the importance of species in the community by averaging their relative density, frequency, and size category. The calculations covered all species sampled in the study area. Changes in species density were analyzed using the paired t-test (alpha was set at = 0.05).

3. RESULTS AND DISCUSSION

3.1. Floristic composition

In general, in both surveys, 77 species were found, represented by 51 genera and 32 botanical families. Specifically, in 2012 and 2016, 50 (12,382 ind ha^{-1}) and 59 species (12,313 ind ha^{-1}) were found, respectively, of which 18 were exclusive to the first survey and 28 were exclusive to the second (Table 1). The species richness found in this study was similar to that found by Aguiar *et al.* (2017) in an MOF experiment in Lages, SC, Brazil, and by Santos *et al.* (2015) in a fragment with the same forest typology also in Lages, SC, Brazil.

The family with the greatest richness was Myrtaceae, followed by Lauraceae. Emphasizing the ecological importance of the Myrtaceae family, it has also been classified as highly representative of MOFs by several authors (Vibrans *et al.*, 2011; Meyer *et al.*, 2013; Higuchi *et al.*, 2015; Santos *et al.*, 2015, 2018; Dalla Rosa *et al.*, 2016; Silva et al., 2017; Santana *et al.*, 2018; Vefago *et al.*, 2019), occurring in areas of different altitudes (Dalla Rosa *et al.*, 2016).

Table 1. Floristic and structural descriptors evaluated for natural regeneration in 2012 and 2016 in a remnant of Mixed Ombrophilous Forest in Santa Catarina, Brazil.

Descriptors evaluated	2012	2016
Number of species	50	59
Number of genres	43	37
Number of families	29	24
Shannon's diversity index (H′)	3.15	3.26
Pielou's equability index (J′)	0.81	0.79
Simpson's diversity index (D)	0.94	0.94
Number of individuals per hectare	12,382	12,313

The H′ and J′ values were 3.15 and 0.81 in 2012 and 3.26 and 0.79 in 2016, respectively. The estimated value for D was 0.94 for both surveys (Table 1). The H′ value was similar to that found in an experiment by Aguiar *et al.* (2017) in an MOF in Lages, SC, Brazil (3.34) and by Santos *et al.* (2018), also in an MOF in Lages, SC (3.42). Higher values were found by Dalla Rosa *et al.* (2016) in a remnant of the same forest typology in Urubici, SC, Brazil (2.51). In contrast, lower values were found by Santos *et al.* (2015) in an MOF fragment in Lages, SC, Brazil. According to Nascimento *et al.* (2001), diversity values close to 3.00 characterize a medium diversity, which is expected in secondary succession stage MOF forests that have

suffered anthropic influences.

Regarding J′, Dalla Rosa *et al.* (2016), Santos *et al.* (2015), Aguiar *et al.* (2017) and Santos *et al.* (2018) found values close to that of this study: 0.75, 0.76, 0.82 and 0.83, respectively. This indicates high ecological dominance. According to Brower and Zar (1984), the Simpson diversity index (D) measures the probability that two individuals, selected at random from the same sample, belonging to the same species. That is, the higher the D value, the greater the diversity and the lesser the dominance of species (Klauberg *et al.*, 2010).

The quantitative data of the floristic descriptors evaluated (Table 1) revealed little change between the two surveys. It is observed that the diversity values found in this study reflect the pattern already verified in other studies in the same formation and confirm that the MOF in Santa Catarina is, in general, undergoing regeneration after decades of selective exploration. However, in this study, the observed changes were small, which indicates the existence of disturbances such as gusts and tree falls in the area, which can increase environmental filters and facilitate the entry of pioneer species.

3.2. Phytosociological parameters of natural regeneration

In the 2012 survey, the species *Eugenia* sp., *Allophylus edulis* (A.St.-Hil., Cambess. & A. Juss.) Radlk., *Casearia decandra* Jacq., *Matayba elaeagnoides* Radlk., and *Myrsine umbelata* Mart. were the most important in terms of density, which together accounted for 46.7% of the total stems (Table 2). These species were also the most representative in terms of frequency. In 2016, these same species remained the most important; however, there was a change in their order: *Allophylus edulis*, *Myrsine umbellata*, *Casearia decandra*, *Matayba elaeagnoides* and *Eugenia* sp. The mentioned species added up to 43.4% of the total density (Table 2). According to Higuchi *et al.* (2015), the variation of the most abundant species can be explained due to their different life strategies and respective capacities to develop in the forest understory. Some species may produce more propagules; however, they are inefficient competitors. Other species may produce few propagules, but with good competitive capacity.

Approximately half of the species (51.67%) were found in only 5% of the sample units, demonstrating the great diversity of species present in the regeneration of this forest type. In a study by Vefago *et al.* (2019), *Allophylus edulis* and *Matayba elaeagnoides* were also among the most representative species. *Araucaria angustifolia* (Bertol.) Kuntze, despite being considered the species that most characterizes MOF, went from 7th to 13th rank between the 2012 and 2016 survey; that is, it represented 4.3% of the density in 2012 (535.0 ind ha^{-1}), and only 2.7% in 2016 (331.2 ind ha^{-1}). However, despite the decrease in density in the plots, the species were more concentrated spatially in 2012 (FR: 3.2%) than in 2016 (FR: 4.1%). Other studies have also shown that this species had low representativeness (Dalla Rosa *et al.*, 2016; Vefago *et al.*, 2019). According to Dalla Rosa *et al.* (2016), *A. angustifolia* has a limited number of regenerating individuals in the understory of the MOF and this limitation is even more extreme at high altitudes (>1,500 m).

3.3. Dynamics of floristic composition of natural regeneration

There were considerable changes in the floristic composition of natural regeneration between the two surveys (Table 3). For example, 18 species remained (23.38% of the total) and 27 new species entered (35.06% of the total). From this, we can see the dynamism that occurred in natural regeneration, which shows that the occurrence of species in the regenerative stratum will not guarantee their presence in the tree stratum in the future.

Table 2. Phytosociological parameters of 20 species of greatest of values relative natural regeneration in 2012 and 2016 in a remnant of Mixed Ombrophilous Forest in Santa Catarina, Brazil.

SPECIES	AD (n ha^{-1})		RD (%)		AF (%)		RF (%)		ASC		RSC (%)		ANR		RNR (%)	
	2012	2016	2012	2016	2012	2016	2012	2016	2012	2016	2012	2016	2012	2016	2012	2016
Allophylus edulis (A.St.-Hil., Cambess. & A. Juss.) Radlk.	1248.4	1707.0	10.1	13.9	65.0	65.0	5.9	7.6	22.5	29.1	10.3	15.0	445.3	600.4	8.7	12.1
Annona emarginata (Schltdl.) H.Rainer	382.2	484.1	3.1	3.9	40.0	25.0	3.6	2.9	7.2	8.6	3.3	4.4	143.1	172.6	3.3	3.8
Araucaria angustifolia (Bertol) Kuntze	535.0	331.2	4.3	2.7	35.0	35.0	3.2	4.1	9.4	5.9	4.3	3.0	193.2	124.0	3.9	3.3
Brunfelsia pilosa Plowman	51.0	229.3	0.4	1.9	10.0	20.0	0.9	2.3	1.1	4.1	0.5	2.1	20.7	84.5	0.6	2.1
Campomanesia guaviroba (DC.) Kiaersk.	25.5	101.9	0.2	0.8	5.0	10.0	0.5	1.2	0.4	1.4	0.2	0.7	10.3	37.8	0.3	0.9
Casearia decandra Jacq.	1095.5	917.2	8.8	7.4	80.0	45.0	7.2	5.3	20.6	15.8	9.4	8.1	398.7	326.0	8.5	6.9
Casearia obliqua Spreng.	51.0	25.5	0.4	0.2	10.0	5.0	0.9	0.6	1.1	0.1	0.5	0.0	20.7	10.2	0.6	0.3
Cinnamodendron dinisii Schwacke	229.3	382.2	1.9	3.1	30.0	35.0	2.7	4.1	3.8	6.4	1.7	3.3	87.7	141.2	2.1	3.5
Cupania vernalis Cambess.	458.6	76.4	3.7	0.6	40.0	10.0	3.6	1.2	7.3	1.4	3.3	0.7	168.6	29.3	3.5	0.8
Eugenia sp.	1579.6	738.9	12.8	6.0	90.0	40.0	8.1	4.7	28.2	12.4	12.9	6.4	565.9	263.7	11.2	5.7
Eugenia uniflora L.	203.8	305.7	1.6	2.5	30.0	30.0	2.7	3.5	4.1	4.6	1.9	2.4	79.3	113.4	2.1	2.8
Luehea divaricata Mart. & Zucc.	25.5	76.4	0.2	0.6	5.0	15.0	0.5	1.8	0.5	0.6	0.2	0.3	10.3	30.7	0.3	0.9
Matayba elaeagnoides Radlk.	993.6	789.8	8.0	6.4	70.0	60.0	6.3	7.0	16.1	10.2	7.4	5.2	359.9	286.7	7.2	6.2
Miconia cinerascens Miq.	101.9	509.6	0.8	4.1	15.0	10.0	1.4	1.2	2.0	6.6	0.9	3.4	39.6	175.4	1.0	2.9
Myrsine umbellata Mart.	866.2	1197.5	7.0	9.7	55.0	55.0	5.0	6.4	15.5	19.2	7.1	9.9	312.2	423.9	6.3	8.7
Podocarpus lambertii Klotzsch ex Endl.	178.3	101.9	1.4	0.8	15.0	10.0	1.4	1.2	2.3	1.5	1.0	0.8	65.2	37.8	1.3	0.9
Roupala montana Aubl.	152.9	51.0	1.2	0.4	25.0	10.0	2.3	1.2	2.3	0.6	1.1	0.3	60.1	20.5	1.5	0.6
Rudgea parquioides (Cham.) Müll.Arg.	433.1	356.7	3.5	2.9	50.0	30.0	4.5	3.5	7.9	6.3	3.6	3.2	163.7	131.0	3.9	3.2
Sebastiana brasiliensis Spreng.	687.9	687.9	5.6	5.6	45.0	25.0	4.1	2.9	13.9	11.3	6.4	5.8	248.9	241.4	5.3	4.8
Styrax leprosus Hook. & Arn.	433.1	254.8	3.5	2.1	50.0	25.0	4.5	2.9	7.2	4.5	3.3	2.3	163.4	94.8	3.8	2.4

AD: absolute density; RD: relative density; AF: absolute frequency; RF: relative frequency; ASC: absolute size class; RSC: relative size class; ANR: absolute natural regeneration; RNR: relative natural regeneration.

Table 3. Dynamics of the structure of the regenerative stratum in a remnant of Mixed Ombrophilous Forest in Santa Catarina, Brazil.

SPECIES	RD (%)		RF (%)		RSC (%)		RNR (%)		CHANGES
	2012	2016	2012	2016	2012	2016	2012	2016	RNR (%)
Allophylus edulis (A.St.-Hil., Cambess. & A. Juss.) Radlk.	10.1	13.9	5.9	7.6	10.2	15.0	8.7	12.1	3.4
Allophylus guaraniticus (A. St.-Hil.) Radlk.		5.2		4.7		5.6		5.2	
Annona emarginata (Schltdl.) H.Rainer	3.1	3.9	3.6	2.9	3.3	4.4	3.3	3.8	0.5
Araucaria angustifólia (Bertol) Kuntze	4.3	2.7	3.2	4.1	4.3	3.0	3.9	3.3	-0.6
Baccharis dentata (Vell.) G.Barroso		0.6		0.6		0.5		0.6	
Bernardia pulchella (Baill.) Müll.Arg	0.2	0.4	0.5	0.6	0.2	0.5	0.3	0.5	0.2
Brunfelsia cuneifólia J.A.Schmidt		0.6		1.2		0.7		0.8	
Brunfelsia pilosa Plowman	0.4	1.9	0.9	2.3	0.5	2.1	0.6	2.1	1.5
Calyptranthes concinna DC.	2.1		3.2		2.1		2.4		
Campomanesia guaviroba (DC.) Kiaersk.	0.2	0.8	0.5	1.2	0.2	0.7	0.3	0.9	0.6
Capsicum sp.	0.2		0.5		0.2		0.3		
Casearia decandra Jacq.	8.8	7.4	7.2	5.3	9.4	8.1	8.5	6.9	-1.6
Casearia obliqua Spreng.	0.4	0.2	0.9	0.6	0.5	0.0	0.6	0.3	-0.3
Cinnamodendron dinisii Schwacke	1.9	3.1	2.7	4.1	1.7	3.3	2.1	3.5	1.4
Cinnamomum amoenum (Nees & Mart.) Kosterm.		0.2		0.6		0.2		0.3	
Citronella gongonha (Mart.) R.A.Howard	0.2		0.5		0.2		0.3		
Cupania vernalis Cambess.	3.7	0.6	3.6	1.2	3.3	0.7	3.5	0.8	-2.7
Dalbergia frutescens (Vell.) Britton	0.4		0.5		0.4		0.4		
Daphnopsis racemosa Griseb.	0.2	0.2	0.5	0.6	0.2	0.2	0.3	0.3	0.0
Drimys brasiliensis Miers	0.2	0.2	0.5	0.6	0.2	0.2	0.3	0.3	0.0
Eugenia pyriformis Cambess.	0.2		0.5		0.2		0.3		
Eugenia rostrifolia D.Legrand	2.3	0.2	2.7	0.6	2.3	0.2	2.4	0.3	-2.1
Eugenia uniflora L.	1.6	2.5	2.7	3.5	1.9	2.4	2.1	2.8	0.7
Eugenia sp.	12.8	6.0	8.1	4.7	12.8	6.4	11.2	5.7	-5.5
Ilex theezans Mart. ex Reissek	1.2		1.8		1.3		1.4		

Continue...

Continued...									
Lamanonia ternata Vell.	0.2		0.5		0.2		0.3		
Leandra regnellii (Triana) Cogn.		0.2		0.6		0.2		0.3	
Ligustrum lucidum W.T.Aiton		0.2		0.6		0.2		0.3	
Lonchocarpus campestris Mart. ex Benth	0.4		0.5		0.4		0.4		
Lonchocarpus latifolius (Willd.) DC.		0.4		0.6		0.5		0.5	
Luehea divaricata Mart. & Zucc.	0.2	0.6	0.5	1.8	0.2	0.3	0.3	0.9	0.6
Matayba elaeagnoides Radlk.	8.0	6.4	6.3	7.0	7.4	5.2	7.2	6.2	-1.0
Maytenus aquifolia Mart.	0.2		0.5		0.2		0.3		
Miconia cinerascens Miq.	0.8	4.1	1.4	1.2	0.9	3.4	1.0	2.9	1.9
Mimosa scabrella Benth.	0.2		0.5		0.2		0.3		
Myrceugenia mesomischa (Burret) D. Legrand et Kausel		0.2		0.6		0.2		0.3	
Myrceugenia sp.	0.4		0.9		0.4		0.6		
Myrcia glabra (O.Berg) D. Legrand		0.2		0.6		0.2		0.3	
Myrcia hartwegiana (O.Berg) Kiaersk.		0.2		0.6		0.2		0.3	
Myrcianthes pungens (O.Berg) D.Legrand	0.4		0.9		0.5		0.6		
Myrocarpus frondosus Allemão	1.2		0.9		1.4		1.2		
Myrsine lorentziana (Mez) Arechav.		0.4		0.6		0.5		0.5	
Myrsine sp.	0.2		0.5		0.2		0.3		
Myrsine umbellata Mart.	7.0	9.9	5.0	7.0	7.1	10.1	6.3	9.0	2.7
Nectandra lanceolata Nees	0.2	0.4	0.5	0.6	0.2	0.5	0.3	0.5	0.2
Nectandra megapotamica (Spreng.) Mez	2.7	1.2	2.3	2.3	2.0	1.4	2.3	1.7	-0.6
Ocotea puberula (Rich.) Nees.	1.2	0.2	2.3	0.6	0.7	0.2	1.4	0.3	-1.1
Ocotea pulchella (Nees) Mez	4.3	0.2	4.5	0.6	4.4	0.2	4.4	0.3	-4.1
Ocotea pulchra Vattimo-Gil		0.8		1.8		0.9		1.2	
Ocotea sp.		0.4		1.2		0.5		0.7	
Pavonia sepium A.St.-Hil.		1.2		1.2		1.2		1.2	
Pera glabrata (Schott) Poepp. ex Baill.	0.2		0.5		0.2		0.3		
Pimenta pseudocaryophyllus (Gomes) Landrum		0.4		0.6		0.5		0.5	
Continue...									

Continued...									
Piptocarpha angustifolia Dusén ex Malme	0.2	0.2	0.5	0.6	0.2	0.2	0.3	0.3	0.0
Podocarpus lambertii Klotzsch ex Endl.	1.4	0.8	1.4	1.2	1.0	0.8	1.3	0.9	-0.4
Prunus myrtifolia (L.) Urb.	0.8		1.8		0.9		1.2		
US – 1		0.6		1.2		0.7		0.8	
US – 2		0.8		1.2		0.9		1.0	
US – 3		0.4		0.6		0.5		0.5	
US – 4		0.2		0.6		0.2		0.3	
US – 5		0.2		0.6		0.2		0.3	
US – 6		0.6		0.6		0.7		0.6	
US – 7		0.2		0.6		0.2		0.3	
US – 8		0.4		0.6		0.3		0.4	
US – 9	0.2	0.2	0.5	0.6	0.2	0.2	0.3	0.3	0.0
Roupala montana Aubl.	1.2	0.4	2.3	1.2	1.1	0.3	1.5	0.6	-0.9
Rudgea parquioides (Cham.) Müll.Arg	3.5	2.9	4.5	3.5	3.6	3.2	3.9	3.2	-0.7
Schaefferia argentinensis Speg.		0.2		0.6		0.2		0.3	
Sebastiania brasiliensis Spreng.	5.6	5.6	4.1	2.9	6.3	5.8	5.3	4.8	-0.5
Sebastiania commersoniana (Baill.) L.B. Sm. & Downs		4.2		1.2		0.7		2.0	
Seguieria aculeata Jacq.	0.2		0.5		0.2		0.3		
Strychnos brasiliensis (Spreng.) Mart.	0.2	0.2	0.5	0.6	0.2	0.2	0.3	0.3	0.0
Styrax leprosus Hook. & Arn.	3.5	2.1	4.5	2.9	3.3	2.3	3.8	2.4	-1.4
Trichilia elegans A. Juss.		0.2		0.6		0.2		0.3	
Xylosma ciliatifolia (Clos) Eichler	0.4		0.9		0.4		0.6		
Zanthoxylum kleinii (R.S.Cowan) P.G.Waterman	0.2	0.6	0.5	1.2	0.2	0.7	0.3	0.8	0.5
Zanthoxylum rhoifolium Lam.		0.2		0.6		0.2		0.3	

RD: relative density; RF: relative frequency; RSC: relative size class; RNR: relative natural regeneration; US: unidentified species.

The greatest increases were observed for *Allophylus edulis* (+3.4%), *Myrsine umbellata* (+2.7%), and *Miconia cinerascens* Miq. (+1.9%), of which only *M. cinerascens* was classified as a pioneer, while the others were classified as secondary species. This fact indicates that this remnant forest is in a reestablishment phase after disturbance, since there is sufficient light shining into the forest to initiate the development/ recruitment of both pioneer and secondary species. Regarding the decreases, the species *Eugenia* sp., *Ocotea pulchella* (Nees & Mart.) Mez, and *Cupania vernalis* Cambess. stood out (–5.5%, –4.1%, and –2.7%) and the latter two were classified as pioneers. A study by Gross *et al.* (2018) reported that the dynamics of the Araucaria forest varied mainly in terms of tree mortality and rates of basal area loss.

3.4. Dynamics of the regeneration of ecological groups

Analyzing the dynamics of regeneration in ecological groups, it was observed that the pioneer species had similar values in both surveys (29.4% and 29.6%, respectively) (Figure 2). In contrast, secondary species decreased from 56.6% to 52.8%, while late-successional species increased from 0.2% to 6.0% between the first and the second survey, respectively. Meyer *et al.* (2013), when evaluating the natural regeneration of the MOF in Santa Catarina, Brazil, observed that the secondary, pioneer, and late-successional species corresponded to 54.37%, 29.66% and 15.97% of the total, respectively, which partially reflects the history of use of this forest.

In general, pioneer species showed the highest rates of positive change (189.8%), while secondary species showed the highest rates of negative change (–573.25%) (Figure 3). In this case, it becomes evident that the availability of light in the interior of the forest is caused by the fall of individuals from the tree layer due to the actions of climatic events, which is reflected in the increase of pioneer individuals, also resulting in the mortality of secondary species in natural regeneration. In this sense, the changes observed in the floristic composition and distribution of ecological groups can be attributed to disturbances that occur in the forest.

Chazdon (2016) mentioned that disturbances in natural forests can be caused by either natural or anthropogenic activities. Considering that selective logging ceased more than 40 years ago in the study area, natural disturbances, such as gales and the fall of mature trees, are undoubtedly causing the regeneration gaps. This, consequently, provides opportunities for changes in the distribution of ecological groups in the forest, especially with the increased representativeness of pioneer species that are extremely important for the forest succession, creating conditions for the species of more advanced successional stages to establish themselves. Thus, the colonization of clearings by pioneer species detected in this study shows the occurrence of forest reestablishment after disturbances (Narvaes *et al.*, 2005).

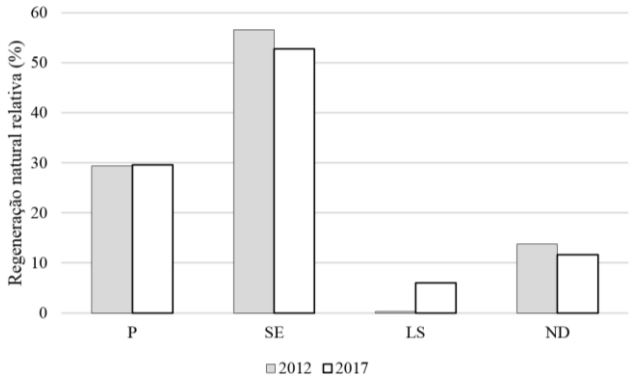

Figure 2. Relative natural regeneration by ecological groups in a remnant of Mixed Ombrophilous Forest in Santa Catarina, Brazil. P: Pioneers species; SE: Secondary species; LS: late-successional species; ND: Ecological group not defined.

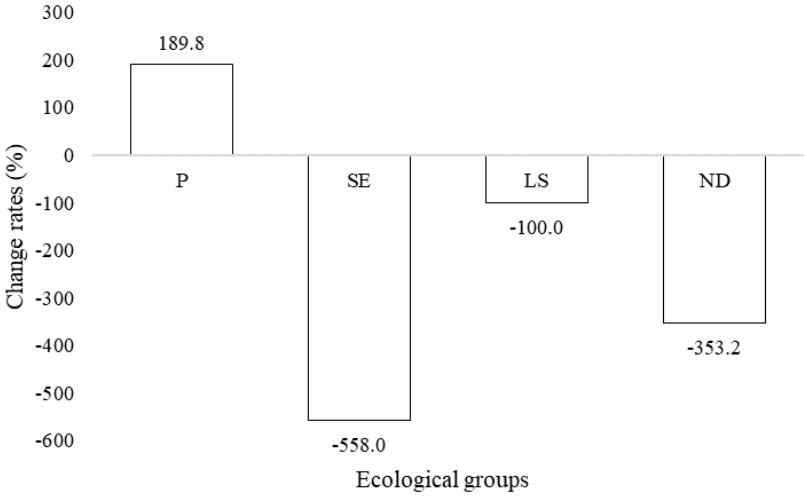

Figure 3. Average rates of change in the regenerative stratum by ecological groups in a remnant of Mixed Ombrophilous Forest in Santa Catarina, Brazil.
P: Pioneers species; SE: Secondary species; LS: late-successional species; ND: Ecological group not defined.

The changes that occurred in this fragment of MOF in the period of four years between the two vegetation censuses show that there was an increase in pioneer species and decreases in secondary and late-successional species. Therefore, the results show that the dynamics of natural regeneration of the forest may not follow the path theoretically expected in such a short period of time, as internal and external disturbances can affect the succession processes.

4. CONCLUSIONS

Considerable changes occurred in the structure and floristic composition dynamics of natural regeneration between the two data surveys.

Pioneer species had the highest rates of positive change, while secondary species had the highest rates of negative change.

This studied remnant forest fragment is in the healing phase after disturbance, since there is a sufficient amount of light falling inside the forest.

5. REFERENCES

AGUIAR, M. D.; SILVA, A. C.; HIGUCHI, P.; NEGRINI, M.; SCHOLLEMBERG, A. L. Similaridade entre adultos e regenerantes do componente arbóreo em floresta com araucária. **Floresta e Ambiente**, v. 24, 2017. https://doi.org/10.1590/2179-8087.083214

ALVARES, C. A.; STAPE, J. L.; SENTELHAS, P. C.; GONÇALVES, J. L. M.; SPAROVEK, G. Köppen's climate classification map for Brazil. **Meteorologische Zeitschrift**, v. 22, n. 6, p. 711-728, 2013. https://doi.org/10.1127/0941-2948/2013/0507

BROWER, J. E.; ZAR, J. H. **Field and laboratory methods for general ecology**. Dubuque: W. M. C. Brow, 1984. 226 p.

CHAZDON, R. L. **Renascimento de florestas**: regeneração na era do desmatamento. São Paulo: Oficina de Textos, 2016. 430 p.

DALLA ROSA, A.; SILVA, A. C.; HIGUCHI, P.; MARCON, A. K.; MISSIO, F. F.; BENTO, M. A.; SILVA, J. O.; GONÇALVES, D. A.; RODRIGUES JÚNIOR, L. C. Natural regeneration of tree species in a cloud forest in Santa Catarina, Brazil. **Revista Árvore**, v. 40, n. 6, p. 1073-1082, 2016. https://doi.org/10.1590/0100-67622016000600013

FELFILI, J. M.; REZENDE, R. P. **Conceitos e métodos em fitossociologia**. Brasília: Departamento de Engenharia Florestal, Universidade de Brasília, 2003. 68 p.

FINOL, U. H. Nuevos parámetros a considerarse en el analisis estructural de las selvas vírgenes tropicales. **Revista Florestal Venezuelana**, v. 14, p. 337-1144, 1971.

GROSS, A.; SILVA, A. C.; CRUZ, A. P.; KILKA, R. V.; NUNES, A. S.; DUARTE, E.; VEFAGO, M. B.; SANTOS, G. S.; LIMA, C. L.; SALAMI, B.; HIGUCHI, P. Fragmentation as a key driver of tree community dynamics in mixed subtropical evergreen forests in Southern Brazil. **Forest Ecology and Management**, v. 411, p. 20-26, 2018. https://doi.org/10.1016/j.foreco.2018.01.013

HESS, A. F.; CALGAROTTO, A. R.; PINHEIRO, R.; WANGINIAK, T. C. R. Propostas de manejo de *Araucaria angustifolia* utilizando o quociente de Liocourt e análise de incremento, em propriedade rural no município de Lages, SC. **Pesquisa Florestal Brasileira**, v. 30, n. 64, p. 337-345, 2010. https://doi.org/10.4336/2010.pfb.30.64.337

HIGUCHI, P.; SILVA, A. C.; FERREIRA, T. S.; SOUZA, S. T.; GOMES, J. P.; SILVA, K. M.; SANTOS, K. F.; LINKE, C.; PAULINO, P. S. Influência de variáveis ambientais sobre o padrão estrutural e florístico do componente arbóreo, em um fragmento de Floresta Ombrófila Mista Montana em Lages, SC. **Ciência Florestal**, v. 22, n. 1, p. 79-90, 2012a. http://dx.doi.org/10.5902/198050985081

HIGUCHI, P.; SILVA, A. C.; FERREIRA, T. S.; SOUZA, S. T.; GOMES, J. P.; SILVA, K. M.; SANTOS, K. F. Floristic composition and phytogeography of the tree component of Araucaria Forest fragments in southern Brazil. **Brazilian Journal of Botany**, v. 35, n. 2, p. 145-157, 2012b. https://doi.org/10.1590/S0100-84042012000200004

HIGUCHI, P.; SILVA, A. C.; BUZZI JUNIOR, F.; NEGRINI, M.; FERREIRA, T. S.; SOUZA, S. T.; SANTOS, K. F.; VEFAGO, M. B. Fatores determinantes da regeneração natural em um fragmento de floresta com araucária no Planalto Catarinense. **Scientia Forestalis**, v. 43, n. 106, p. 251-259, 2015.

KLAUBERG., C.; PALUDO, G. F.; BORTOLUZZI, R. L. C.; MANTOVANI, A. Florística e estrutura de um remanescente de Floresta Ombrófila Mista no Planalto Catarinense. **Revista Biotemas**, v. 23, n. 1, p. 35-47, 2010. https://doi.org/10.5007/2175-7925.2010v23n1p35

LARSEN, J. G.; DUARTE, E.; DREYER, J. B. B.; DALLABRIDA, J. P.; MUZEKA, L. M.; SANTOS, G. N.; RODRIGUES JÚNIOR, L. C.; LIMA, C. L. L.; SILVA, A. C.; HIGUCHI, P. Variación espacio-temporal de la regeneración natural arbórea y arbustiva de bosque de alta montaña en etapa inicial de desarrollo en el sur de Brasil. **Bosque**, v. 40, n. 2, p. 185-193, 2019. https://doi.org/10.4067/S0717-92002019000200185

MAGURRAN, A. E. **Measuring biological diversity**. Oxford: Blackwell Science, 2004. 256 p.

MEYER, L.; GASPER, A. L.; SEVEGNANI, L.; SCHORN, L. A.; VIBRANS, A. C.; LINGNER, D. V.; VERDI, M.; STIVAL-SANTOS, A.; DREVECK, S.; KORTE, A. Regeneração natural da Floresta Ombrófila Mista em Santa Catatina. *In*: VIBRANS, A. C.; SEVEGNANI, L.; GASPER, A. L.; LINGNER, D. **Inventário Florístico Florestal de Santa Catarina**: Floresta Ombrófila Mista. Blumenau: Edifurb, 2013. p. 191-222.

MUELLER-DOMBOIS, D.; ELLENBERG, D. **Aims and methods of vegetation ecology**. New York: Wiley, 1974. 547 p.

NARVAES, I. S.; BRENA, D. A.; LONGHI, S. J. Estrutura da regeneração natural em Floresta Ombrófila Mista na Floresta Nacional de São Francisco de Paula, RS. **Ciência Florestal**, v. 15, n. 4, p. 331-342, 2005. https://doi.org/10.5902/198050981871

NASCIMENTO, A. R. T.; LONGHI, S. J.; BRENA, D. A. Estrutura e padrões de distribuição espacial de espécies arbóreas em uma amostra de Floresta Ombrófila Mista em Nova Prata, RS. **Ciência Florestal**, v. 11, n. 1, p. 105-119, 2001. https://doi.org/10.5902/19805098499

RIBEIRO, M. C.; METZGER, J. P.; MARTENSEN, A. C.; PONZONI, F. J.; HIROTA, M. M. The Brazilian Atlantic Forest: How much is left, and how is the remaining forest distributed? Implications for conservation. **Biological conservation**, v. 42, n. 6, p. 1141-1153, 2009. https://doi.org/10.1016/j.biocon.2009.02.021

SANTANA, L. D.; RIBEIRO, J. H. C.; IVANAUSKAS, N. M.; CARVALHO, F. A. Estrutura, diversidade e heterogeneidade de uma floresta ombrófila mista altomontana em seu extremo norte de distribuição (Minas Gerais). **Ciência Florestal**, v. 28, n. 2, p. 567-579, 2018. https://doi.org/10.5902/1980509832039

SANTOS, K. F.; FERREIRA, T. S.; HIGUCHI, P.; SILVA, A. C.; VANDRESEN, P. B.; COSTA, A.; SPADA, G.; SCHMITZ, V.; SOUZA, F. Regeneração natural do componente arbóreo após a mortalidade de um maciço de taquara em um fragmento de Floresta Ombrófila Mista em Lages – SC. **Ciência Florestal**, v. 25, n. 1, p. 107-117, 2015. https://doi.org/10.1590/1980-509820152505107

SANTOS, G. N.; HIGUCHI, P.; SILVA, A. C.; FARIAS, K. J.; MACHADO, F. D.; DUARTE, E. D.; FERNANDES, C.; VIEIRA, F.; AMARAL, R. S.; AGUIAR, V.; WALTER, F. F.; MORES, B.; REIS, M. A. Regeneração natural em uma floresta com araucária: inferências sobre o processo de construção da comunidade de espécies arbóreas. **Ciência Florestal**, v. 28, n. 2, p. 483-494, 2018. https://doi.org/10.5902/1980509832029

SILVA, J. O.; SILVA, A. C.; HIGUCHI, P.; MAFRA, A. L.; GONÇALVES, D. A.; BUZZI JÚNIOR F.; DALLA ROSA, A.; CRUZ, A. P.; FERREIRA, T. S. Floristic composition and phytogeography contextualization of the natural regeneration of an alluvial forest located in the "Planalto Sul Catarinense" Region, SC, Brazil. **Revista Árvore**, v. 41, 2017. https://doi.org/10.1590/1806-90882017000200003

SOUZA, K.; FAXINA, T. C.; SILVA, G. O.; DIAS, R. A. R.; SILVA, A. C., HIGUCHI, P. Análise fitossociológica de trilha ecológica em Floresta Ombrófila Mista. **Revista de Ciências Agroveterinárias**, v. 13, n. 3, p. 266-274, 2014.

VEFAGO, M. B.; SILVA, A. C.; CUCHI, T.; SANTOS, G. N.; NUNES, A. S.; RODRIGUES JUNIOR, L. C.; LIMA, C. L.; GROSS, A.; KILCA, R. V.; HIGUCHI, P. What explains the variation on the regenerative component dynamics of Araucaria Forests in southern Brazil? **Scientia agrícola**, v. 76, n. 5, p. 405-414, 2019. https://doi.org/10.1590/1678-992x-2017-0304

VIBRANS, A. C.; SEVEGNANI, L.; UHLMANN, A.; SCHORN, L. A.; SOBRAL, M. G.; GASPER, A. L.; LINGNER, D. V.; BROGNI, E.; KLEM, G.; GODOY, M. B.; VERDI, M. Structure of mixed ombrophyllous forests with *Araucaria angustifolia* (Araucariaceae) under external stress in Southern Brazil. **Revista de Biologia Tropical**, v. 59, n. 3, p. 1371-1387, 2011.

VIBRANS, A. C.; MCROBERTS, R.; LINGNER, D. V.; NICOLETTI, A. L.; MOSER, P.; NICOLETTI, A. Extensão original e remanescentes da Floresta Ombrófila Mista em Santa Catarina. *In*: VIBRANS A. C.; SEVEGNANI L.; GASPER A. L.; LINGNER D. V. Inventário Florístico Florestal de Santa Catarina: Floresta Ombrófila Mista. Blumenau: Edifurb, 2013. p. 25-31.

ZELLER, R. H. **Plano de Manejo**: Reserva Particular do Patrimônio Natural Emílio Einsfeld Filho, Santa Catarina. Campo Belo do Sul: Florestal Gateados; 2010.

Ambiente & Água - An Interdisciplinary Journal of Applied Science
ISSN 1980-993X – doi:10.4136/1980-993X
www.ambi-agua.net
E-mail: ambi.agua@gmail.com

Freshwater mollusks as proxies for assessing agrochemicals hazards in Volta Grande Reservoir, Brazil

ARTICLES doi:10.4136/ambi-agua.2681

Received: 26 Nov. 2020; Accepted: 12 Apr. 2021

Andressa Mendes Sene[1*]; Daniel Melo Rosa[2,3]; Silvia Maria Millan Gutierre[1]; Paulo Santos Pompeu[1]

[1]Instituto de Ciências Naturais. Departamento de Ecologia e Conservação. Universidade Federal de Lavras (UFLA), Avenida Doutor Sílvio Menicucci, s/n, CEP: 37200-900, Lavras, MG, Brazil. E-mail: sil.m.gutierre@gmail.com, pompeu@ufla.br
[2]Programa de Pós-graduação em Ciências (FIMAT). Departamento de Física. Universidade Federal de Ouro Preto (UFOP), Rua Cinco, n° 2, CEP: 35400-000, Ouro Preto, MG, Brazil. E-mail: danielnativa@gmail.com
[3]Centro de Bioengenharia de Espécies Invasoras de Hidrelétricas (CBEIH), Avenida José Cândido da Silveira, n° 21000, CEP: 31035-536, Belo Horizonte, MG, Brazil. E-mail: danielnativa@gmail.com
[*]Corresponding author. E-mail: andressasene@hotmail.com

ABSTRACT

Brazil has experienced a rise in the use of agrochemicals in recent years, representing a potential threat to nearby ecosystems. The Volta Grande Reservoir (Minas Gerais/São Paulo, Brazil) has about 87% of its area surrounded by agricultural systems, and many compounds used in agriculture end up being carried into nearby water bodies. Given the potential ecological risk, our purpose was to assess pesticides in the reservoir. We collected specimens of two bivalves and three gastropods using bottom dredging and visual investigation in three different sites within the reservoir. The sampling sites were classified according to their distance from the dam, and all were close to agricultural lands. The samples were processed and frozen for qualitative toxicological analysis using mass spectrophotometry. Eight pesticides were identified, including four organochlorines (Aldrin, p,p'-DDE, Heptachlor epoxide, and Endrin) and organophosphates (Disulfoton, Malathion, Parathion- methyl, and Parathion-ethyl). All five studied species (*Limnoperna fortunei*, *Corbicula fluminea*, *Melanoides tuberculata*, *Aylacostoma tenuilabris*, and *Pomacea* aff. *canaliculata*) presented traces of pesticides in their bodies. Of the eight pesticides found in our analysis, six are illegal in Brazil, raising awareness about the continuous use of forbidden pesticides, and also the ecological risk in the Volta Grande Reservoir area. Our results suggest stricter control by environmental agencies regarding the use and commercialization of these illegal toxic compounds.

Keywords: bivalve, gastropoda, high contamination-risk, organic agrochemicals, pesticides.

Moluscos de água doce como indicadores da presença de agrotóxicos no reservatório de Volta Grande, Brasil

RESUMO

O Brasil tem vivenciado um aumento no uso de agroquímicos nos últimos anos, representando uma ameaça potencial aos ecossistemas. O reservatório de Volta Grande (Minas Gerais/São Paulo, Brasil) tem cerca de 87% de sua área cercada por sistemas agrícolas, e muitos

This is an Open Access article distributed under the terms of the Creative Commons Attribution License, which permits unrestricted use, distribution, and reproduction in any medium, provided the original work is properly cited.

compostos usados na agricultura acabam sendo transportados para corpos d'água próximos. Dado o potencial risco ecológico, nosso objetivo foi avaliar a presença de pesticidas utilizando moluscos de água doce como bioindicadores no reservatório de Volta Grande. Coletamos espécimes de dois bivalves e três gastrópodes usando dragas de fundo e sondagem visual, em três locais diferentes dentro do reservatório. Todos os pontos de amostragem foram classificados de acordo com suas distâncias da barragem, e todos estavam próximos a terras agrícolas. As amostras foram processadas e congeladas para análise toxicológica qualitativa por espectrofotometria de massa. Oito pesticidas foram identificados, incluindo quatro organoclorados (Aldrin, p,p'-DDE, Heptacloro epóxido e Endrin) e organofosforados (Disulfato, Malation, Paration-metil e Paration-etil). Todas as cinco espécies estudadas (*Limnoperna fortunei, Corbicula fluminea, Melanoides tuberculata, Aylacostoma tenuilabris* e *Pomacea* aff. *canaliculata*) apresentaram vestígios de pesticidas nos tecidos. Dos oito agrotóxicos encontrados em nossa análise, seis são ilegais no Brasil, reforçando a preocupação sobre o uso contínuo de agrotóxicos proibidos e também o risco ecológico na área do reservatório de Volta Grande. De acordo com os nossos resultados sugere-se um controle ambiental mais rigoroso por parte dos órgãos ambientais em relação ao uso e comercialização desses compostos tóxicos ilegais.

Palavras-chave: agroquímicos orgânicos, bivalve, gastropoda, pesticidas, risco de contaminação.

1. INTRODUCTION

Brazil has been experiencing intense growth in its agriculture sector for more than three decades. The country is considered one of the greatest agricultural exporters in South America and is projected to continually increase production for the next ten years (OECD/FAO, 2019). To sustain such growth in the agricultural sector, there has been also an increase in the production and use of agrochemicals, especially in the Southwestern region of Brazil (Bombardi, 2017). A great concern regarding the use of agrochemicals is the contamination of water bodies (Srivastav, 2020). A significant part of the agrochemical compounds used end up being transported by atmospheric processes, reaching aquatic environments (Bombardi, 2017). Man-made structures, such as dams and reservoirs, are constantly influenced by agricultural activities in the surrounding areas (Nilsson *et al*., 2005; Morais *et al*., 2014), and are subjected to inputted compounds carried through the watersheds (Frascareli *et al*., 2018). The disruptions of nutrient loads, sediment accumulation, water-flow, surrounded vegetation, and longitudinal gradients (Cantonati *et al*., 2020) caused by man-made reservoirs make them areas of high contamination-risk (Thornton *et al*., 1990).

Agrochemicals such as fertilizers (Khan *et al*., 2018) and pesticides (Starling *et al*., 2019) can be harmful to the environment, and especially to aquatic fauna. Previous studies have shown pesticide assimilation in invertebrates and consumers due to their chemical and physical properties, including hydrophobicity and linkage with total suspended solids (Rao and Ahmad, 2015). When invertebrates feed on nutrients contaminated with toxic compounds, these compounds accumulate in their bodies (bioaccumulation, Vidotti and Rollermber, 2004) and can be passed through the food web via trophic magnification, causing problems to consumers as well as to the predators that feed on invertebrates, including fish and humans (Gall *et al*., 2015; Rao and Ahmad, 2015).

Many mollusks are used as bioindicators of water quality, since they can greatly reflect diversity of species as well as environmental health and impacts (McGeoch, 1998; Oehlmann and Schulte-Oehlmann, 2003). Additionally, mollusks also present fairly long life cycles, the great majority are sessile or have low mobility range, and are relatively large, which facilitates sampling and understanding of ecological conditions in an area (Ligeiro *et al*., 2014). Such

species are ideal tools to evaluate biomagnification and bioaccumulation of metal pollution in the water (Gupta and Singh, 2011), and can be indicators of anthropic alterations in the habitat (Asif *et al*., 2018). There are, for example, many suggestions in the literature of bivalves as bioindicators for organochlorine pesticide contamination in aquatic ecosystems (Larramendy and Soloneski, 2016; Shirapova and Morozov, 2020). Therefore, the sensitivity of mollusks to a wide range of environmental disturbances makes them good proxies for detecting environmental impacts.

Despite the contamination risk that mollusks are subject to in agriculturally-surrounded areas, little information is available about the presence of agrochemical pesticides in these water systems or their inhabitants. With the aim of filling this gap, the present study was performed to determine the presence of pesticides in the Volta Grande Reservoir's most abundant mollusks, to discuss the consequences of pesticide contaminants for the local aquatic fauna, and to point out concerns regarding the use of toxic compounds in the area.

2. MATERIAL AND METHODS

The study was conducted in three sites in the Volta Grande Reservoir, located in the Grande River Basin, a sub-basin of the upper Paraná River Basin (S 20°2′5″ W 48°13′22″; Figure 1). The hydroelectric power plant (HPP) of Volta Grande is located in the municipality of Conceição do Alagoas, between the states of Minas Gerais and São Paulo (Sanches *et al*., 2014). Site 1 is the closest to the dam, with crops and surrounding urban areas (S 20°01′06″ W 48°09′00″); Site 2 is the middle site, surrounded mainly by crops (S 20°06′51″ W 48°02′16″); Site 3 is the most distant from the dam and is also mainly surrounded by crops (S 20°04′06″ W 47°57′13″).

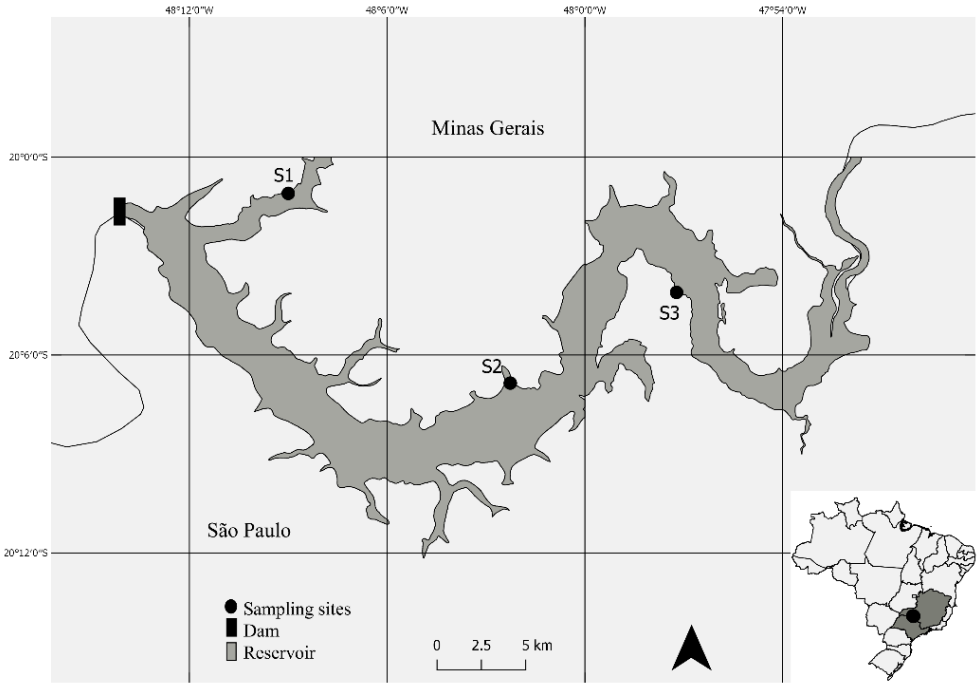

Figure 1. Three sampling sites (S1, S2, and S3) in the reservoir of the Volta Grande Hydroeletric Power Plant, Brazil (QGIS 2.18.22).

The Volta Grande Reservoir is located in São Paulo, the largest agricultural producing state of Brazil (IBGE, 2015). About 87% of the reservoir area is surrounded by agricultural lands (Macedo *et al*., 2014). The area is characterized by mean annual temperatures between 17° and 26°C and annual accumulated precipitation of 1673 mm (INMET, 2010). The rainy season is

between October and March and the dry season from April to September (data from local hydro-meteorological reports). The soil around the reservoir is used for crops of soy and corn in the summer, beans, corn, or sorghum in the winter, and sugar cane year-round (Macedo *et al*., 2014). From the original vegetation cover (Rolla *et al*., 1992), only 6% of forest patches remain; the rest is represented by other crops, open fields (4%), cattle run, buildings, and roads (3%) (Macedo *et al*., 2014).

We sampled three sites of the littoral zone in the Volta Grande Reservoir in January, April, and July 2016. We collected animals once each month, and we made an extra effort in January because the water was too turbid for visual collection. We selected the mollusks to be analyzed according to their abundance in the reservoir (Macedo *et al*., 2014). In order to collect mollusks, a Petersen-type bottom dredging and visual examination were employed. Via bottom dredging, three samples were obtained at each sampling site near the lakeshore, at depths ranging between 2 and 6 m. In the visual examination, visual sediment surveys and hand catches were made at depths up to 1.5 m, with a three-person sampling effort for 25 minutes at each site. Individuals found were sorted by species into 200 mL bottles. In total, 60 full bottles were collected (4 bottles/species for 5 species at each of the 3 sites). The captured specimens were identified (according to Simone, 2006 and Pereira *et al*., 2012), sorted by species, frozen and transported in sealed ice-boxes to be analyzed in the laboratory.

The frozen samples were submitted to qualitative toxicological analysis to determine the presence or absence of organic compounds. We put the macerate of viscera, muscle, and shell in the centrifuge to get the supernatant. Target organic analytes were isolated from the aqueous samples using solid-phase extraction (SPE) media, extracted by the methods EPA 8270-D (according to Lehotay and Schenck, 2000), and analyzed using mass spectrophotometry (EPA 8260C, 5021A, 525.3) in an ISO 17.025 certified laboratory. The compounds found, and further analyzed, were organochlorine (OC) and organophosphate (OP) pesticides, classified according to their chemical nature.

The pesticides were analyzed according to their bioaccumulation potential. According to Walters *et al*. (2016), the bioaccumulation potential is calculated using Trophic Magnification Factors (TMFs - "trophic level change in the log-concentration of a chemical"), which considers the relationship between compounds hydrophobicity values (Kow) and the metabolization time (Km), to represent the compound's biomagnification potential in the food web. The octanol/water partition coefficient (hydrophobicity, Kow) corresponds to the solute affinity in a solution containing equal parts of octanol and water. This affinity property reflects the compound's reaction in a living organism's body with water and lipids (Silva and Ferreira, 2003). Meanwhile, the Km coefficient corresponds to the rate of metabolic biotransformation, or how long it takes for the compound to be metabolized by the organism (Walters *et al*., 2016). We obtained each compound's Kow and Km values from the literature (Kim *et al*., 2020), and applied the numerical relationship between Kow and Km in the figure model proposed by Walters *et al.* (2016, p. 4654) for TMF in freshwater ecosystems.

3. RESULTS AND DISCUSSION

The most abundant mollusks in the Volta Grande Reservoir selected for analysis were the non-native species *Limnoperna fortunei* (Dunker, 1857), *Corbicula fluminea* (Muller, 1774), and *Melanoides tuberculata* (Muller, 1774); and the native species *Aylacostoma tenuilabris* (Reeve, 1860), and *Pomacea* aff. *canaliculata* (Lamarch, 1822). The toxicological analyses showed the presence of eight pesticides, four OC: Aldrin, p,p'-DDE (Dichlorodiphenyldichloroethylene, DDT [dichlorodiphenyl-trichloroethane] metabolite), Heptachlor epoxide, and Endrin; and four OP: Disulfoton, Malathion, Parathion-methyl, and Parathion-ethyl (Table 1). The less frequently found pesticides in the analyzed animals were: Heptachlor epoxide (only in *P.* aff. *canaliculata*, Sites 1

and 3), and Parathion-methyl (only in *C. fluminea*, Site 1) (Table 1, Figure 2). The OPs Disulfoton, Parathion-ethyl, and Malathion were found in all five analyzed mollusks (Table 1). *Pomacea* aff. *canaliculata, L. fortunei, and A. tenuilabris* were found in all sampled sites; *C. fluminea* and *M. tuberculata* were not contaminated in Site 2 (Figure 3, Table 1). Each of the five species analyzed were contaminated with at least five contaminants. The species *C. fluminea* presented a higher number of contaminants (seven), followed by *A. tenuilabris*, and *P.* aff. *canaliculata* (six), while *L. fortunei*, and *M. tuberculata* presented five different contaminants. Site 1 was the most contaminated, with the presence of all pesticides across all samples.

Table 1. Presence of pesticides for each mollusk's species, (*P. can = P. canaliculata; C. flu = C. fluminea; L. for = L. fortunei; A. ten = A. tenuilabris; M. tub = M. tuberculata*) in the Volta Grande reservoir for each sampling sites 1, 2, or 3.

Pesticides	Analyzed species				
	P. can	*C. flu*	*L. for*	*A. ten*	*M. tub*
Aldrin	-	1	-	1	1
Endrin	1, 3	1, 3	1, 2, 3	2, 3	-
p,p'-DDE	1, 2	3	2, 3	1, 2, 3	1
Heptachlor epoxide	1, 3	-	-	-	-
Disulfoton	1, 2, 3	1, 3	1, 3	1, 2	1, 3
Malathion	2	3	1, 3	1, 2	1, 3
Parathion-ethyl	1, 2	1, 3	1, 3	1, 2, 3	1, 3
Parathion- methyl	-	1	-	-	-

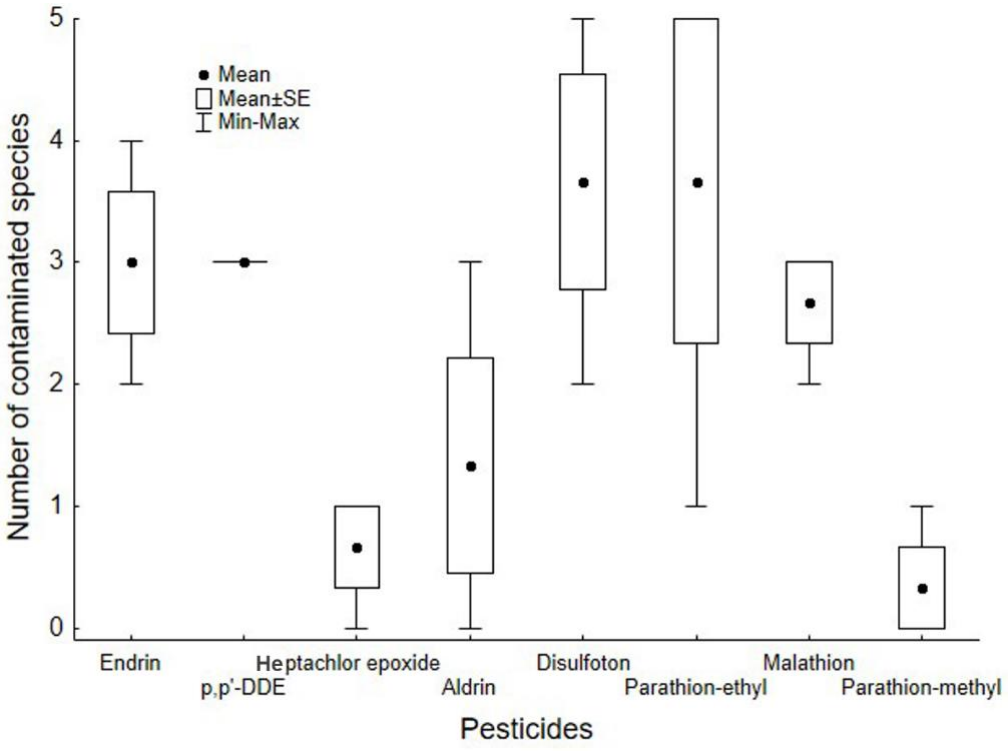

Figure 2. Mean (±SE) number of contaminated species per pesticide.

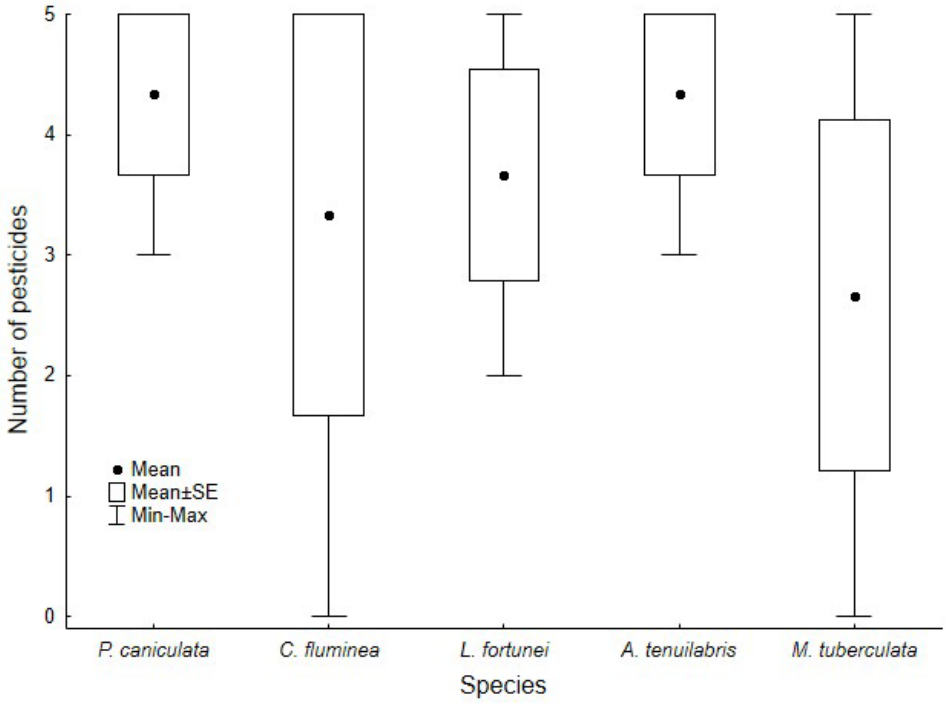

Figure 3. Mean (±SE) number of pesticides found in each analyzed species.

The compounds found are well-known pesticides used in agricultural systems worldwide (Rao and Ahmad, 2015; Srivastav, 2020). The potential health hazards of these pesticides contributed to their prohibition in Brazil. From the pesticides we found contaminating the mollusk species in our study, Aldrin, DDT (the original form of p,p'-DDE), and Heptachlor epoxide were prohibited in Brazil in 1985 by the Ordinance nº 329 (Ministério da Agricultura, Pecuária e Abastecimento) and Parathions in 1998, by the Ordinance nº 11 (Ministério da Saúde). Heptachlor epoxide, for example, was prohibited about 30 years ago, while both Parathions were prohibited about 19 years ago, and yet we found those compounds in most of the analyzed invertebrates across the sampling sites. Disulfoton and Malathion are not prohibited in Brazil, therefore their presence in the analyzed invertebrates implies a constant use in agricultural systems around the reservoir. Starling *et al*. (2019) reviewed the presence of pesticides in different watersheds across Brazil, and presented data on the widespread findings of prohibited pesticides in Brazilian waters. The authors' review corroborates our results that even forbidden compounds are still present in the environment, which can be potentially harmful to aquatic life. Furthermore, the presence of these pesticides in the animals can indicate continuous use of illegal compounds in agricultural areas (reinforced in Starling *et al*., 2019). The presence of DDT in all analyzed species is even more alarming due to its well-known toxicity (Blaylock, 2005) and extensive harmful effects discussed since the renewed publication of Rachel Carson's book, Silent Spring.

Based on the compounds' half-life (Mostafalou and Abdollahi, 2013), it is notable in our study that Heptachlor epoxide (2 years) and Parathion-ethyl (58 days) are still being used in Brazil even after their prohibition decades ago. Parathion-methyl has a very short half-life (1-12 days) and possibly does not stay long enough in the environment to contaminate most of the mollusks, explaining why we found only one species (*P. canaliculata*) contaminated with Parathion-methyl in one site. This contamination may have happened very shortly before the animal collection. By contrast, Tong *et al*. (2018) indicated a tendency of bivalve mollusks to accumulate Heptachlor, Aldrin, or Endrin more than DDT, and it is important to reinforce that

the contamination and accumulation can vary in different environmental conditions and species. The OPs Parathion-ethyl, Malathion, and Disulfoton were found in all studied mollusk species. Of those, Parathion-ethyl is the only one prohibited in Brazil, and should not be found in the environment.

To better visualize TMF results, we adapted the figure from Walters *et al.* (2016, p. 4654) and plotted the values found in our analysis for each compound (Figure 4). Our results showed that Aldrin presented a greater probability of being biomagnified when compared to the other OC, followed by p,p'-DDE, Endrin, and Heptachlor epoxide. For the OPs, Parathion-ethyl and Disulfoton presented low biomagnification probability (Figure 4). High TMF values, or high biomagnification potential, are represented by organic compounds that are moderately hydrophobic (Walters *et al*., 2016; log Kow 6-8) and are slowly metabolized by animals (Km < 0.01). The bioaccumulation potential shown by TMF values is important to indicate the possible effects of pesticides on the food web. The Aldrin found in our results (prohibited in Brazil), has a high probability of biomagnification and a relatively high half-life of 4-7 years (Walters *et al*., 2016). Malathion and Parathion-methyl (logKow 2.36 and 2.86, respectively; Hansch *et al.*, 1996) were not represented in the graph since these two compounds have logKow values lower than 3.5 and therefore do not present a reliable relationship between Kow and Km that could demonstrate their biomagnification potential (Walters *et al*., 2016). According to the International Programme on Chemical Safety (IPCS) and the Food and Agriculture Organization of the United Nations (FAO), the low logKow of Parathion-methyl (and here extrapolated to Malathion), together with the compounds' short environmental persistence, indicate no potential to bioconcentrate.

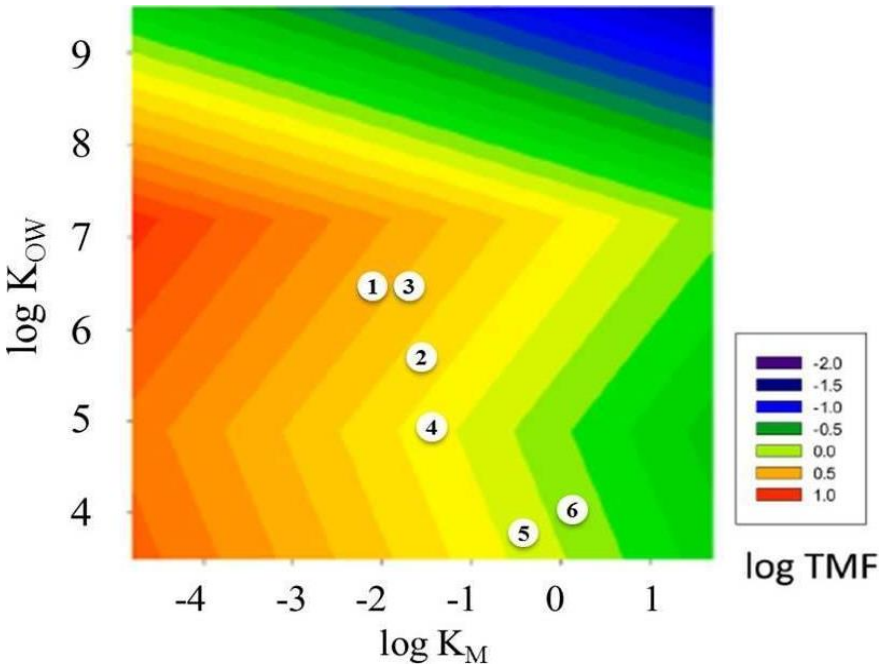

Figure 4. Relationship between metabolization time (logKm) and hydrophobicity (logKow) with log TMFs (presented as a colored gradient in z dimension). Each compound corresponds to a number: 1- Aldrin, 2- Endrin, 3- p,p'-DDE, and 4- Heptachlor epoxide, 5- Parathion ethyl, 6- Disulfoton. The colors indicate the accumulation probability, hot colors (red, orange, and yellow) indicate a high probability of accumulation (TMF>0) and cool colors (greens and blues) indicate a low probability of accumulation (TMF<1).
Source: Walters *et al.*, 2016 (adapted).

We found Aldrin in three species of mollusks in Site 1 (*C. fluminea, A. tenuilabris, M.*

tuberculata). Those same three species are important prey in the Volta Grande Reservoir (Rosa *et al*., 2021), meaning that this pesticide, with its high bioaccumulation potential and environmental persistence (Blaylock, 2005), may have been incorporated in the food chain. The one with the second-highest chance of bioaccumulation that we found, p,p'-DDE, has an even higher half-life (about 10 years) than Aldrin, and it is also prohibited in Brazil (Starling *et al*., 2019). Due to its known contamination harm and the high environmental persistence (Blaylock, 2005), it is alarming that we identified p,p'-DDE in all five mollusk species and all three sampling sites. Endrin presents moderate biomagnification potential and a very wide half-life range (1-12 years). This compound is not prohibited in Brazil, but because it is relatively persistent in the environment (Blaylock, 2005) and the food chain, it can be potentially harmful for the four contaminated mollusk species and the reservoir in general.

The presence of eight pesticides in the analyzed mollusks suggests that the agricultural activity in the surrounding areas of the Volta Grande Reservoir may be impacting the local fauna (as seen in Rao and Ahmad, 2015; Baqar *et al.*, 2018). Some of the pesticides found in our study were also reported in the Parana River Basin's (which includes the Rio Grande) water and sediment samples, including Parathions, Heptachlor, and Aldrin (Lenardon *et al*., 1984). A more recent study in the Furnas Reservoir (in the Rio Grande sub-basin), showed the presence of OC in the water, gills, and liver of two fish species (*Psalidodon fasciatus* and *Pimelodus maculatus*) (Paulino *et al*., 2014). The harmful and even deadly effects of Endrin in fish and birds that feed on *Pomacea* have been already demonstrated (Vermeer *et al*., 1974). Vertebrates such as fish and birds may have been contaminated in the Volta Grande Reservoir since they rely on *L. fortunei* and *P.* aff. *canaliculata* as important items in their diets (Halwart, 1994; Sylvester *et al*., 2007). The fish *Leporinus friderici*, with commercial and environmental importance in the region, may also be contaminated, since it intensely feeds on *L. fortunei* (Rosa *et al.*, 2021). Coat *et al*. (2011) detected a strong and widespread food-web contamination by OC in freshwater ecosystems and the pesticides strongly accumulated by mollusks and shrimps can be affecting higher level animals such as fishes. Organochlorines present higher bioaccumulation potential and environmental persistence than other pesticides (Baird and Cann, 2011). Even though the OC found in our work presented reduced or non-determined bioaccumulation potential, their presence in all species and sites raises an alert regarding the control of prohibited pesticides and the need for further studies on the potential damages caused by these compounds in local environments. However, to assess the trophic contamination risk and food web contamination, more detailed studies are encouraged, including the predators' diets and toxicological analysis to complement our results.

Besides the legal implications of pesticide use and their effects on the food chain, these compounds may also be directly harmful to the animals in the reservoir. As reviewed by Nowell *et al.* (1999), the effects of pesticide on aquatic organisms, specifically mollusks, may include development, reproduction, and behavior changes, endocrine disruption, decreased reproductive success, and defeminization and masculinization of females. Since we found pesticides contaminating all five analyzed mollusks species, as well as some species contaminated with multiple pesticides, there is an increasing concern regarding the reservoir wildlife health and the ecological implications of populations disruptions caused by contamination.

4. CONCLUSIONS

From our results, we suggest that stronger and continuous control is necessary for the Volta Grande Reservoir area to avoid the selling and use of prohibited pesticides. The presence of some pesticides (Heptachlor epoxide, Parathion-methyl, and Parathion-ethyl) in the analyzed mollusks implies that they are still being used even after decades of prohibition. With the

agriculture sector continuously expanding, pesticide use tends to rise as well, and therefore the control should also arise to avoid environmental damages and trophic contamination.

More studies are necessary for the Grande and Paraná River Basins, as well as other similar locations surrounded by agricultural systems, to address how the pesticides are impacting the food web and to support management actions to avoid further contamination. The present work is the first to provide information about pesticide contamination in mollusks of the Grande River Basin. This work is an advisory about the present scenario of pesticide contamination in the region, and raises questions about the environmental health in areas surrounded by agriculture. Considering all the problems pointed out by our work regarding pesticide contamination in the Volta Grande Reservoir area, we emphasize the need for further work to show more details of contamination in the whole food web, the need for a more controlled use of pesticides, and the importance of bringing more awareness and information to local communities regarding the laws and risks of agrochemical use.

5. ACKNOWLEDGEMENTS

We would like to thank Márcia, Paulo and the UFLA Fish Ecology lab group for the support in the field. Jessica Schulte for the English review. André Maciel for textual review. The funding of FAPEMIG (Fundação de Amparo à Pesquisa do Estado de Minas Gerais), CAPES (Coordenação de Aperfeiçoamento de Pessoal de Nível Superior), FUNDECC (Fundação de Desenvolvimento Científico e Cultural), and CEMIG (Companhia Energética de Minas Gerais).

6. REFERENCES

ASIF, N.; MALIK, M.; CHAUDHRY, F. N. A review of environmental pollution bioindicators. **Pollution**, v. 4, n. 1, p. 111-118, 2018. https://dx.doi/10.22059/poll.2017.237440.296

BAIRD, C.; CANN, M. Pesticidas. *In*: BAIRD, C.; CANN, M. **Química ambiental.** Porto Alegre: Bookman, 2011. p. 471-489.

BAQAR, M.; SADEF, Y.; AHMAD, S.; MAHMOOD, A.; LI, J.; ZHANG, G. Organochlorine contaminants in freshwater mussels; occurrence, bioaccumulation pattern, spatio-temporal distribution and human health risk assessment from the tributaries of River Ravi, Pakistan. **Human and Ecological Risk Assessment: An International Journal**, v. 24, n. 5, p. 1268-1290, 2018. https://dx.doi/10.1080/10807039.2017.1411780

BLAYLOCK, B. L. DDT (Dichlorodiphenyltrichloroethane). **Encyclopedia of Toxicology**, v. 2, p. 725-727, 2005. https://dx.doi/10.1016/B0-12-369400-0/00291-X

BOMBARDI, L. M. **Geografia do uso de agrotóxicos no Brasil e conexões com a União Europeia.** São Paulo: FFLCH – USP, 2017. E-book (296 p.).

CANTONATI, M.; POIKANE, S.; PRINGLE, C. M.; et al. Characteristics, main impacts, and stewardship of natural and artificial freshwater environments: Consequences for biodiversity conservation. **Water**, v. 12, n. 1, p. 260, 2020. https://dx.doi/10.3390/w12010260

COAT, S.; MONTI, D.; LEGENDRE, P.; BOUCHON, C.; MASSAT, F.; LEPOINT, G. Organochlorine pollution in tropical rivers (Guadeloupe): role of ecological factors in food web bioaccumulation. **Environmental Pollution**, v. 159, n. 6, p. 1692-1701, 2011. https://dx.doi/10.1016/j.envpol.2011.02.036

FRASCARELI, D.; CARDOSO-SILVA, S.; MIZAEL, J. O. S. et al. Spatial distribution, bioavailability, and toxicity of metals in surface sediments of tropical reservoirs, Brazil. **Environmental monitoring and assessment**, v. 190, n. 4, p. 190-199, 2018. https://dx.doi/10.1007/s10661-018-6515-8

GALL, J.E.; BOYD, R. S.; RAJAKARUNA, N. Transfer of heavy metals through terrestrial food webs: a review. **Environmental monitoring and assessment**, v. 187, n. 4, p. 201, 2015. https://dx.doi/10.1007/s10661-015-4436-3

GUPTA, S. K.; SINGH, J. Evaluation of mollusc as a sensitive indicator of heavy metal pollution in an aquatic system: a review. **The II OAB Journal**, v. 2, n. 1, p. 49-57, 2011.

HALWART, M. The golden apple snail *Pomacea canaliculata* in Asian rice farming systems: present impact and future threat. **International Journal of Pest Management**, v. 40, n. 2, p. 199-206, 1994. https://dx.doi/10.1080/09670879409371882

HANSCH, C.; LEO, A.; HOEKMAN, D. Exploring QSAR – Hydrophobic, Electronic, and Steric Constants. **Journal of American Chemical Society**, n.118, p. 1189-1191, 1996. https://dx.doi/10.1021/ja965433

IBGE. **Produção Agrícola Municipal (PAM)**. 2015. Available in: https://www.ibge.gov.br/estatisticas/economicas/agricultura-e-pecuaria/9117-producao-agricola-municipal-culturas-temporarias-e-permanentes.html?edicao=9118&t=sobre. Access in: August 2017.

INMET. **Normais climatológicas do Brasil.** 2010. Available in: https://portal.inmet.gov.br/normais. Access in: February 2020.

KHAN, M. N.; MOBIN, M.; ABBAS, Z. K.; ALAMRI, S. A. Fertilizers and their contaminants in soils, surface and groundwater. **Encyclopedia of the Anthropocene**, v. 5, p. 225-240, 2018. https://dx.doi/10.1016/B978-0-12-809665-9.09888-8

KIM, S.; THIESSEN, P.A.; BOLTON, E.E.; et al. PubChem Substance and Compound databases. **Nucleic Acids Research**, v. 44, n. D1, p. D1202-1213, 2020. https://dx.doi/10.1093/nar/gkv951

LARRAMENDY, M.; SOLONESKI, S. **Invertebrates**: Experimental Models in Toxicity Screening. 1. ed. Rijeka: InTech, 2016. 117.

LEHOTAY, S. J.; SCHENCK, F. J. Multi-residue methods: extraction. *In:* WILSON, I. D. *et al.* (ed.) **Encyclopedia of separation Science.** Cambridge: Academic Press, 2000. p. 3409-3415.

LENARDON, A. M.; HEVIA, M. I. M.; FUSE, J. A.; NOCHETTO, C. B.; DEPETRIS, P. J. Organochlorine and organophosphorus pesticides in the Parana River (Argentina). **Science of the total environment**, v. 34, n. 3, p. 289-297, 1984. https://dx.doi/10.1016/0048-9697(84)90070-6

LIGEIRO, R.; FERREIRA, W.; CASTRO, D.; FIRMIANO, K. R.; SILVA, D.; CALLISTO, M. Macroinvertebrados bentônicos em riachos de cabeceira: múltiplas abordagens de estudos ecológicos em bacias hidrográficas. *In:* CALLISTO, M.; ALVES, C. B. M.; LOPES, J. M.; CASTRO, M. A. (org.). **Condições ecológicas em bacias hidrográficas de empreendimentos hidrelétricos.** Belo Horizonte: Companhia Energética de Minas Gerais, 2014. cap. 6, p. 127-160.

MACEDO, D. R.; POMEPU, P. S.; MORAIS, L.; CASTRO, M.; ALVES, C. B. M.; FRANÇA, J. S.; SANCHES, B.; UCHÔA, J.; CALLISTO, M. Uso e ocupação do solo, sorteio de sítios amostrais, reconhecimento em campo e realização de amostragens. *In*: **Condições ecológicas em bacias hidrográficas de empreendimentos hidrelétricos**. Belo Horizonte: Companhia Energética de Minas Gerais, 2014. p. 47-68.

MCGEOCH, M. A. The selection, testing and application of terrestrial insects as bioindicators. **Biological reviews**, v. 73, n. 2, p. 181-201, 1998. https://dx.doi/10.1111/j.1469-185X.1997.tb00029.x

MORAIS, L; FARIAS R. L.; MARTINS, I.; BARBOSA, J. E. L.; MOLOZZI, J.; ANACLÉTO, M. J.; CALLISTO, M. Bioindicadores bentônicos de qualidade ambiental em reservatórios da CEMIG. In: **Condições ecológicas em bacias hidrográficas de empreendimentos hidrelétricos**. Belo Horizonte: Companhia Energética de Minas Gerais, 2014. p. 161-184.

MOSTAFALOU, S.; ABDOLLAHI, M. Pesticides and human chronic diseases: evidence, mechanisms, and perspectives. **Toxicology and applied pharmacology**, v. 268, n. 2, p. 157-177, 2013. https://dx.doi/10.1016/j.taap.2013.01.025

NILSSON, C.; REIDY, C. A.; DEYNESIUS, M.; REVENGA, C. Fragmentation and flow regulation of the world's large river systems**. Science**, v. 308, n. 5720, p. 405-408, 2005. https://dx.doi/10.1126/science.1107887

NOWELL, L. H.; CAPEL, P. D.; DILEANIS, P. D. Analysis of key topics-Environmental significance. *In:* NOWELL, L. H.; CAPEL, P. D.; DILEANIS, P. D. **Pesticides in stream sediment and aquatic biota:** distribution, trends, and governing factors. 1. ed. Boca Raton, Florida: CRC Press, 1999. 971 p.

OECD/FAO. Latin American Agriculture: Prospects and Challenges. In: OECD/FAO. **Agricultural Outlook 2019-2028**. Rome, 2019. p. 70-124.

OEHLMANN, J.; SCHULTE-OEHLMANN, U. Molluscs as bioindicators. **Trace Metals and other Contaminants in the Environment**, v. 6, p. 577-635, 2003. https://dx.doi/10.1016/S0927-5215(03)80147-9

PAULINO, M. G.; BENZE, T. P.; SADAUSKAS-HENRIQUE, H.; SAKURAGUI, M. M.; FERNANDES, J. B.; FERNANDES, M. N. The impact of organochlorines and metals on wild fish living in a tropical hydroelectric reservoir: bioaccumulation and histopathological biomarkers. **Science of the Total Environment**, v. 497, p. 293-306, 2014. https://dx.doi/10.1016/j.scitotenv.2014.07.122

PEREIRA, D.; MANSUR, M. C. D.; PIMPÃO, D. M. Identificação e diferenciação dos bivalves límnicos invasores dos demais bivalves nativos do Brasil. *In:* MANSUR, M. C. D.; SANTOS, C. P.; PEREIRA, D.; PAZ, I. C. P.; ZURITA, M. L. L.; RODRIGUEZ, M. T. R.; NEHRKE, M. V.; BERGONCI, P. E. A. (org.) **Moluscos límnicos invasores no Brasil:** biologia, prevenção e controle. Porto Alegre: Redes, 2012. cap. 5, p. 75-94.

RAO, M. R. J.; AHMAD, K. Occurrence of Organochlorine and Organophosphorus Pesticides in *M. scabra* and *M. tuberculata* Species in Tighra Reservoir, Gwalior, India. **Environmental Claims Journal**, v. 30, n. 3, p. 216-227, 2015. https://dx.doi/10.1080/10406026.2018.1467089

ROLLA, M. E.; DEBÉS, M. B. G. S; FRANÇA, R. C.; FERREIRA, E. M. V. M. Inventário limnológico do rio Grande na área de influência da futura usina hidrelétrica (UHE) de Igarapava. **Acta Limnologica Brasiliensia**, v. 4, p. 139-162, 1992.

ROSA, D.M.; SENE, A.M.; MOREIRA, M.Z.; POMPEU, P.S. Non-native prey species supporting fish assemblage biomass in a Neotropical reservoir. **Biol Invasions**, 2021. https://doi.org/10.1007/s10530-021-02510-x

SANCHES, B. O.; BECKER, B.; GOMES, P. L. A.; SANTOS, G. B. A ictiofauna de quatro reservatórios da CEMIG: caracterização das comunidades. In: Condições **ecológicas em bacias hidrográficas de empreendimentos hidrelétricos**. Belo Horizonte: Companhia Energética de Minas Gerais, 2014. p. 185-214.

SHIRAPOVA, G.; MOROZOV, S. Organochlorine pesticides in Baikal bivalve mollusc Colletopterum ponderosum sedakovi. **IOP Conference Series: Materials Science and Engineering**, v. 962, n. 4, p. 042042, 2020. https://dx.doi/10.1088/1757-899X/962/4/042042

SILVA, L.; FERREIRA, M. Estudo do coeficiente de partição octanal-água de bifenilas policloradas (PCBs) utilizando parâmetros topológicos. **Química Nova**, v. 26, n. 3, p. 312-318, 2003. https://dx.doi/10.1590/s0100-404220

SIMONE, L. R. L.; **Land and freshwater molluscs of Brazil**. 2. ed. São Paulo: EGB; Fapesp, 2006. 390 p.

SRIVASTAV, A. L. Chemical fertilizers and pesticides: Role in groundwater contamination. **Agrochemicals Detection, Treatment and Remediation**. Oxônia: Butterworth-Heinemann, 2020. p. 143-159. https://dx.doi/10.1016/B978-0-08-103017-2.00006-4

STARLING, M. C. V.; AMORIM, C. C.; LEÃO, M. M. D. Occurrence, control and fate of contaminants of emerging concern in environmental compartments in Brazil. **Journal of hazardous materials**, v. 372, p. 17-36, 2019. https://dx.doi/10.1016/j.jhazmat.2018.04.043

SYLVESTER, F.; BOLTOVSKOY, D.; CATALDO, D. H. Fast response of freshwater consumers to a new trophic resource: predation on the recently introduced Asian bivalve *Limnoperna fortunei* in the lower Paraná River, South America. **Austral Ecology**, v. 32, n. 4, p. 403-415, 2007. https://dx.doi/10.1111/j.1442–9993

THORNTON, K. W.; KIMMEL, B. L.; PAYNE, F. E. **Reservoir Limnology**: Ecological Perspectives. New York: John Wiley and Sons, 1990. 256 p.

TONG, N. X.; THI, T.; HUONG, T.; THUY, D. T.; HUONG, M.; TRONG, D.; LUC, H. C.; LOAN, P. T.; THI, L.; QUYNH, P. Bioaccumulation of organochlorine pesticides (OCPs) in molluscs and fish at the Sai Gon – Ding Nai estuary. **Journal of Viernamese Environment**, v. 9, n. 5, p. 248-254, 2018. https://dx.doi/10.13141/jve.vol9.no5.pp248-254

VERMEER, K.; RISEBROUGH, R. W.; SPAANS, A. L.; REYNOLDS, L. M. Pesticide effects on fishes and birds in rice fields of Surinam, South America. **Environmental Pollution**, v. 7, n. 3, p. 217-236, 1974.

VIDOTTI, E. C.; ROLLERMBERG, M. D. C. E. Algas: da economia nos ambientes aquáticos à biorremediação e à química analítica. **Química Nova**, v. 27, p. 139-145, 2004. https://dx.doi/10.1590/S0100-4042

WALTERS, D. M.; JARDINE, T. D.; CADE, B. S.; KIDD, K. A.; MUIR, D. C. G.; LEIPZIG-SCOTT, P. Trophic magnification of organic chemicals: A global synthesis. **Environmental Science & Technology**, v. 50, n. 9, p. 4650-4658, 2016. https://dx.doi/10.1021/acs.est.6b00201

Ambiente & Água - An Interdisciplinary Journal of Applied Science
ISSN 1980-993X – doi:10.4136/1980-993X
www.ambi-agua.net
E-mail: ambi.agua@gmail.com

Evaluation of the environmental life cycle of an STP that employs a low-rate trickling filter as post-treatment of a UASB reactor and different sludge-management alternatives

ARTICLES doi:10.4136/ambi-agua.2648

Received: 14 Sep. 2020; Accepted: 19 Apr. 2021

Karina Guedes Cubas do Amaral*; Julio Cezar Rietow; Miguel Mansur Aisse

Departamento de Hidráulica e Saneamento (DHS). Universidade Federal do Paraná (UFPR),
Avenida Coronel Francisco Heráclito dos Santos, n° 100, CEP: 81530-000, Curitiba, PR, Brazil.
E-mail: juliorietow@gmail.com, miguel.dhs@ufpr.br
*Corresponding author. E-mail: kacubas@gmail.com

ABSTRACT

This study aimed to undertake an environmental life cycle assessment (LCA) of a sewage treatment plant (STP) equipped with low-rate trickling filters (TFs) as post-treatment of upflow anaerobic sludge blanket (UASB). The STP is located in South Brazil and uses landfill and agriculture as sludge-disposal alternatives. The evaluation was performed using the LCA technique and SimaPro® 9 software. The results revealed that the gases methane (CH_4) and sulfur dioxide (SO_2), emitted into the atmosphere after the partial burning of the biogas in flares, are mainly responsible for impacts in the categories of global warming (GW) and terrestrial acidification (TA), respectively. Due to the low rate of hydraulic sewage application in TFs, nitrous oxide (N_2O) emissions stood out due to their high impact in the category of stratospheric ozone depletion (SOD). The use of sludge in agriculture obtained a greater potential for environmental impact compared to landfills in five of the eight categories evaluated. The main impacts of agricultural use were in the category of human toxicity (HT), due to the high concentration of zinc present in the sludge, and in the category TA, due to the emission of ammonia (NH_3) during hygienization of the sludge. In turn, the main positive aspects were avoided products, such as urea, phosphate fertilizer and limestone. The results contribute to a greater discussion of sewage-treatment processes, as well as sludge-management alternatives used in developing countries.

Keywords: alkaline stabilization, biogas, biological sludge, environmental assessment, nitrogen dioxide, sanitary landfill.

Avaliação do ciclo de vida ambiental de uma ETE que emprega filtro biológico percolador, de baixa taxa, como pós-tratamento de um reator UASB e diferentes alternativas de gerenciamento de lodo

RESUMO

O presente estudo teve por objetivo realizar a avaliação de ciclo de vida (ACV) ambiental de uma estação de tratamento de esgoto (ETE), dotada de filtros biológicos percoladores (FBPs) de baixa taxa, como pós-tratamento de reatores anaeróbios - UASB. A ETE está localizada no sul do Brasil e emprega como alternativas de destinação do lodo o aterro sanitário e o uso

This is an Open Access article distributed under the terms of the Creative Commons Attribution License, which permits unrestricted use, distribution, and reproduction in any medium, provided the original work is properly cited.

agrícola. Para realizar a avaliação, utilizou-se a técnica de ACV, empregando o software SimaPro® 9. Os resultados evidenciaram que os gases metano (CH_4) e dióxido de enxofre (SO_2), emitidos para a atmosfera, após a queima parcial do biogás em queimadores abertos, são os principais responsáveis pelos impactos nas categorias de mudanças climáticas (GW) e acidificação terrestre (TA), respectivamente. Devido à baixa taxa de aplicação hidráulica de esgoto nos FBPs, as emissões de óxido nitroso (N_2O) se destacaram pelo elevado impacto na categoria de depleção de ozônio estratosférico (SOD). O emprego do lodo na agricultura obteve um maior potencial de impacto ambiental, em relação ao aterro sanitário, em 5 das 8 categorias avaliadas. Os principais impactos do uso agrícola foram na categoria de toxicidade humana (HT), devido à elevada concentração de zinco presente no lodo, e na categoria de acidificação terrestre (TA), em virtude da emissão de amônia (NH_3) durante a higienização do lodo. Por sua vez, os principais aspectos positivos foram os produtos evitados como ureia, fertilizante fosfatado e calcário. Os resultados reportados contribuem para uma maior discussão dos processos de tratamento de esgoto, bem como de alternativas de gerenciamento de lodo, empregados em países em desenvolvimento.

Palavras-chave: aterro sanitário, avaliação ambiental, biogás, dióxido de nitrogênio, estabilização alcalina, lodo biológico.

1. INTRODUCTION

Population growth in Latin America and the Caribbean (LAC) has surpassed the capacity of national and local governments to meet the demand for basic sanitation services, especially those inherent in the collection and treatment of sewage (Noyola *et al.*, 2012). In Brazil, recent data from Agência Nacional de Águas (ANA; National Water Agency) confirm this problem by disclosing that the sanitary sewage collection rate in the country is 61.4%, and that only 42.6% of all sewage generated is treated (ANA, 2017). These data indicate that approximately 65 million Brazilians still do not have access to a collective system to remove sewage, and about 97 million do not have the sewage from their homes treated. Therefore, new sewage treatment plants (STPs) and the expansion of the capacity and treatment level of existing STPs should be planned in the coming years, since the intention is to universalize sewage servicers in the country.

One of the sewage technologies that should continue to be widely used in Brazil is that of upflow anaerobic sludge blanket (UASB) rectors. Present in 1,047 STPs, UASB reactors represent the most used treatment technology in the country (ANA, 2017). This is mainly due to low costs of implementation and operation compared to aerobic treatment systems (Chernicharo *et al.*, 2018). In addition, UASB reactors are responsible for the production of biogas, which is endowed with energy potential because it contains methane (CH_4) in its composition and can therefore be used for energy purposes within the treatment plant itself (Moran *et al.*, 2010). However, it should be noted that most Brazilian STPs collect biogas and conducted it to flares, in order to reduce rates of greenhouse gas emissions (Amaral *et al.*, 2018; Possetti *et al.*, 2019), since CH_4 has a global warming potential 34 times greater than that of carbon dioxide (CO_2) (IPCC, 2014). An additional aim of burning biogas is to reduce problems related to bad odors and equipment corrosion due to hydrogen sulfide (H_2S) present in the medium (Possetti *et al.*, 2018). However, if H_2S destruction occurs in low-efficiency burners, sulfur dioxide (SO_2) may form in the atmosphere (Possetti *et al.*, 2018).

Despite the recognized advantages, it should be emphasized that exclusive use of UASB reactors may be insufficient to meet legal requirements for discharging effluents into bodies of water (Almeida *et al.*, 2018). Thus, aerobic treatment processes, such as activated sludge and, mainly, trickling filters (TFs), are being used in Brazil as a stage for post-treatment of effluents

from UASB reactors. The efficiency of removing organic matter in TFs systems can vary according to the hydraulic rate applied to its surface, or even the organic load applied to the volume of the percolating filter media, thus resulting in three possible types of TFs: low rate (1 to 4 $m^3.m^{-2}.d^{-1}$ or 0.08 to 0.4 $kgBOD.m^{-3}.d^{-1}$), intermediate rate (4 to 10 $m^3.m^{-2}.d^{-1}$ or 0.4 to 0.48 $kgBOD.m^{-3}.d^{-1}$) and high rate (10 to 40 $m^3.m^{-2}.d^{-1}$ or 0.48 to 1.0 $kgBOD.m^{-3}.d^{-1}$) (Metcalf & Eddy, 2016).

Low-rate TFs have an organic removal efficiency of more than 80%, with high effluent nitrification capacity (Corrêa, 2019). Although nitrification reduces the environmental problems intrinsic to the discharge of effluents into water bodies, it should be emphasized that it is responsible for the production of nitrous oxide (N_2O) (Vasilaki *et al.*, 2019), which has a global warming potential 265 times greater than CO_2 (IPCC, 2014). Still, TFs can also be a source of CH_4 emissions, since up to 40% of this biogas remains dissolved in the effluent of the UASB reactors and can be released in the post-treatment stage (Souza *et al.*, 2011). Within this context, STPs that employ UASB reactors followed by low-rate TFs can become a significant source of CH_4 and N_2O (El-Fadel e Massoud, 2001). Studies referring to the assessment of environmental impacts of systems composed of UASB reactors followed by low-rate TFs are incipient (Bressani-Ribeiro *et al.*, 2017), and there is still no integrated discussion of the environmental problems inherent to these two treatment technologies.

In addition to the issues of gaseous emissions arising from sewage treatment, another by-product generated by STPs that can bring a series of significant environmental impacts is sludge (Amaral *et al.*, 2019). Characterized by high concentrations of nutrients and organic matter, sludge can be used as a fertilizer in agriculture (Bittencourt, 2014; Cieslik *et al.*, 2015). However, sludge also has high levels of water and pathogenic microorganisms and, thus, processes of dewatering and hygienization must be performed for its use as a biofertilizer (Lobato *et al.*, 2018). A practice adopted by some sanitation companies in Brazil is to dewater sludge, in drying beds or in centrifuges, followed by prolonged alkaline stabilization (PAS).

The process of PAS consists of raising the pH of the sludge to 12 for a minimum period of 2 hours by the application of chemical products, such as lime, for example. The mixture must be sufficient to ensure that the entire mass of the sludge in contact with the lime suffers an increase in pH (USEPA, 1992). It should be noted that during this process there is a release of ammonia (NH_3), which is another significant point of emission in an STP that employs such a procedure (Amaral *et al.*, 2019). After the mixing step, the sludge must be sent to a curing and storage yard, where it will remain for a period of 35 to 45 days (Andreoli *et al.*, 2014). Despite being considered a recognized practice worldwide, the agricultural destination of sewage sludge is performed by few sanitation companies in Brazil. This is mainly due to the difficulty that these companies have in meeting the criteria and procedures established by Brazilian legislation for agricultural use (Bittencourt *et al.*, 2014). Thus, the main destination of the sludge produced in Brazilian STPs remains the sanitary landfill. Studies of environmental impacts resulting from sludge disposal alternatives in developing countries (Hernandez-Padilla *et al.*, 2017; Amaral *et al.*, 2018), whether in agricultural areas or landfills, are also incipient.

Based on the understanding of the need for new studies based on the survey of environmental impacts in STPs, it should be emphasized that the development of inventories, as well as the application of decision-making tools such as the Life Cycle Assessment (LCA), are fundamental for the identification of strategies to mitigate environmental impacts and in the choice of environmentally correct alternatives for sewage treatments and final disposal of sludge. In this context, the objective of this article was to carry out an environmental LCA of an STP that employs UASB reactors followed by low-rate TFs, with the a primary focus on CH_4, H_2S, N_2O and NH_3 emissions to the atmosphere, as well as on comparing environmental impacts between the sludge disposal alternatives of landfills and agricultural areas.

2. MATERIALS AND METHODS

2.1. Study area

To meet the objective of the present study, a small STP located in the South Region of Brazil, was used as a study area. With a capacity to treat sewage of a population of up to 52 thousand inhabitants, the plant has a design flow equal to 90 $L.s^{-1}$. The treatment system adopted at the STP, consists: preliminary treatment (course and fine screens, grit chamber and a Parshall flow meter); 03 (three) UASB reactors; 02 (two) low-rate TFs and 02 (two) circular secondary decanters. To maintain the active biota in the biofilm during periods of low flow (dawn, for example), the effluent from the TFs is recirculated. More detailed information about the UASB reactors and the TFs implanted in the studied STP are shown in Table 1.

Table 1. Characteristics of the UASB reactors and the TFs implanted in the STPs under study.

Parameters	**UASB reactors**	**TFs**
Population (inhab)	34,000 (52,000)*	
Flow rate ($L.s^{-1}$)	33 (90)*	
Hydraulic retention time (h)	11.3 (8.0)*	–
Volumetric organic load ($kgBOD.m^{-3}.d^{-1}$)	0.8	0.1 – 0.4
Volumetric hydraulic load ($m^3.m^{-2}.d^{-1}$)	–	1 – 4
Number of reactors	3	2
Type	Trunk-conical	Circular
Diameter of each reactor (m)	18	22
Useful depth of each reactor (m)	5.75	3.0
Useful volume of each reactor (m^3)	800	1,140

* Values in parentheses refer to design parameters.

The waste produced in the preliminary treatment (waste from the screens and grit chamber) is sent to a landfill. The sludge from the UASB reactors and secondary decanters is directed to cover conventional drying beds. After the dewatering process, the sludge is sent for hygienization in a Sludge Management Unit (SMU) for the PAS process to be carried out. After the curing period, the sludge can be made available for agricultural areas. In sporadic situations, after the dewatering process in the drying beds, the sludge can be sent to a sanitary landfill without the need, therefore, for the hygienization step. Finally, the biogas produced in the UASB reactors is collected and conducted to flares with low CH_4 destruction efficiency.

2.2. Elaboration of environmental inventories for LCA

The elaboration of environmental inventories of the domestic sewage treatment processes, as well as the sludge management alternatives used in the STP, took place through the use of primary (measured) and secondary (bibliographical references/data of Ecoinvent® database) data of parameters correlated with the gaseous, liquid and solid phases of the STP (Figure 1). The chosen functional unit for the study was the treatment of 1 m^3 of sewage. Another parameter considered in the study was the consumption of electricity in the treatment plant. These data were obtained directly from the sanitation company responsible for the STP.

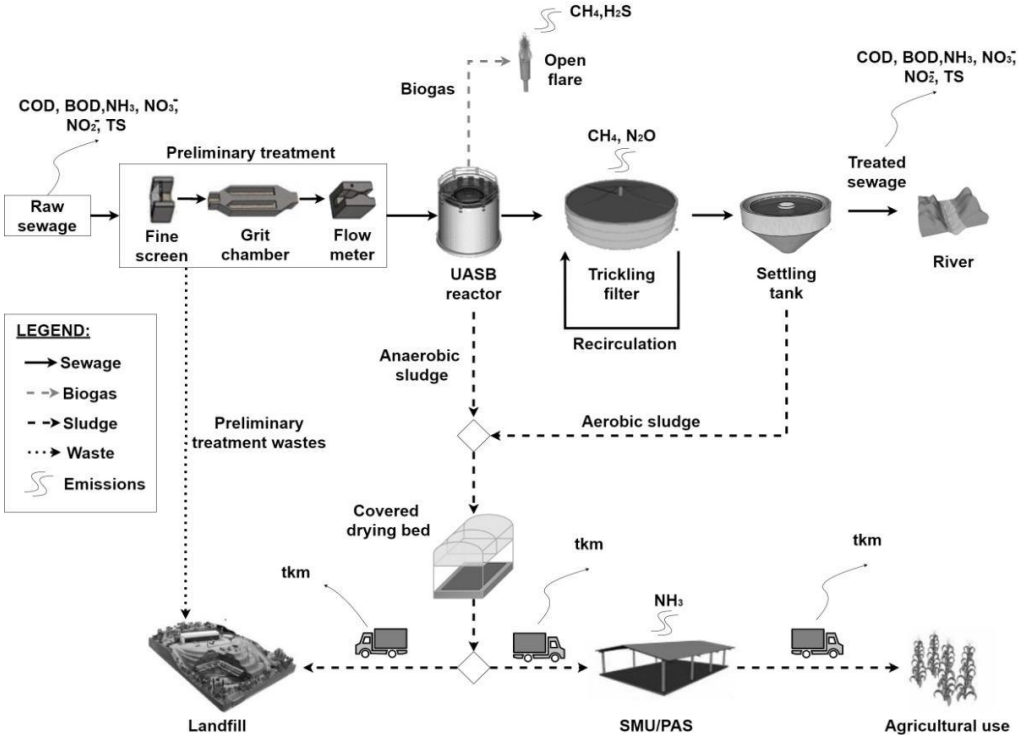

Figure 1. Schematic diagram of the gaseous, liquid and solid phases in the STP under study.

2.2.1. Gaseous phase

Environmental inventory of the gaseous phase included the following: flow and characterization of the biogas produced in the UASB reactors; efficiency of flares with respect to the destruction of CH_4 and H_2S; emission rates of N_2O and CH_4 in TFs; and emissions of NH_3 during PAS of the sewage. The study also took into account emissions related to the transportation of lime to the STP (for the PAS process), the transportation of sludge to the agricultural area or sanitary landfill, and the process of applying the sanitized sludge to the agricultural area.

The flow of biogas produced in the UASB reactors was calculated using ProBio 1.0 *software* (2021). The input data required by the *software* were sewage flow and chemical oxygen demand (COD) affluent to the UASB reactors. These data were obtained from the STP and refer to average values found during 2018. The values reported by Lobato *et al.* (2012) were used for biogas composition, being, in volumetric relations ($v.v^{-1}$), equal to: 70% for CH_4 and 1,500 ppm for H_2S. The destruction efficiency for CH_4 and H_2S in flares was obtained through studies carried out by Kaminski *et al.* (2018). According to these authors, this type of burner has a destruction efficiency, on average, for these gases of 50%.

Regarding emissions of N_2O and CH_4 in the TFs of the STP, the reference values of a domestic sewage treatment system of the constructed vertical *wetland* type were used (Fuchs *et al.*, 2011; Gutierrez, 2014). It should be noted that the adoption of these values was due to the hydraulic similarity between the systems and also due to the fact there are no emission data in literature for N_2O and CH_4 in TFs at full scale. Thus, emissions of 2.68 $gCH4.m^{-3}{}_{sewage}$ and 0.23 $gN2O.m^{-3}{}_{sewage}$ in TFs were considered. The NH_3 emission value, in the PAS of sludge, was obtained from studies carried out by Amaral *et al.* (2018), who found an average emission value of 1.2 $gNH_3.m^{-3}{}_{sewage}$. Emissions related to the transportation of lime to the STP, as well as the destinations of the waste from the preliminary treatment and the dewatered sludge, whether an agricultural area or landfill, were reported according to the parameter tkm, which considers the mass transported (in tons) and the distance covered (round trip in kilometers). Finally,

emissions related to the application of sludge in agriculture areas followed the models presented by Nemecek and Schnetzer (2011), according to the study of Amaral *et al.* (2018).

2.2.2. Liquid phase

Environmental inventory of the liquid phase considered the following parameters for the influent and effluent of the STP: COD, biochemical oxygen demand (BOD_5), NH_3, nitrate (NO_3^-), nitrite (NO_2^-) and total solids (TS). Collections were performed at these points during two 24-hour sampling campaigns in the years of 2017 and 2018. The analyses followed the procedures established in *Standard Methods for the Examination of Water and Wastewater* (Apha *et al.*, 2012).

2.2.3. Solid phase

The amount of waste from the preliminary treatment was obtained from the monthly average of 2018 in the STP. The amount of total solids (TS) in the biological sludge from the UASB reactors and the TFs was estimated from the COD applied at the STP. For this, the production of TS in UASB reactors followed by aerobic-post-treatment was used, which is 0.25 kgST.kgCOD applied (Andreoli *et al.*, 2014).

The environmental inventory of the hygienized sludge application process in agricultural areas took into account the models reported by Nemecek and Schnetzer (2011). The input data required for the modeling were: nitrogen (N) and phosphorus (P) content in the hygienized sludge, characteristics of the soil where the sludge is to be disposed and the products avoided by the agricultural use of the sludge. Thus, the levels of N and P used were 10.2 $g.kg^{-1}$ and 3.6 $g.kg^{-1}$, respectively. The soil type considered was Haplic Cambisol with its specific characteristics of clay content, organic carbon content and the amount of eroded soil. For the application of hygienized sludge in the agricultural area, urea (with 45% nitrogen content), phosphate fertilizer (P_2O_5) and limestone were considered as avoided products. This step used the characterization data for hygienized sludge reported by Amaral *et al.* (2018).

Data relating to the manufacture of products avoided in agricultural use, the manufacture of polymer (used for dewatering), the manufacture of lime, the type of transport by motor vehicles and the production of diesel for fuel and electricity generation were obtained through the Ecoinvent® database. For lime, Relative Power of Total Neutralization (RPNT) of 75% was considered, while a RPNT of 110% was considered for lime (contained in biological sludge) (Bittencourt, 2014). Finally, since there are no specific environmental inventories of impacts related to sludge deposited in landfills, the present study used data of environmental inventories of a landfill that receives sludge from the paper industry. This consideration was made due to the composition and biodegradability of this material being closer to those of STP sludge used in Brazilian landfills.

2.3. Assessment of environmental impacts

The environmental impact was calculated using the LCA methodology and SimaPro® 9 *software*. The method used was ReCiPe 2016 Midpoint (H). The assessed impact categories were: global warming (GW), stratospheric ozone depletion (SOD), ozone formation - terrestrial ecosystems (OTE), terrestrial acidification (TA), aquatic eutrophication (fresh water) (EUT-AW), terrestrial ecotoxicity (TE), freshwater ecotoxicity (FWE) and human toxicity – non cancer (HT).

3. RESULTS AND DISCUSSION

3.1. Environmental inventory of the processes used in the STP

Table 2 shows the environmental inventory of the flows, into and out, of the phases

(gaseous, liquid and solid) referring to the sewage treatment processes (preliminary treatment, UASB reactors, TFs, secondary decanters) and the different sludge management alternatives (destination for landfill or agricultural area) employed at the studied STP.

Samples of sewage affluent to the STP had values within the ranges for typical concentrations of domestic sewage found in the literature (Aisse, 2002; Von Sperling, 2014). The average efficiency of the STP for removing COD and BOD_5 was over 87%. For the nitrification process, the average reduction of NH_3 in the TFs was 43%. Similar results were obtained by Lopes *et al.* (2018) in vertical *wetlands* as a post-treatment step for UASB reactors. The estimate of biogas production in the UASB reactors was 341 $m^3.d^{-1}$. Considering the lower calorific power (LCP) of CH_4 equal to 9.9 $kWh.m^{-3}$, the chemical potential that could be used in the STP would be approximately 3,376 $kWh.d^{-1}$. This potential is not greater, due to fugitive emissions in the reactor and the CH_4 not recovered in the biogas, that remains dissolved in the treated effluent. According to Souza *et al.* (2011), concentrations of 17 to 22 $mg.L^{-1}$ of CH_4 can be found in liquid medium. Regarding the destination of the sludge, it should be noted that the distance from the STP to the SMU, and from this to the agricultural area, increased the parameter of tkm by approximately two times in relation to disposal in landfill.

Table 2. Inventory of the Life Cycle of processes used in the STP.

Inputs (Pollutants in domestic wastewater)	**Concentration ($mg.L^{-1}$)**	**Correlated to functional unit**
Chemical oxygen demand (COD)	565.0	0.565 $kg.m^{-3}$
Biochemical oxygen demand (BOD)	293.0	0.293 $kg.m^{-3}$
Unionized ammonia (NH_3 - N)	65.7	0.066 $kg.m^{-3}$
Nitrate (NO_3^- - N)	1.2	0.0012 $kg.m^{-3}$
Nitrite (NO_2^- - N)	0.2	0.0002 $kg.m^{-3}$
Input (energy)	**Demand ($kWh.d^{-1}$)**	**Correlated to functional unit**
Electricity consumed	1,086.5	0.38 $kWh.m^{-3}$
Emissions to water (final treated effluent)	**Concentration ($mg.L^{-1}$)**	**Correlated to functional unit**
Chemical oxygen demand (COD)	68.0	0.068 $kg.m^{-3}$
Biochemical oxygen demand (BOD)	17.0	0.017 $kg.m^{-3}$
Unionized ammonia (NH_3 - N)	37.5	0.0375 $kg.m^{-3}$
Nitrate (NO_3^- - N)	9.0	0.009 $kg.m^{-3}$
Nitrite (NO_2^- - N)	5.0	0.005 $kg.m^{-3}$
Total solids (TS)	19.0	0.019 $kg.m^{-3}$
Biogas production in UASB reactors	**Flow rate ($m^3.d^{-1}$)**	**Correlated to functional unit**
Biogas (70% – CH_4 and 1,500 ppm – H_2S)	341.1	
Emissions to air	**Flow rate ($m^3.d^{-1}$)**	**Correlated to functional unit**
Methane (CH_4)[a]	119.4	0.042 $m^3.m^{-3}$
Hydrogen sulfide (H_2S)[a]	0.26	0.00009 $m^3.m^{-3}$
Nitrous oxide (N_2O) – Trickling filter		0.23 $g.m^{-3}$
Methane (CH_4) – Trickling filter[b]		2.68 $g.m^{-3}$
Solid waste	**Production ($kg.d^{-1}$)**	**Correlated to functional unit**
Preliminary treatment waste	82.6	0.029 $kg.m^{-3}$
Dewatered sludge	500.0	0.17 $kg.m^{-3}$
Solid waste transportation	**Mass x distance (tkm)**	**Correlated to functional unit**
Preliminary treatment waste – Landfill		0.0033 $tkm.m^{-3}$
Dewatered sludge – Landfill		0.066 $tkm.m^{-3}$
Dewatered sludge – Agricultural area		0.01412 $tkm.m^{-3}$

[a]Considering an efficiency of 50% destruction in the flare; [b]Methane dissolved ($CH_{4\ dissolved}$) in the UASB reactor effluent emitted in the Trickling filter.

3.2. Environmental assessment of the STP with sludge being destined to landfill

Figure 2 shows the contribution of each process used in the STP to the impact categories evaluated for the landfill sludge disposal scenario. The biggest contribution to the GW category, with a 53% influence, was the stage of burning the CH_4 produced in the UASB reactors. Due to the low efficiency of flares (~50%), a significant portion of CH_4 is still emitted into the atmosphere. With a CH_4 flow rate equal to 238 $m^3.d^{-1}$ in the UASB reactors (70% in relation to biogas), it is calculated that 119 $m^3.d^{-1}$ of this gas is emitted into the atmosphere by the burners. Considering a density of 0.657 $kg.m^{-3}$ and a global warming potential 34 times higher than CO_2, the flow of CH_4 emitted corresponds to an average rate of greenhouse gas emissions of approximately 1,000 $tCO_2eq.year^{-1}$. The TFs and the final effluent of the STP are also considered to be CH_4 emission sources, contributing about 25% of the impacts to the GW category. Finally, the sending of sludge to landfill contributed about 14% to the environmental impacts that occurred in the GW category. This percentage is associated with CH_4 and CO_2 produced during the degradation of this material in landfill cells.

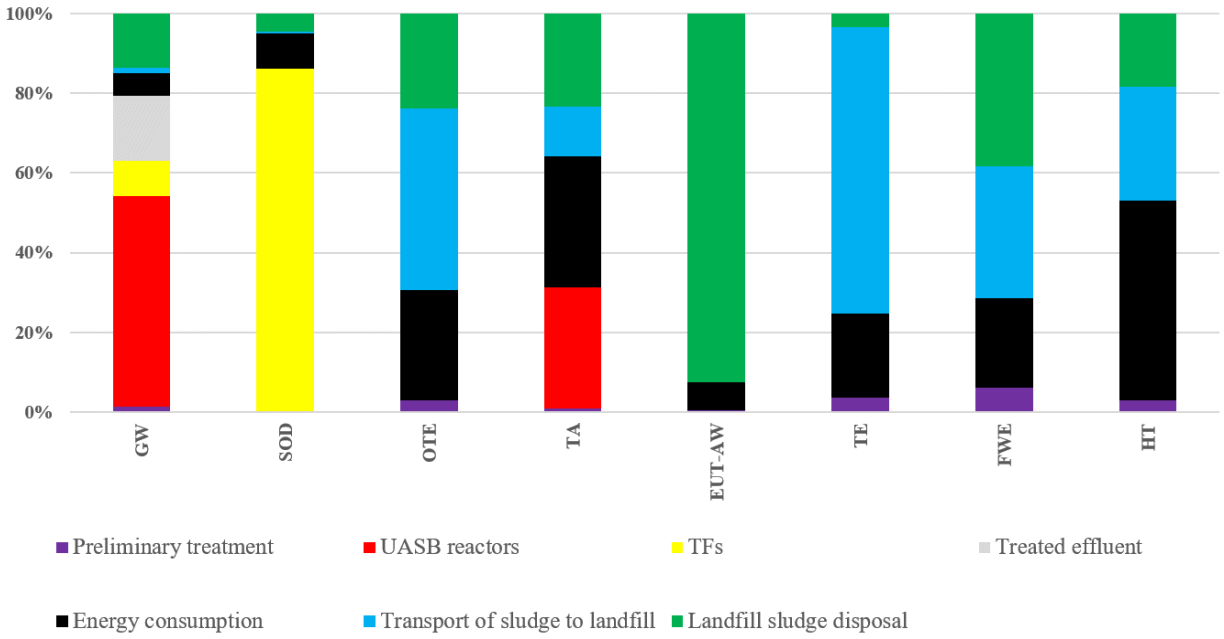

Figure 2. Contribution of each treatment step in the categories of environmental impacts evaluated considering the destination of sludge in landfill.

The process with the greatest influence on the SOD category was the TFs (86%) due to N_2O emissions. In the stratosphere, N_2O plays an important catalytic role in the consumption of stratospheric ozone (O_3), having a residence time in the media of up to 120 years (Ravishankara *et al.*, 2009). One way to reduce the impacts caused by the emission of this gas in TFs is to carry out more adequate control of the aeration process. It should be noted that the alternative of sending the sludge to landfill contributes only about 5% to the environmental impacts of the SOD category.

The process of transporting sludge to landfills had an approximately 45% influence on the impacts caused in the OTE category. This is mainly due to emissions of nitrogen oxides (NO_x) from the use of diesel as a fuel in motor vehicles. NO_x is a major contributor to increased ozone concentration on the Earth's surface, which in turn contributes to the worsening of air pollution in cities and acid rain (Quiros *et al.*, 2017). As for OTE, the TE category also had the transport of sludge to the landfill as the main environmental impact process, with an influence of approximately 72%. This influence is due to copper (heavy metal) emissions resulting from wear and tear on brakes in motor vehicles. Vehicle brake systems are made up of brake pads

composed mainly of copper fibers. The pad, when forced by the rotating brake disc, generates wear on the fibers causing the emission of copper (Simons, 2013). Tire wear during the sludge transport process was one of the main factors responsible for the impacts measured in the FWE category. Still, for this category, zinc present in landfill leachate contributed approximately 40% of the impacts.

The most impactful process in the TA category, with a 30% influence, was the emission of sulfur dioxide (SO_2) and H_2S in the burners of the UASB reactors. As the burners are unable to fully combust the biogas, SO_2 is formed and emitted into the atmosphere. The transportation and disposal of sludge in landfills had an influence of about 36% on the TA category. This is also due to SO_2 (produced during sludge transport due to the possibility of incomplete burning of diesel).

The process that contributed most to the EUT-AW category was the destination of sludge in landfills, with 92%. This is due to the high presence of phosphate (PO_4^{3-}) in the leachate in the landfill. The inventory used considered the emission of 0.437 $gPO_4^{3-}.kg^{-1}$ of waste to the river and 0.272 $gPO_4^{3-}.kg^{-1}$ to groundwater. In the HT category, the processes of transportation and disposal of sludge in landfills had an influence of approximately 50%.

3.3. Environmental assessment of the STP with sludge destined for agriculture use

Figure 3 shows the contribution of each process used in the STP considering sludge disposal in agriculture. For the GW category, CH_4 emissions to the atmosphere in the UASB reactors, TFs and final effluent remain the main sources of environmental impact. Sludge transport and final destination for agriculture only had a 5% influence on this category. In turn, the agricultural use of sludge was responsible for approximately 80% of the impacts in the TA category, which is mainly due to the emission of NH_3 in the PAS process. Although the application of lime raises the pH in the sludge, ensuring the reduction of pathogenic microorganisms (Bittencourt, 2014), this process also causes a significant amount of NH_3 to be volatized.

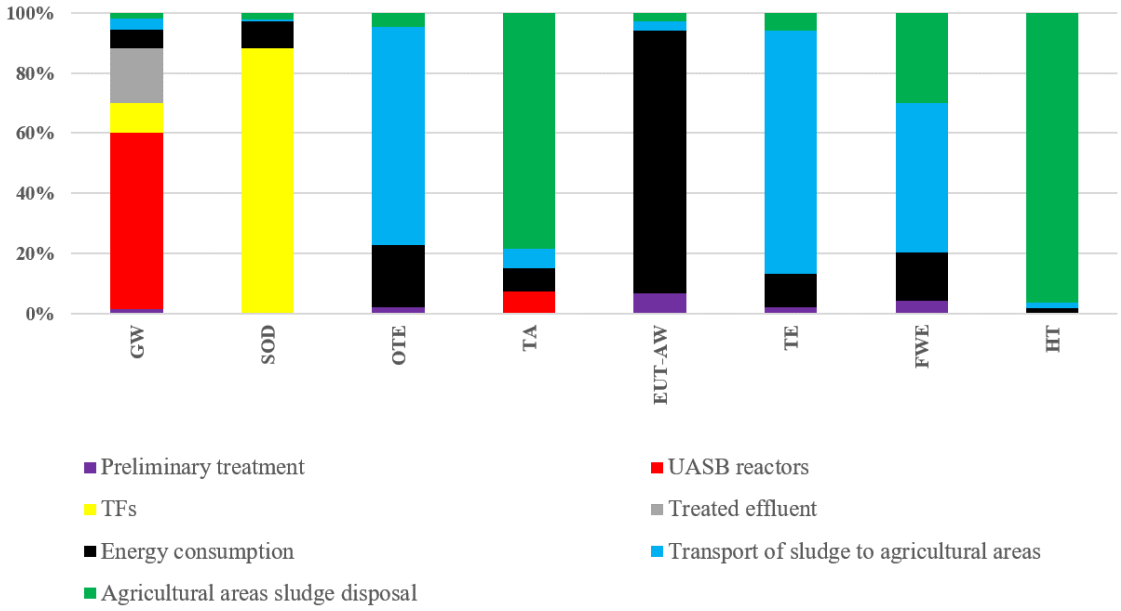

Figure 3. Contribution of each treatment step in the categories of environmental impacts evaluated considering the destination of sludge in agricultural areas.

In the SOD category, N_2O emissions in TFs continued to be the main contributor responsible for the measured environmental impacts. The destination of sludge in agriculture

was responsible for only 3% of the impacts caused in this category. Sludge transport was responsible for contributing approximately 70% of the impacts caused in the OTE category (due to NO_x emissions form the use of diesel) and 80% of the impacts in the TE category (due to copper emissions).

The transport and use of sludge in the agricultural area were responsible for about 80% of the impacts measured in the FWE category. With regard to transport, tire wear was the main source of impact. In sludge application, the high concentration of zinc (heavy metal) in the sludge (514 $mg.kg^{-1}$) used in the present study, and reported by Amaral *et al.* (2018), was responsible for the impacts in this category. According to Kummer *et al.* (2018), zinc has a low potential for adsorption in soils and, thus, is easily leached into rivers and groundwater.

The avoided products (urea, phosphate fertilizer and limestone), due to the use of sludge in agricultural areas, contributed to this alternative, having an impact on the EUT-FW category of only 4%. Finally, in the HT category, the agricultural disposal of sludge was responsible for 95% of the environmental impacts, which was due to the high concentration of zinc (heavy metal) in the sludge. Results obtained by Yoshida *et al.* (2018) also highlighted the impact of the application of sludge containing a high concentration of zinc on the soil. According to these authors, zinc was responsible for 85 to 92% of the impacts caused in the HT category.

3.4. Comparative LCA

The absolute values of the contribution of each process used in the STP, with the different alternatives for final disposal of the sludge, are shown in Table 3. In general, the agricultural use of sludge obtained a greater potential for environmental impact in the following categories: OTE, TA, TE, FWE and HT.

The agricultural use of the sludge had a greater impact on the categories OTE, TE and FWE compared to destination in landfill due to the greater distances traveled to carry out the hygienization and disposal of the sludge, thus resulting in greater wear and tear on vehicle and also higher rates of NO_x and copper emissions into the atmosphere. In the TA category, NH_3 emissions during the PAS process were responsible for the greater impact of the agricultural use of sludge. As shown in Figure 3, of all the categories investigated, the one with the greatest impact from the agricultural disposition of sludge was HT, due to the high concentration of zinc in the sludge. This parameter has a characterization factor of $1.29x10^6$ by the method used for emission in agricultural soil, which causes a great impact for this destination.

Table 3. Life Cycle Assessment of processes used in the STP.

Impact categories	Units	Transport		Disposal	
		Landfill	Agricultural areas	Landfill	Agricultural areas
GW	kg CO_2 eq	0.027	0.059	0.241	0.029
SOD	kg CFC11 eq	8.18×10^{-9}	1.75×10^{-8}	1.37×10^{-7}	5.99×10^{-8}
OTE	kg NO_x eq	1.83×10^{-4}	3.92×10^{-8}	9.64×10^{-5}	2.74×10^{-5}
TA	kg SO_2 eq	9.50×10^{-5}	2.03×10^{-4}	1.79×10^{-4}	2.54×10^{-3}
EUT-AW	kg P eq	3.24×10^{-8}	6.93×10^{-8}	2.63×10^{-5}	6.54×10^{-8}
TE	kg 1,4-DCB eq	6.84×10^{-5}	1.46×10^{-4}	3.27×10^{-6}	1.06×10^{-5}
FWE	kg 1,4-DCB eq	4.56×10^{-5}	9.75×10^{-5}	5.29×10^{-5}	5.90×10^{-5}
HT	kg 1,4-DCB eq	0.113	0.243	7.38×10^{-2}	12.69

4. CONCLUSIONS

The destination of sewage sludge for agriculture, under the conditions addressed here, had a greater potential for impact in five of the eight categories evaluated. It should be noted that in this article, for comparison purposes, a landfill from the Ecoinvent® database was used, which receives sludge form the paper and cellulose industry. The main impacts observed in the process

of agricultural use of sludge are related to the concentration of zinc present, which significantly affects the FWE and HT categories. On the other hand, the main benefits of the agricultural use of sludge were avoided products, such as urea, phosphate fertilizer and limestone. The main impacts related to the disposal of sludge in landfills were limited to CH_4 emissions to the atmosphere and the PO_4^{3-} load present in the leachate. The results of the sewage treatment processes used in the studied STP showed the problem of CH_4 and N_2O emissions. With regard to CH_4, the use of burners with greater burning efficiency, as well as the use of energy from this gas, could lessen the impact on the GW category. In addition, the CH_4 dissolved in the effluent from the UASB reactors caused the TFs and the final effluent from the STP to become significant emission points. Emissions of N_2O in the low-rate TFs contributed the most to the SOD category. Finally, it is recommended that future studies carry out environmental inventories of emissions in landfills that receive sewage sludge and in low-rate TFs, as a post-treatment step for anaerobic processes.

5. ACKNOWLEDGMENT

The authors would like to acknowledge the support obtained from the following Brazilian institutions: Coordenação de Aperfeiçoamento de Pessoal de Nível Superior – CAPES; Instituto Nacional de Ciência e Tecnologia em Estações Sustentáveis de Tratamento de Esgoto – INCT ETEs Sustentáveis and Companhia de Saneamento do Paraná – SANEPAR.

6. REFERENCES

AISSE, M. M. **Tratamento de efluentes de reatores anaeróbios**. 2002. Tese (Doutorado em Engenharia) - Escola Politécnica, Universidade de São Paulo, 2002.

ALMEIDA, P. G. S.; RIBEIRO, T. B.; SILVA, B. S.; AZEVEDO, L. S.; CHERNICHARO, C. A. L. Contribuição para o aprimoramento de projeto, construção e operação de reatores UASB aplicados ao tratamento de esgoto sanitário - Parte 6: Qualidade do efluente. **Revista DAE**, v. 66, p. 90-108, 2018. https://dx.doi.org/10.4322/dae.2018.043

AMARAL, K. G. C.; AISSE, M. M.; POSSETTI, G. R. C.; PRADO, M. R. Use of life cycle assessment to evaluate environmental impacts associated with the management of sludge and biogas. **Water Science and Technology**, v. 77, n. 9, p. 2292–2300, 2018. https://doi.org/10.2166/wst.2018.146

AMARAL, K. G. C.; AISSE, M. M.; POSSETTI, G. R. C. Avaliação da sustentabilidade no gerenciamento do lodo e biogás, em estação de tratamento de esgotos, utilizando a técnica de ACV. **Revista Ambiente & Água**, v. 14, n. 5, 2019. http://dx.doi.org/10.4136/ambi-agua.2371

ANA (Brasil). **Atlas esgotos**: despoluição de bacias hidrográficas. Brasília, 2017.

ANDREOLI, C. V.; VON SPERLING, M.; FERNANDES, F. **Lodo de esgotos**: tratamento e disposição final. Belo Horizonte: UFMG, 2014.

APHA; AWWA; WEF. **Standard Methods for the examination of water and wastewater**. 22nd ed. Washington, 2012. 1496 p.

BITTENCOURT, S. **Gestão do processo de uso agrícola de lodo de esgoto no estado do Paraná**: aplicabilidade da resolução CONAMA 375/06. 190f. 2014. Tese (Doutorado em Engenharia de Recursos Hídricos e Ambiental) – Departamento de Hidráulica e Saneamento, Universidade Federal do Paraná, Curitiba, 2014.

BITTENCOURT, S.; SERRAT, B. M.; AISSE, M. M.; GOMES, D. Sewage sludge usage in agriculture: a case study of its destination in the Curitiba Metropolitan Region, Paraná, Brazil. **Water, Air, and Soil Pollution,** v. 225, n. 2074, 2014. https://doi.org/10.1007/s11270-014-2074-y

BRESSANI-RIBEIRO, T.; BRANDT, E. M. F.; GUTIERREZ, K. G.; DÍAZ, C. A.; GARCIA, G. B.; CHERNICHARO, C. A. L. Potential of resource recovery in UASB/trickling filter systems treating domestic sewage in developing countries. **Water Science and Technology**, v. 75, n. 7, p. 1659–1666, 2017. https://doi.org/10.2166/wst.2017.038

CHERNICHARO, C. A. L.; RIBEIRO, T. B.; PEGORINI, E. S.; POSSETTI, G. R. C.; MIKI, M. K.; SOUZA, S. N. Contribuição para o aprimoramento de projeto, construção e operação de reatores UASB aplicados ao tratamento de esgoto sanitário - Parte 1: Tópicos de Interesse. **Revista DAE**, v. 66, p. 5-16, 2018. https://dx.doi.org/10.4322/dae.2018.038

CIESLIK, B. M.; NAMIESNIK, J.; KONIECZKA, P. Review of sewage sludge management: standards, regulations and analytical methods. **Journal of Cleaner Production,** v. 90, p. 1–15, 2015. https://doi.org/10.1016/j.jclepro.2014.11.031

CORRÊA, W. C.; AISSE, M. M. Avaliação do filtro biológico percolador de baixa taxa como pós tratamento de reatores de manto de lodo. *In:* SIMPÓSIO DO PROGRAMA DE PÓS-GRADUAÇÃO EM ENGENHARIA DE RECURSOS HÍDRICOS E AMBIENTAL, 1., Curitiba, 2018. **Anais[...]** Curitiba: UFPR, 2019.

EL-FADEL, M.; MASSOUD, M. Methane emissions from wastewater management. **Environmental Pollution**, v. 114, n. 2, p. 177–185, 2001. https://doi.org/10.1016/S0269-7491(00)00222-0

FUCHS, V. J.; MIHELCIC, J. R.; GIERKE, J. S. Life cycle assessment of vertical and horizontal flow constructed wetlands for wastewater treatment considering nitrogen and carbon greenhouse gas emissions. **Water Research**, v. 45, n. 5, p. 2073–81, 2011. https://doi.org/10.1016/j.watres.2010.12.021

GUTIERREZ, K. G. **Análise e gerenciamento de impactos ambientais no tratamento de esgoto doméstico mediante avaliação de ciclo de vida**. 112 f. 2014. Tese (Doutorado em Saneamento, Meio Ambiente e Recursos Hídricos) - Escola de Engenharia, Universidade Federal de Minas Gerais, Belo Horizonte, 2014.

HERNANDEZ-PADILLA, F.; MARGNI, M.; NOYOLA, A.; GUERECA-HERNANDEZ, L.; BULLE, C. Assessing wastewater treatment in Latin America and the Caribbean: Enhancing life cycle assessment interpretation by regionalization and impact assessment sensibility. **Journal of Cleaner Production,** v. 142, p. 2140-2153, 2017. https://doi.org/10.1016/j.jclepro.2016.11.068

IPCC. **Climate Change Synthesis Report**. Contribution of Working Groups I, II and III to the Fifth Assessment Report of the Intergovernmental Panel on Climate Change. Geneva, 2014. 151 p.

KAMINSKI, G. F.; WAGNER; L. G.; SILVA, F. O. M.; POSSETTI, G. R. C. Análise crítica acerca da aplicação de queimadores enclausurados em ETEs para destruição de biogás. *In*: SIMPÓSIO MAUI BRASIL – ALEMANHA, 3., 2018, Curitiba. **Anais[...]** Curitiba: Universität Stuttgart; UFPR; SENAI; ABES-PR, 2018.

KUMMER, L.; GONÇALVES, M. S.; MELO, Z.; EMIANI. A.; MELO, V. F.; GOMES, S. D. Individual and competitive adsorption of copper, zinc and lead in soils with contrasting texture. **Journal of Experimental Agriculture International**, v. 27, n. 1, p. 1–11, 2018. https://doi.org/10.9734/JEAI/2018/43891

LOBATO, L. C. S.; CHERNICHARO, C. A. L; SOUZA, C. L. Estimates of methane loss and energy recovery potential in anaerobic reactors treating domestic wastewater. **Water Science & Technology**, v. 66, n. 12, p. 2745-2753, 2012. https://doi.org/10.2166/wst.2012.514

LOBATO, L. C. S.; RIBEIRO, T. B.; SILVA, B. S.; FLÓREZ, C. A. D.; NEVES, P. N. P.; CHERNICHARO, C. A. L. Contribuição para o aprimoramento de projeto, construção e operação de reatores UASB aplicados ao tratamento de esgoto sanitário - Parte 3: Gerenciamento de lodo e escuma. **Revista DAE**, v. 66, p. 30-55, 2018. https://dx.doi.org/10.4322/dae.2018.040

LOPES, T. A. S.; QUEIROZ, L. M.; KIPERSTOK, A. Environmental performance of a full-scale wastewater treatment plant applying Life Cycle Assessment. **Revista Ambiente & Água**, v. 13, n. 4, 2018. https://dx.doi.org/10.4136/ambi-agua.2216

METCALF & EDDY INC. **Wastewater engineering**: Treatment and Reuse. 5. ed. New York: McGraw Hill, 2016.

MORAN, M. J.; SHAPIRO, H. N.; BOETTNER, D.D.; BAILEY M. B. **Fundamentals of Engineering Thermodynamics**. 7th ed. New York: John Wiley & Sons, 2010.

NEMECEK, T.; SCHNETZER, J. **Methods of assessment of direct field emissions for LCIs of agricultural production systems**. Zurich: ART, 2011.

NOYOLA, A.; PADILLA, A. R.; MORGAN, J. M. S.; GUERECA, L. P.; HERNANDEZ, F. P. Typology of Municipal Wastewater Treatment Technologies in Latin America. **Clean – Soil, Air, Water**, v. 40, n. 9, p. 926-932, 2012. https://doi.org/10.1002/clen.201100707

POSSETTI, G. R. C.; RIETOW, J. C.; COSTA, F. J. O. G.; WAGNER, L. G.; LOBATO, L. C. S.; RIBEIRO, T. B.; MELO, D. F.; REIS, J. A.; CHERNICHARO, C. A. L. Contribuição para o aprimoramento de projeto, construção e operação de reatores UASB aplicados ao tratamento de esgoto sanitário - Parte 5: Biogás e emissões fugitivas de metano. **Revista DAE**, v. 66, p. 73-89, 2018. https://dx.doi.org/10.4322/dae.2018.042

POSSETTI, G. R. C.; RIETOW, J. C.; CABRAL, C. B. G.; MOREIRA, H. C.; PLATZER, C.; BRESSANI-RIBEIRO, T.; CHERNICHARO, C. A. L. Energy recovery from biogas in UASB reactors treating sewage. Chapter 8. *In*: CHERNICHARO, C. A. L.; BRESSANI-RIBEIRO, T. (Eds.). **Anaerobic Reactors for Sewage Treatment**: Design, Construction and Operation. London: IWA Publishing, 2019.

PROBIO 1.0. **Programa de estimativa de produção de biogás em reatores UASB**. Available at: site.sanepar.com.br/probio/probio.zip. Access: feb. 2021.

QUIROS, D. C.; SMITH, J.; THIRUVENGADAM, A.; HUAI, T.; HU, S. Greenhouse gas emissions from heavy-duty natural gas, hybrid, and conventional diesel on-road trucks during freight transport. **Atmospheric Environment**, v. 168, p. 36–45, 2017. https://doi.org/10.1016/j.atmosenv.2017.08.066

RAVISHANKARA, A. R.; DANIEL, J. S.; PORTMANN, R. W. Nitrous oxide (N2O): the dominant ozone-depleting substance emitted in the 21st century. **Science**, v. 326, n. 5949, 2009. https://dx.doi.org/10.1126/science.1176985

SIMONS, A. Road transport: new life cycle inventories for fossil-fuelled passenger cars and non-exhaust emissions in ecoinvent v3. **The International Journal of Life Cycle Assessment**, v. 21, n. 9, p. 1299–1313, 2013. https://doi.org/10.1007/s11367-013-0642-9

SOUZA, C. L.; CHERNICHARO, C. A. L.; AQUINO, S. F. Quantification of dissolved methane in UASB reactors treating domestic wastewater under different operating conditions. **Water Science & Technology**, v. 64, n. 11, 2011. https://doi.org/10.2166/wst.2011.695

USEPA. **Environmental regulation and technology control of pathogens and vector attraction in sewage sludge. 40 CFR. Part 503. 625/R-92/013**. Washington, 1992.

VASILAKI, V.; MASSARA, T. M.; STANCHEV, P.; FATONE, F.; KATSOU, E. A decade of nitrous oxide (N_2O) monitoring in full-scale wastewater treatment processes: A critical review. **Water Research,** v. 161, p. 392-412, 2019. https://doi.org/10.1016/j.watres.2019.04.022

VON SPERLING, M. **Introdução à qualidade das águas e ao tratamento de esgoto**. 4. ed. Belo Horizonte: UFMG, 2014.

YOSHIDA, H.; TEN HOEVE, M.; CHRISTENSEN, T. H.; BRUUN, S.; JENSEN, L. S.; SCHEUTZ, C. Life cycle assessment of sewage sludge management options including long-term impacts after land application. **Journal of Cleaner Production**, v. 174, p. 538–547, 2018. https://doi.org/10.1016/j.jclepro.2017.10.175

Ambiente & Água - An Interdisciplinary Journal of Applied Science
ISSN 1980-993X – doi:10.4136/1980-993X
www.ambi-agua.net
E-mail: ambi.agua@gmail.com

Evaluation of anaerobic and anoxic reactors installed in serial to treat fish tank effluent

ARTICLES doi:10.4136/ambi-agua.2678

Received: 18 Nov. 2020; Accepted: 12 Apr. 2021

Maria Lidia Carra[1]; Vitória Teodoro Gonçalves[1]; Tiago Palladino Delforno[2]; Valéria Maia de Oliveira[2]; Ariovaldo José da Silva[1*]

[1]Faculdade de Engenharia Agrícola. Laboratório de Meio Ambiente e Saneamento. Universidade Estadual de Campinas (UNICAMP), Avenida Cândido Rondon, n° 501, Cidade Universitária, CEP: 13083-875, Campinas, SP, Brazil. E-mail: malidiacarra@gmail.com, vitoriatgoncalves@yahoo.com.br
[2]Centro Pluridisciplinar de Pesquisas Químicas, Biológicas e Agrícolas. Divisão de Recursos Microbianos. Universidade Estadual de Campinas (UNICAMP), Avenida Alexandre Cazellato, n° 999, CEP: 13148-218, Paulínia, SP, Brazil. E-mail: tiago.palladino@gmail.com, vmaia@cpqba.unicamp.br
[*]Corresponding author. E-mail: arijs@unicamp.br

ABSTRACT

Effluent from a fish tank with Nile tilapia (*Oreochromis niloticus*) was treated in a system of two parallel fixed-bed anaerobic reactors followed by a suspended stirred, anoxic reactor for solids, organic matter and nitrogen removal. Microbial community structure was compared between the reactors and an enriched anammox culture originated from anaerobic sludge by using the PCR (Polymerase Chain Reaction) and DGGE (Denaturing Gradient Gel Electrophoresis) techniques. DGGE analysis revealed three large microbial clusters, namely, the biomass in the inoculum, the biomass growing in the reactors, and the enriched anammox culture. The similarity between the microbial community recovered from the anaerobic reactors and the anammox community was considered low (32.7%), suggesting differentiation of the bacterial community as a function of the selection of specific anammox groups. The last step in the anoxic reactor had worsened the effluent quality. The potential of organic matter and ammonia removal in a single anaerobic reactor was demonstrated.

Keywords: anaerobic reactors, anammox, denitrification, DGGE, nitrification.

Avaliação de reatores anaeróbios e anóxico instalados em série para tratamento de efluentes de tanques de piscicultura

RESUMO

Efluentes de um tanque de peixes de cultivo de tilápia do Nilo (*Oreochromis niloticus*) foram tratados em um sistema de dois reatores anaeróbios de leito fixo paralelos e seguido por um reator agitado suspenso sob ambiente anóxico para remoção de sólidos, matéria orgânica e nitrogênio. A estrutura da comunidade microbiana foi comparada entre os reatores e uma cultura enriquecida de anammox originada de lodo anaeróbio por PCR (Reação em Cadeia de Polimerase) e DGGE (Eletroforese em Gel de Gradiente Desnaturante). A análise de DGGE revelou três grandes aglomerados microbianos, a saber, a biomassa do inóculo, a biomassa nos reatores e a cultura de anammox enriquecida. A similaridade entre a comunidade microbiana recuperada dos reatores anaeróbios e a comunidade anammox foi considerada baixa (32,7%),

This is an Open Access article distributed under the terms of the Creative Commons Attribution License, which permits unrestricted use, distribution, and reproduction in any medium, provided the original work is properly cited.

sugerindo diferenciação da comunidade bacteriana em função da seleção de grupos específicos de anammox. Embora o reator anóxico tenha piorado a qualidade do efluente, os resultados indicam o potencial de remoção de matéria orgânica e amônia em um único reator anaeróbio.

Palavras-chave: anammox, desnitrificação, DGGE, nitrificação, reator anaeróbio.

1. INTRODUCTION

Fish production is carried out in intensive and semi-intensive systems by small producers. Fish farming in excavated tanks is largely responsible for semi-intensive and intensive systems, where animals are kept and raised throughout the growing period at high stocking densities (Malpartida Pasco *et al*., 2018). Animals are fed with high levels of protein that are only partially assimilated, resulting in an excess of this nutrient in the environment (Kaushik and Seiliez, 2010). The main product excreted by aquatic organisms that have been fed with proteins is ammonia. Excessive feeding and excretion contributes to the increase of nitrogen concentration in fish ponds, which can cause toxicity by nitrogen compounds such as ammonia, nitrite and nitrate (Silva *et al*., 2017). In order to minimize the impacts of nitrogen compounds in fish ponds, producers constantly renew the water without treating the discharged effluent, impacting the receiving rivers. (Coldebella *et al*., 2017).

The conventional process of nitrogen removal from wastewater is carried out through aerobic nitrification and anaerobic denitrification. In the first aerobic phase, Nitrosomonas spp. oxidize ammonia to nitrite and, in the second phase, Nitrobacter spp. oxidize nitrite to nitrate. Anaerobic denitrifying bacteria reduce nitrate and nitrite to nitrogen gas (Khin and Annachhatre, 2004). These reactions are widely known and have been successfully applied in most wastewater treatment systems (Egli *et al*., 2001). However, this process has some limitations when the objective is to treat effluents containing high concentrations of nitrogen and low concentration of carbon (low C / N ratio) since there are difficulties in the transfer of large amounts of oxygen necessary for nitrification and the need for a large amount of biodegradable organic matter in the denitrification phase (Xing and Clark, 2012). Fish farming effluents are characterized by the high concentration of biochemical oxygen demand (BOD) and the presence of organic and inorganic matter; in this way the efficiency of the process can be impaired and other processes must be explored.

Anammox has become an important subject in the fields of microbiology and environmental engineering because this process has several advantages, including low sludge production, low energy consumption, and no requirement for external organic carbon (Daverey *et al*., 2015).

The anammox process was investigated in a denitrifying reactor by Mulder *et al*. (1995). Ammonia (NH_4^+) is converted into gaseous nitrogen using nitrite (NO_2^-) as an electron acceptor. The anammox process can completely replace the conventional denitrification step of wastewater treatment systems, and save half of the aeration costs in the nitrification phase (Ma *et al*., 2016).

Anammox bacteria have been detected in several ecosystems. Devol (2003) states that they participate in the nitrogen cycle, and are responsible for 30 to 50% of the total N_2 production of the planet. In addition, they have also been detected in several effluent treatment plants in Germany (Helmer *et al*., 1999), Switzerland (Egli *et al*., 2001), England (Schmidt *et al*., 2003), Belgium (Pynaert *et al*., 2003), and Australia (Toh and Ashbolt, 2002). The presence of such bacteria in aquatic ecosystems suggests that they are found in any ecosystem that contains nitrogen and has anaerobic zones (Francis *et al*., 2007).

CANON (Completely Autotrophic Removal of Nitrogen Over Nitrite) is another innovative process. It is the combination of nitrification processes via nitrite and anammox,

developed in a single reactor aerated by two groups of bacteria (Sliekers *et al*., 2002). The first group is *Nitrosomonas spp.*, which oxidizes ammonia to nitrite by consuming oxygen and creating anaerobic conditions for the second group, represented by the anaerobic bacteria *Planctomycetales*, which are responsible for the anammox nitrogen removal process. (Ahn, 2006).

The anammox and CANON processes are considered to be a good alternative for biological nitrogen removal in wastewater treatment (Van Dongen *et al*., 2001), and can reduce up to 90% of operating costs (Jetten *et al*., 2001). In the review study by Nozhevnikova *et al.* (2012) on the application of the anammox process in the biotechnological treatment of effluents, the authors pointed out a 25% reduction in aeration costs compared to a complete nitrification process, a 40% reduction in costs by not adding organic carbon and a reduction of carbon dioxide emissions of 20%.

The anammox process has been used for the treatment and reduction of nitrogen compounds in agricultural environments in recent years, including treatment of anaerobic digestion effluents from food and fruit/vegetable waste, livestock manure, cannery wastewater, and sludge (Dapena-Mora *et al*., 2006; Fernandes *et al*., 2018; Kindaichi *et al*., 2016; Wu *et al*., 2019; Zhao *et al*., 2015).

Castine *et al*. (2012) observed in a settlement pond for the treatment of aquaculture waste the removal of nitrogen compounds and the production of nitrogen gas by denitrification and anammox processes. Other authors have also found the presence of anammox bacteria in fish production systems (Van Duc *et al.*, 2018; Li and Gu, 2016; Tal *et al*. 2006; Van Kessel *et al*. 2011; Shen *et al.* 2016; Lahav *et al*. 2009) showing the potential for the study and development of technologies for this production system.

According to Dapena-Mora *et al*. (2006), the anammox bacteria have specific conditions of development and very slow growth, an 11-day period according to Jetten *et al*. (2001). Therefore, some techniques were developed to obtain anammox biomass.

To have an optimal performance in the anammox process, the effluent must have some specific characteristics, such as low organic load and high ammonia concentration. For the success of the anammox process, it is necessary to have anammox bacteria in the system and to provide the appropriate anaerobic conditions (Nozhevnikova *et al.*, 2012).

Van Duc *et al.* (2018) enriched anammox bacteria in continuous compacted bed columns with marine sediment from a shrimp pond and had a nitrogen removal efficiency of 88% at a nitrogen loading rate of 1 $kg.m^{-3}.h^{-1}$. The authors showed that it is possible to obtain an anammox culture from marine sediment and also to reduce nitrogen compounds in an aquaculture treatment system with the anammox process.

Ding *et al*. (2017) tested three conventional sludges in sequencing batch reactors for Anammox enrichment, including conventional aerobic sludge, denitrification sludge, and anaerobic sludge. The anammox process was completely stabilized in the reactor with denitrifying sludge, obtaining 80% nitrogen removal in 150 days. Despite the favorable environment for the development of bacteria, the authors observed a fluctuation of nitrogen removal rates throughout the process. Microbiological analysis helped to more easily diagnose what was happening in each reactor.

Mirza *et al*. (2020) evaluated three different inoculum sources for the anammox process, i.e., anaerobic, aerobic and anoxic sludge from conventional sewage treatment plants. Anaerobic sludge was close to stoichiometric nitrite in ammonia utilization (1.2:1) and resulted in the highest ammonia removal (12.2 mg NH_4^+ g VS^{-1} day).

Microbial community analysis was carried out by molecular biology tools in treatment systems (Xiao *et al*., 2009). Genetic fingerprinting of microbial communities provides banding patterns or profiles that reflect the genetic diversity of the community in a given environment. Denaturing gradient gel electrophoresis (DGGE) of PCR amplified gene fragments is one of

the genetic fingerprinting techniques most widely used in microbial ecology studies on bioreactors (Cabezas *et al*., 2015). DGGE allows the simultaneous analysis of multiple samples and the comparison of microbial communities based on temporal and spatial differences (Muyzer and Smalla, 1998).

Therefore, it is interesting to look for alternatives and new discoveries for the removal of ammonia, technologies that help fish farmers in managing their production or building an effluent treatment system. It is also important to look for new sources of anammox bacteria and how different groups of bacteria can help remove nutrients and organic matter in a treatment system.

In this study, we evaluated the performance of an anaerobic and anoxic mixed biomass for the treatment of fish waste effluent in anaerobic reactors, and an agitated anoxic reactor for removing organic matter, ammonia, nitrite and nitrate by partial nitrification and the anammox process.

2. MATERIAL AND METHODS

2.1. Treatment System for effluent from fish tank

Figure 1 shows the scheme of the experimental setup and the sampling points for monitoring. The glass fish tank F, with a volume of 140 L, was supplied with dechlorinated water from tank W, of 250 L by gravity at a flow rate of 50 L h^{-1} for 90 days and thereafter was reduced to 20 L h^{-1}. The higher flow rate was applied for fish adaptation and observation of the treatment system. Nevertheless, the ammonia concentration was not high enough for the selection of anammox bacteria and for this reason the flow rate was decreased to 20 L h^{-1} and maintained throughout the experiment. Therefore, from the 90th day, the flow rate was reduced to 20 L h^{-1} to increase the concentration of ammonia in the treatment system.

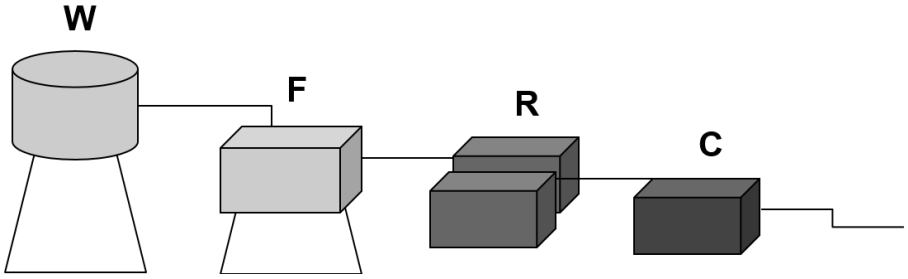

Figure 1. Experimental scheme. W, water supply reservoir; F, fish tank; R, upflow fixed-bed anaerobic reactor; C, suspended stirred reactor.

To simulate the intensive culture, the fish tank was inhabited by juvenile fish Nile's tilapia species (*Oreochromis niloticus*) with an initial weight of 27 ± 3 g and a biomass density of 5 g L^{-1}. The fish were donated by a Nile tilapia producer from the city of Mogi Mirim, SP, Brazil. The fishes were fed three times a day with a balanced ration containing 30% crude protein until satiety, limited to 3% of the average weight of the animals (Kubitza, 2000). Dissolved oxygen (DO) was measured daily to keep the concentration of 3.4±1.06 mg L^{-1} by the air compressor Boyu® ACQ-001. The low DO in the fish tank is in order to not compromise the anaerobic activity of the treatment reactors. The tolerance of low DO of tilapia is higher than other farmed fish, some tilapia can tolerate an environment with DO between 2.5-3.0 mg L^{-1} for 12 weeks without affecting their growth or mortality (Abdel-Tawwab *et al*., 2015; Li *et al*., 2018). A Nile tilapia was chosen for this study because it is a species that adapts to these extreme conditions.

For anaerobic treatment, two parallel upflow fixed-bed anaerobic reactors (FBR) were assembled, made in polypropylene, R (Figure 1) and with volume of 170 L, with dimensions 0.40 x 0.60 x 0.74 m (height x width x length) each, containing immobilized biomass from an

anaerobic baffled reactor sludge (ABRS), treating cattle manure plus dairy barn effluent. Biomass was immobilized in polyurethane foam (Biobob®) randomly disposed upon a steel plate with holes of 2 cm, up to the upper edge of the reactors, at a height of 0.35 m.

Later, the effluent was treated in the stirred reactor, C (Figure 1), also made in polypropylene, and with the same volume and dimensions of the FBR; the biomass grew in suspension, under limited aeration by a submerged pump to enable partial nitrification. This reactor was conceived to operate according to the CANON process, in which nitrite and ammonia should be later removed by anammox biomass in a single reactor (Khin and Annachhatre, 2004).

All the reactors were kept at room temperature; however, they were externally coated with styrofoam plates to minimize the changes of the inside temperature. The treatment system operated for 240 days.

2.2. Chemical Analysis

The pH, temperature, dissolved oxygen (DO), turbidity, color, and conductivity of the water were measured daily to ensure the welfare of the animals. Analyses of pH, temperature, conductivity and DO were measured by precision electrodes. Turbidity and color were measured by spectrometry. These analyses were performed according to Standard Methods for Examination of Water and Wastewater (APHA *et al.*, 2005).

During monitoring, samples of supply water (W) and fish tank (F), anaerobic reactors (R) and anoxic reactor effluent (C) (Figure 1), were collected weekly for analyzing chemical oxygen demand (COD), total nitrogen (TN), total carbon (TC), and total solids (TS). Analyses of TN and TC were performed by catalytic oxidation with combustion at 680ºC in a Shimadzu® brand analyzer, Model TNM-L. The COD measurement was performed by oxidizing organic matter using potassium dichromate as an oxidant in the presence of sulfuric acid and silver ions. The samples were digested in the digester block HACH COD Reactor, and after 2 hours they were read by absorbance on a spectrophotometer HACH DR4000U, according to Standard Method 5220 D (APHA *et al.*, 2005).

For TS, the porcelain capsule was cleaned and dried in a drying oven at a temperature ranging between 103-105°C for 1 hour. After cooling to room temperature the capsule was weighed and the value recorded. The sample was well homogenized, taking care to eliminate previously possible interference. One hundred mL of the sample was measured, and transferred to the porcelain capsule. Again the evaporation process was done, this time using the sample in the oven at 103-105°C for 60 minutes. After evaporation, the capsule was taken to the desiccator and allowed to cool. The capsule was then weighed again. The TS value was obtained by the difference in the weighing values. TS analyses were performed according to Standard Methods for Examination of Water and Wastewater (APHA *et al.*, 2005).

2.3. Statistical Analysis

All statistical analyses were performed with a 5% significance. Parametric or nonparametric data were verified by D' Agostino's method (D'Agostino *et al*., 1990). Hypotheses were tested by ANOVA and Kruskal-Wallis methods (Kruskal, 2007), for parametric and nonparametric data, respectively.

2.4. Bacterial community analysis

The similarity between the microbial community growing in the anaerobic and anoxic reactors and an enriched anammox microbial community was assayed by the molecular tool PCR/DGGE. All microbial communities were obtained from the same original inoculum, i.e., ABRS. Anaerobic Sludge is a suitable inoculum for anammox enrichment (Mirza *et al*. 2020). The enriched anammox culture originated from a parallel study, with the objective of obtaining anammox bacteria, which had the biomass of an ABRS as inoculum, and was selected in a

sequential batch reactor after 210 d fed with autotrophic medium according to Dapena-Mora *et al*. (2006) (data not shown).

An aliquot from inoculum (I), anammox biomass (E), anaerobic reactor sludge (R), and stirred reactor sludge (C) were centrifuged at 3,000 rpm for 5 minutes until at least 5 mL of biomass in triplicate.

Total DNA of the microbial community was extracted from each biomass sample (300 µL) using *PowerSoil DNA Isolation Kit* (Mobio), according to manufacturer's instructions. The 16S rRNA gene was partially amplified by PCR reactions using total DNA of the microbial community as a template and the primer pair 341f (coupled to a clamp with high GC content) and 907r (Muyzer *et al*., 1993; Muyzer and Smalla, 1998), which are complementary to conserved regions of the 16S rRNA gene of Domain Bacteria. PCR reactions were performed at a final volume of 50 µL containing 1X PCR buffer (Invitrogen), 1.5 mM $MgCl_2$, 0.2 µM dNTP Mix (Invitrogen), 0.5 µM of each primer, 2.0 U *Taq* DNA Polymerase (Invitrogen), and 5.0 µL of the DNA sample (~50 ng).

Amplification was carried out on a GeneAmp PCR System 9700 (Applied Biosystems), and the amplification program consisted of 1 denaturation cycle at 94°C for 5 min; 35 cycles at 94°C for 1 min, 60°C for 1 min, and 72°C for 2 min, followed by 10 cycles at 60°C for 30 seconds and 72°C for 1 min. PCR products were first confirmed on 1% agarose gel stained with 0.02 µL / mL SYBR Safe 10,000X in DMSO (Invitrogen). Amplicons were then subjected to denaturing gradient gel electrophoresis (DGGE) in the *Ingeny phor U-2* system (Ingeny International BV®), in which 15 µL of PCR products were applied to a 6% polyacrylamide gel at a voltage of 100 V for 15 hours. The denaturing gradient (urea and formamide) of the gel used for separation of the DNA fragments ranged from 40% to 65%. After electrophoresis, the gel was stained with 10 mL of a solution containing 4 µL SYBR Gold (Invitrogen®) in 1X TAE buffer for 1 hour in the dark.

DGGE polymorphic band profiles were analyzed by the Bionumerics software (Version 6.6; Applied Maths, Kortrijk, Belgium) after conversion and normalization of the profiles using the bands present in the molecular marker as standard. Band profiles were combined in a single image and analyzed per band, where the bands were automatically selected by the program and visually inspected and corrected, using default parameters and the Dice coefficient. The UPGMA (Unweighted Pair Group Method with Arithmetic Mean) algorithm was used to construct the similarity dendrogram.

3. RESULTS AND DISCUSSION

3.1. Performance of anaerobic and anoxic reactors for removal of organic matter and nitrogen

Table 1 shows the water quality in the fish tank (F) and in the biological reactors R and C (Figure 1). The mean values of temperature, pH, DO, turbidity, color and electrical conductivity (EC) of the fish tank water were in accordance with the recommended values for the fish species used (Makori *et al*., 2017).

In Figure 2, we show the content of the pollutants, organic matter, total nitrogen, total carbon, ammonia, nitrite, and nitrate, expressed in volumetric load in the fish tank (F), anaerobic reactors (R) and after the stirred reactor (C).

There was a 20.7% reduction in turbidity after treatment in the anaerobic reactor due to the retention of solids. The C reactor reduced an additional 55.4%, resulting in a total reduction of 64.6%. The total solids load was reduced from 179.5 g TS d^{-1} to 127.0 g TS d^{-1} (29.2% less) (data not shown). Beli *et al*. (2010) observed a reduced turbidity in 87% operating an aerobic/anaerobic combined treatment using anaerobic baffled reactor followed by a sand filter. Sánchez *et al*. (2016) achieved 58.2% in suspended solid removal with a biofilter using sand as

support material. In our study, we obtained TS removal of 48% combining the anaerobic reactor and the stirred reactor. The total removal efficiency showed that the system of anaerobic and aerobic reactors in series was effective in the retention of solids from Nile tilapia production.

Table 1. Quality parameters for water in the fish tank (F), upflow fixed-bed anaerobic reactor (R), suspended stirred reactor (C).

	F	R	C
Temperature (°C)	24 ± 1.8	24 ± 1.7	24 ± 1.8
pH	7.27 ± 0.29	7.25 ± 0.23	7.30 ± 0.24
DO (mg O_2 L^{-1})	3.4 ± 1.06	0.5 ± 0.1	0.5 ± 0.1
Turbidity (NTU)	2.32 ± 2.04	1.84 ± 0.78	0.82 ± 0.49
Color	32 ± 46	14 ± 12	11 ± 7
Conductivity (µS cm^{-1})	340 ± 76	319 ± 137	318 ± 132

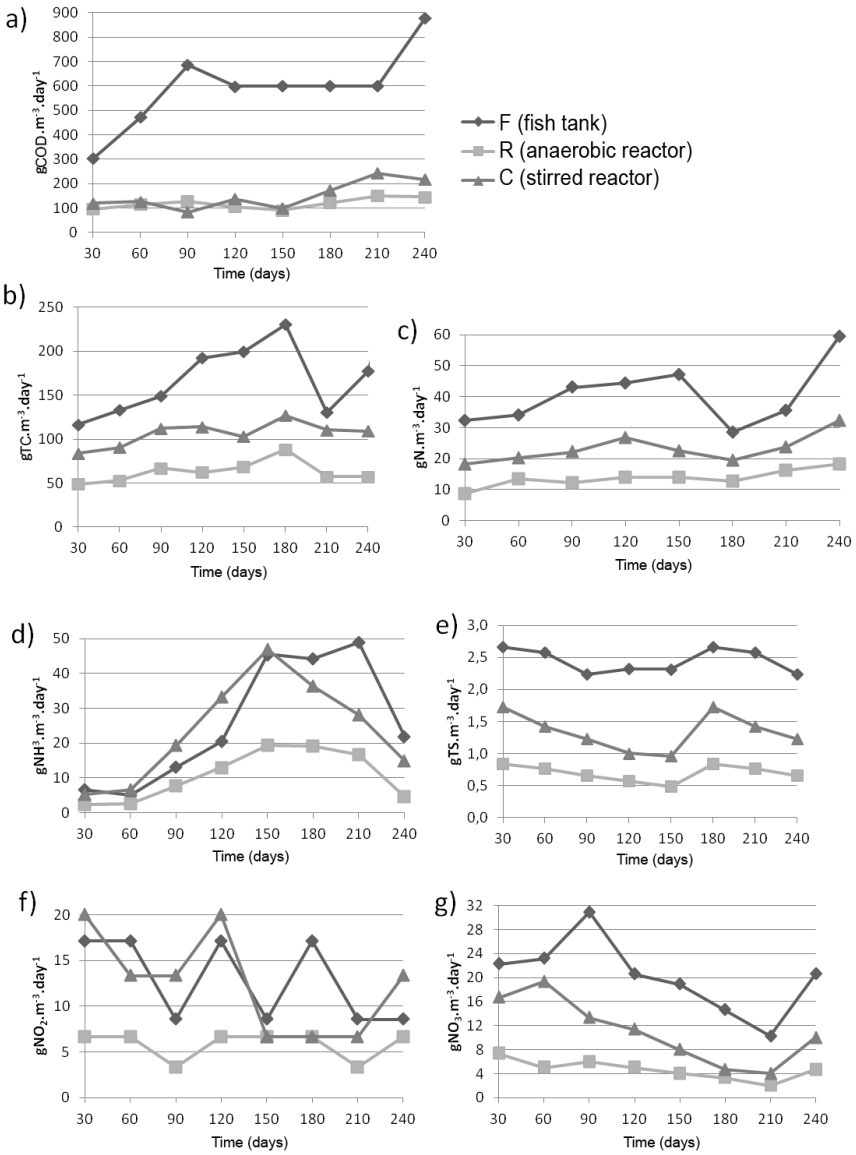

Figure 2. Volumetric loads of COD (a), TC (b), TN (c), Ammonia (d), TS (e), Nitrate (f) and Nitrite (g) in the fish tank (F), anaerobic reactor (R) and after stirred reactor (C) for 240 days.

The DO in the aquarium was 3.2 mg L^{-1}. In the anaerobic reactor, the DO was 0.5 mg L^{-1}.

The reduction of dissolved oxygen in the anaerobic reactor was due to the low flow and the period of stabilization of the liquid in the anaerobic tank. The low concentration of DO in the reactor C makes it possible to remove nitrogen by the CANON process. The concentration of organic matter and the NO_2^- / NH_3 ratio close to 1 also favors the CANON process.

According to Figure 2, carbon and nitrogen (b and c) mean loading rate of the anaerobic reactor was 186.85 g m^{-3} d^{-1} and 48.91 g m^{-3} d^{-1}, i. e., ratio C/N 3.82. The mean carbon and nitrogen load were reduced to 69.90 g m^{-3} d^{-1} (62.59%) and 15.99 g m^{-3} d^{-1} (67.31%) in the anaerobic reactors, resulting in a C/N ratio of 4.37 for the anoxic reactor. In reactor C, there was an increase in the average carbon and nitrogen load to 55.55 g m^{-3} d^{-1} and 10.48 g m^{-3} d^{-3}, respectively. In reactor R, the volumetric organic load (COD) (a) was reduced from 585.27 to 113.73 g m^{-3} d^{-1} (80.6%), and in reactor C it was increased to 149.95 g COD m^{-3} d^{-1}. This increase was due to biomass growth, since the sample was not filtered before the analysis.

During the first 60 days, the rate of water renewal in the fish tank was higher (50 L h^{-1} for 90 days, and then the flow rate decreased to 20 L h^{-1}), so the organic load in the anaerobic reactor was lower (388 ± 120 gCOD m^{-3} d^{-1}), increasing to 635 ± 106 gCOD m^{-3} d^{-1} in the next 240 days due to the reduction of water flow and the consequent increase in the COD concentration in the fish tank and in the reactors. The growth of biomass in the anaerobic reactor was able to remove organic matter, the average COD load was reduced by 80.6% and the total organic carbon was reduced by 69.0%.

Hussar and Bastos (2008), treating fish effluents with aquatic macrophytes had a COD removal efficiency of 77.7%, considered satisfactory for the system. Correia *et al*. (2012), evaluated the performance of aerobic fluidized bed reactors with internal circulation in removing carbon through the treatment of different wastewater. When assessing the fish farming effluent, they had 75% carbon removal. Other authors, such as Davidson *et al*. (2008), reported the removal of carbon above 60% in biphasic fluidized bed reactors, with sand as a support and biofilm thickness control for the treatment of fish effluent.

Although the anaerobic reactor (R) is efficient in removing COD, in the stirred reactor (C) the COD load increased by 24.15%, suggesting that the combination of the fixed bed anaerobic reactor and the agitated reactor with suspended biomass was not suitable for removal of organic matter.

The low electrical conductivity measured in average 319 μS cm^{-1} also was a consequence of renewal water. Conductivity is a very important factor for the operation of the Anammox process. Tsai *et al*. (2019) verified that when the conductivity was between 1250–7500 μS cm^{-1}, the total nitrogen removal rate begins to decrease slowly from 64 to 57%, being greatly reduced when the conductivity was higher than 7500 μS cm^{-1}, i.e, from 57.1 to 40.9%.

For ammonia, the mean loading rate was reduced from 26.25 g m^{-3} d^{-1} to 11.57 g m^{-3} d^{-1} (55.92%) in reactor R, but it increased in reactor C to 25.11 g m^{-3} d^{-1} (Figure 2d). The mean load of nitrite and nitrate (Figure 2f) was also reduced in the anaerobic reactors, from 12.86 gNO_2^- m^{-3} d^{-1} to 5.83 gNO_2^- m^{-3} d^{-1} (54.66%) (Figure 2e), and from 22.29 gNO_3^- m^{-3} d^{-1} to 7.33 gNO_3^- m^{-3} d^{-1}(67.11%), respectively. However, it increased in the stirred reactor, resulting in a final effluent load of 12.50 gNO_2^- m^{-3} d^{-1} and 16.67 gNO_3^- m^{-3} d^{-1}, respectively. The influent NH_3/NO_2^- ratio at anaerobic reactor decreased from 2.04 to 1.98 in the effluent. In the stirred reactor, this ratio increased to 2.01, higher than the stoichiometric value for the complete anammox process, i.e., 1.23, thus indicating a lack of nitrite.

In this experiment, the water renewal rate of 20 L h^{-1} maintained a low ammonia concentration, 3.23±2.08 mg L^{-1}. However, some authors found higher ammonia concentration in fish farming; for instance, Gonzaga *et al.* (2008) found 10.3 mgNH_3 L^{-1} in Nile 's tilapia tank, and Zamboni-Filho *et al*. (1997) found concentration above 70 mg.L^{-1} of ammonia in polyculture tank.

Despite receiving an effluent with DO concentrations above 3 mg L^{-1}, the DO values in the anaerobic reactor were kept close to zero. In the conventional nitrification process, low concentrations of DO are more restrictive for the growth of nitrite-oxidizing bacteria in comparison with ammonia oxidizing bacteria, which can cause nitrite accumulation in the system (Philips *et al*., 2002). This explains the partial removal of ammonia and nitrite in the anaerobic reactors. Ding *et al*. (2017) observed the inhibition of anammox activity and the accumulation of nitrite and nitrate in reactors for enriching anammox bacteria with DO values above 1 mg L^{-1}. Corroborating the study by Jetten *et al*. (2001), which determines the maximum concentration of 0.2 mgO_2 L^{-1} for the development of anammox activity.

According to Peng and Zhu (2006), low concentrations of DO can cause low rates of nitrification, and they suggest DO concentration between 1.0 and 1.5 mg L^{-1} for nitrification. Here, the DO concentration was maintained below 1 mg L^{-1} in order to produce nitrite for the anammox process, according to a stoichiometric NH_4^+/NO_2^- ratio close to 1.31, as shown in Equation 1 (Khin and Annachhatre, 2004). In Equation 1, the last factor represents the biomass.

$$NH_4^+ + 1.31NO_2^- + 0.0425CO_2 \rightarrow 1.045N_2 + 0.22NO_3^- + 1.87H_2O + 0.09OH^- + 0.0425CH_2O \quad (1)$$

The values of the NH_4^+/NO_2^- ratio in the system effluent were found above the theoretical value for the anammox process, i.e., close to 1, indicating a lack of nitrite. We may infer that the NH_4^+/NO_2^- ratio in the anaerobic and anoxic reactors did not present the best ratio for anammox, indicating that partial nitrification in both reactors had ended.

Because the stoichiometric ratio for the anammox process NH_3/NO_2^- is 1.23, and this value is lower than values verified in the influent and effluent of the anaerobic and anoxic reactors, 2.04 and 1.98, ammonia and nitrite were partially removed in 56% and 55%, respectively.

Unfortunately, in this experiment, the effluent quality worsened after being treated in the anoxic reactor, and ammonia and nitrite concentrations increased, suggesting that a suspended anoxic reactor can be used to supply an anaerobic FBR with nitrite, and improve the efficiency in the latter and not as a final unity.

Therefore, ammonia and nitrite removal should occur in a single reactor. In fact, Xiao *et al.* (2009) confirmed the coexistence of nitrifiers, denitrifiers, and anammox bacteria in a single batch sequencing reactor by using PCR-DGGE, and justified that ammonia removal occurred due to the growth of aerobic bacteria in the surface and anaerobic bacteria inside the biofilm. According to the authors, aerobic bacteria supply nitrite to anammox bacteria. These data corroborate the fact that in this study we found nitrite and nitrate in the reactors, indicating the coexistence of nitrification and anammox reactions.

The low efficiency in the anoxic reactor concerning ammonia and nitrite removal could be explained by the presence of dissolved oxygen. The average DO concentration was 0.5 mg L^{-1}, considering that the anammox process takes place under anoxic conditions, and low concentrations of oxygen in the medium may already interfere with the efficiency of the process. Strous *et al*. (1997) demonstrated that the activity of the anammox bacteria undergoes a temporary inhibition if the DO concentration is up to 0.2 mg L^{-1}, and this inhibition can be reversed under anoxic conditions. At DO concentrations between 0.2-1.0 mg L^{-1}, the bacteria undergo complete inhibition (Strous *et al*., 1997).

3.2. Bacterial community

The 16S rDNA fragments were successfully amplified from the community DNA obtained from the sludge samples (data not shown). Dendrograms generated from the DGGE band profiles by DICE correlation coefficients are shown in Figure 3.

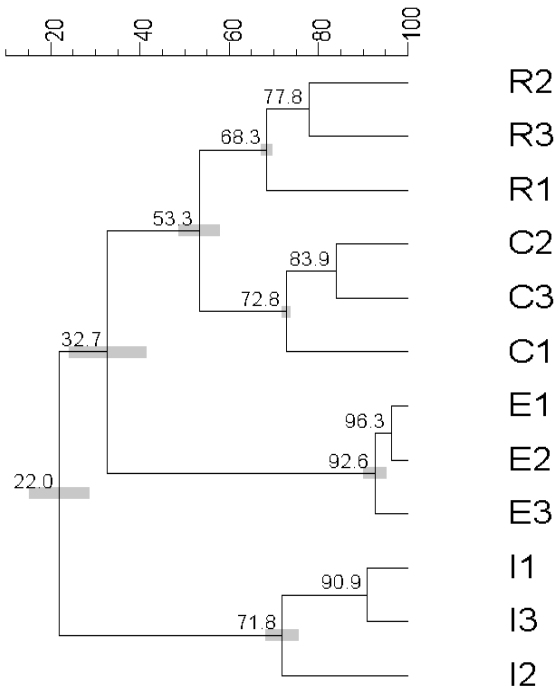

Figure 3. Dendrogram of similarity based on the DGGE band profiles of the samples, obtained using the DICE coefficient and the UPGMA algorithm (BioNumerics program v. 6.6). I1, I2, and I3 correspond to inoculum samples; E1, E2 and E3, to anammox biomass; R1, R2 and R3, to samples from the anaerobic reactor; and C1, C2, and C3, to samples from the stirred reactor. Values in each node represent the percentage of similarity, and the bar is the standard deviation.

Three distinct bacterial clusters were recovered based on the similarity dendrogram, which corresponded to the different groups of samples analyzed. The first cluster, R, contains microorganisms developed in the anaerobic reactor; the second cluster, C, refers to microorganisms developed in the anoxic reactor. These two clusters were more similar (53.3%) among each other in comparison to the others. Cluster E, which corresponds to the enriched anammox biomass, showed 32.7% similarity with clusters R and C; whereas cluster I, which corresponds to the inoculum used for the enrichment and starting of the reactors, was the most distinct (22% similarity with the others).

Cultivation-independent analysis by DGGE allowed us to evaluate and compare the complexity of the bacterial community present in the inoculum (I), enriched anammox biomass (E), and biomass from reactors (R) and (C). The dendrogram showed the formation of three large groups, the biomass growing in anaerobic and anoxic reactors, the enrichment biomass anammox, and the inoculum.

The level of similarity observed between the R group and C group was 53.3% for the DICE coefficient. The anaerobic reactor (group R) and the anoxic reactor (group C) were operated in series, in such a way that the microorganisms developed in the anaerobic reactor were probably taken to the anoxic reactor by the effluent. The level of similarity in the R and C reactors was not higher because different processes of nutrient removal occurred in the reactors, which influenced the microbial community developed in each one.

Replicates were consistent and more similar to each other than between the samples.

Bacterial communities of R and C reactors were more similar (53.3% in the case of the DICE coefficient) when compared with inoculum and enrichment samples. These reactors were operated in the same conditions of dissolved oxygen, 0.5 mg L^{-1}, and both showed nitrification and denitrification activity.

The low similarity between the band profiles of the reactor biomass (Groups R and C) in relation to the inoculum (Group I) may suggest that operating conditions and the characteristics of the substrate possibly enabled the selection of specific bacterial populations that were in low abundance in the inoculum.

Biomass from reactors also demonstrated some similarity with the anammox biomass, 32.7% as determined by DICE coefficients. The consumption of nitrite and ammonia in the R reactor and the production of nitrate in the C reactor suggest that anammox activity took place in both reactors.

Authors of recent studies have indicated the presence of anammox bacteria in sediments of fish culture tanks (van Kessel *et al*., 2011; Lahav *et al.*, 2009; Tal *et al*., 2006). The origin of these bacteria would be the feces of the animals, and some aquatic animals possess bacteria of the phylum *Planctomycetes* in their intestines (Fuerst, 2004). Some similarities observed between fish tank treatment and enriched anammox bacteria can be explained both by the origin of the inoculum and the possible development of anammox bacteria in fish feces.

4. CONCLUSIONS

- The rate of water renewal used in this experiment resulted in a low concentration of ammonia, total nitrogen, nitrite and nitrate compared to values reported in the literature, and the assay was ineffective for removing ammonia and nitrite;
- The anaerobic reactor was effective in the removal of COD, ammonia, nitrite, and nitrate probably due to the anammox and simultaneous denitrification;
- The increase in the load of organic matter, ammonia, nitrate and nitrite in the stirred reactor showed that this configuration of the reactor after the anaerobic reactor was not viable for the CANON process;
- The presence of oxygen in the stirred reactor may have caused the removal of ammonia by the partial nitrification process. However, further studies must be carried out to prove the system as a nitrite supplier for an anaerobic reactor for the removal of ammonia by anammox process;
- There was some similarity in the microbial community of the reactors and the anammox community. However, the biggest similarity was observed among the anaerobic and anoxic reactors.

5. ACKNOWLEDGMENTS

The authors are grateful to the Environmental Control Laboratory of the School of Agriculture Engineering, University of Campinas, for the space to experimental installation, to the Bioproj Environment Technology, for donation of support material, Piscicultura Pollettini, for donation of fish and to Capes Foundation from the Brazilian Ministry of Education, for the scholarship, and to the National Council of Scientific and Technological Development – CNPq, for the financial support process no. 481361/2013-8, and to Espaço da Escrita – Pró-Reitoria de Pesquisa – UNICAMP – for the language services provided.

6. REFERENCES

AHN, Y. H. Sustainable nitrogen elimination biotechnologies: A review. **Process Biochemistry**. v. 41, n. 8, p.1709–1721, 2006. https://dx.doi.org/10.1016/j.procbio.2006.03.033

ABDEL-TAWWAB, M.; HAGRAS, A. E.; ELBAGHDADY, H. A. M. Effects of dissolved oxygen and fish size on Nile tilapia, Oreochromis niloticus (L.): growth performance, whole-body composition, and innate immunity. **Aquaculture,** v. 23, p. 1261–1274, 2015. https://doi.org/10.1007/s10499-015-9882-y

APHA; AWWA; WEF. **Standard Methods for the Examination of Water and Wastewater**. 21. ed. Washington, 2005.

BELI, E.; HUSSAR, G. J.; HUSSAR, D. H. Redução de DQO e Turbidez de efluente de uma unidade suinícultura empregando reator anaeróbio compartimentado (RAC) seguido de filtro biológico e filtro de areia. **Engenharia Ambiental,** v. 7, n. 1, p. 5-19, 2010.

CASTINE, S. A.; ERLER, D. V.; TROTT, L. A.; PAUL, N. A.; NYS, R.; EYRE, B. D. Denitrification and anammox in tropical aquaculture settlement ponds: an isotope tracer approach for evaluating N2 production. **PLos ONE**, v. 7, n.9, 2012. https://doi.org/10.1371/journal.pone.0042810

CABEZAS, A.; de ARAUJO, J. C.; CALLEJAS, C.; GALÈS, A.; HAMELIN, J.; MARONE, A.; SOUZA, D. Z.; TRABLY, E.; ETCHEBEHERE, C. How to use molecular biology tools for the study of the anaerobic digestion process? **Reviews in Environmental Science Biotechnology,** v. 14, n.4, p. 555–593, 2015. https://dx.doi.org/10.1007/s11157-015-9380-8

COLDEBELLA, A.; GENTELINI, A. L.; PIANA, P. A.; COLDEBELLA, P. F.; BOSCOLO, W. R.; FEIDEN, A. Effluents from fish farming ponds: A view from the perspective of its main components. **Sustainability.** v. 10, n.1, p.1–16, 2017. https://dx.doi.org/10.3390/su10010003

CORREIA, G. T.; ANDRÉS, I.; ORTIZ, S.; GEBARA, D.; SOBRINHO, M. D.; MATSUMOTO, T. Desempenho de Reatores Aeróbios de Leito Fluidizado com Circulação interna na remoção de matéria carbonácea tratando diferentes águas residuárias. **Interciência**, v. 37, n. 4, p. 266–271, 2012.

D'AGOSTINO, R. B.; BELANGER, A.; D'AGOSTINO Jr., R. B. A Suggestion for Using Powerful and Informative Tests of Normality. **The American Statistician**, v. 44, p. 316–321, 1990. https://doi.org/10.2307/2684359

DAPENA-MORA, A.; CAMPOS, J. L.; MOSQUERA-CORRAL, A.; MÈNDEZ, R. Anammox process for nitrogen removal from anaerobically digested fish canning effluents. **Water Science Technology.** v. 53, n. 12, p. 265–274, 2006. https://dx.doi.org/10.2166/wst.2006.429

DAVEREY, A.; CHEI, P. C.; DUTTA, K.; LIN, J. G. Statistical analysis to evaluate the effects of temperature and pH on anammox activity. **International Biodeterioration and Biodegradation,** n. 102, p. 89–93, 2015. https://dx.doi.org/10.1016/j.ibiod.2015.03.006

DAVIDSON, J.; HELWIG, N.; SUMMERFELT, S.T. Fluidized sand biofilters used to remove ammonia, biochemical oxygen demand, total coliform bacteria, and suspended solids from an intensive aquaculture effluent. **Aquacultural Engineering,** v. 39, n. 1, p. 6–15, 2008. https://dx.doi.org/10.1016/j.aquaeng.2008.04.002

DEVOL, A. H. Solution to a marine mystery. **Nature,** v. 422, p. 575–576, 2003. https://dx.doi.org/doi.org/10.1038/422575a

DING, Z.; VENTORINO, V.; PANICO, A.; PEPE, O.; VAN HULLEBUSCH, E.D.; PIROZZI, F.; BOURVEN, I.; GUIBAUD, G.; ESPOSITO, G. Enrichment of Anammox Biomass from Different Seeding Sludge: Process Strategy and Microbial Diversity. **Water, Air and Soil Pollution,** v. 228, n. 1, p. 1–13, 2017. https://dx.doi.org/10.1007/s11270-016-3181-8

EGLI, K.; FANGER, U.; ALVAREZ, P. J. J.; SIEGRIST, H.; VAN DER MEER, J. R.; ZEHNDER, A. J. B. Enrichment and characterization of an anammox bacterium from a rotating biological contactor treating ammonium-rich leachate. **Archives of Microbiology,** v. 175, n. 3, p. 198–207, 2001. https://dx.doi.org/10.1007/s002030100255

FERNANDES, L.A.; PEREIRA, A. D.; LEAL, C. D.; DAVENPORT, R.; WERNER, D.; MOTA FILHO, C. R.; BRESSANI-RIBEIRO, T.; LEMOS CHERNICHARO, C. A.; ARAÚJO, J. C. Effect of temperature on microbial diversity and nitrogen removal performance of an anammox reactor treating anaerobically pretreated municipal wastewater. **Bioresource Technology**., v. 258, p. 208-219, 2018. https://doi.org/10.1016/j.biortech.2018.02.083

FRANCIS, C. A.; BEMAN, J. M.; KUYPERS, M. M. M. New processes and players in the nitrogen cycle: The microbial ecology of anaerobic and archaeal ammonia oxidation. **ISME Journal**, v. 1, n. 1, p.19–27, 2007. https://dx.doi.org/10.1038/ismej.2007.8

FUERST, J. A. Planctomycetes – a phylum of emerging interest for microbial evolution and ecology. **World Federation for Culture Collections Newsletter,** v. 38, p.1–11, 2004.

GONZAGA, G.; ANTONIO, H.; MONTEIRO, F. Impacto das Atividades de Aqüicultura e Sistemas de Tratamento de Efluentes com Macrófitas Aquáticas - Relato de Caso. **Boletim do Instituto de Pesca,** v. 34, p.163–173, 2008. http://orcid.org/0000-0003-3565-6838

HELMER, C.; KUNST, S.; JURETSCHKO, S.; SCHMID, M. C.; SCHLEIFER, K. H.; WAGNER, M. Nitrogen Loss in a Nitrifying Biofilm System. **Water Science and Technology,** v. 39, p.13–21, 1999. https://doi.org/10.1016/S0273-1223(99)00145-6

HUSSAR, G. J.; BASTOS, M. C. Tratamento de efluente de piscicultura com macrófitas aquáticas flutuantes. **Engenharia Ambiental,** v. 5, n. 3, p. 274–285, 2008.

JETTEN, M. S. M.; WAGNER, M.; FUERST, J.; VAN LOOSDRECHT, M. C. M.; KUENEN, J. G.; STROUS, M. Microbiology and application of the anaerobic ammonium oxidation ('anammox') process. **Environmental Biotechnology,** v. 12, p. 283–288, 2001. https://dx.doi.org/10.1016/S0958-1669(00)00211-1

KAUSHIK, S. J.; SEILIEZ, I. Protein and amino acid nutrition and metabolism in fish: current knowledge and future needs. **Aquaculture Research**, v. 41, n. 3, p. 322–332, 2010. https://dx.doi.org/10.1111/j.1365-2109.2009.02174.x

KINDAICHI, T.; AWATA, T.; MUGIMOTO, Y.; RATHNAYAKE, R. M. L. D.; KASAHARA, S.; SATOH, H. Effects of organic matter in livestock manure digester liquid on microbial community structure and in situ activity of anammox granules. **Chemosphere**. v. 159, p. 300-307, 2016. https://doi.org/10.1016/j.chemosphere.2016.06.018

KHIN, T.; ANNACHHATRE, A. P. Novel microbial nitrogen removal processes. **Biotechnology Advances,** v. 22, n. 7, p. 519–532, 2004. https://dx.doi.org/10.1016/j.biotechadv.2004.04.003

KRUSKAL, W. H. A Nonparametric test for the Several Sample Problem. **The Annals of Mathematical Statistics,** v. 23, p. 525–540, 2007. https://dx.doi.org/10.1214/aoms/1177729332

KUBITZA, F. Tilápias. **Panorama da Aquicultura**, v. 10, n. 59, p. 44–53, 2000. https://dx.doi.org/10.3109/14764172.2011.552607

LAHAV, O.; MASSADA, I.B.; YACKOUBOV, D.; ZELIKSON, R.; MOZES, N.; TAL, Y.; TARRE, S. Quantification of anammox activity in a denitrification reactor for a recirculating aquaculture system. **Aquaculture,** v. 288, n. 1-2, p. 76–82, 2009. https://dx.doi.org/10.1016/j.aquaculture.2008.11.020

LI, M.; XIAODAN, W.; CHANGLE, Q.; ERCHAO, L.; ZHENYU, D.; JIAN, G.Q.; LIQIAO, C. Metabolic response of Nile tilapia (Oreochromis niloticus) to acute and chronic hypoxia stress. **Aquaculture**, v. 495, p. 187-195, 2018. https://dx.doi.org/10.1016/j.aquaculture.2018.05.031

LI, M; GU, J. The diversity and distribution of anammox bacteria in the marine aquaculture zones. **Applied Microbiology and Biotechnology**, v. 100, n. 20, p. 8943-8953, 2016. https://doi.org/10.1007/s00253-016-7690-6

MA, B.; WANG, S.; CAO, S.; MIAO, Y.; JIA, F.; DU, R.; PENG, Y. Biological nitrogen removal from sewage via Anammox: Recent advances. **Bioresource Technology**, v. 200, p. 981–990, 2016. https://doi.org/10.1016/j.biortech.2015.10.074

MAKORI, A. J.; ABUOM, P. O.; KAPIYO, R.; ANYONA, D. N.; DIDA, G. O. Effects of water physico-chemical parameters on tilapia (Oreochromis niloticus) growth in earthen ponds in Teso North Sub-County, Busia County. **Fisheries and Aquatic Sciences,** v. 20, n. 1, p. 1–10, 2017. https://dx.doi.org/10.1186/s41240-017-0075-7

MALPARTIDA PASCO, J. J.; CARVALHO FILHO, J. W.; de ESPIRITO SANTO, C. M.; VINATEA, L. Production of Nile tilapia Oreochromis niloticus grown in BFT using two aeration systems. **Aquaculture Research,** v. 49, n. 1, p. 222–231, 2018. https://dx.doi.org/10.1111/are.13451

MULDER, A. A.; VAN DE GRAFF, L. A.; ROBERTSON, J. G. K. Anaerobic Ammonium Oxidation Discovered in a denitrifying fluidized bed reactor. **FEMS Microbiology Ecology,** v. 16, n. 3, p. 177–184, 1995. https://doi.org/10.1111/j.1574-6941.1995.tb00281.x

MIRZA, M. W.; D'SILVA, T.; GANI, M. K.; AFSAR, S. S.; GAUR, R. Z.; MUTIYAR, P. K.; KHAN, A. A.; DIAMANTIS, V.; LEW, B. Cultivation of anaerobic ammonium oxidizing bacteria (AnAOB) using different sewage sludge inoculums: process performance and microbial community analysis. **Journal of Chemical Technology and Biotechnology**, v. 96, n. 2, p. 454-464, 2020. https://doi.org/10.1002/jctb.6560

MUYZER, G.; SMALLA, K. Application of denaturing gradient gel electrophoresis (DGGE) and temperature gradient gel electrophoresis (TGGE) in microbial ecology. **Antonie Van Leeuwenhoek,** v. 73, p. 127–141, 1998. https://doi.org/10.1023/A:1000669317571

MUYZER, G., WAAL, E. C. D. E.; UITTERLINDEN, A. G. Profiling of Complex Microbial Populations by Denaturing Gradient Gel Electrophoresis Analysis of Polymerase Chain Reaction-Amplified Genes Coding for 16S rRNA. **Applied and Environmental Microbiology**, v. 59, n. 3, p. 695-700, 1993.

NOZHEVNIKOVA, A.N.; SIMANKOVA, M. V.; LITTI, Y. V. Application of the microbial process of anaerobic ammonium oxidation (ANAMMOX) in biotechnological wastewater treatment. **Applied Biochemistry and Microbiology,** v. 48, n. 8, p. 667–684, 2012. https://dx.doi.org/10.1134/s0003683812080042

PENG, Y., ZHU, G. Biological nitrogen removal with nitrification and denitrification via nitrite pathway. **Applied Microbiology and Biotechnology,** v. 73, n. 1, p. 15–26, 2006. https://dx.doi.org/10.1007/s00253-006-0534-z

PHILIPS, S.; LAANBROEK, H. J.; VERSTRAETE, W. Origin, causes and effects of increased nitrite concentrations in aquatic environments. **Reviews in Environmental Science and Bio/Technology,** v. 1, p. 115–141, 2002. https://dx.doi.org/10.1023/A:1020892826575

PYNAERT, K.; SMETS, B. F.; WYFFELS, S.; BEHEYDT, D.; SICILIANO, S.D.; VERSTRAETE, W. Characterization of an autotrophic nitrogen-removing biofilm from a highly loaded lab-scale rotating biological contactor. **Applied and Environmental Microbiology,** v. 69, n. 6, p. 3626–3635, 2003. https://dx.doi.org/10.1128/AEM.69.6.3626-3635.2003

SÁNCHEZ, O. I.; DOLLY REVELO, R.; ÁLVARO BURBANO, M.; ROBERTO GARCÍA, C.; CAMILO GUERRERO, R.; DIANA BELTRÁN, T.; LUIS BENAVIDES, M. Performance of different biofilters in a recirculating system for rainbow trout farming. **Revista MVZ Cordoba,** v. 21, n. 2, p. 5426–5440, 2016. https://doi.org/10.21897/rmvz.608

SCHMIDT, I.; SLIEKERS, O.; SCHMID, M.; BOCK, E.; FUERST, J.; KUENEN, J.G.; JETTEN, M. S. M.; STROUS, M. New concepts of microbial treatment processes for the nitrogen removal in wastewater. **FEMS Microbiology Reviews.** v. 27, n. 4, p.481–492, 2003. https://dx.doi.org/10.1016/S0168-6445(03)00039-1

SHEN, L.; WU, H.; GAO, Z. Q.; RUAN Y. J.; XU, X. H.; LI, J.; MA, S. J.; ZHENG, P. H. Evidence for anaerobic ammonium oxidation process in freshwater sediments of aquaculture ponds. **Environmental Science and Pollution Research,** v. 23, n. 2, p. 1344-1352. 2016.

SILVA, L.; ESCALANTE, E.; VALDÉS-LOZANO, D.; HERNÁNDEZ, M; GASCA-LEYVA, E. Evaluation of a semi-intensive aquaponics system, with and without bacterial biofilter in a tropical location. **Sustainability,** v. 9, n. 4, p. 592, 2017. https://dx.doi.org/10.3390/su9040592

SLIEKERS, A. O. *et al*. Completely autotrophic nitrogen removal over nitrite in one single reactor. **Water research**, v. 36, n. 10, p. 2475-2482, 2002. https://doi.org/10.1016/S0043-1354(01)00476-6

STROUS, M.; VAN GERVEN, E.; KUENEN, J.G.; JETTEN, M. Effects of aerobic and microaerobic conditions on anaerobic ammonium- oxidizing (anammox) sludge. **Applied and Environmental Microbiology,** v. 63, n. 6, p. 2446–2448, 1997.

TAL, Y; WATTS, J.; SCHREIER, H. Anaerobic ammonium-oxidizing (anammox) bacteria and associated activity in fixed-film biofilters of a marine recirculating aquaculture system. **Applied and Environmental Microbiology,** v. 72, n. 4, p. 2896-2904, 2006. https:/dx.doi.org/10.1128/AEM.72.4.2896-2904.2006

TOH, S.; ASHBOLT, N. Adaptation of anaerobic ammonium-oxidising consortium to synthetic coke-ovens wastewater. **Applied Microbiology and Biotechnology.** v. 59, n.2-3, p.344–352, 2002. https://dx.doi.org/10.1007/s00253-002-1007-7

TSAI, T-Y.; LO, H-S.; CHUANG, H-P.; JI, Y-LYANG, M.; JOU C-J. Effects of conductivity in wastewater for the anaerobic ammonium oxidation (anammox) process. **Journal of Environmental Protection and Ecology**, v. 20, n. 4, p. 1904–1911, 2019.

VAN DONGEN, U.; JETTEN, M. S. M.; LOOSDRECHT, M. C. M. Sharon-anammox process for the treatment of ammonium rich wastewater. **Water Science & Technology,** v. 44, p.153–160, 2001. https://doi.org/10.2166/wst.2001.0037

VAN DUC, L.; SONG, B.; ITO, H.; HAMA, T.; OTANI, M.; KAWAGOSHI, Y. High growth potential and nitrogen removal performance of marine anammox bacteria in shrimp-aquaculture sediment. **Chemosphere.** v. 196, p. 69–77, 2018. https://dx.doi.org/10.1016/j.chemosphere.2017.12.159

VAN KESSEL, M.A.H.J.; HARHANGI, H.R.; FLIK, G., JETTEN, M.S.M.; KLAREN, P.H.M.; OP DEN CAMP, H.J.M. Anammox bacteria in different compartments of recirculating aquaculture systems. **Biochemical Society Transactions,** v. 39, n. 6, p. 1817–1821, 2011. https://dx.doi.org/10.1042/BST20110743

XIAO, Y.; ZENG, G. M.; YANG, Z. H.; LIU, Y. S.; MA, Y. H.; YANG, L.; WANG, R. J.; XU, Z. Y. Coexistence of nitrifiers, denitrifiers and Anammox bacteria in a sequencing batch biofilm reactor as revealed by PCR-DGGE. J **Journal of Applied Microbiology,** v. 106, n. 2, p. 496–505, 2009. https://dx.doi.org/10.1111/j.1365-2672.2008.04017.x

XING, Y.; CLARK, I. Anaerobic Ammonium Oxidation in Waste Water -An Isotope Hydrological Perspective. *In:* EINSCHLAG, F. S. G. (ed.). **Waste Water**: treatment reutilization. Rijeka: InTech, 2012. https://dx.doi.org/10.5772/16154

WU, L.; SHEN, M.; LI, J.; HUANG, S.; LI, Z.; YAN, Z.; PENG, Y. Cooperation between partial-nitrification, complete ammonia oxidation (comammox), and anaerobic ammonia oxidation (anammox) in sludge digestion liquid for nitrogen removal. **Environmental Pollution**, v. 254, p. 112965, 2019. https://dx.doi.org/10.1016/j.envpol.2019.112965

ZAMBONI-FILHO, E.; BARBOSA, N. D.; GONÇALVES, S. M. Caracterização e tratamento do efluente das estações de Piscicultura. **Revista Unimar,** v. 19, p. 537–548, 1997.

ZHAO, J.; ZUO, J.; LIN, J.; LI, P. The performance of a combined nitritation–anammox reactor treating anaerobic digestion supernatant under various C/N ratios. **Journal of Environmental Science**, v. 30, p. 207-214, 2015. https://dx.doi.org/10.1016/j.jes.2014.08.022

Ambiente & Água - An Interdisciplinary Journal of Applied Science
ISSN 1980-993X – doi:10.4136/1980-993X
www.ambi-agua.net
E-mail: ambi.agua@gmail.com

Machine-learning methods for hydrological imputation data: analysis of the goodness of fit of the model in hydrographic systems of the Pacific - Ecuador

ARTICLES doi:10.4136/ambi-agua.2708

Received: 11 Feb. 2021; Accepted: 12 Apr. 2021

Diego Heras; Carlos Matovelle*

Center for Research, Innovation and technology transfer. Environmental Engineering. Catholic University of Cuenca, Avenida de las Americas, EC 010101, Cuenca, Azuay, Ecuador. E-mail: dherasb@ucacue.edu.ec
*Corresponding author. E-mail: cmmatovelleb@ucacue.edu.ec

ABSTRACT

Computational methods based on machine learning have had extensive development and application in hydrology, especially for modelling systems that do not have enough data. Within this problem, there are data series that are missing, and that should not necessarily be discarded; this is achieved by means of the imputation of the same ones, obtaining complete sets. For this reason, this research proposes a comparison of computer-learning techniques to identify those best suited for hydrographic systems of the Pacific of Ecuador. For the elaboration of this investigation, the hydro-meteorological records of the monitoring stations located in the watersheds of the Esmeraldas, Cañar and Jubones Rivers were used for 22 years, between 1990 and 2012. The variables that were imputed were precipitation and flow. Automatic learning machines of the Python Scikit_Learn module were used; these modules integrate a wide range of automated learning algorithms, such as Linear Regression and Random Forest. Finally, results were obtained that led to a minimum useful mean square error for Random Forest as an automatic machine-learning imputation method that best fits the systems and data analyzed.

Keywords: data imputation, hydrographic systems, machine learning.

Métodos de aprendizado de máquina para dados de imputação hidrológica: análise da qualidade de ajuste do modelo em sistemas hidrográficos do Pacífico - Equador

RESUMO

Métodos computacionais baseados em aprendizado de máquina tiveram amplo desenvolvimento e aplicação em hidrologia, especialmente para modelagem de sistemas que não possuem dados suficientes. Dentro deste problema faltam séries de dados que não devem ser necessariamente descartadas. Isso é feito por meio da imputação das mesmas obtendo-se conjuntos completos. Por este motivo, esta pesquisa propõe uma comparação de técnicas de aprendizagem computacional para identificar aquelas mais adequadas aos sistemas hidrográficos do Pacífico do Equador pelo interesse representado pelo estudo destes sistemas por complementaridade hidrológica. Para a elaboração desta investigação foram utilizados os registros hidrometeorológicos das estações de monitoramento localizadas nas bacias dos rios Esmeraldas, Cañar e Jubones durante 22 anos, compreendidos entre 1990 e 2012. As variáveis

This is an Open Access article distributed under the terms of the Creative Commons Attribution License, which permits unrestricted use, distribution, and reproduction in any medium, provided the original work is properly cited.

imputadas foram precipitação e vazão. Foram utilizadas máquinas de aprendizagem automática do módulo Python Scikit_Learn; esses módulos integram uma ampla gama de algoritmos de aprendizagem automatizados, como Linear Regression e Random Forest. Finalmente, foram obtidos resultados que levaram a um erro quadrático médio útil mínimo para Random Forest como um método de imputação de aprendizado de máquina automático que melhor se ajusta aos sistemas e dados analisados.

Palavras-chave: aprendizado de máquina, imputação de dados, sistemas hidrográficos.

1. INTRODUCTION

In recent years, methods based on machine learning have advanced considerably and have been applied in several areas of science and technology. Within hydrology, they have been widely applied in the development of basin behavior models, especially those that do not have enough information to apply physical models. In this aspect, another problem is that much of the available information is incomplete, and the series that are available are useless, further reducing the data for the work of hydrological modelling.

Hydrologists and water managers have made use of observed relationships between rainfall and runoff to predict streamflow ever since the creation of the rational method in the 19th century (Beven, 2012), a properly designed monitoring network with optimal data allows us to know the relationship between these behaviours and to be able to apply this in studies of water interest. However, streamflow and rainfall records suffer from missing observations, mostly resulting from unexpected causes including the loss of records, sensor problems, or disruption of data collection (Ng *et al*., 2009).

In the area of analysis, one of the problems is that there are not enough nor adequate monitoring systems, and from those that exist a large amount of missing data is evident. This makes the process of modelling these watersheds complicated and inaccurate; the application of this type of study generates knowledge of the area and its subsequent exploitation for different activities linked to water. These data would result in an incorrect response of hydrological models, but it is illogical to ignore abnormal or missing values if there is limited data available; substantial uncertainty in hydrologic and water quality modelling can be driven by these missing records (Kim *et al*., 2015). There are several methods to solve the problem of missing observations from statistics based on linear regressions that have already been validated in other investigations. These depend on the amount of data existing in the series and the data and relationships that they have with neighbouring weather stations (Mwale *et al.*, 2012; Rees, 2009). For these reasons, authors such as (Adeloye, 2009) indicate that regression methods might only be applicable when all predictors exist.

Artificial neural networks (ANNs), regression trees, and support vector machines have been shown to be powerful tools for predictive modelling and exploratory data analysis, particularly in areas that do not meet the conditions for using traditional statistical methods (Shortridge *et al*., 2016). These methods have mathematical formulations that require a high cost of computational processes, but are very effective when there are non-linear relationships to use traditional statistical methods (Dawson *et al.*, 2010). These strengths make them very useful, especially in countries with poor monitoring traditions, where gaps of information in climatological and hydrologic time series are ubiquitous (Campozano *et al*., 2014).

2. MATERIALS AND METHODS

The analysis stations are located in three main river basins of the coastal zone of Ecuador. These are the Cañar River, the Jubones River and the Esmeraldas River. These basins have

around 318 weather stations and 106 hydrological stations. The three systems have been chosen because they have the largest monitoring network in the country and represent a significant area of analysis (see Figure1).

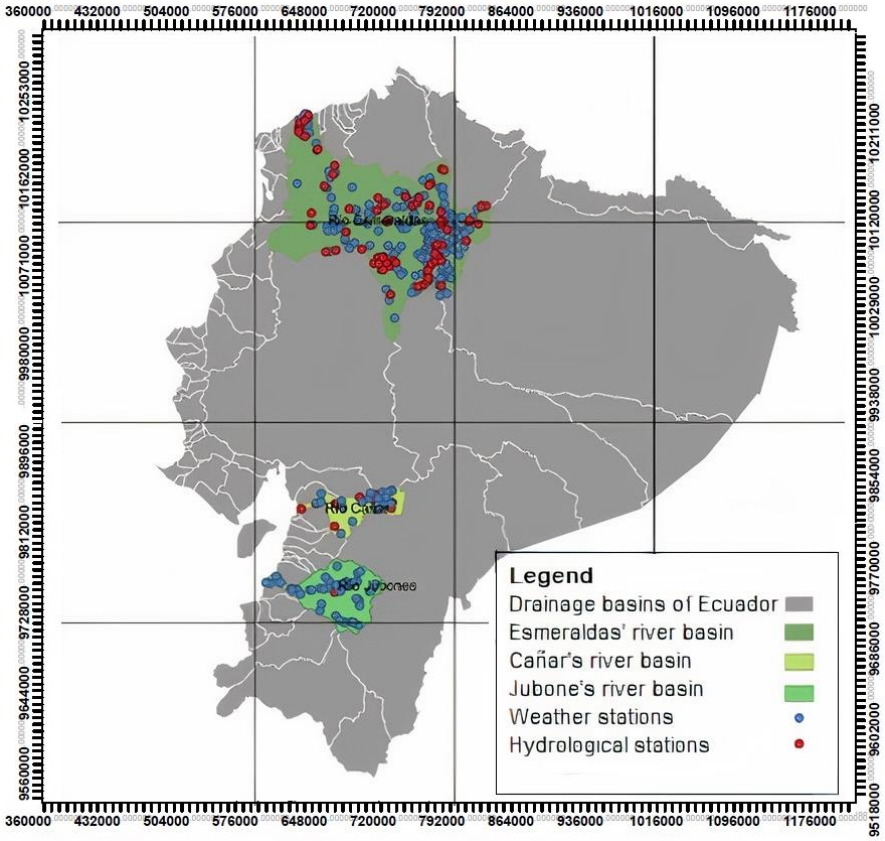

Figure 1. Location of the hydrographic systems for the analysis.

The sample of the stations to be analyzed was obtained by simple random sampling. One meteorological station and one hydrological station were selected per basin, as well as two nearby reference stations for the case of meteorological stations and a reference station for the example of hydrological stations. These nearby reference stations were selected as predictors at the time of analysis of data.

2.1. Data Imputation Methods

For the development of the imputation model with the uses of machine learning, we work with a pattern search to optimize parameters and later cross-validation for the periods of analysis of the research (Kim *et al*., 2015) (Carpenter, 1999[1]). This imputation method is based on supervised learning models, that is, the machine is presented with the response information at the same time as the input information, with which the machine will learn to arrive at the

[1] CARPENTER, J. **Personal Communication**. Virginia Tech, 1999.

answer through an iterative process. Within the operation of a machine learning, we have an input data vector that transfers it to the network where the complexity of the training is determined, thus obtaining a vector of data output as a result of the model (Guo *et al*., 2015).

The process is divided into training data, test data, and validation data; this division is established through cross-validation that allows an adequate distribution of the data between test data and validation so that the model does not over-fit in the trained data and have deficiencies in the validation data (see Figure 2). Followed by the supervised learning machine, this information is processed and a linear model based on the least square's method is established. The multiple iterations that the learning machine performs with the training and test data allow us to identify the best linear model, which will allow the imputation of hydro-meteorological data.

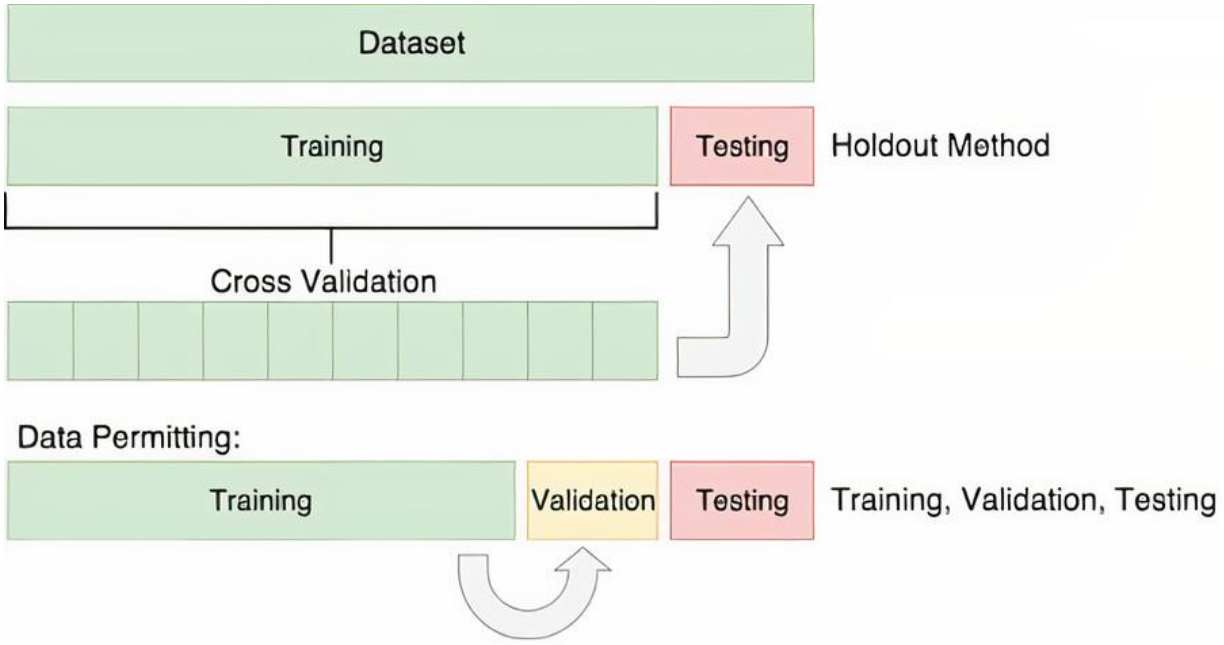

Figure 2. Cross-validation operation, between training, testing and validation data.
Source: www.towardsdatascience.com

The Tansig Function is used as a transfer function since it gives efficient results within hydrological studies (Kim *et al*., 2015; Akhter, 2017), the function is as Equation 1 follows:

$$y = f \sum_{i=1}^{N} w_i x_i + b \quad (1)$$

Where x_i is the input in the network, y is the output in the network, N is the number of neurons in the input vector, w_i is the connection weight between input and output, f is the transfer function, and b is the bias term.

To analyze the weight of each calculation, the neural networks use a back-propagation algorithm, where the error in the output data and the observed data are analyzed. It is a type of supervised learning based on the generalization of the delta rule (Veintimilla-Reyes and Cisneros, 2015; Hsu *et al.*, 1995; Bisoyi *et al*., 2019). This algorithm updates weights by moving along the gradient descent of the error function, which allows the steepest decreasing change. The advantages of this algorithm are its ability to adjust the learning rate by updating the learning rate parameter and it also guarantees less oscillation with the momentum constant (Kim *et al.*, 2015). The process is repeated until the error is minimized. This method is widely used in hydrological studies (Dawson and Wilby, 2001).

In this research, we analyze and compare two methods. The first method is autonomous learning based on linear regression, which integrates statistical models for relating responses to linear combinations of predictor variables (Ahmad *et al*., 2010; Srivastava *et al.*, 2013). The second method is the random forest algorithm, which is widely used for the study of water resources. Applications falling under this category include streamflow modeling using data-driven rainfall-runoff models, while streamflow imputation of missing values is also generating increased interest (Tyralis *et al.*, 2019).

Random Forest is a supervised Machine Learning algorithm based on a stochastic model that relates a result to explanatory variables or characteristics. Each decision within the tree can be viewed as a set of conditions, organized hierarchically and applied successively to the data set. For regression applications, they provide independent numerical predictions of the phenomenon of interest. In the end, the result corresponds to the mean forecast of all individual trees (Muñoz *et al*., 2018).

3. RESULTS AND DISCUSSIONS

The machine of autonomous learning based on linear regression and in random decision forests produced models that allowed the imputation of missing data in the hydro-meteorological records of the stations located in the study basins, i.e., the stations of the basins of the Esmeraldas, Cañar and Jubones Rivers. The following models are calibrated to meet the imputation of missing data from each station within the period of records comprising 22 years, from 1990 to 2012, for both meteorological stations and hydrological stations. It should also be taken into account that we worked only with the hydro-meteorological stations near the hydrographic basin, and that in the analysis of correlations they maintained between them a correlation value greater than or equal to 0.75.

The analysis of the best regressions obtained for each imputed data in the selected meteorological stations is presented (see Figure 3). These models were established with the Linear Regression learning machine of the Sklearn Python library, and their data sets were applied for cross-validation as a fundamental pillar for the validation of results (Hastie *et al*., 2017). The analyses have a relationship between the test values and the predicted values. As a result of these results, the linear models allowed imputation of missing data in the hydro-meteorological records. In the figure, it can be seen that there is a linear relationship for each of the data and the stations. This relationship has to be validated by statistical indicators of goodness-of-fit between observed and predicted data (Tyralis *et al.*, 2019; Zambrano-Bigiarini, 2017; 2011). These analyses are presented in Section 3.1, where they are compared between the two methods presented in this research.

Table 1 shows the equations of the linear models that have been obtained for each station with the stations with which it has been correlated with the previous spatial analysis. This line regression model is obtained by the Machine Learning Linear Regression algorithm between test values and the predicted values of the stations.

Similarly, the analysis of the allocation models based on the Random Forest learning machine (see Figure 4) is presented. The relationship between the values of the data of the reference station and the data of the analysis station is evaluated; each parameter of the model is calibrated so the statistical indicator is the most reliable.

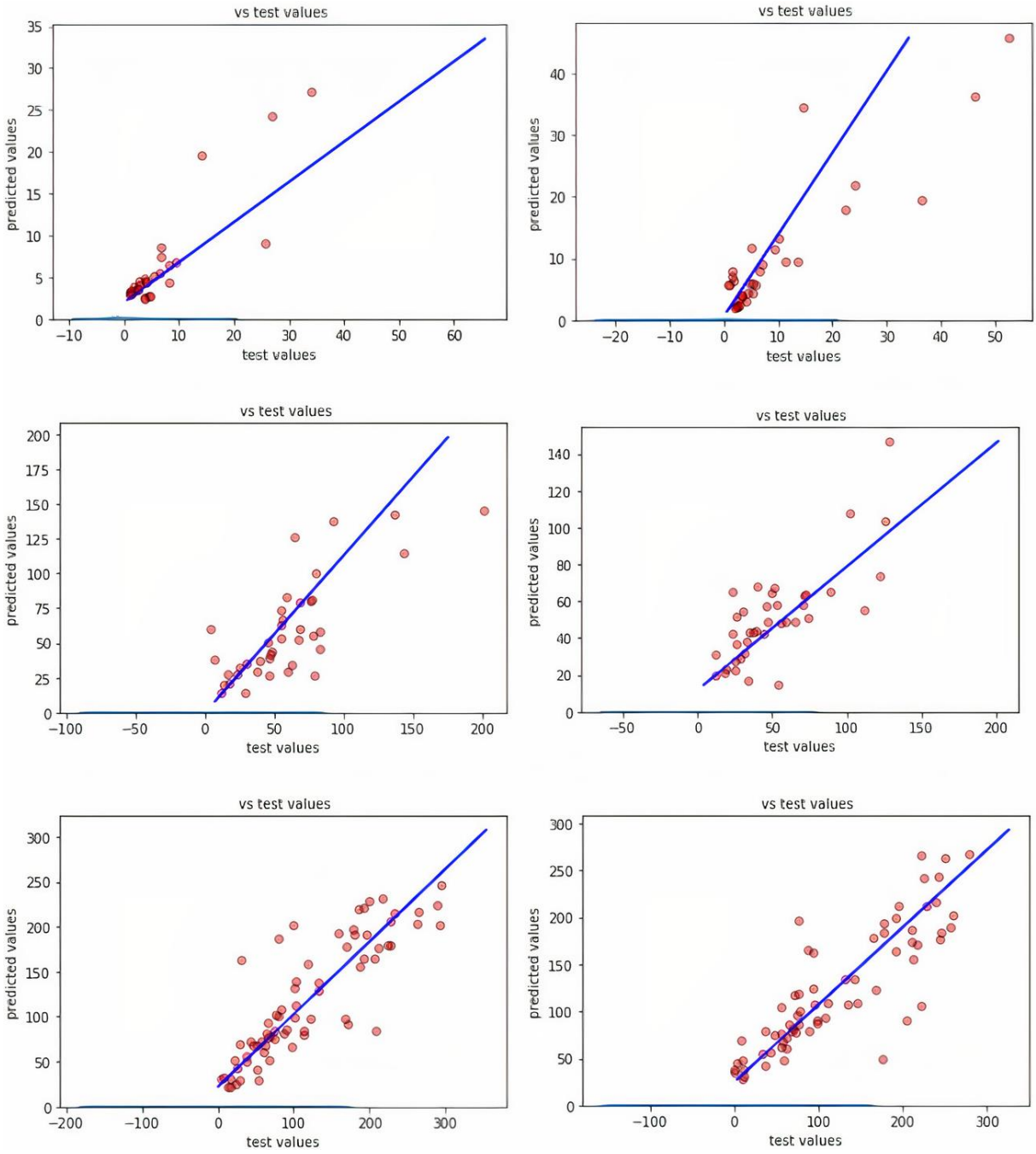

Figure 3. Linear regression line obtained by the Machine Learning Linear Regression algorithm between test values and the predicted values of the stations.

Table 1. Linear models for each weather station.

Weather station	Linear Model
M003	20.91 + 0.8150 M364
M364	22.68 + 0.8370 M003
M411	1.59 + 1.0939 M31
M031	10.52 + 0.6960 M411
M040	24.75 + 0.2145 M185 + 0.5375 M292
M185	23.25 + 0.3488 M040 + 1.2632 M292

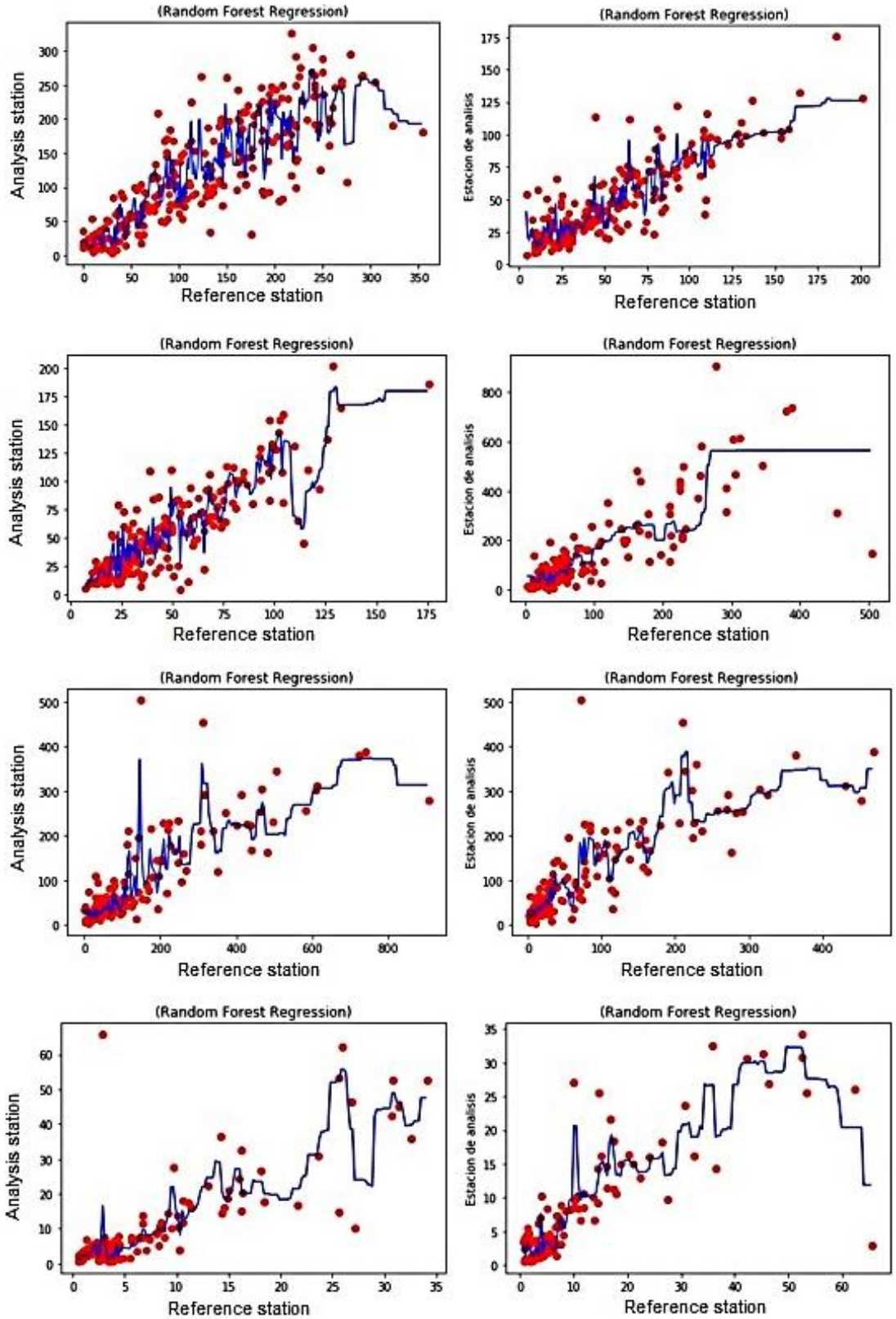

Figure 4. Predictive model obtained by the Machine Learning Random Forest algorithm between test values and the predicted values of the stations.

3.1. Analysis of statistical index for model validation

To perform an interpretation, comparison, and analysis of applicability for large hydrographic systems where the basin has many variations in both meteorological and hydrological behaviour, it is necessary to obtain indicators of goodness-of-fit that indicate

which is the optimal model. The statistical significance of the performance statistics is an aspect that is generally ignored that helps in reducing subjectivity in the proper interpretation of the model performance (Ritter and Muñoz-Carpena, 2013). To obtain these indicators, the data observed in the meteorological stations have been compared with the simulated data (imputed through the techniques analyzed). This process allows us to validate which of the two methods has a better fit, and therefore, which would be more efficient and result better in subsequent applications.

The indicators have been analyzed, and the efficiency coefficient of Nash and Sutcliffe (Nash and Sutcliffe, 1970) has received considerable attention in hydrological modelling (Gupta and Kling, 2011; Moussa, 2010). It has already been used for the imputation of missing data and it is generally used in other fields of science (Schaefli and Gupta, 2007). It is also tested by the Kling-Gupta Index of Efficiency (KGE) (Galleguillos *et al.*, 2017), which uses the values between -1 and 1, with the value 1 as an ideal and positive values greater than 0.5 as sufficiently robust correctors. The Mean Square Error is a standard indicator for this type of analysis (Gupta *et al*., 2009).

To determine the best method for data imputation, the indices are compared (Table 2). It is observed that the best method in the three reliability analyses is the Random Forest. The Mean Square Error is the one that indicates the highest relation of the imputed values and, observed with 0.01, the NSE and KGE index has values of 0.76 and 0. 67 respectively, indicating good data adjustments.

Table 2. Comparison of indexes of the evaluated methods.

LINEAR REGRESSION				RANDOM FOREST			
STATION	**MSE**	**NSE**	**KGE**	**STATION**	**MSE**	**NSE**	**KGE**
M003	0	0.75	0.55	M003	0	0.78	0.68
M364	0	0.75	0.55	M364	0	0.78	0.68
M411	0.02	0.71	0.52	M411	0	0.78	0.68
M031	0.1	0.7	0.50	M031	0	0.78	0.68
M040	0	0.75	0.45	M040	0.06	0.7	0.65
M185	0.32	0.68	0.4	M185	0.07	0.7	0.65
M292	0.08	0.65	0.45	M292	0.02	0.73	0.66
H172	0.05	0.6	0.45	H172	0	0.78	0.68
H173	0	0.65	0.43	H173	0	0.78	0.68
MEAN	**0.06**	**0.69**	**0.48**	**MEAN**	**0.01**	**0.76**	**0.67**

The evaluations of the indices verify that the models have given good results. Reliable indices are appreciated with the tools of artificial intelligence, although reviewing each accurate indicator the NSE index for Linear Regression is 0.69 compared to 0.76 for Random Forest; the two values show right adjustments between the data (Waseem *et al*., 2017). The KGE index between the models has more noticeable differences between Linear Regression (0.48) and Random Forest (0.67), the Random Forest indicator has given values that establish (Näschen *et al*., 2018; Pool *et al.*, 2018) the use of that model as the best for analysis of large river basins with variations of the Pacific climatology.

For several decades the need to have complete time series to validate subsequent studies has meant that many studies are done, and various techniques have been used. In Aissia *et al.* (2017), a review of multivariate methods and their application to reduce the loss of information is made; these range from simple relationships such as linear regressions that are based on spatial approximations, artificial intelligence techniques, and even much more innovative methods, such as those presented by Williams *et al.* (2018), who formed two methods with Bayesian structures to generate an algorithm that represented the signal of the time series of

temperatures. In Teegavarapu (2019) research, spatial interpolation methods were evaluated, although Euclidean distances were substituted to improve fit indicators' goodness.

In another study carried out by Chen *et al.* (2019), several techniques were tested to impute precipitation data with the premise that having complete series improves analyses within hydrographic basins. After using several methods, they decide to perform the hydrological model with the best fit; This leads us to consider that there is no "best" technique, but rather that the analysis must be based on several determining factors such as the type of hydrometeorological variable, the years of the series, the time scale, spatial variations, conditioning factors or external phenomena.

The apparent difference compared to traditional methods is that the response to abnormal weather patterns can be better exploited, which is of great interest for rainfall patterns as variable as that of the Pacific in Ecuador, which is influenced by various external phenomena.

4. CONCLUSIONS

In this study, we propose the analysis of two traditional methods of artificial intelligence to study the accuracy and use for imputation of missing data in Hydrographic Systems on the slope of the Pacific in Ecuador. The two methods proposed and evaluated were Linear Regression and Random Forest, which were tested in the three most representative Hydrographic Systems of the country, in the basins of the Esmeraldas, Cañar and Jubones Rivers, intending to cover the extension of the surface and the water from north to the south of Ecuador.

After carrying out a preliminary analysis of the data, we worked with 9 test stations in the three systems, observing goodness-of-fit indicators for each of the stations and each model, we worked with Medium Squared Error (MSE), Nash and Sutcliffe (NSE) and Kling-Gupta Index of efficiency (KGE). The values obtained after the goodness-of-fit analysis mark ranges for good efficiency analyses, but the Random Forest model has the three best indicators both on average and for each of the analysis stations. It is important to highlight the importance of carrying out this type of analysis in watersheds of the Pacific slope of Ecuador, since available information is scarce and the hydro-meteorological behaviour is different from the Amazon slope. They are also very large systems in extension but with hypsometries marked by very marked altitudinal differences in a small area of land and with a lower amount of water compared to the Amazon slope.

After the data analysis and the discussion process with authors who have carried out similar works worldwide for several decades, it can be seen that techniques that can reproduce atypical effects should be evaluated in the first place and then validated before their application to the management of water resources.

5. REFERENCES

ADELOYE, A. The relative utility of regression and artificial neural networks models for rapidly predicting the capacity of water supply reservoirs. **Environmental Modelling and Software**, v. 24, n. 10, p. 1233–1240, 2009. https://doi.org/10.1016/j.envsoft.2009.04.002

AHMAD, S.; KALRA, A.; STEPHEN, H. Estimating soil moisture using remote sensing data: A machine learning approach. **Advances in Water Resources**, v. 33, n. 1, p. 69–80, 2010. https://doi.org/10.1016/j.advwatres.2009.10.008

AISSIA, M.-A. B.; CHEBANA, F.; OUARDA, T. B. M. J. Multivariate missing data in hydrology–Review and applications. **Advances in Water Resources**, v. 110, p. 299-309, 2017. https://doi.org/10.1016/j.advwatres.2017.10.002

AKHTER, M. Application of ANN for the Hydrological Modeling. **International Journal for Research in Applied Science & Engineering Technology**, v. 5, n. 7, p. 203–213, 2017.

BEVEN, K. Rainfall-Runoff Modelling. *In*: ABRAHART, R.; KNEALE, P. E.; SEE, L. M. (eds.). **Neural Networks for Hydrological Modeling**. 2nd ed. New York: John Wiley & Sons, 2012. https://doi.org/10.1201/9780203024119.ch9

BISOYI, N.; GUPTA, H.; PADHY, N. P.; CHAKRAPANI, G. J. Prediction of daily sediment discharge using a back propagation neural network training algorithm: A case study of the Narmada River, India. **International Journal of Sediment Research**, v. 34, n. 2, p. 125–135, 2019. https://doi.org/10.1016/j.ijsrc.2018.10.010

CAMPOZANO, L.; SÁNCHEZ, E.; AVILÉS, Á.; SAMANIEGO, E. Evaluation of infilling methods for time series of daily precipitation and temperature: The case of the Ecuadorian Andes. **Maskana**, v. 5, n. 1, p. 99–115, 2014. https://doi.org/10.18537/mskn.05.01.07

CHEN, L.; XU, J.; WANG, G.; SHEN, Z. Comparison of the multiple imputation approaches for imputing rainfall data series and their applications to watershed models. **Journal of Hydrology**, v. 572, p. 449–460, 2019. https://doi.org/10.1016/j.jhydrol.2019.03.025

DAWSON, C. W.; HARPHAM, C.; WILBY, R. L.; CHEN, Y. Evaluation of artificial neural network techniques for flow forecasting in the River Yangtze, China. **Hydrology and Earth System Sciences**, v. 6, n. 4, p. 619–626, 2010. https://doi.org/10.5194/hess-6-619-2002

DAWSON, C. W.; WILBY, R. L. Hydrological modelling using artificial neural networks. **Progress in Physical Geography**, v. 25, n. 1, p. 80–108, 2001. https://doi.org/10.1191/030913301674775671

GALLEGUILLOS, M.; ZAMBRANO, M.; PUELMA, C.; JOPIA, A. Evaluación espacio-temporal del déficit hídrico para las cuencas de Chile a partir de información satelital. *In:* **Escenarios Hídricos 2030**. 2017. Available at: http://escenarioshidricos.cl/multimedia/ Access: 2018.

GUO, H.; JEONG, K.; LIM, J.; JO, J.; KIM, Y. M.; PARK, J.-P.; KIM, J. H.; CHO, K. H. Prediction of effluent concentration in a wastewater treatment plant using machine learning models. **Journal of Environmental Sciences**, v. 32, p. 90–101, 2015. https://doi.org/10.1016/j.jes.2015.01.007

GUPTA, H. V.; KLING, H. On typical range, sensitivity, and normalization of Mean Squared Error and Nash-Sutcliffe Efficiency type metrics. **Water Resources Research**, v. 47, n. 10, p. 2–4, 2011. https://doi.org/10.1029/2011WR010962

GUPTA, H. V.; KLING, H.; YILMAZ, K. K.; MARTINEZ, G. F. Decomposition of the mean squared error and NSE performance criteria: Implications for improving hydrological modelling. **Journal of Hydrology**, v. 377, n. 1–2, p. 80–91, 2009. https://doi.org/10.1016/j.jhydrol.2009.08.003

HASTIE, T.; TIBSHIRANI, R.; FRIEDMAN, J. **The Elements of Statistical Learning**. Springer, 2017.

HSU, K.; GUPTA, H. V.; SOROOSHIAN, S. Artificial neural network modeling of the rainfall-runoff process that arises and based on Background and Scope. **Water Resources**, v. 31, n. 10, p. 2517-2530, 1995. https://doi.org/10.1029/95WR01955

KIM, M.; BAEK, S.; LIGARAY, M.; PYO, J.; PARK, M.; CHO, K. H. Comparative studies of different imputation methods for recovering streamflow observation. **Water**, v. 7, n. 12, p. 6847–6860, 2015. https://doi.org/10.3390/w7126663

MOUSSA, R. When monstrosity can be beautiful while normality can be ugly: assessing the performance of event-based flood models. **Hydrological Sciences Journal**, v. 55, n. 6, p. 1074–1084, 2010. https://doi.org/10.1080/02626667.2010.505893

MUÑOZ, P.; ORELLANA-ALVEAR, J.; WILLEMS, P.; CÉLLERI, R. Flash-flood forecasting in an andean mountain catchment-development of a step-wise methodology based on the random forest algorithm. **Water**, v. 10, n. 11, 2018. https://doi.org/10.3390/w10111519

MWALE, F. D.; ADELOYE, A. J.; RUSTUM, R. Infilling of missing rainfall and streamflow data in the Shire River basin, Malawi - A self organizing map approach. **Physics and Chemistry of the Earth**, v. 50–52, p. 34–43, 2012. https://doi.org/10.1016/j.pce.2012.09.006

NÄSCHEN, K.; DIEKKRÜGER, B.; LEEMHUIS, C.; STEINBACH, S.; SEREGINA, L. S.; THONFELD, F.; VAN DER LINDEN, R. Hydrological modeling in data-scarce catchments: The Kilombero floodplain in Tanzania. **Water**, v. 10, n. 5, p. 1–27, 2018 https://doi.org/10.3390/w10050599

NASH, J. E.; SUTCLIFFE, J. V. River flow forecasting through conceptual models part I — A discussion of principles. **Journal of Hydrology**, v. 10, n. 3, p. 282–290, 1970 https://doi.org/https://doi.org/10.1016/0022-1694(70)90255-6

NG, W. W.; PANU, U. S.; LENNOX, W. C. Comparative Studies in Problems of Missing Extreme Daily Streamflow Records. **Journal of Hydrologic Engineering**, v. 14, n. 1, p. 91–100, 2009. https://doi.org/10.1061/(asce)1084-0699(2009)14:1(91)

POOL, S.; VIS, M.; SEIBERT, J. Evaluating model performance: towards a non-parametric variant of the Kling-Gupta efficiency. **Hydrological Sciences Journal**, v. 63, n.13–14, p. 1941–1953, 2018. https://doi.org/10.1080/02626667.2018.1552002

REES, G. Hydrological data. *In:* WMO. **Manual on Low-flow Estimation and Prediction**. Geneva: WMO, 2009. (Operational Hydrology Report, n. 1029).

RITTER, A.; MUÑOZ-CARPENA, R. Performance evaluation of hydrological models: Statistical significance for reducing subjectivity in goodness-of-fit assessments. **Journal of Hydrology**, v. 480, p. 33–45, 2013. https://doi.org/10.1016/j.jhydrol.2012.12.004

SCHAEFLI, B.; GUPTA, H. V. Do Nash values have value? **Hydrological Processes**, v. 21, p. 2075–2080, 2007. https://doi.org/10.1002/hyp

SHORTRIDGE, J. E.; GUIKEMA, S. D.; ZAITCHIK, B. F. Machine learning methods for empirical streamflow simulation: A comparison of model accuracy, interpretability, and uncertainty in seasonal watersheds. **Hydrology and Earth System Sciences**, v. 20, n. 7, p. 2611–2628, 2016. https://doi.org/10.5194/hess-20-2611-2016

SRIVASTAVA, P. K.; HAN, D.; RAMIREZ, M. R.; ISLAM, T. Machine Learning Techniques for Downscaling SMOS Satellite Soil Moisture Using MODIS Land Surface Temperature for Hydrological Application. **Water Resources Management**, v. 27, n. 8, p. 3127–3144, 2013. https://doi.org/10.1007/s11269-013-0337-9

TEEGAVARAPU, R. S. V. Precipitation Imputation with Probability Space-based Weighting Methods. **Journal of Hydrology**, v. 581, 2019. https://doi.org/10.1016/j.jhydrol.2019.124447

TYRALIS, H.; PAPACHARALAMPOUS, G.; LANGOUSIS, A. A Brief Review of Random Forests for Water Scientists and Practitioners and Their Recent History in Water Resources. **Water**, v. 11, n. 5, p. 910, 2019. https://doi.org/10.3390/w11050910

VEINTIMILLA-REYES, J.; CISNEROS, F. Predicción de Caudales Basados en Redes Neuronales Artificiales (RNA) para Períodos de Tiempo Sub Diarios. **Revista Politécnica**, v. 35, n. 3, p. 42–49, 2015.

WASEEM, M.; MANI, N.; ANDIEGO, G.; USMAN, M. A Review of Criteria of Fit for Hydrological Models. **International Research Journal of Engineering and Technology**, v. 4, n. 11, 2017.

WILLIAMS, D. A.; NELSEN, B.; BERRETT, C.; WILLIAMS, G. P.; MOON, T. K. A comparison of data imputation methods using Bayesian compressive sensing and Empirical Mode Decomposition for environmental temperature data. **Environmental Modelling and Software**, v. 102, p. 172–184, 2018. https://doi.org/10.1016/j.envsoft.2018.01.012

ZAMBRANO-BIGIARINI, M. Goodness-of-fit Measures to Compare Observed and Simulated Values with hydroGOF Installation Installing hydroGOF. p. 1–5, 2011. Available at: https://mran.microsoft.com/snapshot/2017-05-24/web/packages/hydroGOF/vignettes/hydroGOF_Vignette.pdf Access: 2018.

ZAMBRANO-BIGIARINI, M. **HydroGOF**. 2017. Available at: http://hzambran.github.io/hydroGOF/. Access: 2017.

Ambiente & Água - An Interdisciplinary Journal of Applied Science
ISSN 1980-993X – doi:10.4136/1980-993X
www.ambi-agua.net
E-mail: ambi.agua@gmail.com

Statistical study of growth kinetics and lipid content of microalgae grown in brackish waters for bioenergetic purposes

ARTICLES doi:10.4136/ambi-agua.2649

Received: 15 Sep. 2020; Accepted: 19 Apr. 2021

Bruna da Silveira Guimarães*; Kepler Borges França

Unidade Acadêmica de Engenharia Química. Laboratório de Referência em Dessalinização (LABDES). Universidade Federal de Campina Grande (UFCG), Rua Aprígio Veloso, nº 882, CEP: 58429-900, Campina Grande, PB, Brazil. E-mail: kepler123@gmail.com
*Corresponding author. E-mail: brunasilveiraguimaraes@hotmail.com

ABSTRACT

This study aimed to statistically prove the influence of salinity on growth kinetics and intracellular lipid accumulation in microalgae. The species *Chlorella* sp., *Scenedesmus acuminatus*, *Nannochloropsis* sp., *Monoraphidium contortum* and *Pediastrum tetras* were studied, which were isolated in the Brazilian semi-arid region and cultivated in synthetic media with the addition of NaCl. From the crops, growth kinetics, dry biomass production and lipid content were analyzed, using the experimental planning for one factor as a tool, with the NaCl concentration as an independent variable. The kinetic parameters maximum growth speed (μ_{max}) and generation time (t_g), as well as lipid concentration were the response variables studied. The results showed that, in the species *Scenedesmus acuminatus*, *Nannochloropsis* sp. and *Pediastrum tetras*, salt stress contributed to the increase in μ_{max} and the consequent decrease in t_g. The highest levels of lipid accumulation were obtained in *Nannochloropsis* sp. (62.04%), in the medium with the highest salinity and *Pediastrum tetras* (54.04%) in the lowest. Dry biomass production was higher in *Scenedesmus acuminatus* (1,941.37 $mg.L^{-1}$) and *Nannochloropsis* sp. (1237.05 $mg.L^{-1}$), both at a concentration of 4.0 $g.L^{-1}$. Therefore, saline stress acted directly on the cell growth and lipid content of the species, which can be used as a device to enhance lipid production for the purpose of producing biofuels.

Keywords: biofuels, biomass, biotechnology, brackish waters, lipids.

Estudo estatístico da cinética de crescimento e teor de lipídeos de microalgas cultivadas águas salobras com fins bioenergéticos

RESUMO

O presente trabalho teve como objetivo comprovar, estatisticamente, a influência da salinidade na cinética de crescimento e acumulação lipídica intracelular em microalgas. Foram estudadas as espécies *Chlorella* sp., *Scenedesmus acuminatus*, *Nannochloropsis* sp., *Monoraphidium contortum* e *Pediastrum tetras*, as quais foram isoladas na região semiárida nordestina brasileira e cultivadas em meios sintéticos com adição de NaCl. A partir dos cultivos foram analisados a cinética de crescimento, produção de biomassa seca e teor de lipídeos, utilizando-se como ferramenta o planejamento experimental para um fator, tendo a concentração de NaCl como variável independente. Os parâmetros cinéticos velocidade máxima de crescimento ($\mu_{máx}$) e tempo de geração (t_g), bem como concentração lipídica foram

This is an Open Access article distributed under the terms of the Creative Commons Attribution License, which permits unrestricted use, distribution, and reproduction in any medium, provided the original work is properly cited.

as variáveis resposta estudadas. Os resultados mostraram que, nas espécies *Scenedesmus acuminatus*, *Nannochloropsis* sp. e *Pediastrum tetras*, o estresse salino contribuiu para o aumento de $\mu_{máx}$ e consequente diminuição de t_g. Os maiores níveis de acumulação lipídica foram obtidos na *Nannochloropsis* sp. (62,04%), no meio com maior salinidade e *Pediastrum tetras* (54,03%) no de menor. A produção de biomassa seca foi maior nas espécies *Scenedesmus acuminatus* (1.941,37 $mg.L^{-1}$) e *Nannochloropsis* sp. (1237,05 $mg.L^{-1}$), ambas na concentração de 4,0 $g.L^{-1}$. Portanto, o estresse salino atuou diretamente no crescimento celular e teor de lipídeos das espécies, podendo este ser utilizado como artifício para potencializar a produção lipídica, com fins de produção de biocombustíveis.

Palavras-chave: águas salobras, biocombustíveis, biomassa, biotecnologia, lipídeos.

1. INTRODUCTION

Since the middle of the twentieth century, it has been well known that rapid population growth and technological advances contribute to the increase in the planet's energy demand. According to studies, the tendency is that this demand will increase by up to 50% by 2030. Fossil-fuel oil products cannot satisfy the current demand, as demand is 105 times greater than nature can replenish. It is well known that excessive dependence on fuels derived from petroleum causes great environmental damage in the medium- and long-term, including the reduction of fuel reserves, in addition to climate changes caused by the increase in the emission of gases such as CO_2 (Shuba and Kifle, 2018).

The use of biofuels has been shown to be a viable alternative to solve dependence on petroleum derivatives, which can be produced from raw materials such as starch, vegetable oils, animal fats, biomass residues and algae biomass. As environmental benefits, biofuels reduce CO_2, hydrocarbon and particulate matter emissions, in addition to eliminating emissions of SO_X-type compounds, with a consequent reduction in greenhouse gases. The CO_2 capture capacity of microalgae is between 10 and 50 times greater than many higher plants. Thus, greater photosynthetic efficiency is observed, in relation to higher plants, which is one of the positive points for use as a raw material for the production of biodiesel (Zhu *et al*., 2017).

Shuba and Kifle (2018) also point out that the productivity of biodiesel production from microalgae biomass can generally surpass the values of the best oil-producing crops. They also show that, compared to other crops, biomass has more potential for production, without negatively affecting the supply of food and other products of agricultural origin, since the crops can be grown on non-arable land, not used for agricultural purposes. Thus, there is no territorial competition with crops destined for food purposes.

Bellou *et al*. (2014) note that some species of microalgae are capable of accumulating considerable amounts of lipids, the main raw material for the production of biodiesel, being compared to higher oilseed plants. Zhao *et al*. (2021) show that saline stress is a device widely used and researched to maximize the synthesis of lipids in microalgae, since they are more viable processes, economically speaking. Qiao *et al*. (2021) also highlight that causing salt stress directly affects physiological and biochemical mechanisms linked to cell growth and consequent biomass production, causing ionic, osmotic and oxidative stress. Ionic and osmotic changes caused by salt stress reduce the activity of the Na^+/H^+ ion, which impacts on photosynthetic activity. Thus, during lipid accumulation, the saline medium causes an increase in oxidative stress or accumulation of reactive oxygen species in the microalgal cells.

Zhang *et al*. (2017) still emphasize that the understanding of the regulatory mechanism for the production of lipids in microalgae cells is important in the development of technologies for the production of biofuels derived from microalgal biomass. Chew *et al*. (2018) show that recent research with the species *Tetraselmis suecica* and *Nannochloropsis oculata* shows the high

potential for the production of biodiesel, being considered suitable species for large-scale production. Such research has also shown that some species, such as *T. suecica*, are able to grow in saline and brackish environments due to the presence of Na^+ pumps, which act on the osmoregulatory mechanism of cells, making them adaptable to rapid and gradual changes in salinity. Srivastava *et al*. (2017) found that the salinity of the medium contributes significantly in the synthesis of neutral lipids, more specifically the triacylglycerides (TAG) in the form of secondary metabolite, allowing the microalgal cells to support the increase in salinity. The exploitation of these factors can be of vital importance, implying the economic viability of the production of microalgae on a large scale for bioenergetic purposes. The author also points out that the salinity of the medium also interferes with the rate of respiration, assimilation of nutrients and carbon uptake.

Pancha *et al*. (2015) show that salt stress has been studied in the cultivation of species such as *Chlamydomonas* sp., *Desmodesmus abundans* and *Nannochloropsis* sp. In his work, the author studied the effect of salinity on the growth of freshwater microalgae *Scenedesmus* sp. The authors observed that saline stress caused physiological, biochemical and growth changes. Parameters were analyzed, such as biomass production, lipid content, carbohydrates, proteins, photosynthetic pigments, mineral contents, among others. The results showed an increase in lipid and carbohydrate levels in crops grown in a single phase, but with lower amounts of biomass.

Based on the literature review and the authors' knowledge, no studies were found to statistically prove the positive or negative influence of salinity on growth kinetics and on the content of microalgae intracellular lipids. Thus, the objective of this work is to prove, using experimental planning for one factor, the influence of the salinity of the medium in the cultivation of five species of microalgae, cultivated in brackish media, by the addition of NaCl in different concentrations. Based on the monitoring of growth in each medium and their comparison with the culture medium without the addition of this salt, the work analyzes which species increased cell growth, biomass production and lipid accumulation, thus proving the potential for the production of biodiesel.

2. MATERIALS AND METHODS

The study was carried out in a controlled environment at the Laboratório de Referência em Dessalinização (LABDES) located at the Universidade Federal de Campina Grande (UFCG) in Campina Grande, Paraíba, Brazil. Five strains of species were used, isolated in the semiarid region of northeastern Brazil. The species were: *Chlorella* sp., *Scenedesmus acuminatus*, *Nannochloropsis* sp., *Monoraphidium contortum* and *Pediastrum tetras*. *Secenedesmus acuminatus*, *Monoraphidium contortum*, *Pediastrum tetras* and *Nannochloropsis* sp. were replicated in synthetic Water Culture, recommended by Guillard and Lorenzen (1972). *Chlorella* sp. was replicated in Bold's Basal Medium synthetic medium, with a composition described by Bischoff and Bold (1963).

The methodology used for crops was developed by the authors. It was carried out from the inoculum in the synthetic media in photobioreactors (Figure 1), with a volume of 2 liters, adding NaCl, in concentrations of 2.0; 4.0 and 6.0 $g.L^{-1}$. In addition to these, the strains were also inoculated into the medium without the addition of salts, called Control for comparison between brackish media. The cultivation environment was controlled, with a temperature between 22.0 and 25.0ºC, based on Chisti (2008), who recommends a range between 20.0 and 30.0ºC in the cultivation of microalgae. Light/dark photoperiod 12/12h (384.0 lux) and constant aeration through micro pumps at a flow rate of 150.0 $L.h^{-1}$ was used.

After this stage, cell growth was monitored solely by daily counting the number of cells per mL, aiming at calculating the kinetic parameters based on the observance of the growth phases, as shown by Lee *et al.* (2015). The authors report that batch microalgal growth has six

phases; lag, exponential or log, linear, of declining growth, stationary and of death. In addition, this process also had the purpose of visualizing viable and non-viable cells in each culture medium. Monitoring of pH also took place, aimed at observing changes in the media.

Figure 1. Photobioreactors in a controlled environment.

The counts were performed until the phase of stationary cell growth was reached, with the total cultivation time for *Chlorella* sp. between 10 and 13 days, between 15 and 18 days for *Scenedesmus acuminatus* and *Nannochloropsis* sp., for *Monoraphidium contortum* and *Pediastrum tetras* the cultivation time was 15 days. With the data obtained, the growth curves were plotted and the beginning and end of the exponential growth phase were observed for the kinetic calculations. After reaching the maximum number of cells, the biomass was separated by centrifuge and dried in an oven at 45.0ºC to check the lipid content, according to the methodology recommended by Folch *et al.* (1957), modified for microalgae. However, the production of dry biomass per liter of cultivation was previously calculated by weighing.

From the kinetic results, a statistical study was made using the Hypothesis Test, from the experimental planning for one factor, testing the equality between means of the kinetic parameters of the treatments. This study was carried out through Test F ($\alpha = 0.05$), applying analysis of variance (ANOVA) and Tukey's Test, aiming to know the influence of salinity (input variable) on the growth of species, comparing them the average values of the kinetic parameters of each medium with the Control. The levels varied according to the salinity of the media under study, that is, 0 (Control); 2.0 $g.L^{-1}$; 4.0 $g.L^{-1}$ and 6.0 $g.L^{-1}$. The response variables were the maximum growth speed (μ_{max}, given day^{-1}) and generation time (t_g, given day), which depend on the cell concentrations obtained through the daily count. Such parameters are calculated from Equations 1 and 2, as discussed by Schmidell *et al*. (2001), where, X_i is the cellular concentration (in $cells.mL^{-1}$) at the beginning of the exponential phase and X is the final concentration, just as t_i is the initial time of the exponential phase and t the final time, in days. With this treatment, it was possible to compare the means of the kinetic parameters at the levels 2.0 $g.L^{-1}$; 4.0 $g.L^{-1}$ and 6.0 $g.L^{-1}$ with the Control, observing which results showed significant differences.

$$ln\ \frac{X}{X_i} = \mu_{max}.(t - t_i) \quad (1)$$

$$\mu_{máx} = \frac{ln\,2}{t_g} = \frac{0{,}693}{t_g} \quad (2)$$

3. RESULTS AND DISCUSSION

3.1. Growth kinetics

As shown in Figure 2, the X axis represents the NaCl concentration and the Y axis the kinetic parameters (μ_{max} and t_g). For *Chlorella* sp., the highest value of μ_{max} and lowest t_g occurred in the Control and, among the brackish media; the best values were observed in the concentration of 4.0 g.L^{-1}. In contrast, the *Scenedesmus acuminatus* species had better growth kinetics in the medium with higher salinity, reaching values much higher than that of the Control, which points to the fact that the cell growth of this species is favored in the media with higher salinities.

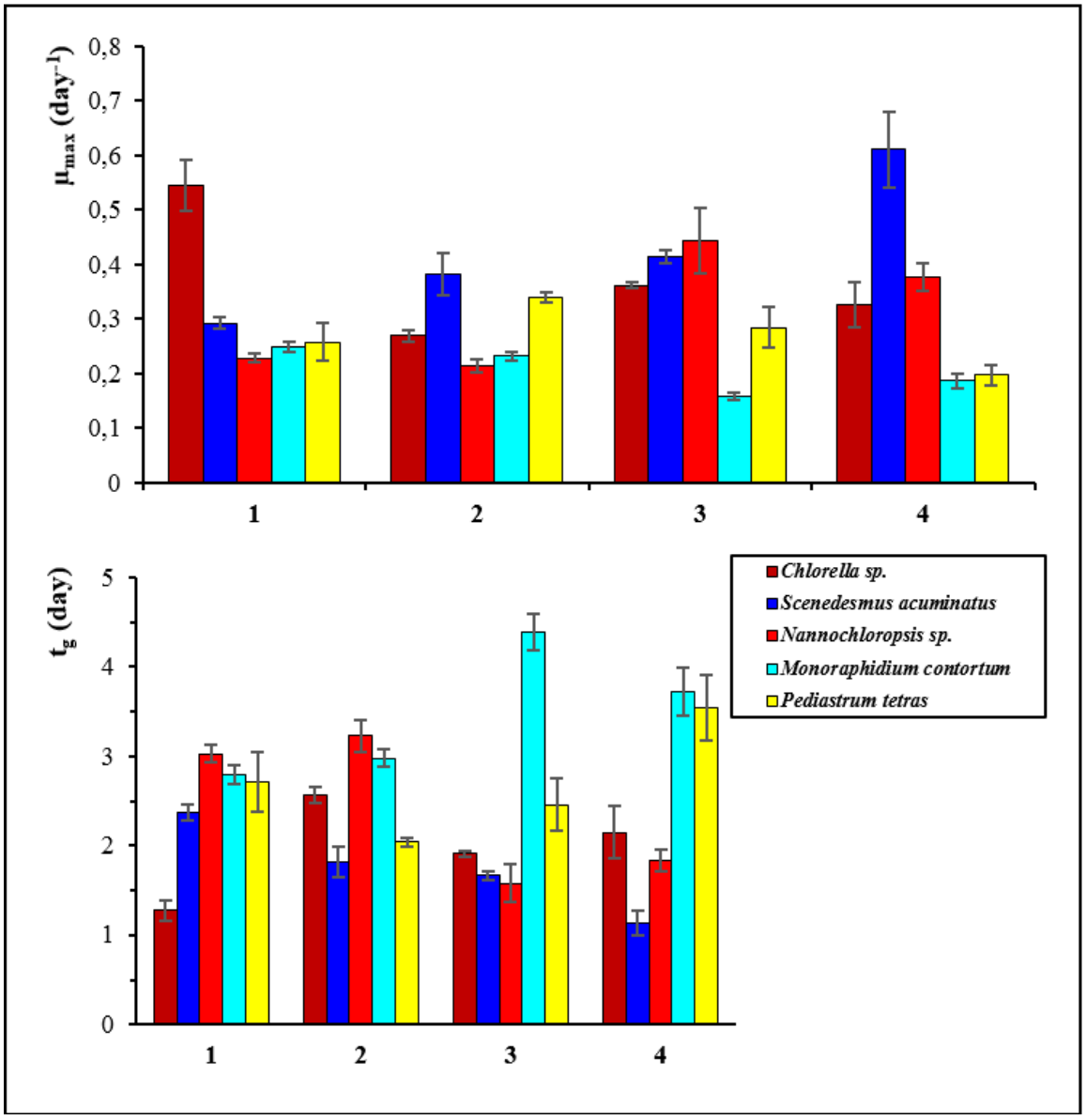

Figure 2. Maximum growth speed and generation time for all species in brackish and control environments.

The same occurred with *Nannochloropsis* sp., in which the values of μ_{max} and t_g in the medium 4.0 g.L^{-1} were more satisfactory than those of the Control. Similar results were not

observed in the microalgae *Monoraphidium contortum*, where there were no major differences between the Control and the other concentrations. It appears that μmax and t_g, in brackish environments, did not exceed those of Control. For *Pediastrum tetras* species, the maximum growth speed and generation time were slightly higher in the media with salinity of 2.0 $g.L^{-1}$ and 4.0 $g.L^{-1}$, but without great increases in relation to the Control.

Comparing the species, the growth kinetics was favored in the media with higher salinities for *Scenedesmus acuminatus* and *Nannochloropsis* sp., and *Chlorella* sp., in this order. Nevertheless, it is observed in the latter that the kinetic results were not better than those of the Control. However, relating to *Monoraphidium contortum* and *Pediastrum tetras*, the results in concentrations of 4.0 and 6.0 $g.L^{-1}$ were more expressive for *Chlorella* sp.

Abubakar (2016) cultivated the microalgae *Dunaliella* sp., studying the ideal salinity in cell growth. The author shows that the growth rate was maximum in the medium with NaCl concentration of 1.0 Molar (0.1680 day^{-1}). This shows the great diversity of halotolerant species, that is, those that are able to adapt to brackish environments. The present study also shows this diversity, to the extent that species with greater adaptability were used, since they were obtained, mainly in the cultivation of *Chlorella* sp., *Scenedesmus acuminatus* and *Nannochloropsis* sp., higher rates of maximum growth and generation time in media with higher salinities.

3.2. Statistical analysis of growth kinetics

As can be seen in Table 1, the $F_{calculated}$ values are all higher than the $F_{tabulated}$, confirming the significant difference between the means.

Table 1. F test for μ_{max} and t_g with $\alpha = 0.05$. ($F_{tabulated} = 4.07$).

	$F_{calculate}$ (μ_{max})	$F_{calculate}$ (t_g)	R^2 (μ_{max})	R^2 (t_g)
Chlorella sp.	42.25	32.37	94.06	92.39
Scenedesmus acuminatus	32.88	50.52	92.50	94.99
Nannochloropsis sp.	34.62	80.71	92.85	96.80
Monoraphidium contortum	54.90	48.84	95.37	94.82
Pediastrum tetras	14.54	14.47	84.51	84.33

It can be seen in Figure 3 that the test is approached graphically through the comparison between pairs of means. The X axis represents the difference between them and the Y axis all possible combinations between the culture media, performed by the Tukey Test. For the present study, the following were observed: Control-2.0 $g.L^{-1}$, Control-4.0 $g.L^{-1}$ and Control-6.0 $g.L^{-1}$, both with respect to μ_{max} and t_g. For *Chlorella* sp. (1) between the pair Control and 2.0 $g.L^{-1}$ medium, the greatest significant difference occurred. As the interval is to the right of zero, the salt concentration is therefore influencing the value of μ_{max} in order to decrease this parameter, which confirms the results obtained in Figure 2.

In *Scenedesmus acuminatus* (2), the biggest significant difference was between the Control and 6.0 $g.L^{-1}$ media. The range is further away from the zero on the left, indicating that the salinity at the 6.0 $g.L^{-1}$ level is influencing in order to increase the value of μ_{max}. This result is confirmed by the fact that the maximum growth speed in the Control was the lowest value observed among the crops. For *Nannochloropsis* sp. (3) there was no significant difference between the Control and the concentration of 2.0 $g.L^{-1}$. A greater influence of salinity can be observed in the medium with 4.0 $g.L^{-1}$, followed by 6.0 $g.L^{-1}$, with both influences of salinity

being positive. These results confirm what was shown in Figure 1, where the highest values of μ_{max} occurred in these concentrations.

For *Monoraphidium contortum* (4), there was a greater influence of salinity in the concentration of 4.0 $g.L^{-1}$ in order to decrease μ_{max}. Thus, this species does not have favored kinetics in brackish environments. It is also noticed that there was a significant difference between the Control and the concentration of 6.0 $g.L^{-1}$, without influence of salinity at the level 2.0 $g.L^{-1}$ at maximum speed. The test for *Pediastrum tetras* (5) showed a significant difference in 2.0 $g.L^{-1}$ media, being positively influenced by the salt concentration. In the other concentrations, salinity did not statistically affect the average value of the maximum growth speed.

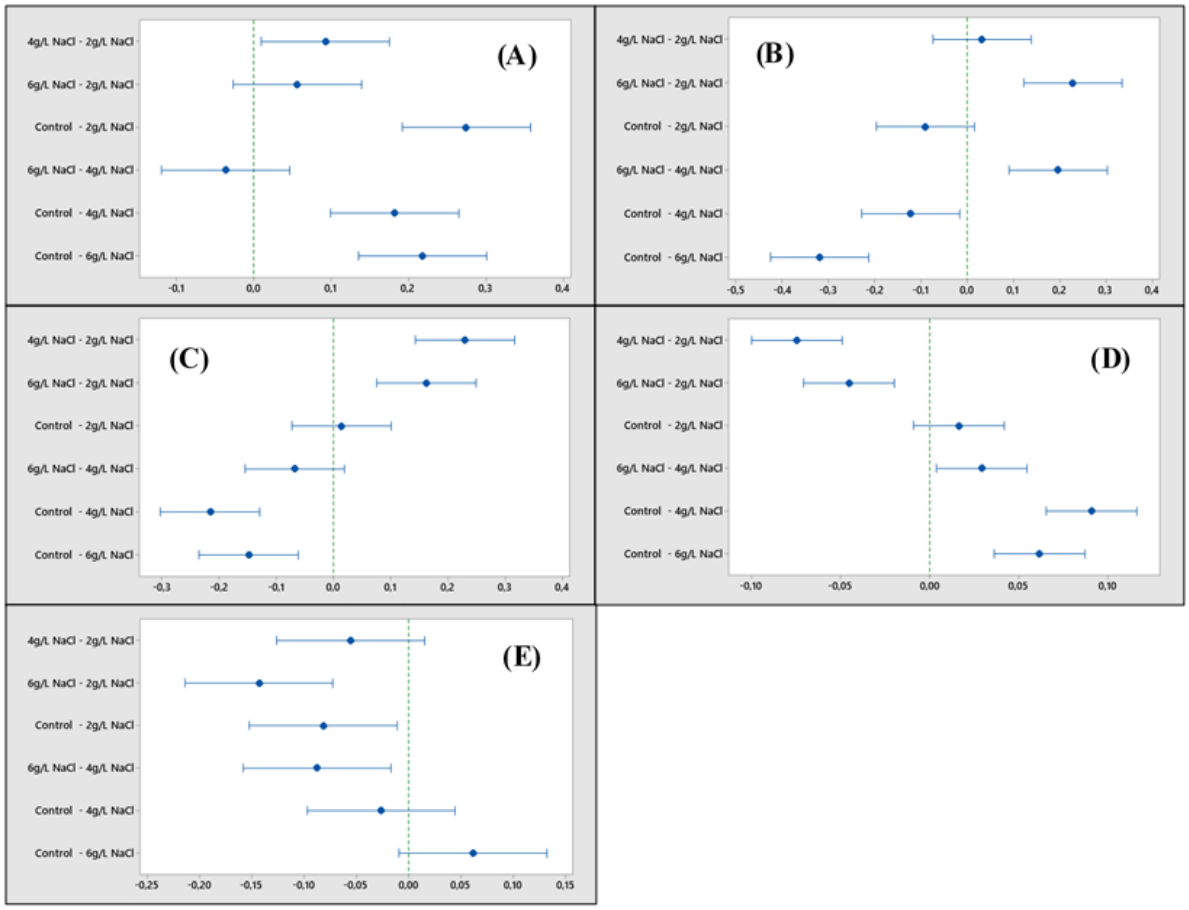

Figure 3. Tukey test between the averages of the maximum velocity of growth in synthetic brackish media. A. *Chlorella* sp., B. *Scenedesmus acuminatus*, C. *Nannochloropsis* sp., D. *Monoraphidium contortum*, E. *Pediastrum tetras.*

Looking at Figure 4, *Chlorella* sp. (1) showed a significant difference in all concentrations compared to the Control, with the greatest influence observed in that of 2.0 $g.L^{-1}$. It also occurred in all medium pairs for *Scenedesmus acuminatus* (2), but the highest was between Control and the medium with the highest salinity. For *Nannochloropsis* sp. (3), there was a greater difference with the concentrations of 4.0 $g.L^{-1}$ and 6.0 $g.L^{-1}$, but salinity was more influential in the first. The same happened with the species *Monoraphidium contortum* (4), with a greater influence of t_g for medium with a concentration of 4.0 $g.L^{-1}$ of NaCl. In *Pediastrum tetras* (5) cultures, there were significant differences between the Control and the concentrations of 2.0 $g.L^{-1}$ and 4.0 $g.L^{-1}$, with no impact on salinity. Therefore, the species that proved to be more suitable for cultivation in brackish environments are *Chlorella* sp., *Scenedesmus acuminatus* and *Nannocholopsis* sp.

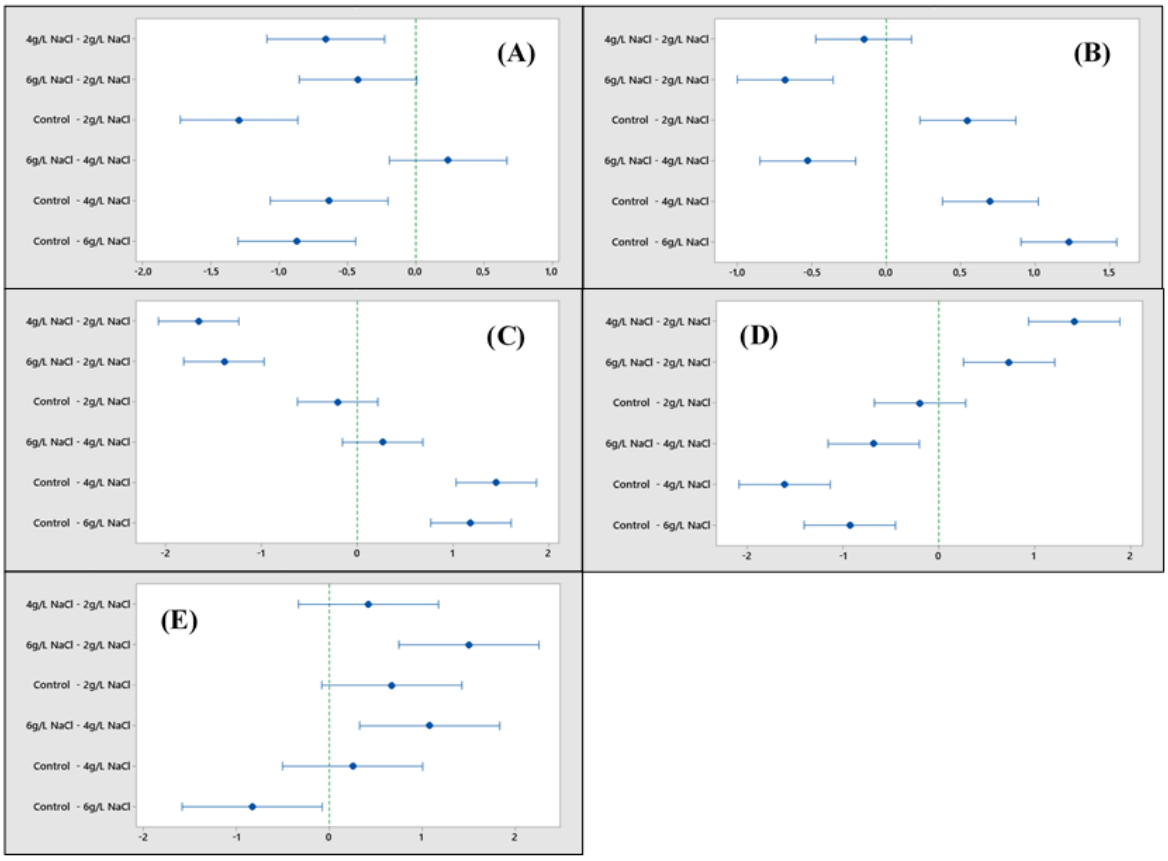

Figure 4. Tukey test between the generation time averages in the synthetic brackish media. A. *Chlorella* sp., B. *Scenedesmus acuminatus*, C. *Nannochloropsis* sp., D. *Monoraphidium contortum*, E. *Pediastrum tetras*.

3.3. Lipid content and biomass production

Figure 5 reveals that *Chlorella* sp. was the species that presented the lowest values of the lipid content, if compared with the others. Shuba and Kifle (2018) show that the levels of lipids for this species in standard culture media can vary between 14 and 22%. In the present study, values close to 10% were obtained among brackish media, the highest observed in the concentration 4.0 $g.L^{-1}$ of NaCl (11.69%).

Chlorella sp. had the highest biomass production in Control (621.90 $mg.L^{-1}$), followed by the concentration of 4.0 $g.L^{-1}$ (559.65 $mg.L^{-1}$), highest production among brackish media, 2.0 gL^{-1} (428.90 $mg.L^{-1}$) and the highest salinity (342.60 $mg.L^{-1}$). However, in all media in which salt was added, the lipid percentage did not increase compared to the Control. Regarding the *Scenedesmus acuminatus*, the results show that the highest lipid accumulation among brackish media occurred at 6.0 $g.L^{-1}$, which is the medium that came closest to the Control. This result points to the fact that cultivation in media with higher salinity can favor the accumulation of lipids, caused by the salt stress in the cells. The highest biomass production occurred at a concentration of 4.0 $g.L^{-1}$, surpassing the Control.

Pancha *et al*. (2015) cultivated the species *Scenedesmus* sp. in brackish media and obtained a lipid percentage of 33.13% at a saline concentration of 400 mM, this being the highest studied. In the present study, the lipid content was higher (41.96%) in the culture with greater addition of salts, showing that the intracellular lipid production can be favored in higher salinities. This fact was also verified in the species *Nannochloropsis* sp., where the highest content of lipids in dry biomass also occurred in the medium with a concentration of 6.0 $g.L^{-1}$, reaching the highest result among the studied species. Therefore, for this microalgae the highest salinities have also maximized the accumulation.

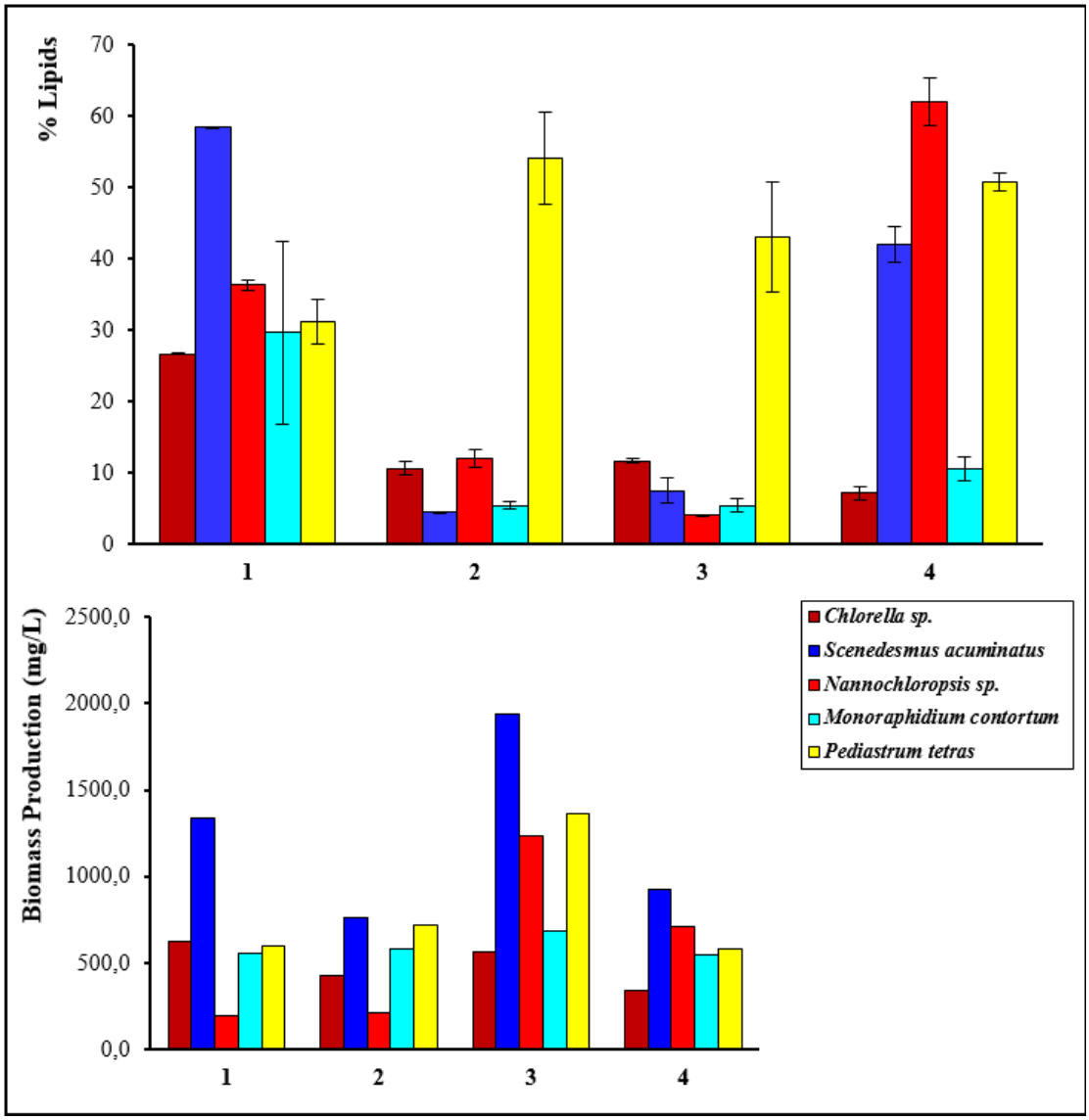

Figure 5. A. Percentage of the concentration of lipids and B. Production in dry biomass of brackish media.

According to Khatoon *et al*. (2014), *Nannochloropsis* sp. is among the microalgae with the highest lipid concentrations, remaining between 20 and 50% of dry biomass. In the present study, production was higher (62.04%), showing that the highest salt concentration provided this expressive result. The authors also point out that the acceptable levels of salinity vary with the species, and each has an optimal range for growth and lipid production. Kalita *et al*. (2011) point out that saline stress has a direct impact on physiological and biochemical mechanisms directly related to cell growth. For this reason, cultivation in brackish environments can increase the lipid content and the production of biomass.

On the other hand, the lowest results between species occurred in *Monoraphidium contortum*, where the highest lipid level did not exceed 10.57% in the 6.0 $g.L^{-1}$ concentration of NaCl and the highest productivity was for the 4.0 $g.L^{-1}$ concentration (684.61 $mg.L^{-1}$). Meanwhile, Bogen *et al*. (2013), when cultivating this same species in a synthetic medium to evaluate the lipid content and productivity in dry biomass, obtained the values of 22.2% of lipid accumulation; however, with 300 $mg.L^{-1}$ of biomass production. Therefore, the cultivation of this species in brackish environments can increase the production of biomass, but no increase in lipid accumulation is observed. The *Pediastrum tetras* species showed a very satisfactory percentage of lipids, and it was observed that in all brackish environments there was an increase

in relation to the Control. The highest value was observed in the concentration of 2.0 $g.L^{-1}$, reaching 54.03%. However, the study authors note that this species is not widely studied and cultivated, and there are no relevant works to be mentioned.

Concerning the production in dry biomass, no significant increases were observed with salinity in relation to the Control for *Chlorella* sp. as for *Monoraphidium contortum*. It is verified that the salt levels did not cause a significant increase in the production of biomass. *Scenedesmus acuminatus*, *Nannochloropsis* sp. and *Pediastrum tetras*, however, showed a considerable increase in the concentration of 4.0 $g.L^{-1}$, and it was verified that this salinity potentiated the production of biomass.

Observing the results and, relating growth kinetics, lipid accumulation and dry biomass production, it appears that the species that were most favorable to be cultivated in synthetic brackish media were Scenedesmus *acuminatus* and *Nannochloropsis* sp. It is observed that in the first, the medium with 6.0 $g.L^{-1}$ had the best combination of results, showing that the production of biomass and lipid content are favored in the medium with greater salinity, in addition to the kinetic aspects. For the second species, the brackish medium was also shown to be the most suitable for cultivation, because despite having a lower biomass production and slightly slower growth kinetics, it was in this medium that the lipid production was maximum.

3.4. Statistical analysis of lipid content

Table 2 shows that for all cultures there was a significant difference between the mean results of lipid percentage.

Table 2. F test for the % of Lipids in cultures in brackish media ($F_{tabulated}$ = 4.07).

	$F_{calculate}$	R^2
Chlorella sp.	519.83	99.49
Scenedesmus acuminatus	347.12	99.78
Nannochloropsis sp.	619.65	99.57
Monoraphidium contortum	9.56	78.19
Pediastrum tetras	7.31	84.54

From Figure 6, it can be seen that in the brackish cultivations of *Chlorella* sp. (1) there was a significant difference between the Control and all means. Due to the fact that the intervals are to the right of zero, it can be seen that salinity is affected in a way to decrease lipid accumulation, having a greater impact on the medium with a concentration of 6.0 $g.L^{-1}$. The same occurred with *Scenedesmus acuminatus* (2) and *Monoraphidium contortum* (4), with the greatest influence observed in media with a concentration of 2.0 and 4.0 $g.L^{-1}$, respectively. Note that in *Nannochloropsis* sp. (3), the medium with 6.0 $g.L^{-1}$ salinity increased the percentage of lipids, since the interval is to the left of zero. In the other media, salinity affected lipid accumulation in order to decrease it, which points to the increase in the percentage of lipids from cultures grown in salinity media for this species. Pediastrum tetras showed only a significant difference between the Control and the 2.0 $g.L^{-1}$ media, which was positive.

Kaewkannetra *et al*. (2012) studied the effect of salinity in cultures of the microalgae *Scenedesmus obliquus* in the presence of NaCl, in concentrations of 0.05, 0.2 and 0.3 M. Compared with the non-brackish medium, the highest lipid accumulation was obtained in the cells that grew under salt stress, obtaining a 36.0% lipid content. Duan *et al*. (2012) used the same strategy for the species *Chlorella vulgaris*, through the osmotic stress caused by the salinity. The author reports that he obtained a 21.1% increase in lipids compared to non-brackish medium. It also shows that higher concentrations of salt increased the content of lipids to 70% in the cultivation of *Dunaliella*. Xia *et al*. (2014) tested several sodium salts to cause an

increase in the lipid content, with NaCl increasing the productivity of *Desmodesmus abundans* to 68.08 $mg.L^{-1}.dia^{-1}$. The author points out that the increase in salinity is a simple mechanism to promote cell growth for the production of biomass for bioenergetic purposes.

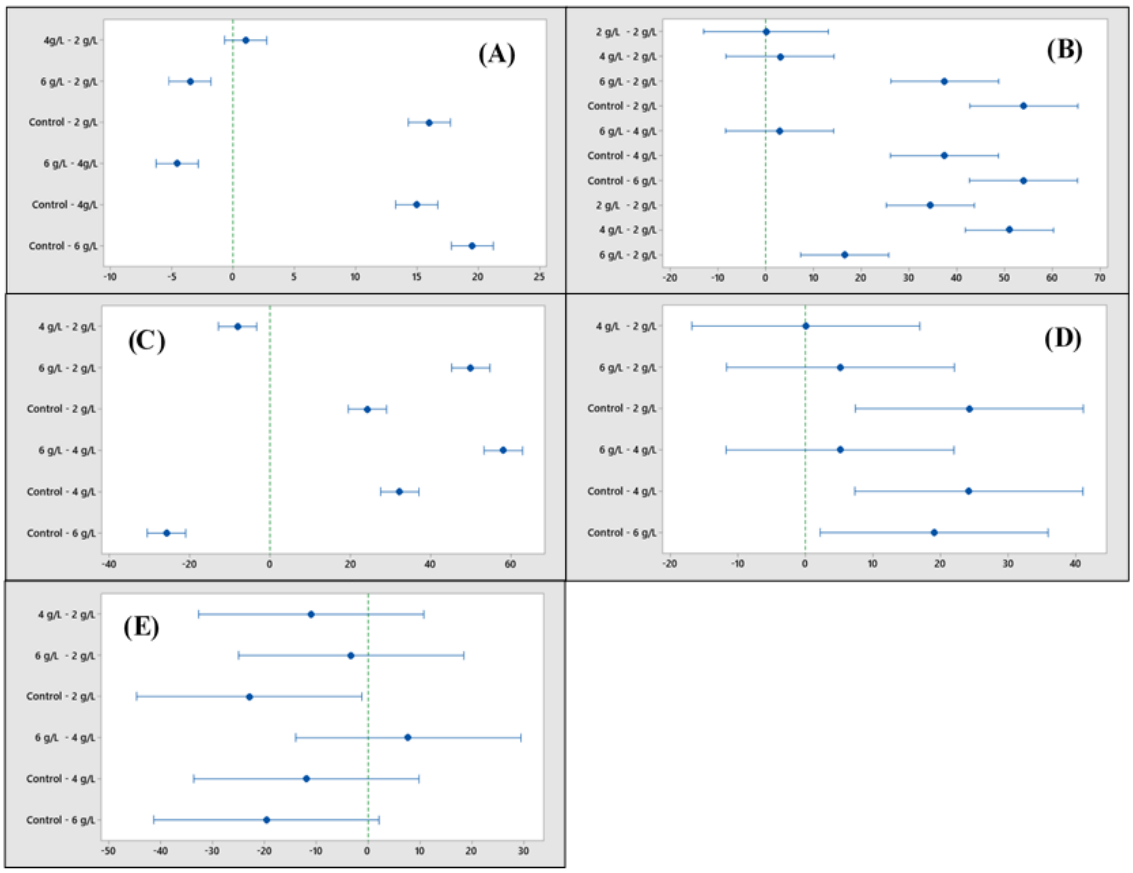

Figure 6. Tukey test for % lipids in synthetic brackish cultures. A. *Chlorella* sp., B. *Scenedesmus acuminatus*, C. *Nannochloropsis* sp., D. *Monraphidium contortum*, E. *Pediastrum tetras*.

The present study obtained a higher percentage of lipid accumulation for the microalgae *Scenedesmus acuminatus*, when compared with the work by Kaewkannetra *et al*. (2012). It is also observed that for *Nannochloropsis* sp. and *Pediastrum tetras*, the values also exceeded those of the author. This fact indicates the feasibility of using several species of microalgae in the production of biomass for the purpose of producing biodiesel. As a differential, this study highlights the use of the statistical tool to prove the influence of salinity on the growth kinetics and production of lipids. It appears that, in all the studied species, there was an interference of salinity in the physiological cellular mechanisms that, depending on the concentration of the salt and the species, increased or decreased the growth and lipid production.

3.5. Monitoring the pH

It can be seen in Figure 7 that in all crops there was an increase in pH over time. Dahmani *et al*. (2016) show that this fact is directly linked to photosynthetic activity, where the CO_2 in the medium is consumed by the cells, thus decreasing the concentration and consequently increasing the pH of the medium. The authors also point out that the optimal range for most microalgae species is between 7.0 and 12.0. For *Scenedesmus acuminatus*, *Nannochloropsis* sp., *Monoraphidium contortum* and *Pediastrum tetras* (grown in Water Culture synthetic medium) the pH has always been alkaline, in the range specified by the authors. It is noticed that, on the day of the inoculum, the pH was between 9.0 and 10.0 and then dropped to 7.0 on the first day. From the fifth day on, it increased again, to between 8.0 and 10.0.

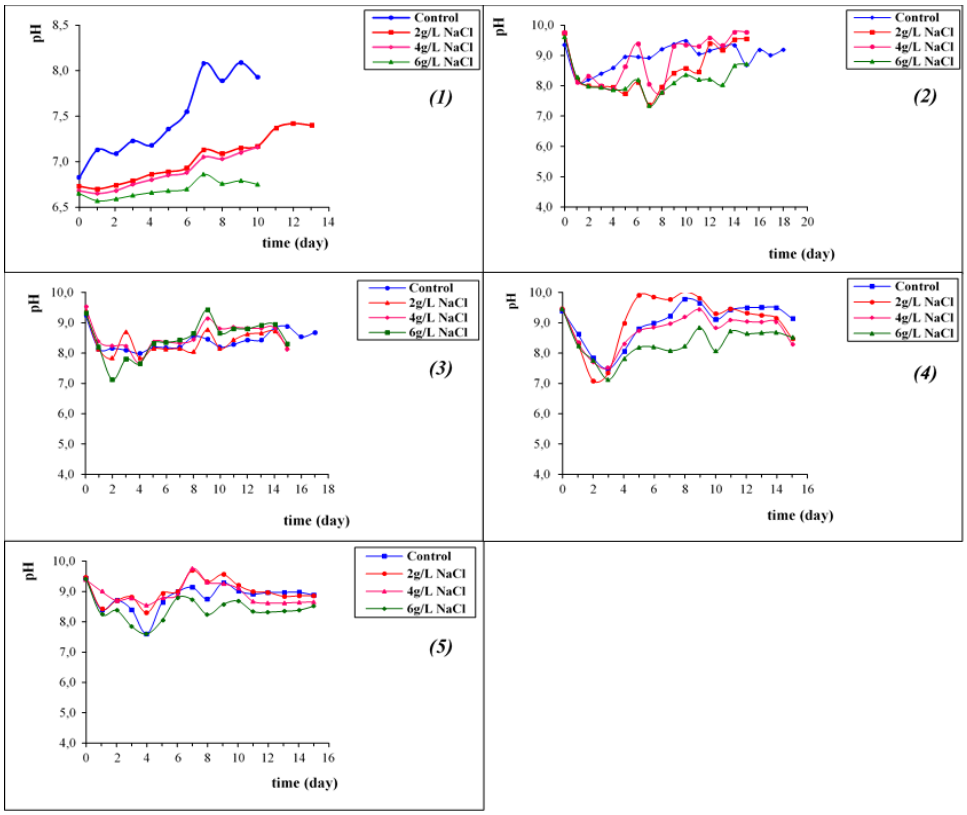

Figure 7. pH of synthetic brackish media over the time of cultivation. (1) *Chlorella* sp., (2) *Scenedesmus acuminatus*, (3) *Nannochloropsis* sp., (4) *Monoraphidium contortum*, (5) *Pediastrum tetras*.

Chlorella sp. showed that pH of the synthetic culture medium (Bold's Basal Medium) on the day of the inoculum was close to neutral. During the cell growth there was an increase, however, among the brackish media pH did not exceed 7.5 and the Control reached pH 8.0. Thus, the influence of both pH and salinity on the low production of biomass and lipids for this species can be seen.

4. CONCLUSIONS

The study found the influence of saline stress on growth, production of dry biomass and accumulation of lipids in all species. It is observed that among them *Scenedesmus acuminatus* and *Nannochloropsis* sp. were the ones that most adapted to the brackish environment. It has been proven that, depending on the species, the concentration can positively or negatively influence the growth kinetics and accumulation of lipids. In the species *Scenedesmus acumnatus* and *Nannochloropsis* sp., the growth was benefited by the salinity in the concentrations 6.0 and 4.0 $g.L^{-1}$, respectively. Regarding lipids, *Nannochloropsis* sp. and *Pediastrum tetras* had the accumulation maximized with the concentration in 6.0 and 2.0 $g.L^{-1,}$ respectively.

The species that reached the highest levels of lipids were *Nannohchloropsis* sp., *Pediastrum tetras* and Scenedesmus *acuminatus*, as well as showing the highest production of dry biomass, both at concentrations of 4.0 $g.L^{-1}$. The results confirm the feasibility of using microalgae as an alternative for the production of biodiesel. The lipid content and the amount of biomass produced become crucial in the choice of the species to be cultivated. It is worth mentioning that it is necessary to observe these two factors together in order to obtain the highest possible yield for the production of biofuel.

5. ACKNOWLEDGMENT

The authors would like to thank the Coordenação de Aperfeiçoamento de Pessoal de Nível Superior (CAPES) for their financial support.

6. REFERENCES

ABUBAKAR, A. L. Effect of Salinity on the Growth Parameters of Halotolerant Microalgae, *Dunaliella* spp. **Nigerian Journal of Basic and Applied Science,** v. 24, n. 2, p. 85-91, 2016. https://doi.org/10.4314/njbas.v24i2.12

BELLOU, S.; BAESHEN, M.; ELAZZAZY, A. M.; AGGELI, D.; SAYEGH, F. Microalgal lipids biochemistry and biotechnological perspectives. **Bioresource Technology**, v. 288, 2014. https://dx.doi.org/10.1016/j.biotechadv.2014.10.003

BISCHOFF, H. W; BOLD, H. C. **Some Soil Algae from Enchanted Rock and Related Algal Specie**. Austin: University of Texas, 1963. (Phycological Studies IV, n. 6318). p. 1-95.

BOGEN, C.; KLASSEN, V.; WICHMANN, J.; LA RUSSA, M.; DOEBBE, A.; GRUNDMANN, M.; URONEN, P.; KRUSE, O.; MUSSGNUG, J. H. Bioresource Technology Identification of *Monoraphidium contortum* as a promising species for liquid biofuel production. **Bioresource Technology**, v. 133, p. 622–626, 2013. https://dx.doi.org/10.1016/j.biortech.2013.01.164

CHEW, K. W.; CHIA, S. R.; SHOW, P. L.; YAP, Y. J.; LING, T. C.; CHANG, J. S. Effects of water culture medium, cultivation systems and growth modes for microalgae cultivation: A review. **Journal of the Taiwan Institute of Chemical Engineers**, v. 0, p. 1-13, 2018. https://dx.doi.org/10.1016/j.jtice.2018.05.039

CHISTI, Y. Biodiesel from microalgae beats bioethanol. **Trends in Biotechnolo gy**, v. 26, n. 3, p. 126-131, 2008. https://dx.doi.org/10.1016/j.tibtech.2007.12.002

DAHMANI, S.; ZERROUKI, D.; RAMANNA, L.; RAWAT, I.; BUX, F. Cultivation of *Chlorella pyrenoidosa* in outdoor open raceway pond using domestic wastewater as medium in arid desert region. **Bioresource Technology**, v. 219, p. 749-752, 2016. https://dx.doi.org/10.1016/j.biortech.2016.08.019

DUAN, X.; REN, G. Y.; LIU. L. L.; ZHU W. X.; Salt-induced osmotic stress for lipid overproduction in batch culture of *Chlorella vulgaris*. **African Journal of Biotechnology**, v. 11, p. 7072-7078, 2012. https://dx.doi.org/10.5897/AJB11.3670

FOLCH, J.; LESS, M.; STALEY, G. H. A Simple Method for the Isolation and Purification of Total Lipids from Animal Tissues. **The Journal of Biological Chemistry,** v. 226, p. 497-509, 1957.

GUILLARD, R. R. L.; LORENZEN, C. J. Yelow-green algae with chlorophyllide. **Journal Phycology**, v. 8, p. 10-14, 1972. https://doi.org/10.1111/j.1529-8817.1972.tb03995.x

KAEWKANNETRA, P.; ENMAK, P.; CHIU, T. The Effect of CO_2 and Salinity on the Cultivation of *Scenedesmus obliquus* for Biodiesel Production. **Biotechnology and Bioprocess Engineering**, v. 17, p. 591-597, 2012. https://doi.org/10.1007/s12257-011-0533-5

KALITA, N.; BARUAH, G.; GOSWAMI, R. C. D.; TALUKDAR, J.; KALITA, M. C. Ankistrodesmus falcatus: A promising candidate for lipid production, its biochemical analysis and strategies to enhance lipid productivity. **Journal of Microbiology and Biotechnology Research**, v. 1, p. 148-157, 2011.

KHATOON, H.; RAHMAN, N. A.; BANERJEE, S.; HARUN, N.; SULEIMAN, S. S.; ZAKARIA, N. H.; LANANAN, F.; HAMID, S. H. A.; ENDUT, A. International Biodeterioration & Biodegradation Effects of different salinities and pH on the growth and proximate composition of *Nannochloropsis* sp. and *Tetraselmis* sp . isolated from South China Sea cultured under control and natural conditions. **International Biodeterioration & Biodegradation**, v. 95, p. 11-18, 2014. https://doi.org/10.1016/j.ibiod.2014.06.022

LEE, E.; JALALIZADEH, M.; ZHANG, Q. Growth kinetic models for microalgae cultivation: A review. **Algal Research**, v. 12, p. 497-512, 2015. https://dx.doi.org/10.1016/j.algal.2015.10.004

PANCHA, I.; CHOKSHI, K.; MAURYA, R.; TRIVEDI, K.; PATIDAR, S. K.; GHOSH, A.; MISHRA, S. Salinity induced oxidative stress enhanced biofuel production potential of microalgae *Scenedesmus* sp. CCNM 1077. **Bioresource Technology**, v. 189, p. 341-348, 2015. https://dx.doi.org/10.1016/j.biortech.2015.04.017

QIAO, T.; ZHAO, Y.; ZHONG, D.; YU, X. Hydrogen peroxide and salinity stress act synergistically to enhance lipids production in microalga by regulating reactive oxygen species and calcium. **Algal Research**, v. 53, Article 102017, 2021. https://dx.doi.org/10.1016/j.algal.2020.102017

SCHMIDELL, W.; BORZANI, W.; LIMA, U. A.; AQUARONE, E. **Biotecnologia Industrial, Volume 2.** 1ª ed. São Paulo: Editora Blucher, 2001. 560 p.

SHUBA, E. S.; KIFLE, D. Microalgae to biofuels: 'Promising' alternative and renewable energy, review. **Renewable and Sustainable Energy Reviews**, v. 81, n. April 2016, p. 743-755, 2018. https://dx.doi.org/10.1016/j.rser.2017.08.042

SRIVASTAVA, G.; NISHCHAL; GOUD, V. V. Salinity induced lipid production in microalgae and cluster analysis (ICCB 16-BR_047). **Bioresource Technology**, v. 242, p. 244-252, 2017. https://dx.doi.org/10.1016./j.biortech.2017.03.175

XIA, L.; RONG J.; YANG, H.; HE, Q.; ZHANG, D.; HU, C. NaCl as an effective inducer for lipid accumulation in fresh water microalgae *Desmodesmus abundans*. **Bioresource Technology**, v. 161, p. 402-409, 2014. https://dx.doi.org/10.1016/j.biortech.2014.03.063

ZHANG, X.; TANG, X.; WANG, M.; ZHANG, W.; ZHOU, B.; WANG, Y. J. ROS and calcium signaling mediated pathways involved in stress responses of the marine microalgae *Dunaliella salinato* enhanced UV-B radiation. **Journal of Photochemistry & Photobiology, B: Biology**, v. 173, p. 360-367, 2017. https://dx.doi.org/10.1016/j.jphotobiol.2017.05.038

ZHAO, Y.; SONG, X.; ZHAO, P.; LI, T.; XU, J.; YU, X. Role of melatonin in regulation of lipid accumulation, autophagy and salinity-induced oxidative stress in microalga Monoraphidium sp. QLY-1. **Algal Research**, v. 54, p. 1-9, 2021. https://dx.doi.org/10.1016/j.algal.2021.102196

ZHU, B.; CHEN, G.; CAO, X.; WEI, D. Molecular characterization of CO_2 sequestration and assimilation in microalgae and its biotechnological applications. **Bioresource Technology**, v. 244, p. 1207-1215, 2017. https://dx.doi.org/10.1016/j.biortech.2017.05.199

Ambiente & Água - An Interdisciplinary Journal of Applied Science
ISSN 1980-993X – doi:10.4136/1980-993X
www.ambi-agua.net
E-mail: ambi.agua@gmail.com

Analysis of microbial community biodiversity in activated sludge from a petrochemical plant

ARTICLES doi:10.4136/ambi-agua.2655

Received: 02 Oct. 2020; Accepted: 03 May 2021

Themis Collares Antunes[1]; Leticia Marconatto[2]; Luiz Gustavo dos Anjos Borges[2]; Adriana Giongo[2]; Sueli Teresinha Van Der Sand[3*]

[1]Instituto de Ciências Básicas da Saúde. Programa de Pós-graduação em Microbiologia Agrícola e do Ambiente. Universidade Federal do Rio Grande do Sul (UFRGS), Rua Sarmento Leite, n°500, CEP: 90050-170, Porto Alegre, RS, Brazil. E-mail: themis.antunes@gmail.com
[2]Instituto do Petróleo e dos Recursos Naturais. Pontifícia Universidade Católica do Rio Grande do Sul (PUCRS), Avenida Ipiranga, n° 6681, CEP: 90619-900, Porto Alegre, RS, Brazil. E-mail: leticia.marconatto@pucrs.br, luizgaborges@gmail.com, adrianagiongo@gmail.com
[3]Departamento de Microbiologia, Imunologia e Parasitologia. Intituto de Ciências Básicas da Saúde. Universidade Federal do Rio Grande do Sul (UFRGS), Rua Sarmento Leite, n°500, CEP: 90050-170, Porto Alegre, RS, Brazil.
[*]Corresponding author. E-mail: svands@ufrgs.br

ABSTRACT

The1active sludge process is one of the most-used techniques for the biodegradation of organic compounds present in effluents from an assortment of wastewaters. This study investigated the bacterial community structure of a petroleum industry's activated sludge and its physical and chemical parameters using high-throughput sequencing. Samples were collected over one year: autumn 2015 (C1), winter 2015 (C2), spring 2015 (C3), and summer 2016 (C4). Total DNA was extracted, and the primers targeting the V4 region of the 16S rRNA gene were used for amplicon sequencing. The majority of the detected microorganisms were considered rare microbiota, presenting a relative abundance below 1% of the total sequences. All of the sequences were classified at the phylum level, and up to 55% of the ASVs (Amplicon Sequence Variants*)* were associated with known bacterial genera. Proteobacteria was the most abundant phylum in three seasons, while the phylum *Armatimonadota* dominated in one season. The genus *Hyphomicrobium* was the most abundant in autumn, winter and summer, and an ASV belonging to the family *Fimbriimonadaceae* was the most abundant in the spring. Canonical Correspondence Analysis showed that physicochemical parameters of SS, SD and TSS are correlated, as well as ammoniacal nitrogen. Sample C3 presented the highest values of COD, AN and solids (SS, SD and TSS). The highest COD, AN, and solids values are correlated to the high frequency of the phylum *Armatimonadota* in C3.

Keywords: bacterial community, high throughput sequencing, wastewater sludge.

This is an Open Access article distributed under the terms of the Creative Commons Attribution License, which permits unrestricted use, distribution, and reproduction in any medium, provided the original work is properly cited.

O lodo ativo da planta de uma indústria de petróleo é constituído por uma microbiota ainda a ser identificada

RESUMO

O processo de lodo ativo é uma das técnicas mais utilizadas para biodegradação de compostos orgânicos presentes nos efluentes de uma variedade de águas residuais. A estrutura da comunidade bacteriana do lodo ativado de uma indústria de petróleo e sua relação com parâmetros físicos e químicos foram investigadas por meio de sequenciamento de alto rendimento. As amostras foram coletadas durante um período de um ano: outono de 2015 (C1), inverno de 2015 (C2), primavera de 2015 (C3) e verão de 2016 (C4). O DNA total foi extraído e para amplificação foram utilizados primers específicos para região V4 do gene 16S rRNA. A maioria dos microrganismos detectados foi considerada microbiota rara, apresentando abundância relativa abaixo de 1% do total de sequências. Em geral, quase a totalidade das sequências (99,9%) foi classificada em nível de filo, mas apenas algumas ASVs (23,7%) foram associadas a gênero bacteriano conhecido. As proteobactérias foram o filo mais abundante em três das estações, enquanto o filo Armatimonadota dominou em uma estação. O gênero *Hyphomicrobium* foi o gênero mais abundante no outono, inverno e verão, e uma ASV pertencente à família *Fimbriimonadaceae* (filo Armatimonadetes) foi o microrganismo mais abundante na primavera. A Análise de Correspondência Canônica (CCA) indica uma diferença consistente da comunidade bacteriana da primavera quando comparada com amostras de outras estações. Os resultados mostram uma correlação entre o filo Armatimonadota e a alta concentração de DQO, NA e sólidos.

Palavras-chave: comunidade bacteriana, lodo ativado, sequenciamento de alto rendimento.

1. INTRODUCTION

Biological and industrial wastewater treatment plants (WWTP) are standout biotechnological processes in operation worldwide (Figuerola and Erijman, 2007), whose significance is increasing in a consistently developing human society. Most wastewater treatment processes use the natural self-depuration limit of aquatic conditions, which is the effect of microbial activity (Heidenwag *et al.*, 2001). It is crucial to recognize the relationship between microbial communities and their performance in the full-scale installations, since bacterial metabolism is essential for effective biological treatment of wastewater (Kwiatkowska and Zielinska, 2016).

Biological treatment by the active-sludge process is well known. This most-used technique for the biodegradation of organic compounds in effluents from a variety of wastewaters and their microbial community has been studied in urban, industrial, and petrochemical wastewaters (Zhang *et al.*, 2011; Sánchez *et al.*, 2013; Ye and Zhang, 2013). These studies have demonstrated that the most prevalent microorganisms in these samples are *Betaproteobacteria*, *Alphaproteobacteria*, *Nitrobacteria*, *Bacteroidetes*, *Firmicutes*, and *Actinobacteria*.

High-throughput sequencing technologies provide deep insights into the bacterial populations (Ibarbalz *et al.*, 2013) and have been used to reveal the bacterial range of some complex environments, including activated sludge samples (Claesson *et al.*, 2010; Zhang *et al.*, 2011; Yang *et al.*, 2014; Gwin *et al.*, 2018). Some microorganisms have not been completely identified (Krishnan *et al.*, 2016; Abe *et al.*, 2017), showing that there is much more to discover about the biodiversity of activated sludge. In this study, we accessed the microbial community diversity present in activated sludge from the petrochemical industry using amplicon sequencing based on the 16S rRNA gene.

2. MATERIAL AND METHODS

2.1. Active sludge samples collection

Activated sludge samples were collected from a wastewater treatment plant (WWTP) located in Triunfo, Rio Grande do Sul, Brazil (29°51'01.1" S 51°22'50.9" W) previously described by Antunes *et al.* (2018). The WWTP handles 450-m^3 h^{-1} of wastewater and is operated as a conventional activated-sludge treatment process, mechanically aerated by blades. One liter of sludge was collected directly from the input aeration tank (Figure 1) during four sampling collections over one year: Autumn 2015 (C1), Winter 2015 (C2), Spring 2015 (C3), and Summer 2016 (C4). Samples were collected using a collection bucket and transported on ice to the laboratory. The samples were thereafter kept at -80ºC until further analysis. Active sludge chemical composition and physical parameters were summarized in Antunes *et al.* (2018).

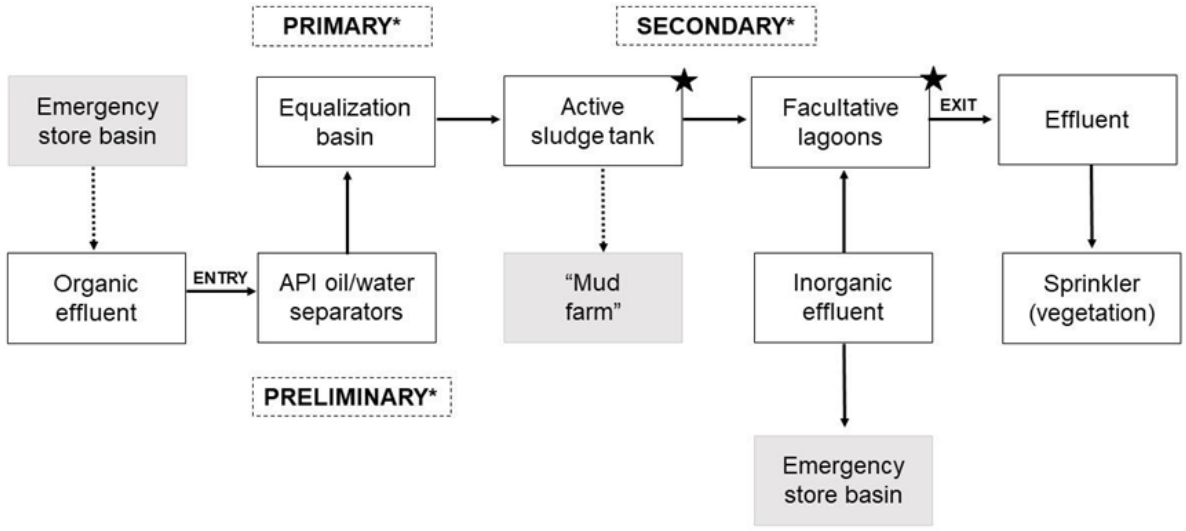

Figure 1. Schematic representation of the wastewater treatment plant. The black star indicates the sampling point. Arrows represent the effluent pathway.

The following parameters were determined by a certified laboratory, according to the American Public Health Association **(**APHA *et al.***,** 2012): total organic carbon (TOC), chemical oxygen demand (COD), dissolved oxygen (DO), total suspended solids (TSS), solids suspended (SS), solids dissolved (SD); and total Kjeldahl nitrogen (TKN). The chemical results are listed in Table 1.

Table 1. Active sludge chemical parameters. Results are shown in mg L^{-1}. (Modified from Antunes *et al.*, 2018).

Parameter	Sampling time			
	C1	C2	C3	C4
Total organic carbon (TOC)	115	20	100	91
Chemical oxygen demand (COD)	399.5	13.33	637	83.6
Dissolved oxygen (DO)	2.1	2.02	0.7	0.5
Total suspended solids (TSS)	1286	788	1477	1625
Solids suspended (SS)	48	22	56	53
Solids dissolved (SD)	1241	678	1428	1508
Total Kjeldahl nitrogen (TKN)	67. 67	13.08	25.54	27.53
Ammoniacal Nitrogen (AN)	8.74	4.32	11.49	8.44

2.2. DNA isolation and 16S rRNA gene fragment sequencing

Total DNA was extracted from 0.25 g of active sludge using the Dneasy PowerSoil Kit (Qiagen) following the manufacturer's standard protocol. The concentration and purity of the isolated DNA were determined using an ND-100Nanodrop spectrophotometer (Thermo Fisher). Partial 16S rRNA gene sequences were amplified using universal primers 515F and 806R, previously identified as suitable for bacteria and archaea (Bates *et al.*, 2011). Amplification was performed in a 25 μL mixture, consisting of 1 μL of genomic DNA, 2 mM $MgCl_2$, 0.2 μM of each primer, 200 μM of each dNTP, 1U Taq DNA polymerase and 1X reaction buffer. These primers amplify 291 bp from the V3-V4 hypervariable region of the prokaryotic 16S rRNA gene. Amplification was carried out in a Mastercycler Personal 5332 Thermocycler (EppendorfR) according to the following program: initial denaturation at 94ºC for 2 min, followed by 25 cycles of 45 s at 94ºC, 45 s at 55ºC, 1 min at 72ºC and a final cycle at 72ºC for 6 min. For library construction, 100 ng of DNA was used as described in the Ion Plus Fragment Library manual kit. Barcode sequences were added to identify each sample from the total sequencing output, since all samples were sequenced in a multiplexed run. Amplicon sequencing was conducted on the Ion PGM System (Thermo Fisher) using an Ion 316 chip, following the manufacturer's instructions.

Sequences from 16S rRNA amplicon sequencing were processed using DADA2 (Divisive Amplicon Denoising Algorithm) (Callahan *et al.*, 2016) in R (R Core Team, 2019). Filtering, dereplication, sample inference, and chimera identification were performed, and the generated amplicon sequence variants (ASVs) were taxonomically assigned based on the SILVA database v. 138 (Quast *et al.*, 2013). The ASV data were imported into R using phyloseq (McMurdie and Holmes, 2013). Unassigned taxa and any residual ASVs identified as chloroplast, mitochondria, or eukaryote were excluded from the analysis. The remaining sequences were analyzed as described by Heinz *et al.* (2017). Sequencing results were deposited in the National Center for Biotechnology Information (NCBI) under BioProject ID PRJNA471748.

Canonical Correspondence Analysis (CCA) was used to evaluate linkages between microbial communities (ten most-abundant phyla) and chemical parameters (TOC, COD, DO, TSS, SS, SD, and TKN) using Past3 software (Hammer *et al.*, 2001).

3. RESULTS AND DISCUSSION

After removing the low-quality sequences, the amplicon sequencing from the four samples collected seasonally from the petrochemical industry active sludge yielded a total of 241,859 16S rRNA gene sequences samples, representing an average of 60,465 sequences per sample. The average sequence length was 273 bp.

The microbiota was classified within 31 phyla, 65 classes, 146 orders, 167 families and 185 genera or respective taxa. The domain *Bacteria* had the highest number of classified microorganisms (94.9% of the total sequences). The occurrence of four archaeal phyla was observed: *Crenarchaeota*, *Halobacterota*, *Nanoarchaeota*, *Aenigmarchaeota.* The phylum *Aenigmarchaeota* was present only in sequences from sample C3, comprising 0.10% of the total sequences in sample C3.

The classified bacterial community was composed of thirteen phyla with an abundance higher than 1% of the total sequences (Figure 2). *Proteobacteria* was the most abundant phylum in samples C1, C2, and C4, representing up to 37% of the total sequences in C2, followed by the phylum *Bacteroidota* present in samples C1, C2 and C4 (16.22%, 15.36% and 17.59% of the total sequences, respectively). In sample C3, the most abundant phylum was *Armatimonadota* and *Proteobacteria*; they represented 49.16% and 21.09% of the total sequences, respectively (Figure 2). *Armatimonadota* was the second-most abundant phylum in C1, after *Proteobacteria*, accounting for 11.74% of the total sequences. Unclassified sequences at the phylum level presented an average of 0.01% of the total sequences in the samples.

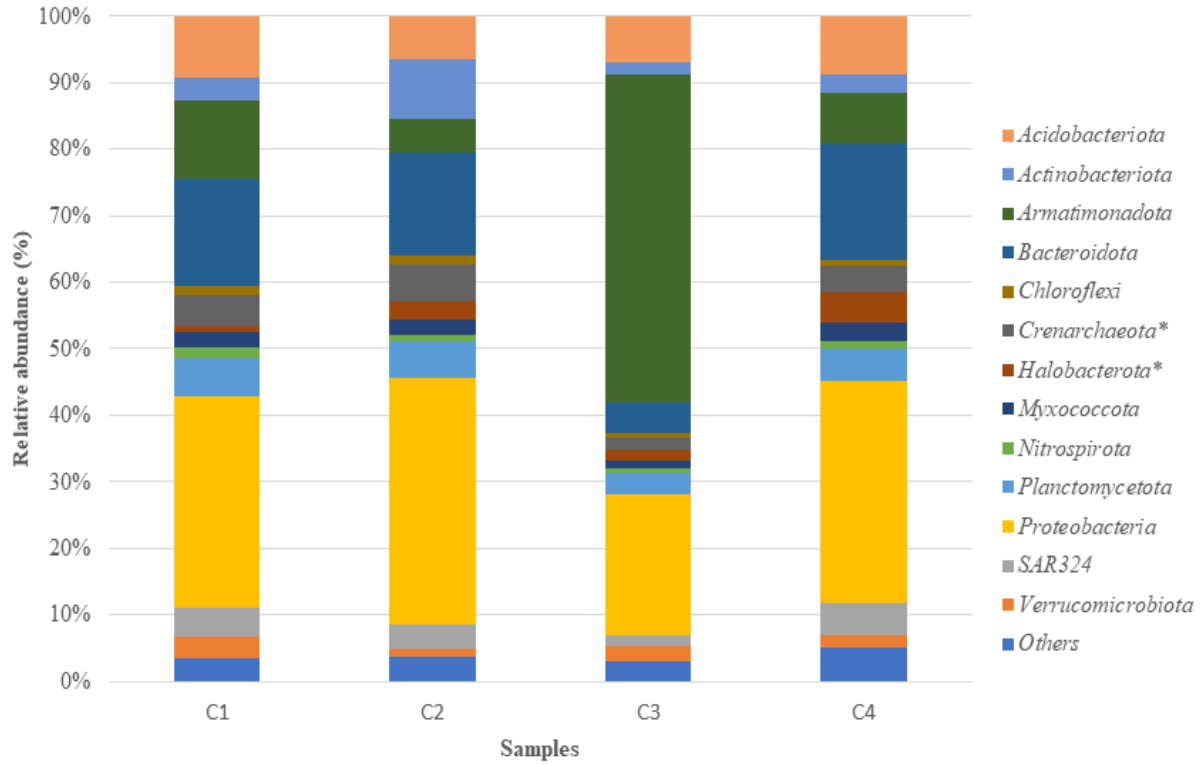

Figure 2. Classification of the most abundant phyla (≥ 1% of the total sequences in at least one sample) of microorganism present in activated sludge samples over a year (samples C1 to C4). "Others" represents the phyla whose abundances are lower than 1% of the total sequences. * *Archaea* phyla.

From the 336 detected taxa, 33 presented a relative abundance higher than 1% in at least one sample (Table 2) and were considered the predominant microbiota. From that, seventeen microorganisms were classified at the genus level. *Hyphomicrobium* was the most abundant genus in samples C1, C2 and, C4, accounting for 13.98%, 12.72% and 13.07% of the total sequences, respectively. The most abundant microorganism of sample C3 was a taxa belonging to the family *Fimbriimonadaceae* (phylum *Armatimonadota*), representing 48.96% of the total sequences in that sample. The majority of the 336 detected taxa were considered rare microbiota for presenting a relative abundance below 1% of the total sequences. From that, 185 microorganisms were classified at the genus level (Supplementary Table 1).

Canonical Correspondence Analysis (CCA) showed that the values of the physicochemical parameters of SS, SD and TSS are correlated, as well as ammoniacal nitrogen (Figure 3). According to the analyzed chemical parameters (Table 1), C3 presents the highest COD, AN and solids (SS, SD and TSS) compared to the other samples. These microbiological and chemical characteristics found in sample C3 make it different from C1, C2, and C4 (Figure 4). The highest COD, AN, and solids values are correlated to the high frequency of the phylum *Armatimonadota*.

Our study provided 16S rRNA gene sequence analyses of the microbial community present in activated sludge from the petrochemical industry. Our findings are in accordance with previous studies of activated sludge, with the predominance of *Proteobacteria* (Xia *et al.*, 2010). Sidhu *et al.* (2017) characterized and dissected the phylogenetic and functional structures from the sludge community at the phylum level and found the dominance of *Proteobacteria* in raw and dried sludge samples, representing 97.9% and 92.6%, respectively.

Table 2. Most abundant bacterial taxa present in the activated sludge samples.

Phylum	Class	Order	Family	Genus (or taxa)	Relative abundance (%)			
					C1	C2	C3	C4
Acidobacteriota	Blastocatellia	Blastocatellales	Blastocatellaceae	Blastocatellaceae	3.59	1.46	2.15	2.03
				OLB17	0.83	0.61	0.98	1.05
				JGI_0001001-H03	1.38	0.64	1.41	2.09
				Stenotrophobacter	1.64	1.41	0.95	1.35
Actinobacteriota	Thermoleophilia	Gaiellales		Gaiellales	1.61	5.61	0.88	1.56
		Solirubrobacterales	67-14	67-14	0.77	1.31	0.23	0.50
Armatimonadota	Fimbriimonadia	Fimbriimonadales	Fimbriimonadaceae	Fimbriimonadaceae	11.07	4.92	48.96	7.49
Bacteroidota	SJA-28			SJA-28	10.64	12.50	1.80	8.61
	Bacteroidia	Sphingobacteriales	AKYH767	AKYH767	3.45	0.41	0.35	2.93
		Chitinophagales	Saprospiraceae	Saprospiraceae	0.66	0.49	0.97	2.81
Crenarchaeota*	Thermoprotei	Desulfurococcales	Desulfurococcaceae	*Sulfophobococcus*	2.51	4.18	1.25	3.03
				Thermogladius	1.49	1.18	0.24	0.04
Halobacterota*	Archaeoglobi	Archaeoglobales	Archaeoglobaceae	*Ferroglobus*	0.59	1.19	0.30	0.67
				Geoglobus	0.39	1.70	0.97	3.11
Myxococcota	Polyangia	Haliangiales	Haliangiaceae	*Haliangium*	1.42	1.05	0.75	1.15
Nitrospirota	Nitrospiria	Nitrospirales	Nitrospiraceae	*Nitrospira*	1.44	0.98	0.65	1.13
Planctomycetota	Phycisphaerae	S-70		S-70	0.87	0.80	0.58	1.31
	OM190			OM190	0.30	1.09	0.32	0.74
	Planctomycetes	Pirellulales	Pirellulaceae	Pirellulaceae	1.59	1.15	0.55	0.69
		Gemmatales	Gemmataceae	Gemmataceae	1.10	0.86	0.35	0.22
Proteobacteria	Alphaproteobacteria	Rhizobiales	Hyphomicrobiaceae	*Hyphomicrobium*	13.98	12.72	4.79	13.07
		Rhodobacterales	Rhodobacteraceae	*Rhodobacter*	1.27	0.79	0.78	0.33
		Rickettsiales	AB1	AB1	0.00	2.09	0.35	0.00
				Alphaproteobacteria	0.27	0.39	0.45	1.08
	Gammaproteobacteria	Burkholderiales	Rhodocyclaceae	Sulfuritalea	1.21	1.24	0.64	0.72
			Nitrosomonadaceae	Ellin6067	0.98	2.19	0.84	1.60
			Comamonadaceae	*Rubrivivax*	1.08	1.82	0.37	0.72
			SC-I-84	SC-I-84	1.57	1.86	0.74	1.75
		Coxiellales	Coxiellaceae	*Coxiella*	1.06	0.99	0.73	0.68
		Diplorickettsiales	Diplorickettsiaceae	Diplorickettsiaceae	0.66	2.74	0.92	0.13
		Gammaproteobacteria	Unknown_Family	*Candidatus* Berkiella	0.83	0.16	2.11	0.93
SAR324				SAR324	4.33	3.59	1.68	4.77
Verrucomicrobiota	Verrucomicrobiae	Chthoniobacterales	Chthoniobacteraceae	*Candidatus* Udaeobacter	1.24	0.36	0.41	0.95

**Archaea* phyla.

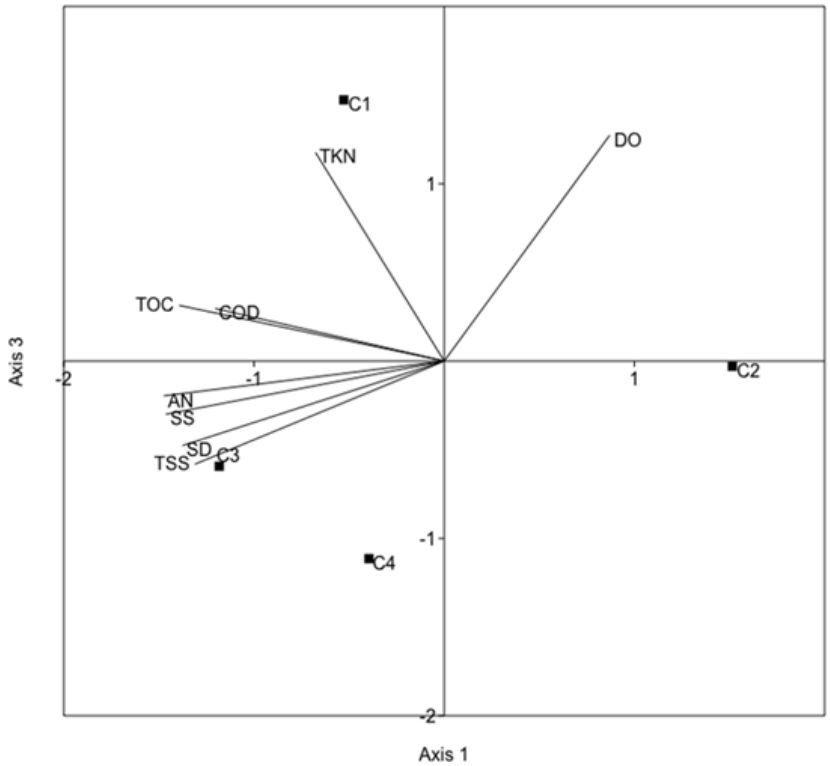

Figure 3. Canonical correlation analysis (CCA) associating the sample collection and chemical parameters to the activated sludge sampling point.

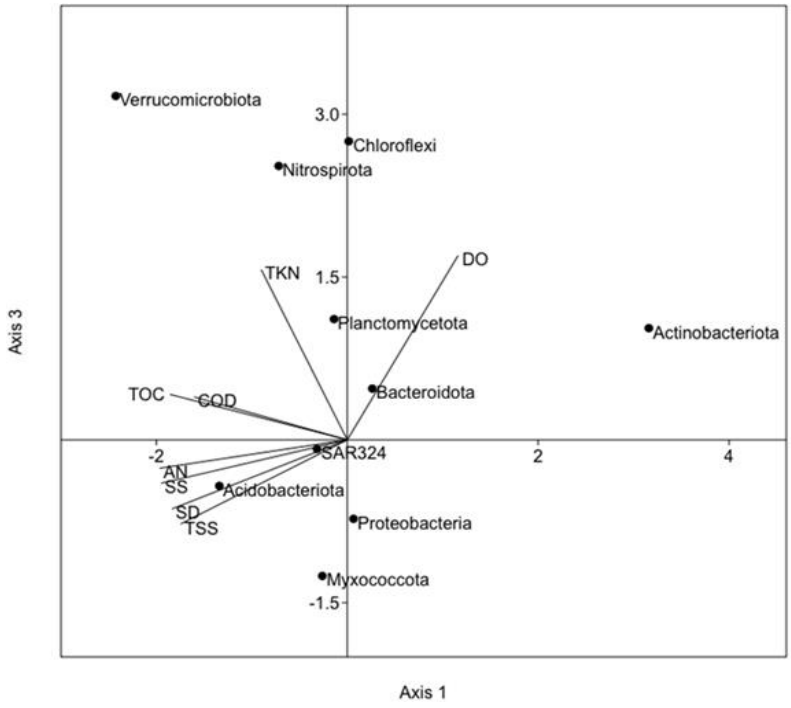

Figure 4. Canonical correlation analysis (CCA) associating the most abundant bacterial phyla and chemical parameters to the activated sludge sampling point.

Analysis of the microbial community revealed key groups for degradation of recalcitrant compounds present in the industrial effluent. *Proteobacteria* prevail in WWTPs treating pharmaceutical, oil refinery, and biological reactors (Xia *et al.*, 2010; Ibarbalz *et al.*, 2013;

Kwiatkowska and Zielinska, 2016). *Alphaproteobacteria* and *Gammaproteobacteria* were the most dominant class in *Proteobacteria*. The filamentous *Alphaproteobacteria* are versatile consumers of various organic substrates (Kragelund *et al.*, 2006). Most species are aerobic or facultatively anaerobic; many are oligotrophic, preferring to grow in environments with low nutrient concentration (Madigan *et al.*, 2016).

Activated sludge has a very diverse microbial community structure depending on both wastewater composition and operational conditions in the treatment plant. However, in several studies of microbial community structure, it has been found that the composition of activated sludge from different plants is quite similar in terms of overall dominating bacterial phylogenetic groups. In nutrient removal of activated sludge, the dominating group frequently found is *Alphaproteobacteria*, *Gammaproteobacteria* and *Betaproteobacteria* (Klausen *et al.*, 2004; Lee *et al.* 2002; Schmid *et al.*, 2003; Wagner and Loy, 2002). Studies in WWTPs suggested a higher diversity of active denitrifiers, including uncharacterized *Alphaproteobacteria*, *Gammaproteobacteria* and *Actinobacteria* (Osaka *et al.* 2006; Hagman *et al.*, 2008; Morgan-Sagastume *et al.*, 2008). Filamentous *Alphaproteobacteria* have been shown as essential microorganisms in industrial WWTPs, often related to bulking incidents or deteriorating settling sludge properties (Levantesi *et al.*, 2004).

At the order level, it was found that the dominant populations in the activated sludge samples were *Burkolderiales* and *Rhizobiales*, which represented 8.03% and 7.44% of those populations. This low percentage indicates a great diversity of the bacterial populations present in the activated sludge.

Sample C3 presented the most different microbial composition of the four samples, mainly because of the dominance of the individuals from the phylum *Armatimonadota* (Lee *et al.*, 2013). This phylum is found in a diverse array of environments, such as geothermal soils (Stott *et al.*, 2008), freshwater lakes and rivers (Crump and Hobbie, 2005), the water discharged from manures (Simpson *et al.*, 2004), and activated sludge (Dalevi *et al.*, 2001). Portillo *et al.* (2009) pointed out that this bacterial phylum could constitute an average of 5% among the total bacterial sequences recovered in hypersaline soils, geothermal springs, lake and river, bioreactors, and endolithic environments. Among the phylum *Armatimonadetes*, a more extensive geographical distribution was found in anaerobic niches (Harris *et al.*, 2004; Stott *et al.*, 2008). Chemical parameters influenced the bacterial community of C3. The canonical correlation analysis (CCA) shows that the phylum *Armatimonadota* presented a positive correlation with the increasing COD, TOC and total dissolved and suspended solids of the C3 sample. This sample showed the highest COD and the second-highest TOC and Solids (TSS, SS, and SD) quantification; these parameters contribute to the formation of an environment with low oxygen concentrations, which may have favored the occurrence of the phylum *Armatimonadota*. Also, sample C3 showed bacterial diversity differences between the other collections of activated sludge, such the phyla *Aenigmarchaeota*, *Caldisericota*, *Cloacimonadota*, MBNT15 and Sva0485, which were only detected in C3 (Supplementary Table 1).

CCA analysis also showed the correlation of *Actinobacteriota* with the presence of dissolved oxygen (DO). Most genera from this phylum are aerobic (Goodfellow and Williams, 1983) and this phylum presented significant quantification in sample C2 (2 mg per liter).

Nitrospirae shows a correlation with the presence of NTK. The ability to perform nitrite reduction was a physiological characteristic observed in *Nitrospirae* (Sidhu *et al.*, 2017). According to Ward *et al.* (2009), genomic evidence suggested that the role of acidobacteria in nitrogen cycling in soils and sediments is the reduction of nitrate, nitrite, and possibly nitric oxide due to assimilatory nitrate reductase gene sequences. The presence of *nif* genes related to conventional nitrogenase was found in a study by Inoue *et al.* (2015), suggesting nitrogen fixation ability in some *Bacteroidetes* species.

Acidobacteriota shows a correlation with the presence of AN, SS, SD and TSS. Bacteria belonging to the phylum *Acidobacteria* have also been observed in a wide variety of environments, including extreme (Hobel *et al.*, 2005), polluted (Bobbink *et al.*, 2010), and effluent wastewater environments (LaPara *et al.*, 2000). Ward *et al.* (2009) found that *Acidobacteria* were involved in nitrogen cycling, promoting the conversion of nitrate and nitrite.

All the sequences were classified at the phylum level, and up to 55% were associated with a bacterial genus. Among the most abundant microorganisms, *Hyphomicrobium* and *Fimbriimonadaceae* were described in the literature as potential denitrifiers and degradators. The genus *Hyphomicrobium* is a denitrifier and can degrade C-1 compounds such as methanol (Rissanen *et al.*, 2017). Sequences representing the phylum *Armatimonadetes* have been isolated by culture-independent methods from various environments, including aerobic and anaerobic wastewater treatment processes, the rhizosphere, hypersaline microbial mats and subsurface geothermal water streams (Portillo and Gonzalez, 2009; Lee *et al.*, 2013; Tamaki *et al.*, 2011). *Fimbriimonadaceae* belonging to *Armatimonadetes* was detected in an anammox consortia where ammonium was removed without nitrite and oxygen (Liang *et al.*, 2014).

4. CONCLUSION

Even with the advances brought about by the new generation sequencing, there are still challenges regarding the classification of the microorganisms in environmental samples. The classification of sequences at a lower taxonomic level, such as family or genus, is essential to understanding a WWTP as a whole and the real participation of each microorganism in the different stages of treatment. The present study contributed to the characterization of the microbial communities involved in the sewage treatment of the petrochemical industry. Identifying the microorganisms has the broader impact of contributing to the knowledge of biological wastewater treatment.

5. ACKNOWLEDGMENTS

We would like to thank Sistema Integrado de Tratamento de Efluentes Líquidos do Polo Petroquímico (SITEL-CORSAN) for authorizing the sample collection. We thank High Performance Computing Lab - LAD/PUCRS for allowing access to run the high-throughput sequences analyses. Luiz Gustavo A. Borges thanks PEGA/PUCRS. We also thank CNPq and CAPES for their financial support.

6. REFERENCES

ABE, T.; USHIKI, N.; FUJITANI, H.; TSUNEDA, S. A rapid collection of yet unknown ammonia oxidizers in pure culture from activated sludge. **Water Research**, v. 108, p. 169-178, 2017. https://doi.org/10.1016/j.watres.2016.10.070

ANTUNES, T. C.; BALLARINI, A. E.; VAN DER SAND, S. Temporal variation of bacterial population and response to physical and chemical parameters along a petrochemical industry wastewater treatment plant. **Annals of the Brazilian Academy of Sciences**, v. 91, n. 2, 2018. https://doi.org/10.1590/0001-3765201920180394

APHA; AWWA; WEF. **Standard Methods for the examination of water and wastewater**. 22nd ed. Washington, 2012. 1496 p.

BATES, S. T.; BERG-LYONS, D.; CAPORASO, W. W. A; KNIGHT, R.; FIERER, N. Examining the global distribution of dominant archaeal populations in soil. **The ISME Journal**, v. 5, p. 908-17, 2011. https://doi.org/10.1038/ismej.2010.171

BOBBINK, R.; HICKS, K.; GALLOWAY, J.; SPRANGER, T.; ALKEMADE, R.; ASHMORE, M. *et al.* Global assessment of nitrogen deposition effects on terrestrial plant diversity: a synthesis. **Ecological Applications**, v. 20, p. 30–59, 2010. http://dx.doi.org/10.1890/08-1140.1

CALLAHAN, B. J.; MCMURDIE, P. J.; ROSEN, M. J.; HAN, A. W.; JOHNSON, A. J.; HOLMES, S. P. DADA2: High-resolution sample inference from Illumina amplicon data. **Nature Methods**, v. 13, p. 581-583, 2016. https://dx.doi.org/10.1038/nmeth.3869

CLAESSON, M. J.; WANG, Q.; O'SULLIVAN, O.; GREENE-DINIZ, R.; COLE J. R.; ROSS, R. P.; O'TOOLE, P. W. Comparison of two next-generation sequencing technologies for resolving highly complex microbiota composition using tandem variable 16S rRNA gene regions. **Nucleic Acids Research**, v. 38, p. e200, 2010. https://doi.org/10.1093/nar/gkq873

CRUMP, B. C.; HOBBIE, J. E. Synchrony and seasonality in bacterioplankton communities of two temperate rivers. **Limnology Oceanography,** v. 50, p. 1718–1729, 2005. https://doi.org/10.4319/lo.2005.50.6.1718

DALEVI, D.; HUGENHOLTZ, P.; BLACKALL, L. L. A multiple-outgroup approach to resolving division-level phylogenetic relationships using 16S rDNA data. **International Journal of Systematic Evolutionary Microbiology**, v. 51, p. 385–391, 2001. https://doi.org/10.1099/00207713-51-2-385

FIGUEROLA, E. L.; ERIJMAN, L. Bacterial taxa abundance pattern in an industrial wastewater treatment system determined by the full rRNA cycle approach. **Environmental Microbiology**, v.9, p.1780-1789, 2007. https://doi.org/10.1111/j.1462-2920.2007.01298.x

GOODFELLOW, M.; WILLIAMS, S. T. Ecology of Actinomycetes. **Annual Review of Microbiology**, v. 37, n. 1, p. 189-216, 1983. https://doi.org/10.1146/annurev.mi.37.100183.001201

GWIN, C. A.; LEFEVRE, E.; ALITO, C. L.; GUNSCH, C. K. Microbial community response to silver nanoparticles and Ag+ in nitrifying activated sludge revealed by ion semiconductor sequencing. **The Science of the Total Environmental,** v. 616–617, p. 1014–1021, 2018. https://doi.org/10.1016/j.scitotenv.2017.10.217

HAGMAN, M.; NIELSEN, J. L.; NIELSEN, P. H.; JANSEN J. Mixed carbon sources for nitrate reduction in activated sludge-identification of bacteria and process activity studies. **Water Research,** v. 42, p. 1539-1546, 2008. https://doi.org/10.1016/j.watres.2007.10.034

HAMMER, O.; HARPER, D. A. T.; RYAN, P. D. PAST: Paleontological Statistics Software Package for Education and Data Analysis. **Palaeontology Electronica**, v. 4, n. 1, p. 1-9, 2001.

HARRIS, J. K.; KELLEY, S. T.; PACE, N. R. New perspective on uncultured bacterial phylogenetic division OP11. **Applied Environmental Microbiology**, v. 70, p. 845–849, 2004. https://dx.doi.org/10.1128/AEM.70.2.845-849.2004

HEIDENWAG, I.; LANGHEINRICH, U.; LÜDERITZ,V. Self Purification in upland and lowland streams. **Acta Hydrochimica at Hydrobiologica**, v. 29, n. 1, p. 22-33, 2001.

HEINZ, K. G. H.; ZANONI, P. R. S.; OLIVEIRA, R. R.; MEDINA-SILVA, R.; SIMÃO, T. L. L.; TRINDADE, F. J. *et al.* Recycled paper sludge microbial community as a potential source of cellulase and xylanase enzymes. **Waste Biomass Valorization**, v. 8, p. 1907-1917, 2017. https://dx.doi.org/10.1007/s12649-016-9792-x

HOBEL, C. F. V.; MARTEINSSON, V. T.; HREGGVIDSSON, G. O.; KRISTJÁNSSON, J. K. Investigation of the microbial ecology of intertidal hot springs by using diversity analysis of 16 S rRNA and chitinase genes. **Applied Environmental Microbiology**, v. 71, p. 2771–2776, 2005. https://dx.doi.org/10.1128/aem.71.5.2771-2776.2005

IBARBALZ, F. M.; FIGUEROLA, E. L. M.; ERIJMAN, L. Industrial activated sludge exhibit unique bacterial community composition at high taxonomic ranks. **Water research**, v. 47, p. 3854-3864, 2013. https://doi.org/10.1016/j.watres.2013.04.010

INOUE, J.; OSHIMA, K.; SUDA, W.; SAKAMOTO, M.; IINO, T.; NODA, S.; OHKUMA, M. Distribution and Evolution of Nitrogen Fixation Genes in the Phylum Bacteroidetes. **Microbes Environmental**, v. 30, n. 1, p. 44–50, 2015. http://doi.org/10.1264/jsme2.ME14142

KLAUSEN, M. M.; THOMSEN, T. R.; NIELSEN, J. L.; MIKKELSEN, L. H.; NIELSEN, P. H. Variations in microcolony strength of probe-defined bacteria in activated sludge flocs. **FEMS Microbiology Ecology**, v. 50, p.123–132, 2004. https://doi.org/10.1016/j.femsec.2004.06.005

KRAGELUND, C.; KONG, Y.; VAN DER, W. J.; THELEN; K.; EIKELBOOM, D.; TANDOI, V. *et al.* Ecophysiology of different filamentous Alphaproteobacteria species from industrial wastewater treatment plants. **Microbiology**, v. 152, p.3003–3012, 2006. https://doi.org/10.1099/mic.0.29249-0

KRISHNAN, M.; SUGANYA, T.; PANDIARAJAN, J. Bacterial community exploration through Ion Torrent sequencing from different treatment stages of CETP for tannery. **Expert Opinion Environmental Biology Journal**, v. 5, p. 3, 2016. https://dx.doi.org/10.4172/2325-9655.1000136

KWIATKOWSKA, A. C.; ZIELINSKA, M. Bacterial communities in full-scale wastewater treatment systems. **World Journal Microbiology Biotechnology**, v. 32, p. 66, 2016. https://dx.doi.org/10.1007/s11274-016-2012-9

LAPARA, T. M.; NAKATSU, C. H.; PANTEA, L.; ALLEMAN, J. E. Phylogenetic analysis of bacterial communities in mesophilic and thermophilic bioreactors treating pharmaceutical wastewater. **Applied Environmental Microbiology,** v. 66, p. 3951–3959, 2000. https://dx.doi.org/10.1128/aem.66.9.3951-3959.2000

LEE, N.; LA COUR JANSSEN, J.; ASPEGREN, H.; HENZE, M. N. P. H.; WAGNER, M. Population dynamics in wastewater treatment plants with enhanced biological phosphorus removal operated without nitrogen removal. **Water Science Technology,** v. 46, p.163–170, 2002. https://doi.org/10.2166/wst.2002.0472

LEE, K. C. Y.; HERBOLD, C. W.; DUNFIELD, P. F.; MORGAN, X. C.; MCDONALD, I. R.; STOTT, M. B. Phylogenetic delineation of the novel phylum Armatimonadetes (former candidate division OP10) and definition of two novel candidate divisions. **Applied Environmental Microbiology**, v. 79, p. 2484-2487, 2013. https://doi.org/10.2166/wst.2002.0472

LEVANTESI, C.; BEIMFOHR, C.; GEURKINK, B.; ROSSETTI, S.; THELEN, K.; KROONEMAN, J. *et al.* Filamentous Alphaproteobacteria associated with bulking in industrial wastewater treatment plants. **System Applied Microbiology**, v. 27, p.716–727, 2004. https://doi.org/10.1078/0723202042369974

LIANG, Y.; LI, D.; ZHANG, X.; ZENG, H.; YANG, Z.; ZHANG, J. Microbial characteristics and nitrogen removal of simultaneous partial nitrification, anammox and denitrification (SNAD) process treating low C/N ratio sewage. **Bioresource Technology**, v.169, p.103-109, 2014. https://doi.org/10.1016/j.biortech.2014.06.064

MADIGAN, M. T.; MARTINKO, J. M.; BENDER, K. S.; BUCKLEY, D. H.; STAHL, D. A. **Microbiologia de Brock**. Porto Alegre: Artmed, 2016. 1032 p.

MCMURDIE P. J.; HOLMES, S. Phyloseq: an R package for reproducible interactive analysis and graphics of microbiome census data. **PLoS ONE,** v. 8, p. e61217, 2013. https://dx.doi.org/10.1371/journal.pone.0061217

MORGAN-SAGASTUME, F.; NIELSEN, J. L.; NIELSEN, P. H. Substrate-dependent denitrification of abundant probe-defined denitrifying bacteria in activated sludge. **FEMS Microbiology Ecology,** v. 66, p. 447-461, 2008. https://doi.org/10.1111/j.1574-6941.2008.00571.x

OSAKA, T.; YOSHIE, S.; TSUNEDA, S.; HIRATA, A.; IWAMI, N.; INAMORI, Y. Identification of acetate- or methanol-assimilating bacteria under nitrate-reducing conditions by stable-isotope probing. **Microbiology Ecology**, v. 52, p. 253-266, 2006. https://doi.org/10.1007/s00248-006-9071-7

PORTILLO, M. C.; GONZALEZ, J. M. Members of the Candidate Division OP10 are spread in a variety of environments. **World Journal Microbiology Biotechnology**, v. 25, p. 347–353, 2009. https://dx.doi.org/10.1007/s11274-008-9895-z

QUAST, C.; PRUESSE, E.; YILMAZ, P.; GERKEN, J.; SCHWEER, T.; YARZA, P. *et al.* The SILVA ribosomal RNA gene database project: improved data processing and web-based tools. **Nucleic Acids Research**, v. 41, p. D590–D596, 2013. https://dx.doi.org/10.1093/nar/gks1219

R CORE TEAM. **R**: A language and environment for statistical computing. Vienna: R Foundation for Statistical Computing, 2019.

RISSANEN, A. J.; OJALA, A.; FRED, T.; TOIVONEN, J.; TIIROLA, M. Methylophilaceae and Hyphomicrobium as target taxonomic groups in monitoring the function of methanol-fed denitrification biofilters in municipal wastewater treatment plants. **Journal of Industrial Microbiology Biotechnology**, v. 44, p. 35–47, 2017. https://doi.org/10.1007/s10295-016-1860-5

SÁNCHEZ, O.; FERRERA, I.; GONZÁLEZ, J.M.; MAS, J. Assessing bacterial diversity in a seawater-processing wastewater treatment plant by 454-pyrosequencing of the 16S rRNA and amoA genes. **Microbial Biotechnology**, v. 6, n. 4, p. 435–442, 2013. https://dx.doi.org/10.1111/1751-7915.12052

SCHMID, M.; THILL, A.; PURKHOLD, U.; WALCHER, M.; BOTTERO, J. Y.; GINESTET, P. *et al.* Characterization of activated sludge flocs by confocal laser scanning microscopy and image analysis. **Water Research**, v. 37, p. 2043–2052, 2003. https://doi.org/10.1016/S0043-1354(02)00616-4

SIDHU, C.; VIKRAM, S.; PINNAKA, A. K. Unraveling the microbial interactions and metabolic potentials in pre- and post-treated sludge from a wastewater treatment plant using metagenomic studies. **Frontiers in Microbiology,** v. 8, p. 1382, 2017. https://dx.doi.org/10.3389/fmicb.2017.01382

SIMPSON, J. M.; DOMINGO, J. W.; REASONER, D. J. Assessment of equine fecal contamination: the search for alternative bacterial source-tracking targets. **FEMS Microbiology Ecology**, v. 47, p. 65–75, 2004. https://doi.org/10.1016/S0168-6496(03)00250-2

STOTT, M. B.; SAITO, J. A.; CROWE, M. A.; DUNFIELD, P. F.; HOU, S.; NAKASONE, E. *et al.* Culture-independent characterization of a novel microbial community at a hydrothermal vent at Brothers volcano, Kermadec arc, New Zealand. **Journal of Geophysical Research: Solid Earth**, v. 113, 2008. https://dx.doi.org/10.1029/2007JB005477

TAMAKI, H.; TANAKA, Y.; MATSUZAWA, H.; MURAMATSU, M.; MENG, X.Y.; HANADA, S. *et al.* Armatimonas rosea gen. nov., sp nov., of a novel bacterial phylum, Armatimonadetes phyl. nov., formally called the candidate phylum OP10. **International Journal Systematic and Evolutionary Microbiology**. v.61, p.1442–1447, 2011. https://doi.org/10.1099/ijs.0.025643-0

WAGNER, M.; LOY, A. Bacterial community composition and function in sewage treatment systems. **Current Opinion Biotechnology**. v. 13, p. 218-227, 2002. https://doi.org/10.1016/S0958-1669(02)00315-4

WARD, N. L.; CHALLACOMBE, J. F.; JANSSEN, P. H.; HENRISSAT, B.; COUTINHO, P. M.; WU, M. *et al.* Three genomes from the phylum Acidobacteria provide insight into the lifestyles of these microorganisms in soils. **Applied Environmental Microbiology**, v. 75, p. 2046-56, 2009. https://dx.doi.org/10.1128/AEM.02294-08

XIA, S.; DUAN. L.; SONG, Y.; LI, J.; PICENO, Y. M.; ANDERSEN, G. L.; COHEN, A. L. *et al.* Bacterial community structure in geographically distributed biological wastewater treatment reactors. **Environmental Science and Technology**, v. 44, p. 7391–7396, 2010. https://doi.org/10.1021/es101554m

YANG, Y.; YU, K.; XIA, Y.; LAU, F. T.; TANG, D. T.; FUNG, W. C.; FANG, H. H. Metagenomic analysis of sludge from full-scale anaerobic digesters operated in municipal wastewater treatment plants. **Applied Microbiology Biotechnology,** v. 98, p. 5709, 2014. https://doi.org/10.1007/s00253-014-5648-0

YE, L.; ZHANG, T. Bacterial communities in different sections of a municipal wastewater treatment plant revealed by 16S rDNA 454 pyrosequencing. **Applied Microbiology Biotechnology**, v. 97, p. 2681, 2013. https://doi.org/10.1007/s00253-012-4082-4

ZHANG, T.; SHAO, M. F.; YE, L. 454 pyrosequencing reveals bacterial diversity of activated sludge from 14 sewage treatment plants. **The ISME Journal**, v. 6, p. 1137–1147, 2011. https://doi.org/10.1038/ismej.2011.188

Supplementary Table 1.

Kingdom	Phylum	Class	Order	Family	Genus (or taxa)	C1	C2	C3	C4
Bacteria	Armatimonadota	Fimbriimonadia	Fimbriimonadales	Fimbriimonadaceae		11.07	4.92	48.96	7.49
Bacteria	Bacteroidota	SJA-28				10.64	12.50	1.80	8.61
Bacteria	Proteobacteria	Alphaproteobacteria	Rhizobiales	Hyphomicrobiaceae	Hyphomicrobium	13.98	12.72	4.79	13.07
Bacteria	Acidobacteriota	Blastocatellia	Blastocatellales	Blastocatellaceae	OLB17	1.38	0.82	1.32	1.01
Bacteria	Acidobacteriota	Blastocatellia	Blastocatellales	Blastocatellaceae	OLB17	0.83	0.61	0.98	1.05
Bacteria	Actinobacteriota	Thermoleophilia	Gaiellales			1.61	5.61	0.88	1.56
Bacteria	Bacteroidota	Bacteroidia	Sphingobacteriales	AKYH767		3.45	0.41	0.35	2.93
Bacteria	Proteobacteria	Gammaproteobacteria	Burkholderiales	Rhodocyclaceae	Sulfuritalea	1.21	1.24	0.64	0.72
Archaea	Crenarchaeota	Thermoprotei	Desulfurococcales	Desulfurococcaceae	Sulfophobococcus	2.51	4.18	1.25	3.03
Bacteria	Proteobacteria	Gammaproteobacteria	Burkholderiales	Nitrosomonadaceae	Ellin6067	0.98	2.19	0.84	1.60
Bacteria	Acidobacteriota	Blastocatellia	Blastocatellales	Blastocatellaceae	JGI_0001001-H03	1.38	0.64	1.41	2.09
Bacteria	Proteobacteria	Gammaproteobacteria	Diplorickettsiales	Diplorickettsiaceae		0.66	2.74	0.92	0.13
Bacteria	SAR324_clade (Marine_group_B)					4.33	3.59	1.68	4.77
Bacteria	Proteobacteria	Alphaproteobacteria	Rhodobacterales	Rhodobacteraceae	Rhodobacter	1.27	0.79	0.78	0.33
Archaea	Halobacterota	Archaeoglobi	Archaeoglobales	Archaeoglobaceae	Ferroglobus	0.59	1.19	0.30	0.67
Bacteria	Proteobacteria	Alphaproteobacteria	Rickettsiales	AB1		0.00	2.09	0.35	0.00
Bacteria	Myxococcota	Polyangia	Haliangiales	Haliangiaceae	Haliangium	1.42	1.05	0.75	1.15
Bacteria	Proteobacteria	Gammaproteobacteria	Burkholderiales	Comamonadaceae	Rubrivivax	1.08	1.82	0.37	0.72
Bacteria	Actinobacteriota	Thermoleophilia	Solirubrobacterales	67-14		0.77	1.31	0.23	0.50
Bacteria	Nitrospirota	Nitrospiria	Nitrospirales	Nitrospiraceae	Nitrospira	1.44	0.98	0.65	1.13
Bacteria	Bacteroidota	Bacteroidia	Chitinophagales	Saprospiraceae		0.66	0.49	0.97	2.81
Bacteria	Acidobacteriota	Blastocatellia	Blastocatellales	Blastocatellaceae		2.20	0.64	0.83	1.02
Bacteria	Acidobacteriota	Blastocatellia	Blastocatellales	Blastocatellaceae	Stenotrophobacter	1.64	1.41	0.95	1.35
Bacteria	Verrucomicrobiota	Verrucomicrobiae	Chthoniobacterales	Chthoniobacteraceae	Candidatus_Udaeobacter	1.24	0.36	0.41	0.95
Bacteria	Proteobacteria	Alphaproteobacteria				0.27	0.39	0.45	1.08
Bacteria	Proteobacteria	Gammaproteobacteria	Coxiellales	Coxiellaceae	Coxiella	1.06	0.99	0.73	0.68
Bacteria	Proteobacteria	Gammaproteobacteria	Burkholderiales	SC-I-84		1.57	1.86	0.74	1.75
Bacteria	Planctomycetota	Phycisphaerae	S-70			0.87	0.80	0.58	1.31
Bacteria	Planctomycetota	Planctomycetes	Pirellulales	Pirellulaceae		1.59	1.15	0.55	0.69
Bacteria	Planctomycetota	OM190				0.30	1.09	0.32	0.74
Bacteria	Planctomycetota	Planctomycetes	Gemmatales	Gemmataceae		1.10	0.86	0.35	0.22
Archaea	Halobacterota	Archaeoglobi	Archaeoglobales	Archaeoglobaceae	Geoglobus	0.39	1.70	0.97	3.11
Archaea	Crenarchaeota	Thermoprotei	Desulfurococcales	Desulfurococcaceae	Thermogladius	1.49	1.18	0.24	0.04
Bacteria	Proteobacteria	Gammaproteobacteria	Gammaproteobacteria_Incertae_Sedis	Unknown_Family	Candidatus_Berkiella	0.83	0.16	2.11	0.93
Bacteria	Proteobacteria	Gammaproteobacteria	Ga0077536			0.53	0.57	0.41	0.79
Bacteria	Verrucomicrobiota	Chlamydiae	Chlamydiales	Waddliaceae	Waddlia	0.15	0.07	0.60	0.19
Bacteria	Bacteroidota	Bacteroidia	Chitinophagales	Chitinophagaceae	Ferruginibacter	0.50	0.73	0.51	0.91
Bacteria	Proteobacteria	Alphaproteobacteria	Sphingomonadales	Sphingomonadaceae	Rhizorhapis	0.57	0.15	0.24	0.75
Bacteria	Acidobacteriota	Blastocatellia	11_24			0.41	0.41	0.40	0.46
Bacteria	Proteobacteria	Gammaproteobacteria	Burkholderiales	Methylophilaceae	Methylotenera	0.07	0.24	0.51	0.26

Continue...

Continued...

Bacteria	Proteobacteria	Alphaproteobacteria	Rhizobiales	Xanthobacteraceae	Bradyrhizobium	0.40	0.48	0.51	0.61
Bacteria	Thermotogota	Thermotogae	Mesoaciditogales	Mesoaciditogaceae		0.17	0.82	0.30	0.39
Archaea	Halobacterota	Halobacteria	Halobacterales	Halobacteriaceae	Salarchaeum	0.00	0.00	0.29	0.71
Bacteria	Proteobacteria	Gammaproteobacteria	Nitrosococcales	Nitrosococcaceae	MSB-1D1	0.00	0.21	0.18	0.76
Bacteria	Proteobacteria	Alphaproteobacteria	Rhodobacterales	Rhodobacteraceae	Paracoccus	0.00	0.68	0.19	0.00
Bacteria	Proteobacteria	Gammaproteobacteria	Burkholderiales	Comamonadaceae		0.46	0.44	0.16	0.33
Archaea	Nanoarchaeota	Nanoarchaeia	Nanoarchaeales	Nanopusillaceae	Candidatus_Nanopusillus	0.82	0.71	0.30	0.81
Bacteria	Proteobacteria	Gammaproteobacteria	Burkholderiales	Sutterellaceae		0.41	0.26	0.11	0.46
Bacteria	Proteobacteria	Gammaproteobacteria	Burkholderiales	B1-7BS		0.46	0.30	0.15	0.47
Bacteria	Verrucomicrobiota	Chlamydiae	Chlamydiales	Simkaniaceae	Ga0074140	0.22	0.04	0.27	0.00
Bacteria	Firmicutes	Clostridia	Clostridiales	Clostridiaceae	Proteiniclasticum	0.00	0.20	0.24	0.09
Bacteria	Proteobacteria	Alphaproteobacteria	Rhizobiales	Hyphomicrobiaceae	Pedomicrobium	0.59	0.92	0.24	0.43
Bacteria	Armatimonadota	Fimbriimonadia	Fimbriimonadales			0.68	0.15	0.21	0.13
Bacteria	Proteobacteria	Alphaproteobacteria	Rhizobiales	Xanthobacteraceae		0.52	0.34	0.21	0.10
Bacteria	Proteobacteria	Alphaproteobacteria	Rhizobiales	Hyphomicrobiaceae		0.54	0.00	0.27	0.00
Bacteria	Acidobacteriota	Vicinamibacteria	Subgroup_17			0.43	0.73	0.30	0.44
Bacteria	Proteobacteria	Alphaproteobacteria	Rhizobiales	Rhizobiales_Incertae_Sedis		0.56	0.18	0.31	0.24
Bacteria	Acidobacteriota	Thermoanaerobaculia	Thermoanaerobaculales	Thermoanaerobaculaceae	Subgroup_10	0.43	0.44	0.26	0.21
Bacteria	Proteobacteria	Gammaproteobacteria	AT-s16			0.04	0.00	0.26	0.00
Bacteria	Proteobacteria	Gammaproteobacteria	EV818SWSAP88			0.36	0.13	0.28	0.10
Bacteria	Proteobacteria	Alphaproteobacteria	Rhizobiales	Rhizobiales_Incertae_Sedis	Nordella	0.33	0.23	0.27	0.32
Bacteria	Gemmatimonadota	Gemmatimonadetes	Gemmatimonadales	Gemmatimonadaceae		0.17	0.17	0.11	0.34
Bacteria	Myxococcota	Polyangia	Blfdi19			0.69	0.33	0.03	0.81
Bacteria	Proteobacteria	Alphaproteobacteria	Rhizobiales	Rhizobiaceae	Aminobacter	0.00	0.83	0.22	0.00
Bacteria	Actinobacteriota	Actinobacteria	Micrococcales	Microbacteriaceae	Leucobacter	0.00	0.26	0.15	0.10
Bacteria	Actinobacteriota	Acidimicrobiia	IMCC26256			0.31	0.42	0.14	0.00
Bacteria	Proteobacteria	Alphaproteobacteria	Rhizobiales	Rhizobiaceae	Pseudaminobacter	0.00	0.00	0.33	0.00
Bacteria	Planctomycetota	Phycisphaerae	mle1-8			0.31	0.41	0.28	0.62
Bacteria	Proteobacteria	Alphaproteobacteria	Rhodobacterales	Rhodobacteraceae	Defluviimonas	0.46	0.00	0.21	0.00
Bacteria	Proteobacteria	Gammaproteobacteria	PLTA13			0.03	0.16	0.13	0.30
Bacteria	Proteobacteria	Alphaproteobacteria	Paracaedibacterales	Paracaedibacteraceae	Candidatus_Paracaedibacter	0.08	0.07	0.07	0.60
Bacteria	Proteobacteria	Alphaproteobacteria	Rhizobiales	Xanthobacteraceae	Pseudorhodoplanes	0.52	0.58	0.21	0.00
Bacteria	Proteobacteria	Alphaproteobacteria	Caulobacterales	Hyphomonadaceae	Hirschia	0.00	0.21	0.14	0.08
Bacteria	Verrucomicrobiota	Verrucomicrobiae	Pedosphaerales	Pedosphaeraceae		0.04	0.19	0.35	0.29
Bacteria	Bacteroidota	Bacteroidia	Chitinophagales	Chitinophagaceae	Terrimonas	0.34	0.46	0.29	0.81
Bacteria	Bacteroidota	Bacteroidia	Cytophagales	Microscillaceae		0.24	0.18	0.17	0.29
Bacteria	Proteobacteria	Gammaproteobacteria	Burkholderiales	Nitrosomonadaceae	966-1	0.00	0.40	0.14	1.04
Bacteria	Planctomycetota	Phycisphaerae	Phycisphaerales	Phycisphaeraceae	SM1A02	0.15	0.38	0.40	0.80
Bacteria	Planctomycetota	Phycisphaerae	CCM11a			0.12	0.04	0.19	0.02
Bacteria	Myxococcota	Polyangia	Polyangiales	Polyangiaceae	Pajaroellobacter	0.00	0.13	0.09	0.43
Bacteria	Dependentiae	Babeliae	Babeliales	Vermiphilaceae		0.00	0.45	0.45	0.09
Bacteria	Proteobacteria	Alphaproteobacteria	Micavibrionales			0.00	0.00	0.00	0.81

Continue...

Continued...

Bacteria	Proteobacteria	Alphaproteobacteria	Sphingomonadales	Sphingomonadaceae		0.00	0.00	0.18	0.00
Bacteria	Desulfobacterota	Desulfobacteria	Desulfobacterales	Desulfolunaceae	Desulfoluna	0.03	0.06	0.13	0.46
Bacteria	Proteobacteria	Gammaproteobacteria	Burkholderiales	Rhodocyclaceae	Uliginosibacterium	0.00	0.17	0.07	0.21
Bacteria	Desulfobacterota					0.10	0.07	0.16	0.16
Bacteria	Planctomycetota	Planctomycetes				0.33	0.40	0.22	0.20
Bacteria	Actinobacteriota	Acidimicrobiia	Microtrichales			0.24	0.40	0.11	0.09
Bacteria	Proteobacteria	Alphaproteobacteria	Sphingomonadales	Sphingomonadaceae	Novosphingobium	0.00	0.00	0.13	0.34
Archaea	Crenarchaeota	Thermoprotei	Geoarchaeales	SCGC_AAA261-C22		0.49	0.00	0.16	0.38
Bacteria	Chloroflexi	KD4-96				0.47	0.54	0.07	0.23
Bacteria	Proteobacteria	Gammaproteobacteria	Burkholderiales	Burkholderiaceae	Limnobacter	0.00	0.23	0.06	0.10
Bacteria	Proteobacteria	Gammaproteobacteria	Burkholderiales	Comamonadaceae	Methylibium	0.00	0.00	0.14	0.00
Bacteria	Proteobacteria	Gammaproteobacteria	Beggiatoales	Beggiatoaceae	Candidatus_Allobeggiatoa	0.00	0.00	0.10	0.37
Bacteria	Actinobacteriota	Actinobacteria	Micrococcales	Microbacteriaceae	Galbitalea	0.33	0.11	0.07	0.00
Bacteria	Proteobacteria	Gammaproteobacteria	Burkholderiales	Rhodocyclaceae	Denitratisoma	0.08	0.05	0.08	0.39
Bacteria	Proteobacteria	Alphaproteobacteria	Reyranellales	Reyranellaceae		0.00	0.27	0.06	0.00
Bacteria	Dependentiae	Babeliae	Babeliales			0.44	0.13	0.13	0.62
Bacteria	Verrucomicrobiota	Chlamydiae	Chlamydiales	Parachlamydiaceae	Candidatus_Protochlamydia	0.27	0.00	0.17	0.00
Bacteria	Chloroflexi	Anaerolineae	RBG-13-54-9			0.32	0.24	0.15	0.16
Bacteria	Proteobacteria	Alphaproteobacteria	Rhodobacterales	Rhodobacteraceae	Amaricoccus	0.00	0.00	0.00	0.54
Bacteria	Bdellovibrionota	Oligoflexia	0319-6G20			0.25	0.06	0.14	0.28
Bacteria	Acidobacteriota	Vicinamibacteria	Vicinamibacterales			0.00	0.08	0.09	0.24
Bacteria	Actinobacteriota	Actinobacteria	Micrococcales	Microbacteriaceae		0.00	0.32	0.00	0.12
Bacteria	Actinobacteriota	Coriobacteriia	Coriobacteriales	Atopobiaceae	Coriobacteriaceae_UCG-002	0.10	0.13	0.13	0.12
Bacteria	Actinobacteriota	Actinobacteria	Corynebacteriales	Mycobacteriaceae	Mycobacterium	0.00	0.15	0.09	0.11
Bacteria	Proteobacteria	Alphaproteobacteria	Sphingomonadales	Sphingomonadaceae	Sphingobium	0.00	0.00	0.11	0.00
Bacteria	Proteobacteria	Gammaproteobacteria	Acidithiobacillales	Acidithiobacillaceae	KCM-B-112	0.16	0.00	0.06	0.09
Bacteria	Acidobacteriota	Vicinamibacteria	Vicinamibacterales	Vicinamibacteraceae		0.00	0.39	0.10	0.25
Bacteria	Acidobacteriota	Blastocatellia	Blastocatellales	Blastocatellaceae	Aridibacter	0.06	0.06	0.08	0.46
Bacteria	Myxococcota	Myxococcia	Myxococcales	Myxococcaceae	Hyalangium	0.02	0.38	0.04	0.00
Archaea	Aenigmarchaeota	Aenigmarchaeia	Aenigmarchaeales	Aenigmarchaeales_fa	Candidatus_Aenigmarchaeum	0.00	0.00	0.10	0.00
Archaea	Crenarchaeota	Thermoprotei				0.08	0.03	0.11	0.34
Bacteria	Bacteroidota	Bacteroidia	Sphingobacteriales	Sphingobacteriaceae	Arcticibacter	0.00	0.00	0.10	0.00
Bacteria	Cloacimonadota	Cloacimonadia	Cloacimonadales	SHA-41		0.00	0.00	0.15	0.00
Bacteria	Chloroflexi	Anaerolineae	Caldilineales	Caldilineaceae		0.38	0.19	0.14	0.24
Bacteria	NB1-j					0.26	0.27	0.06	0.21
Archaea	Crenarchaeota	Thermoprotei	Desulfurococcales	Desulfurococcaceae	Staphylothermus	0.00	0.09	0.12	0.00
Bacteria	Acidobacteriota	Holophagae	Subgroup_7			0.21	0.13	0.09	0.00
Bacteria	Bacteroidota	Kryptonia	Kryptoniales	BSV26		0.23	0.31	0.13	0.69
Bacteria	Myxococcota	Polyangia	MSB-4B10			0.02	0.00	0.09	0.00
Bacteria	Planctomycetota	Phycisphaerae	Tepidisphaerales	WD2101_soil_group		0.27	0.10	0.10	0.09
Bacteria	Chloroflexi	Dehalococcoidia	S085			0.15	0.07	0.06	0.00
Bacteria	Proteobacteria	Gammaproteobacteria	Xanthomonadales	Rhodanobacteraceae	Ahniella	0.10	0.18	0.02	0.00

Continue...

Continued...

Bacteria	Acidobacteriota	Acidobacteriae	Bryobacterales	Bryobacteraceae	Bryobacter	0.00	0.07	0.11	0.15
Bacteria	Bacteroidota	Ignavibacteria	Ignavibacteriales	LD-RB-34		0.03	0.07	0.07	0.16
Bacteria	Verrucomicrobiota	Chlamydiae	Chlamydiales	Parachlamydiaceae	Neochlamydia	0.16	0.30	0.12	0.19
Bacteria	Latescibacterota					0.00	0.20	0.08	0.07
Bacteria	Verrucomicrobiota	Verrucomicrobiae	Pedosphaerales	Pedosphaeraceae	ADurb.Bin063-1	0.00	0.00	0.08	0.00
Bacteria	Verrucomicrobiota	Chlamydiae	Chlamydiales	Simkaniaceae	Candidatus_Fritschea	0.40	0.00	0.05	0.00
Bacteria	Proteobacteria	Alphaproteobacteria	Rhizobiales			0.12	0.00	0.08	0.21
Bacteria	Proteobacteria	Alphaproteobacteria	Caulobacterales	Hyphomonadaceae	SWB02	0.00	0.21	0.16	0.16
Bacteria	Proteobacteria	Alphaproteobacteria	Rhizobiales	Rhizobiales_Incertae_Sedis	Bauldia	0.29	0.26	0.10	0.15
Bacteria	Proteobacteria	Gammaproteobacteria	Burkholderiales	Rhodocyclaceae	Methyloversatilis	0.00	0.00	0.07	0.00
Bacteria	Proteobacteria	Gammaproteobacteria	CCM19a			0.08	0.11	0.05	0.10
Bacteria	Proteobacteria	Alphaproteobacteria	Caulobacterales	Hyphomonadaceae	Fretibacter	0.08	0.00	0.01	0.28
Bacteria	Proteobacteria	Gammaproteobacteria	Chromatiales	Chromatiaceae	Thiocapsa	0.07	0.24	0.00	0.00
Bacteria	Proteobacteria	Alphaproteobacteria	Kordiimonadales	Temperatibacteraceae	Temperatibacter	0.00	0.00	0.07	0.00
Bacteria	Proteobacteria	Alphaproteobacteria	Rhodospirillales	Magnetospiraceae		0.05	0.05	0.07	0.10
Bacteria	Verrucomicrobiota	Chlamydiae	Chlamydiales	Criblamydiaceae	Estrella	0.00	0.00	0.06	0.00
Bacteria	Proteobacteria	Alphaproteobacteria	Rhizobiales	A0839		0.00	0.09	0.08	0.02
Bacteria	Dependentiae	Babeliae	Babeliales	UBA12409		0.00	0.00	0.04	0.10
Bacteria	Verrucomicrobiota	Chlamydiae	Chlamydiales	Parachlamydiaceae	Candidatus_Rubidus	0.31	0.09	0.03	0.07
Bacteria	Bacteroidota	Bacteroidia	Bacteroidales	Bacteroidetes_BD2-2		0.08	0.04	0.06	0.03
Bacteria	Firmicutes	Clostridia	Eubacteriales	Eubacteriaceae	Acetobacterium	0.12	0.04	0.02	0.17
Bacteria	Patescibacteria	Gracilibacteria	Candidatus_Peregrinibacteria			0.05	0.00	0.05	0.03
Bacteria	Bacteroidota	Bacteroidia	Cytophagales	Thermonemataceae	Thermonema	0.00	0.15	0.06	0.00
Bacteria	Planctomycetota	Pla3_lineage				0.14	0.03	0.06	0.05
Bacteria	Myxococcota	Polyangia	Polyangiales	BIrii41		0.00	0.00	0.02	0.25
Bacteria	Planctomycetota	Planctomycetes	Pirellulales	Pirellulaceae	Pir4_lineage	0.08	0.18	0.04	0.08
Bacteria	Proteobacteria	Alphaproteobacteria	Rhizobiales	Rhizobiaceae	Pseudohoeflea	0.03	0.00	0.04	0.05
Bacteria	Proteobacteria	Alphaproteobacteria	Holosporales	Holosporaceae		0.20	0.00	0.05	0.00
Bacteria	Proteobacteria	Gammaproteobacteria	Diplorickettsiales	Diplorickettsiaceae	Aquicella	0.16	0.00	0.00	0.25
Bacteria	Chloroflexi	Anaerolineae	SBR1031	A4b		0.05	0.09	0.09	0.14
Bacteria	Bacteroidota	Bacteroidia	Flavobacteriales	NS9_marine_group		0.00	0.03	0.01	0.14
Bacteria	Proteobacteria	Alphaproteobacteria	Rhizobiales	Rhizobiaceae	Martelella	0.00	0.18	0.00	0.00
Bacteria	Zixibacteria					0.00	0.04	0.05	0.06
Bacteria	Dadabacteria	Dadabacteriia	Dadabacteriales			0.03	0.02	0.03	0.05
Bacteria	Proteobacteria	Alphaproteobacteria	Kiloniellales	Fodinicurvataceae		0.00	0.14	0.05	0.00
Bacteria	Acidobacteriota	Vicinamibacteria	Vicinamibacterales	Vicinamibacteraceae	Luteitalea	0.20	0.05	0.04	0.00
Bacteria	Chloroflexi	Anaerolineae	SBR1031	A4b		0.00	0.04	0.07	0.00
Bacteria	Verrucomicrobiota	Chlamydiae	Chlamydiales	Criblamydiaceae		0.00	0.00	0.04	0.00
Archaea	Crenarchaeota	Thermoprotei	Thermoproteales	Thermoproteaceae	Caldivirga	0.00	0.04	0.04	0.00
Bacteria	Planctomycetota	Planctomycetes	Pirellulales	Pirellulaceae	Rhodopirellula	0.18	0.04	0.04	0.03
Bacteria	Patescibacteria	Microgenomatia	Candidatus_Amesbacteria			0.27	0.00	8.45E-03	0.00
Bacteria	Proteobacteria	Alphaproteobacteria	Rhizobiales	Beijerinckiaceae	Methylocystis	0.00	0.15	0.02	0.00

Continue...

Continued...

Bacteria	MBNT15					0.00	0.00	0.04	0.00
Bacteria	Proteobacteria	Gammaproteobacteria	Legionellales	Legionellaceae	Legionella	0.12	0.03	0.02	0.00
Bacteria	Chloroflexi	Anaerolineae	01_20			0.00	0.03	0.03	0.03
Bacteria	Proteobacteria	Gammaproteobacteria	Burkholderiales	Burkholderiaceae	Lautropia	0.00	0.00	0.04	0.00
Bacteria	Aquificota	Desulfurobacteriia	Desulfurobacteriales	Desulfurobacteriaceae	Balnearium	0.00	0.00	0.04	0.00
Bacteria	Bdellovibrionota	Oligoflexia	Silvanigrellales	Silvanigrellaceae	Silvanigrella	0.00	0.02	0.02	0.26
Bacteria	Verrucomicrobiota	Verrucomicrobiae	Opitutales	Puniceicoccaceae	Cerasicoccus	0.13	0.05	0.00	0.00
Bacteria	Planctomycetota	Planctomycetes	Planctomycetales	Rubinisphaeraceae	Planctomicrobium	0.11	0.08	0.01	0.00
Bacteria	Firmicutes	Clostridia	Peptostreptococcales-Tissierellales	Peptostreptococcaceae	Romboutsia	0.07	0.05	0.02	0.03
Bacteria	Patescibacteria	Saccharimonadia	Saccharimonadales	Saccharimonadaceae	GTL1	0.19	0.00	0.03	0.00
Bacteria	Firmicutes	Clostridia	Clostridiales	Clostridiaceae	Clostridium_sensu_stricto_1	0.11	0.10	0.01	0.05
Bacteria	Dependentiae	Babeliae	Babeliales	Babeliaceae		0.00	0.02	0.04	0.14
Bacteria	Proteobacteria	Gammaproteobacteria	Steroidobacterales	Steroidobacteraceae		0.00	0.00	0.04	0.00
Archaea	Nanoarchaeota	Nanoarchaeia	Woesearchaeales	SCGC_AAA286-E23		0.00	0.12	0.00	0.00
Bacteria	Verrucomicrobiota	Verrucomicrobiae	Chthoniobacterales	Terrimicrobiaceae	FukuN18_freshwater_group	0.01	0.00	0.03	0.00
Bacteria	Patescibacteria	Saccharimonadia	Saccharimonadales			0.05	0.03	0.03	0.00
Bacteria	Acidobacteriota	Acidobacteriae	Acidobacteriales	Koribacteraceae	Candidatus_Koribacter	0.04	0.00	0.02	0.05
Bacteria	Proteobacteria	Alphaproteobacteria	Reyranellales	Reyranellaceae	Reyranella	0.00	0.04	0.08	0.00
Bacteria	Proteobacteria	Gammaproteobacteria	Burkholderiales	T34		0.00	0.00	0.03	0.00
Bacteria	Dependentiae	Babeliae	Babeliales	UBA12411		0.09	8.83E-03	0.03	0.00
Bacteria	Proteobacteria	Gammaproteobacteria	Burkholderiales	Nitrosomonadaceae	MND1	0.00	0.05	0.03	0.00
Bacteria	Proteobacteria	Gammaproteobacteria	Burkholderiales	Alcaligenaceae	Candidimonas	0.00	0.00	0.03	0.00
Bacteria	Verrucomicrobiota	Chlamydiae	Chlamydiales	Parachlamydiaceae		0.00	0.00	0.02	0.14
Bacteria	Verrucomicrobiota	Verrucomicrobiae	Opitutales	Puniceicoccaceae		0.11	0.03	0.01	0.00
Bacteria	Myxococcota	Polyangia	Polyangiales	Sandaracinaceae		0.13	0.13	0.04	0.00
Bacteria	Acidobacteriota	Acidobacteriae	Elev-16S-1166			0.00	0.00	0.03	0.00
Bacteria	Actinobacteriota	Thermoleophilia	Thermophilales	Thermoleophilaceae	Thermoleophilum	0.04	0.02	0.03	0.00
Bacteria	Proteobacteria	Alphaproteobacteria	Azospirillales	Inquilinaceae	Inquilinus	0.05	0.00	0.03	0.00
Bacteria	Chloroflexi	Anaerolineae	SBR1031			0.00	0.00	0.05	0.06
Bacteria	Proteobacteria	Gammaproteobacteria	Burkholderiales	Alcaligenaceae	Derxia	0.00	0.00	0.03	0.00
Bacteria	Proteobacteria	Gammaproteobacteria	Burkholderiales	Nitrosomonadaceae		0.00	0.00	0.03	0.00
Bacteria	Proteobacteria	Gammaproteobacteria	Immundisolibacterales	Immundisolibacteraceae	Immundisolibacter	0.00	0.00	0.03	0.13
Bacteria	Verrucomicrobiota	Chlamydiae	Chlamydiales	cvE6		0.14	0.00	8.45E-03	0
Bacteria	Proteobacteria	Alphaproteobacteria	Azospirillales	Azospirillales_Incertae_Sedis	Stella	0.00	0.00	0.03	0
Bacteria	Bdellovibrionota	Bdellovibrionia	Bdellovibrionales	Bdellovibrionaceae	Bdellovibrio	0.15	0.00	0.03	0.10
Bacteria	Proteobacteria	Gammaproteobacteria	Steroidobacterales	Steroidobacteraceae	Steroidobacter	0.00	0.00	0.04	0.02
Bacteria	Proteobacteria	Gammaproteobacteria	JG36-GS-52			0.05	0.00	0.02	0.06
Bacteria	Chloroflexi	Anaerolineae	Anaerolineales	Anaerolineaceae		0.00	0.02	0.03	0.03
Bacteria	Proteobacteria	Alphaproteobacteria	Rhizobiales	Pleomorphomonadaceae		0.00	0.00	0.02	0.00
Bacteria	Proteobacteria	Alphaproteobacteria	Holosporales	Holosporaceae	Candidatus_Paraholospora	0.00	0.02	0.02	0.00
Bacteria	Verrucomicrobiota	Verrucomicrobiae	Methylacidiphilales	Methylacidiphilaceae		0.00	0.00	0.02	0.00

Continue...

Continued...

Archaea	Crenarchaeota	Nitrososphaeria	Caldiarchaeales	Geothermarchaeaceae		0.00	8.83E-03	0.03	0.05
Bacteria	Chloroflexi	Dehalococcoidia	GIF9	AB-539-J10	Dsc1	0.00	0	0.02	0.00
Bacteria	Bacteroidota	Bacteroidia	Chitinophagales			0.00	0	0.00	0.10
Bacteria	Proteobacteria	Alphaproteobacteria	Rhizobiales	Beijerinckiaceae	Qingshengfania	0.00	0	0.00	0.10
Bacteria	Proteobacteria	Alphaproteobacteria	Rhizobiales	Beijerinckiaceae	Bosea	0.00	0.08	0.00	0.00
Bacteria	Patescibacteria	Parcubacteria	NA			0.00	0.00	0.02	0.05
Bacteria	Desulfobacterota	Desulfarculia	Desulfarculales	Desulfarculaceae	Dethiosulfatarculus	0.03	0.00	0.00	0.10
Bacteria	Proteobacteria	Alphaproteobacteria	Rhizobiales	Methyloligellaceae	Rhodobium	0.00	0.03	0.02	0.00
Bacteria	Myxococcota	Myxococcia	Myxococcales	Myxococcaceae	P3OB-42	0.00	0.04	0.02	0.08
Bacteria	Bacteroidota	Bacteroidia	Bacteroidales	Prolixibacteraceae		0.00	0.00	0.02	0.00
Bacteria	Myxococcota	Polyangia	mle1-27			0.00	0.04	7.25E-03	0.00
Bacteria	Proteobacteria	Gammaproteobacteria	Burkholderiales	Burkholderiales_Incertae_Sedis	Candidatus_Branchiomonas	0.00	0.00	0.02	0.00
Bacteria	Bacteroidota	Bacteroidia	Sphingobacteriales	env.OPS_17		0.02	0.00	0.03	0.03
Bacteria	Proteobacteria	Gammaproteobacteria	Burkholderiales	Neisseriaceae		0.04	0.00	0.02	0.00
Bacteria	Planctomycetota	Phycisphaerae	Tepidisphaerales	Tepidisphaeraceae		0.00	0.00	0.02	0.03
Bacteria	Aquificota	Aquificae	Aquificales	Aquificaceae	Hydrogenivirga	0.00	0.00	0.02	0.05
Bacteria	Planctomycetota	Planctomycetes	Pirellulales	Pirellulaceae	Pirellula	0.10	0.00	0.02	0.08
Bacteria	Proteobacteria	Gammaproteobacteria	Burkholderiales	Oxalobacteraceae	Actimicrobium	0.00	0.00	0.02	0.00
Bacteria	Proteobacteria	Alphaproteobacteria	Rhizobiales	Xanthobacteraceae	Afipia	0.00	0.00	0.02	0.00
Bacteria	Proteobacteria	Gammaproteobacteria	Gammaproteobacteria_Incertae_Sedis	Unknown_Family	Acidibacter	0.09	0.00	0.01	0.00
Bacteria	Actinobacteriota	Acidimicrobiia	Microtrichales	Iamiaceae	Iamia	0.00	0.06	0.00	0.04
Bacteria	Myxococcota	Myxococcia	Myxococcales	Myxococcaceae	Aggregicoccus	0.00	0.00	0.02	0.00
Bacteria	Cyanobacteria	Vampirivibrionia	Obscuribacterales	Obscuribacteraceae		0.08	0.00	7.25E-03	0.04
Bacteria	Proteobacteria	Alphaproteobacteria	Rhizobiales	Devosiaceae	Methyloterrigena	0.00	0.00	0.017	0.00
Bacteria	Proteobacteria	Alphaproteobacteria	Rhizobiales	Stappiaceae	Polymorphum	0.00	0.00	0.017	0.00
Bacteria	Proteobacteria	Alphaproteobacteria	Sphingomonadales	Sphingomonadaceae	MN_122.2a	0.00	0.00	0.017	0.00
Bacteria	Proteobacteria	Gammaproteobacteria	EC3			0.08	0.00	0.000	0.00
Bacteria	Actinobacteriota	Actinobacteria	Frankiales	Nakamurellaceae	Nakamurella	0.00	0.06	0.000	0.00
Bacteria	Verrucomicrobiota	Verrucomicrobiae	Verrucomicrobiales	Verrucomicrobiaceae	Roseimicrobium	0.00	0.00	0.016	0.00
Bacteria	Planctomycetota	Phycisphaerae	Phycisphaerales	Phycisphaeraceae		0.00	8.83E-03	0.016	0.00
Bacteria	Nitrospinota					0.00	0.00	0.016	0.00
Bacteria	Verrucomicrobiota	Verrucomicrobiae	Chthoniobacterales	Chthoniobacteraceae	Chthoniobacter	0.00	0.00	0.016	0.04
Bacteria	Proteobacteria	Gammaproteobacteria	Burkholderiales	T34		0.00	0.00	0.000	0.07
Bacteria	Cyanobacteria	Vampirivibrionia	Vampirovibrionales	Vampirovibrionaceae	Vampirovibrio	0.00	0.00	0.000	0.07
Bacteria	Proteobacteria	Gammaproteobacteria	Methylococcales	Methylococcaceae	Methyloterricola	0.08	0.00	0.000	0.00
Bacteria	Chloroflexi	Anaerolineae	C10-SB1A			0.00	0.02	0.011	0.00
Bacteria	Desulfobacterota	Syntrophobacteria	Syntrophobacterales	Syntrophobacteraceae	Desulfacinum	0.00	0.00	0.014	0.07
Bacteria	Caldisericota	Caldisericia	Caldisericales	TTA-B15		0.00	0.00	0.014	0.00
Bacteria	Proteobacteria	Alphaproteobacteria	Acetobacterales	Acetobacteraceae	Neoasaia	0.00	0.00	0.014	0.00
Bacteria	Bacteroidota	Bacteroidia	Cytophagales	Cyclobacteriaceae	Anditalea	0.00	0.00	2.42E-03	0.07

Continue...

Continued...

Archaea	Halobacterota	Methanomicrobia	Methanomicrobiales	Methanomicrobiaceae	Methanomicrobium	0.00	0.00	0.00	0.07
Bacteria	Proteobacteria	Gammaproteobacteria	Thiomicrospirales	Thiomicrospiraceae	Hydrogenovibrio	0.07	0.00	0.00	0.00
Bacteria	Myxococcota	Polyangia	Polyangiales	Polyangiaceae	Labilithrix	0.00	0.05	0.00	0.00
Bacteria	Chloroflexi	Chloroflexia	Thermomicrobiales	JG30-KF-CM45		0.00	0.05	0.00	0.00
Bacteria	Proteobacteria	Gammaproteobacteria	Gammaproteobacteria_Incertae_Sedis	Unknown_Family	Candidatus_Ovatusbacter	0.00	0.00	0.02	0.00
Bacteria	Planctomycetota	Phycisphaerae	Pla1_lineage			0.06	0.00	0.01	0.00
Bacteria	Verrucomicrobiota	Verrucomicrobiae	Pedosphaerales	Pedosphaeraceae	Pedosphaera	0.01	0.00	0.01	0.00
Bacteria	Firmicutes	Bacilli	Acholeplasmatales	Acholeplasmataceae	DMI	0.00	0.00	0.00	0.06
Bacteria	Verrucomicrobiota	Kiritimatiellae	Kiritimatiellales	Kiritimatiellaceae		0.00	0.04	0.00	0.00
Bacteria	Patescibacteria	Microgenomatia	Candidatus_Gottesmanbacteria			0.00	0.04	0.00	0.00
Bacteria	Proteobacteria	Gammaproteobacteria	Xanthomonadales	Rhodanobacteraceae	Tahibacter	0.00	0.00	0.01	0.00
Bacteria	Chloroflexi	Ktedonobacteria	C0119			0.00	0.00	0.01	0.00
Bacteria	Proteobacteria	Alphaproteobacteria	Rhizobiales	Labraceae	Labrys	0.00	0.00	0.01	0.00
Bacteria	Proteobacteria	Gammaproteobacteria	sediment-surface35			0.00	0.00	0.01	0.00
Bacteria	Proteobacteria	Alphaproteobacteria	Rickettsiales	SM2D12		0.00	0.00	0.00	0.05
Bacteria	Proteobacteria	Alphaproteobacteria	Rickettsiales	Rickettsiaceae	Candidatus_Arcanobacter	0.00	0.00	0.00	0.05
Bacteria	Proteobacteria	Alphaproteobacteria	Rickettsiales	Rickettsiaceae	Candidatus_Megaira	0.00	0.05	0.00	0.00
Bacteria	Actinobacteriota	Thermoleophilia	Solirubrobacterales	Solirubrobacteraceae	Conexibacter	0.00	0.04	0.00	0.00
Bacteria	Proteobacteria	Alphaproteobacteria	Rickettsiales	SM1B06		0.00	0.00	0.01	0.00
Bacteria	Firmicutes	Desulfotomaculia	Carboxydothermales	Carboxydothermaceae	Carboxydothermus	0.00	0.00	0.01	0.00
Bacteria	Bdellovibrionota	Bdellovibrionia	Bdellovibrionales	Bdellovibrionaceae		0.00	0.00	0.01	0.02
Bacteria	Chloroflexi	OLB14				0.00	0.00	0.00	0.05
Bacteria	Planctomycetota	Planctomycetes	Planctomycetales	Schlesneriaceae	Schlesneria	0.05	0.00	7.25E-03	0.00
Bacteria	Actinobacteriota	Acidimicrobiia	Microtrichales	Ilumatobacteraceae		0.05	0.00	0.00	0.00
Bacteria	Actinobacteriota	Actinobacteria	Frankiales	Sporichthyaceae	Longivirga	0.00	0.04	0.00	0.00
Bacteria	Firmicutes	Bacilli	Erysipelotrichales	Erysipelotrichaceae	Bulleidia	0.00	0.00	9.66E-03	0.00
Bacteria	Bdellovibrionota	Oligoflexia	Silvanigrellales	Silvanigrellaceae		0.00	0.00	9.66E-03	0.00
Bacteria	Planctomycetota	Planctomycetes	Planctomycetales			0.01	8.83E-03	0.014491528	0.00
Bacteria	Planctomycetota	Phycisphaerae	Phycisphaerales	Phycisphaeraceae	CL500-3	0.00	0.00	9.66E-03	0.00
Bacteria	Proteobacteria	Gammaproteobacteria	Thiomicrospirales	Thioglobaceae	Candidatus_Vesicomyosocius	0.00	0.00	9.66E-03	0.00
Bacteria	Chloroflexi	Anaerolineae	KZNMV-5-B42			0.00	0.03	7.25E-03	0.00
Bacteria	Actinobacteriota	Acidimicrobiia	Microtrichales	Microtrichaceae		0.00	0.03	0.00	0.00
Bacteria	Bacteroidota	Bacteroidia	Bacteroidales	Prolixibacteraceae	Mangrovibacterium	0.00	0.00	8.45E-03	0.00
Bacteria	Proteobacteria	Alphaproteobacteria	Elsterales	Elsteraceae	Aliidongia	0.00	0.00	8.45E-03	0.00
Bacteria	Cyanobacteria	Cyanobacteriia	Phormidesmiales	Phormidesmiaceae	Phormidium_MBIC10002	0.00	0.00	8.45E-03	0.00
Bacteria	Chloroflexi	JG30-KF-CM66				0.00	0.00	0.011	0.00
Bacteria	Proteobacteria	Alphaproteobacteria	Rhizobiales	Rhizobiales_Incertae_Sedis	Phreatobacter	0.00	0.03	0.000	0.00
Bacteria	Planctomycetota	Planctomycetes	Planctomycetales	Rubinisphaeraceae	SH-PL14	0.00	0.03	8.45E-03	0.00
Bacteria	Proteobacteria	Alphaproteobacteria	Rickettsiales	Rickettsiaceae	Rickettsia	0.00	0.03	0.00	0.00
Bacteria	Actinobacteriota	Acidimicrobiia	Microtrichales	Microtrichaceae	IMCC26207	0.00	0.03	0.00	0.00
Archaea	Halobacterota	Halobacteria	Halobacterales	Halobacteriaceae	Halocalculus	0.00	0.03	0.00	0.00

Continue...

Continued...

Bacteria	Planctomycetota	Planctomycetes	Gemmatales	Gemmataceae	Gemmata	0.00	0.00	0.01	0.00
Bacteria	Proteobacteria	Alphaproteobacteria	Rhodobacterales	Rhodobacteraceae	Nereida	0.00	8.83E-03	0.00	0.03
Bacteria	Planctomycetota	Phycisphaerae	MSBL9			0.06	0.00	0.00	0.00
Bacteria	Proteobacteria	Alphaproteobacteria	Rickettsiales	AB1		0.00	0.00	6.04E-03	0.00
Bacteria	Firmicutes	Clostridia	Oscillospirales	Oscillospiraceae	NK4A214_group	0.00	0.00	6.04E-03	0.00
Bacteria	Proteobacteria	Gammaproteobacteria	Burkholderiales	Alcaligenaceae	Ampullimonas	0.00	0.00	6.04E-03	0.00
Bacteria	Bacteroidota	Bacteroidia	Sphingobacteriales	FFCH9454		0.03	0.00	0.00	0.00
Bacteria	Proteobacteria	Gammaproteobacteria	Nitrococcales	Nitrococcaceae	Arhodomonas	0.03	0.00	0.00	0.00
Bacteria	Verrucomicrobiota	Verrucomicrobiae	Pedosphaerales	Pedosphaeraceae	SH3-11	0.00	0.018	0.00	0.02
Bacteria	Proteobacteria	Alphaproteobacteria	Holosporales	Holosporaceae	Candidatus_Bealeia	0.00	0.018	0.00	0.00
Bacteria	Patescibacteria	Microgenomatia	Candidatus_Pacebacteria			0.00	0.00	4.83E-03	0.00
Bacteria	Patescibacteria	MD2896-B216				0.00	0.00	4.83E-03	0.00
Bacteria	Planctomycetota	Planctomycetes	Isosphaerales	Isosphaeraceae		0.00	0.00	4.83E-03	0.00
Bacteria	Proteobacteria	Alphaproteobacteria	Rickettsiales	Anaplasmataceae	Candidatus_Xenolissoclinum	0.00	0.00	4.83E-03	0.00
Bacteria	Firmicutes	Clostridia	Eubacteriales	Eubacteriaceae		0.00	0.00	4.83E-03	0.00
Bacteria	Sva0485					0.00	0.00	4.83E-03	0.00
Bacteria	Myxococcota	Polyangia	Polyangiales	Amb-16S-1034		0.00	8.83E-03	0.00	0.02
Bacteria	Verrucomicrobiota	Chlamydiae	Chlamydiales	Simkaniaceae		0.00	0.00	0.00	0.02
Bacteria	Acidobacteriota	Acidobacteriae	Acidobacteriae_or	Acidobacteriae_fa	Paludibaculum	0.00	0.00	0.00	0.02
Bacteria	Chloroflexi	Anaerolineae	Anaerolineales	Anaerolineaceae	Anaerolinea	0.02	0.00	2.42E-03	0.00
Bacteria	Actinobacteriota	Actinobacteria				0.02	0.00	0.00	0.00
Bacteria	Proteobacteria	Gammaproteobacteria	Ectothiorhodospirales	Ectothiorhodospiraceae	Thiohalospira	0.00	0.01	0.00	0.00
Bacteria	Firmicutes	Bacilli	Thermoactinomycetales	Thermoactinomycetaceae	Risungbinella	0.00	0.01	0.00	0.00
Bacteria	Firmicutes	Bacilli	Paenibacillales	Paenibacillaceae	Oxalophagus	0.00	0.01	0.00	0.00
Bacteria	Proteobacteria	Gammaproteobacteria	Burkholderiales	Rhodocyclaceae	Niveibacterium	0.00	0.01	0.00	0.00
Bacteria	Proteobacteria	Gammaproteobacteria	Diplorickettsiales	Diplorickettsiaceae		0.00	0.01	0.00	0.00
Archaea	Crenarchaeota	Thermoprotei	Desulfurococcales	Desulfurococcaceae	Thermosphaera	0.00	0.00	3.62E-03	0.00
Bacteria	Planctomycetota	BD7-11				0.00	0.00	3.62E-03	0.00
Bacteria	Verrucomicrobiota	Verrucomicrobiae	Opitutales	Opitutaceae	Ereboglobus	0.00	0.00	3.62E-03	0.00
Bacteria	Armatimonadota					0.00	0.00	3.62E-03	0.00
Bacteria	Proteobacteria	Gammaproteobacteria	Oceanospirillales	Halomonadaceae	HdN1	0.00	0.00	3.62E-03	0.00
Bacteria	Proteobacteria	Gammaproteobacteria	Legionellales	Legionellaceae		0.00	0.00	3.62E-03	0.00
Bacteria	Proteobacteria	Alphaproteobacteria	Rhizobiales	Xanthobacteraceae	Variibacter	0.00	0.00	3.62E-03	0.00
Archaea	Crenarchaeota	Nitrososphaeria	Nitrososphaerales	Nitrososphaeraceae	Candidatus_Nitrocosmicus	0.00	0.00	0.00	0.02
Bacteria	Actinobacteriota	Acidimicrobiia	Acidimicrobiales	Acidimicrobiaceae	Ferrimicrobium	0.00	0.00	0.00	0.02
Bacteria	Firmicutes	Thermovenabulia	Thermovenabulales	Thermovenabulales_fa	Fervidicola	0.00	0.00	0.00	0.02
Bacteria	Proteobacteria	Gammaproteobacteria	Enterobacterales	Enterobacteriaceae	Escherichia/Shigella	0.01	0.00	0.00	0.00
Bacteria	Proteobacteria	Gammaproteobacteria	Xanthomonadales	Rhodanobacteraceae	Pseudofulvimonas	0.00	8.83E-03	0.00	0.00
Bacteria	Firmicutes	Clostridia	Clostridia_or	Hungateiclostridiaceae	Ruminiclostridium	0.00	8.83E-03	0.00	0.00

Continue...

Continued...

Bacteria	Proteobacteria	Alphaproteobacteria	Elsterales			0.00	0.00	2.42E-03	0.00
Bacteria	Actinobacteriota	Acidimicrobiia	Acidimicrobiales	Acidimicrobiaceae		0.00	0.00	2.42E-03	0.00
Bacteria	Verrucomicrobiota	Verrucomicrobiae	Opitutales	Opitutaceae	Lacunisphaera	0.00	0.00	0.00	0.01
Bacteria	Acidobacteriota	Subgroup_11				0.00	0.00	0.00	0.01
Bacteria	Planctomycetota	Phycisphaerae	Phycisphaerales	Phycisphaeraceae	I-8	0.00	0.00	0.00	0.01
Bacteria	Verrucomicrobiota	Verrucomicrobiae	Pedosphaerales	Pedosphaeraceae	Ellin517	0.00	0.00	0.00	0.01
Bacteria	Myxococcota	Polyangia	UASB-TL25			0.00	0.00	0.00	0.01
Bacteria	Proteobacteria	Gammaproteobacteria	Burkholderiales	Nitrosomonadaceae	cr616	0.00	0.00	0.00	0.01
Bacteria	Bacteroidota	Bacteroidia	Flavobacteriales	Flavobacteriaceae	Croceibacter	0.00	0.00	0.00	0.01

Ambiente & Água - An Interdisciplinary Journal of Applied Science
ISSN 1980-993X – doi:10.4136/1980-993X
www.ambi-agua.net
E-mail: ambi.agua@gmail.com

Surveillance of public water supply fluoridation and municipal indicators: an analysis in the state of Espirito Santo, Brazil

ARTICLES doi:10.4136/ambi-agua.2693

Received: 11 Jan. 2021; Accepted: 03 May 2021

Ariane Mendonça[1*]; Katrini Guidolini Martinelli[2]; Carolina Dutra Degli Esposti[2]; Lorrayne Belotti[3]; Karina Tonini dos Santos Pacheco[4]

[1]Departamento de Medicina Social. Programa de Pós-Graduação em Clínica Odontológica. Universidade Federal do Espírito Santo (UFES), Avenida Marechal Campos, n°1468, CEP: 29047-105, Vitória, ES, Brazil.
[2]Departamento de Medicina Social. Programa de Pós-Graduação em Saúde Coletiva. Universidade Federal do Espírito Santo (UFES), Avenida Marechal Campos, n°1468, CEP: 29047-105, Vitória, ES, Brazil. E-mail: katrigm@gmail.com, carolinaesposti@gmail.com
[3]Programa de Pós-Graduação em Saúde Pública. Faculdade de Saúde Pública. Universidade de São Paulo (USP), Avenida Doutor Arnaldo, n°715, CEP: 01246-904, São Paulo, SP, Brazil. E-mail: lorraynebelotti@usp.br
[4]Programa de Pós- Graduação em Ciências Odontológicas. Universidade Federal do Espírito Santo (UFES), Avenida Marechal Campos, n°1468, CEP: 29047-105, Vitória, ES, Brazil. E-mail: kktonini@yahoo.com.br
[*]Corresponding author. E-mail: arianemend@gmail.com

ABSTRACT

This study investigated the demographic, socioeconomic, and municipal health indicators related to the quality of water fluoridation. An ecological study was carried out in Espirito Santo state (ES), based on data from the Drinking Water Quality Surveillance Information, from 2014 to 2017. The non-parametric *Mann-Whitney* and *Spearman* tests were applied to compare municipal indicators with the availability of information and the quality of fluoridation, respectively. Fluoridation quality was calculated to define the percentage of fluoride concentration values in each municipality within the range of the optimal level corresponding to the maximum benefit for preventing dental caries and minimum risk for the occurrence of dental fluorosis. The proportion of 80% or more samples were defined as a compliance criterion. In 2014, 62.8% of the municipalities had information available, and 16.7% performed analyses of fluoride concentration. The percentage of available data increased about 30%, in 2017, with 3.8% referring to fluoride. The quality of fluoridation remained high (> 80%) in ES in almost every year, except in 2014. The municipalities with the largest population, the highest GDP per capita, and the lowest coverage of the oral health team exhibited a greater availability of information about fluoride ($p < 0.05$). The child mortality rate showed a strong negative correlation with the quality of fluoridation. The findings reinforce the importance of directing public policies that ensure the correct practices for monitoring and maintaining the quality of fluoridation.

Keywords: development indicators, environmental health surveillance, fluoridation.

This is an Open Access article distributed under the terms of the Creative Commons Attribution License, which permits unrestricted use, distribution, and reproduction in any medium, provided the original work is properly cited.

Vigilância da fluoretação da água de abastecimento público e indicadores municipais: uma análise no estado do Espírito Santo, Brasil

RESUMO

O objetivo foi investigar os indicadores demográficos, socioeconômicos e de saúde municipais relacionados à qualidade da fluoretação da água. Estudo ecológico que abrangeu municípios do estado do Espirito Santo (ES), com base em dados Sistema de Informação de Vigilância da Qualidade da Água para Consumo Humano, no período de 2014 a 2017. Foram aplicados testes não paramétricos de Mann-Whitney e Spearman para comparar indicadores municipais com a disponibilidade de informação e a qualidade da fluoretação, respectivamente. A qualidade da fluoretação foi calculada para definir o percentual de valores de concentração de flúor dentro da faixa do nível ótimo correspondente ao máximo benefício e baixo risco para ocorrência de fluorose dentária. A proporção de 80% ou mais amostras foi definida como critério de conformidade. Em 2014, 62,8% dos municípios possuíam informações disponíveis no sistema, e 16,7% realizaram análises de concentração de flúor. O percentual de dados disponíveis aumentou cerca de 30%, em 2017, sendo que 3,8% foram referentes ao fluoreto. A qualidade da fluoretação manteve-se elevada (>80%) no ES em quase todos os anos, exceto em 2014. Os municípios com maior população, maior PIB per capita e menor cobertura de equipe de saúde bucal apresentaram maior disponibilidade de informações sobre o fluoreto ($p<0,05$). A taxa de mortalidade infantil apresentou forte correlação negativa com a qualidade da fluoretação. Os resultados encontrados reforçam a importância do direcionamento de políticas públicas que garantam a correta execução das atividades de monitoramento e manutenção da qualidade da fluoretação.

Palavras-chave: fluoretação da água, indicadores de desenvolvimento, vigilância sanitária ambiental.

1. INTRODUCTION

The fluoridation of public water supply is one of the most important measures of comprehensive coverage in public health, being recognized and recommended by the main World Health Organizations (Petersen, 2003). Since its implementation, surveys have shown that water fluoridation is effective at reducing the caries levels in both deciduous and permanent dentition in children (Iheozor-Ejiofor *et al.* 2015). Moreover, depending on the extent of the water supply system, it can reduce social inequality in access to fluoride and benefit the entire population, especially the most vulnerable (Slade *et al.*, 2018; Spencer *et al.*, 2018). Despite the control by the sanitation companies, some studies reinforce that the wide variation in fluoride levels in public water supply fluoridation, the relationship between inadequate levels and the interruption of the process and the rate of dental fluorosis, showing that it is necessary to implement surveillance systems by public institutions (Frazão *et al.*, 2013; Scalize *et al.*, 2018).

In Brazil, water quality control for human consumption was made a public responsibility action in 1977 by the passage of Federal Decree nº 79.367, through Ordinance nº 56 of the Ministry of Health. However, it was only at the end of the 1990s that the National Water Quality Surveillance Program for Human Consumption (Vigiagua) was created, which consists of the set of actions adopted to ensure the control and quality of the water consumed by the population. In order to assist in the management of information, the Drinking Water Quality Surveillance Information System (Sisagua) was developed, systematizing the data routinely generated by professionals in the health sector and those responsible for water supply services (Brasil, 2018).

As a way to ensure the quality and effectiveness of water fluoridation, it is necessary not only to monitor the appropriate levels within the recommended range for each region, but to systematize this information in order to establish priorities, objectives and targets. In a study by Frazão *et al.* (2013), given the information registered in Sisagua, it was found that about half of the Brazilian municipalities (50.4%) were not registered, and 12.3%, although registered, did not feed the system at least four times a year. In the Southeast region, more than 50% of the municipalities in the state of Rio de Janeiro and São Paulo were not registered in Sisagua; however, in Espirito Santo (ES) the percentage was lower, around 26%. In addition to the registration and feeding failures, studies indicate the large number of non-standard samples, the absence of collections, analysis and disclosure of fluoride levels, revealing a possible inadequacy in the fluoridation process and failure of the responsible surveillance (Venturini *et al.*, 2016).

In order to improve the quality of available data and the development of surveillance actions on the fluoridation of public water supply in Brazil, the Vigifluor Project, developed through a partnership between the Collaborating Center of the Ministry of Health in Oral Health Surveillance (CECOL) and specialists in the areas of health surveillance, mapped the coverage of fluoridation of public water supply in municipalities with more than 50 thousand inhabitants and also identified the lack of information on the fluoridation of water supply (Frazão and Narvai, 2017a).

Some municipality-level characteristics, such as population size, per capita income, type of sanitation utility, water supply coverage, and human development index have been associated with both the quality of fluoridation and its process expansion and monitoring (Belotti *et al.* 2020; 2018; Frazão and Narvai, 2017b). Knowing that communities and countries with inadequate fluoridation processes have a higher risk of developing caries disease in their population, it is necessary to understand the relationship between municipal indicators and the fluoridation of public water supply as a way to validate the processes already implemented, identify possible problems and suggest changes aimed at water quality surveillance and, consequently, health promotion.

This study therefore investigated the demographic, socioeconomic, and municipal health indicators related to the quality of water fluoridation, which also includes the availability of information, in Espirito Santo state, Brazil.

2. MATERIALS AND METHODS

An ecological study was conducted based on the data regarding the fluoridation of public water supply and municipal demographic, socioeconomic and health indicators in the state of Espirito Santo (ES) from 2014 to 2017. The period was selected according to the availability of data and Version 4 of Sisagua. Located in the Southeast region of Brazil, the state is composed of 78 municipalities distributed among the health regions: Metropolitan; Central; North and South. The population is about 4,016,356. According to data from the National Survey of Basic Sanitation, all 78 municipalities in ES have piped and treated water (IBGE, 2017). Of the total population, 96.45% live in households with running water (PNUD, 2010). According to data from the CECOL website, in 2016 100% of the population of the capital Vitória had treated and fluoridated water.

Data related to external control of fluoridation were collected in the surveillance system (Sisagua) by an author. Considering the average maximum temperature in the state of ES, the criterion proposed by CECOL/USP (2011) was used to classify the fluoride concentration present in the samples according to the benefit in preventing caries and risk of dental fluorosis. This criterion is divided into six categories: insignificant benefit and risk (0.00 to 0.44 mg F/L); minimal benefit and low risk (0.45 to 0.54 mg F/L); maximum benefit and low risk (0.55 to 0.84 mg F/L); maximum benefit and moderate risk (0.85 to 1.14 mg F/L); questionable benefit

and high risk (1.15 to 1.44 mg F/L); and harmfulness and very high risk (1.45 mg F/L or more).

The Fluoridation Quality Level (FQL) was calculated according to Belotti *et al.* (2018) Equation 1:

$$FQL = \frac{No.of\ suitable\ samples\ (0.55 \leq T_{fluoride} \leq 0.84)}{Total\ number\ of\ samples\ (n)}\ x\ 100 \quad (1)$$

To estimate the quality of water fluoridation, the proportion of 80% or more samples was defined as a high level of quality (Pelletier, 2004). Considering that the control and quality of fluoridation can be assessed using some demographic, socioeconomic and municipal health indicators, the following indicators were selected from official sources and according to the years surveyed or the last census carried out:

- Total population: the availability of treated and fluoridated water tends to be higher in municipalities with a larger population size (Roncalli *et al.*, 2019; Belotti *et al.*, 2020).

- Gross Domestic Product (GDP) *per capita:* municipalities with better economic indicators can be associated with a better quality of fluoridation (Belotti *et al.*, 2020).

- Gini Index (0 to 1): the lack of registration and food in the Sisagua system has been associated with municipalities with the worst social and economic indicators (Frazão *et al.*, 2013)

- Municipal Human Development Index (MHDI): an index that assesses the quality of life and economic development of a population (UNDP, 2010), being able to detect the risk of mortality, the quality of the water offered and, consequently, life expectancy, through basic sanitation and economy (Frazão and Narvai, 2017b).

- Percentage of the population in households with running water: this indicator directly influences access to fluoridated water, limiting this portion of the population to enjoy the benefits of fluoridation.

- Child mortality rate: it is considered a universal indicator in studies that analyze issues that affect the basic sanitation of the population, mainly in children up to 1 year old, as they are more sensitive to several pathologies (Carvalho *et al.*, 2015)

- Hospitalization rates due to diarrhea: the occurrence of diarrhea is linked to access to treated water and environmental sanitation (WHO, 2009). The contamination of the water supplied by the public supply network reveals a flaw in its external control, reflecting the presence of possible irregularities in the control of the fluoride parameter.

- Coverage by oral health teams (COHT): indicator established based on the organization and structuring of the health system (Fernandes and Peres, 2005), attributing a possible correlation between the municipalities with better coverage and the quality of water fluoridation.

- Percentage of extractions in relation to the total of dental procedures: the increase in the number of mutilating procedures may serve as a warning for the presence of possible flaws in the external control of water fluoridation, considering that the decline in the values of the DMFT index (index of decayed, missing and filled teeth) is related to cities that have fluoridated water (Belotti *et al.*, 2018).

- Average of supervised tooth brushing: it is considered one of the priorities of the National Oral Health Policy, aiming at the prevention of oral diseases, mainly dental caries (Brasil, 2004), thus being an indicator of the effectiveness in the offer of public policies aimed at oral health.

Descriptive analyses were performed by calculating absolute and relative frequencies for qualitative variables, and median and interquartile distance for quantitative variables. To analyze the association between municipal indicators and the control of available data regarding fluoridation (municipalities with and without recorded data, at least one month of the year), the Mann-Whitney nonparametric test was performed (comparison of medians), with p-value ≤

0.05 and 95% confidence interval, as the data did not present a normal distribution. Considering only the municipalities that fed the system with fluoridation data in some of the years studied, the nonparametric Spearman test was performed to analyze the correlation between municipal indicators and the quality of fluoridation (FQL). P-value ≤ 0.05 and 95% confidence interval were also used. The data were stored in the program *Statistical Package for the Social Sciences* (SPSS), Version 20.0.

3. RESULTS AND DISCUSSION

Analyzing the availability of information regarding the external control of public water supply in 2014, of the 78 municipalities that make up the state of ES, only 49 (62.8%) recorded data related to the analysis of public water supply in the Sisagua, of which only 13 (16.7%) had data on the fluoride parameter. In 2017, the number of municipalities with available data increased to 72 (92.3%); however, only 16 (20.5%) analyzed fluoride concentration. The Metropolitan region had the highest number of municipalities with data records between the years 2014 (60.0%) and 2017 (80%). On the other hand, the Central, North and South regions did not provide data on fluoridation control for most of the period analyzed. Among the samples with analysis of the fluoride concentration, in all the state, the percentage of the samples with content considered: (a) "adequate" - ranged from 70.7% to 87.6%; (b) "inadequate" - below ranged from 5.1% to 23.6%; and (c) "inadequate" - above ranged from 1.0% to 7.3% (Table 1).

Table 1. Distribution of available data on the external control and of the quality of fluoridation in the municipalities of Espirito Santo in the period from 2014 to 2017.

	2014 n (%)	2015 n (%)	2016 n (%)	2017 n (%)
Available data (n=78)				
Control of public water supply	49 (62.8)	73 (93.6)	68 (87.2)	72 (92.3)
Control of fluoride parameter	13 (16.7)	16 (20.5)	15 (19.2)	16 (20.5)
Fluoridation data by health region (n)				
Metropolitan (20)	12 (60.0)	16 (80.0)	15 (75.0)	16 (80.0)
Central (18)	0 (0.0)	0 (0.0)	0 (0.0)	0 (0.0)
North (14)	01 (7.1)	0 (0.0)	0 (0.0)	0 (0.0)
South (26)	0 (0.0)	0 (0.0)	0 (0.0)	0 (0.0)
Quality of fluoridation				
Total samples with [ ] of fluoride	692	1.177	1.308	713
[ ] Inadequate Below	163 (23.6)	60 (5.1)	105 (8.0)	93 (13.0)
[ ] Adequate	489 (70.7)	1.031 (87.6)	1.155 (88.3)	613 (86.0)
[ ] Inadequate Above	40 (5.8)	86 (7.3)	48 (3.7)	07 (1.0)

Note: [ ] concentration; [ ] inadequate below: 0 to 0.54 mg F/L; [ ] adequate: 0.55 to 0.84 mg F/L; [ ] inadequate above: equal to or greater than 0.85 mg F/L.

Considering only the municipalities that performed the analysis of the fluoride concentration in any year surveyed, the sampling plan (minimum recommended number of samples to be analyzed in the fluoride parameter) was compared with the number of samples in which included an analysis of fluoride concentration. None of these municipalities analyzed the minimum number of samples in all consecutive years. More than half of the municipalities that performed an analysis of the fluoride concentration had the quality level of fluoridation equal

to or above 80%, indicating a high level of quality, except in 2014 (Table 2).

In this study, there was a significant increase (almost 30%) in the registration of data in Sisagua regarding the water supply surveillance between 2014 and 2017. Even so, the analysis of the fluoride parameter was reduced, presenting an increase of only 3.8% in the years surveyed. The lack of analysis of the fluoride parameter in a municipality in the state of ES was also reported by Belotti *et al.* (2019) through an interview with water surveillance system workers. Roncalli *et al.* (2019), assessing municipalities with more than 50 thousand inhabitants in Brazil, observed a significant improvement in the registration of data on external control of water in the surveillance information system; however, the percentage of data referring to the analysis of the fluoride parameter was still deficient.

Table 2. Numerical and percentage distribution of the annual sampling plan, the number of samples with analysis of fluoride concentration and the number of samples considered adequate (according to classification criteria CECOL/USP) by municipality in the state of ES, in the period from 2014 to 2017.

Municipalities	S.P (n)	2014		2015		2016		2017	
		S.A (n)	FQL (%)	S.A (n)	FQL (%)	S.A (n)	FQL (%)	S.A (n)	FQL (%)
Afonso Claudio	60	*	*	*	*	4	100	18	22.2
Brejetuba	60	8	100	8	100	12	100	2	100
Cariacica	156	*	*	1	100	86	80.2	54	85.2
Conceição do Castelo	60	16	75.0	37	91.9	40	95.0	15	93.3
Domingos Martins	60	16	37.5	54	70.4	9	66.7	6	33.3
Fundão	60	*	*	*	*	30	93.3	30	90.0
Guarapari	108	81	90.1	204	90.2	207	89.9	107	93.5
Ibatiba	60	20	75.0	54	88.9	35	94.3	22	81.8
Itaguaçu	60	*	*	31	54.8	*	*	5	100
Itarana	60	23	73.9	56	73.2	51	66.7	25	52.0
Laranja da Terra	60	11	100	3	66.7	*	*	*	*
Santa Maria de Jetibá	60	2	100	9	100	71	91.5	30	90.0
Santa Teresa	60	*	*	8	100	*	*	*	*
São Mateus	108	132	11.4	*	*	*	*	*	*
Serra	156	134	89.6	214	88.8	208	92.8	105	82.9
Venda Nova do Imigrante	60	20	100	37	100	20	90.0	23	95.7
Viana	84	*	*	2	100	35	80.0	15	73.3
Vila Velha	156	85	71.8	208	90.9	227	85.0	83	84.5
Vitória	156	144	89.6	251	88.8	273	90.8	173	94.8

Note: S.P: Sampling Plan according to Brasil (2014); S.A: Samples Analyzed; FQL: Fluoridation Quality Level
*No information available.

Considering the availability of data by health region, only the municipalities in the Metropolitan health region maintained greater regularity in recording external control of fluoridation in Sisagua. The result can be justified by the high number of smaller municipalities in the other health regions of ES, revealing the influence of demographic, socioeconomic and health inequality in different regions in the same state and the success of the activities developed by the surveillance sector, in which less-developed regions face greater difficulties in carrying out all actions relevant to the water quality and control program. When investigating the

perception of professionals in the sector responsible for the Vigiagua program in a small municipality, Queiroz *et al.* (2012) identified that, although there was a record of the data, no analysis or planning of this information was carried out, which demonstrates the difficulty of political organization in these regions.

Even with the better control of information in Sisagua found in this research, workers responsible for the Vigiagua Program in some municipalities that make up the Metropolitan health region also reported difficulties faced in the daily life of the sector, such as work overload, lack of initial training related to the activities of the water surveillance program, deficiency and structural limitation of the sector itself, lack of inputs in the laboratory responsible for the analyses and delay in the reports. The lack of disclosure of the results obtained through the external control process was also pointed out, showing an important non-compliance with the legislation (Belotti *et al.*, 2019).

The quality level of fluoridation in the state of ES was considered high in almost all the years surveyed. Belotti *et al.* (2018) reported optimal fluoride levels in the metropolitan region of Great Vitória, where, despite some irregularities, the quality standard remained high. Other studies that analyzed the quality of fluoridation using the classification criteria for maximum benefit and low risk found results similar to those of this research, considering the same concentration range as appropriate (Buzalaf *et al.*, 2013; Bergamo *et al.*, 2015).

Among the samples in noncompliance with the ideal standard, most of them were below the fluoride dosage suitable for the state of ES. The prevalence of samples with concentrations below those recommended by the current legislation and by CECOL was also identified in other studies (Brito *et al.*, 2016; Scalize *et al.* 2018). In view of the precarious access of a large part of the population to other preventive methods and dental treatment, which is still present today, the absence or insufficient levels of fluoride in public water supply directly affect low-income populations (Alves *et al.*, 2012).

Although the information was recorded in the system, the results found in this research may not reflect the quality of fluoridation offered to the population of ES, given the reduced number of samples with analysis of fluoride concentration. Among the municipalities with data on fluoridation, less than half analyzed the minimum number of samples established annually, indicating noncompliance with the legislation. It is worth mentioning that the sampling plan is defined by the municipalities in accordance with the National Guidelines for the Vigiagua Sampling Plan. This analysis is done on a preventive basis in order to maintain quality and avoid the inherent risks of fluoridation (Brasil, 2018).

In a report released by the Ministry of Health based on data recorded in Sisagua, amounts of samples analyzed by surveillance in the state of ES in 2018 were also found, below the number recommended by the National Directive for the residual parameters of the infectious agent, turbidity and fecal coliforms, in which 53%, 68.1% and 96.6%, respectively, of the total mandatory samples were analyzed (Brasil, 2018). Oliveira Junior *et al.* (2019), exploiting the surveillance system, also identified the quantity of water monitoring data for human consumption lower than that established by the sampling plan of Vigiagua, both in the information relevant to the sanitation company (control) and the surveillance (external control).

The complexity of the water distribution network, the difficulties in transporting the collected samples, the insufficient capacity and the deficiency in the structure of the analysis laboratories are some factors that can contribute to the inadequacy of the operationalization of the method and, consequently, to the achievement of the sampling plan. Other factors related to the unavailability of financial resources, difficulty in maintaining adequate fluoride content due to the small range of recommendation and deficiency in the training of sanitation professionals responsible for fluoridation are also pointed out as difficulties that directly impact control and maintenance of adequate fluorine content and even the systematization of data generated by surveillance (Cesa *et al.*, 2011; Moimaz *et al.*, 2015). However, in order to

guarantee the effectiveness (protection against dental caries) and safety (avoidance of risk of dental fluorosis) of fluoridation, it is necessary that the responsible public authority ensures not only the addition of fluoride but the adequacy of the added concentration levels (Piorunneck *et al.*, 2017).

The availability, access and use of data produced by the surveillance in addition to sharing this data with the public water supply companies responsible for the distribution of water are of extreme importance for decision making in the health sector in structuring and expansion, not only of fluoridation, but of all aspects related to water quality throughout the country. Furthermore, since these data are available, it contributes to the evaluation of the performance of the actions developed by the surveillance and sanitation companies in the possible challenges faced by the sector and in the development of new activities, aiming to guarantee the maintenance of the positive effects of fluoridation.

The association between the availability of data and the municipal indicators revealed that the coverage of the oral health team showed a statistically significant result ($p \leq 0.05$) in all years of the research, indicating that the municipalities with unavailability fluoridation data had a higher median ESB coverage. In 2016, the Gross Domestic Product showed a statistically significant result ($p \leq 0.05$), which reveals that the municipalities with available data on fluoridation had a higher GDP. The total population indicator also showed a statistically significant result ($p \leq 0.05$) for the years 2016 and 2017, indicating that the municipalities with available data on fluoridation had larger populations (Table 3).

The association between greater coverage of the oral health team and the absence of recorded fluoridation data could be explained because, in this study only the metropolitan health region, which comprises a large part of the municipalities with the largest total population, showed these data. In general, large municipalities tend to have less coverage of oral health teams than those with smaller populations (Fischer *et al.*, 2010). It is recognized that the benefits derived from better management of water resources occur much more quickly in large urban centers and metropolitan regions, where the highest levels of income and the greatest technical and business training are concentrated (Tucci *et al.*, 2000).

These statements were reinforced, since the availability of data on fluoridation was associated with more populous and higher GDP municipalities in the state of ES. This finding highlights that the effectiveness of the surveillance information system in the fluoride parameter is unequal and could be related to the better municipal conditions of the structure, organization, and human resources in the water quality control program. Frazão *et al.* (2013) identified the association between underfeeding and lack of registration in Sisagua with smaller municipalities and with worse economic, health and human development indicators nationwide.

According to the Inventory of the National Water Quality Surveillance Program for Human Consumption, some municipalities in the state of Acre, without data recorded in the surveillance system, reported the following difficulties: not having health surveillance actions, unavailability of internet and computers for registration of data generated by Vigiagua and lack of knowledge of the water surveillance program (Brasil, 2018). The reduced number of collaborators in the health surveillance team can interfere in the accomplishment of the activities of collecting and feeding the database, given the possible overload of functions that apply in carrying out all the actions inherent to the responsible sector, the low valuation of the professional and high turnover in teams, contributing to possible failures during the planning and analysis processes of the information generated (Campos *et al.*, 2015; Belotti *et al.* 2019).

When correlating the quality of fluoridation with municipal indicators, only the child mortality rate in 2014 showed a statistically significant result ($p < 0.001$), revealing a strong negative correlation, that is, the lower the percentage of suitable samples, the higher the child mortality rate (Table 4).

Table 3. Association between municipal indicators and the availability of data on the external control of fluoridation of public water supply in the state of ES, from 2014 to 2017.

Municipal Indicators	Available Median (P25-P75)	Unavailable Median (P25-P75)	P- value*
		2014	
Total Population (2014)	34,239 (12,692.5–237,386)	16,946 (12,057–29,920)	0.224
GDP (2014)	16,290.06 (14,674.9-25,152.0)	15,306.40 (11,449.2-20,305.6)	0.252
Gini Index (2010)	0.50 (0.48-0.57)	0.50 (0.49-0.53)	0.421
MHDI (2010)	0.68 (0.66-0.73)	0.68 (0.67-0.71)	0.365
% Piped Water (2010)	91.28 (87.42-98.18)	94.81 (90.93-96.95)	0.722
Child Mortality Rate (2014)	10.47 (7.73-12.64)	11.04 (7.87-18.65)	0.446
Hospitalization rates due to diarrhea (2014)	4.39 (0.90-13.94)	6.90 (0.20-24.13)	0.920
COHT (2014)	48.19 (20.15-65.14)	76.20 (51.23-99.59)	**0.018**
% of Tooth Extractions in relation to Dental Procedures (2014)	2.89 (1.96-5.14)	3.80 (2.85-6.14)	0.116
Average of Supervised Tooth Brushing (2014)	1.65 (1.00-8.27)	1.36 (0.38-4.05)	0.202
		2015	
Total Population (2015)	29,830 (13,281.75-296,856.75)	17,965.5 (11,987.75–30,795.50)	0.161
GDP (2015)	17,628.25 (14,920.2-24,076.6)	16,481.13 (12,566.7-20,112.9)	0.190
Gini Index (2010)	0.49 (0.47-0.53)	0.51 (0.49-0.53)	0.331
MHDI (2010)	0.69 (0.67-0.73)	0.68 (0.66-0.71)	0.287
% Piped Water (2010)	91.65 (88.29-98.63)	94.82 (90.80-96.93)	0.805
Child Mortality Rate (2015)	10.41 (9.04-15.56)	12.19 (7.87-16.43)	0.904
Hospitalization rates due to diarrhea (2015)	3.66 (1.17-10.74)	7.43 (0.23-24.25)	0.675
COHT (2015)	53.30 (17.41-82.94)	77.87 (55.19-97.57)	**0.050**
% of Tooth Extractions in relation to Dental Procedures (2015)	3.60 (2.37-5.86)	4.37 (3.06-5.98)	0.366
Average of Supervised Tooth Brushing (2015)	1.60 (0.48-2.51)	1.54 (0.27-3.97)	0.963

Continue...

Continued...			
		2016	
Total Population (2016)	34,589 (20,376–359,555)	16,339 (11,957-29,743)	**0.003**
GDP (2016)	19,826.5 (17,124.8-26,483.8)	16,574.3 (14,302.8-20,763.8)	**0.026**
Gini Index (2010)	0.50 (0.47-0.53)	0.50 (0.49-0.53)	0.909
MHDI (2010)	0.69 (0.67-0.73)	0.68 (0.66-0.71)	0.264
% Piped Water (2010)	92.73 (87.72-99.07)	94.18 (90.84-96.91)	0.884
Child Mortality Rate (2016)	10.25 (8.98-14.70)	12.52 (9.85-16.00)	0.262
Hospitalization rates due to diarrhea (2016)	5.97 (0.93-12.70)	4.49 (0.29-18.11)	0.960
COHT (2016)	46.88 (20.16-52.76)	77.97 (55.83-96.43)	**0.001**
% of Tooth Extractions in relation to Dental Procedures (2016)	3.87 (2.85-6.15)	4.84 (2.93-7.19)	0.385
Average of Supervised Tooth Brushing (2016)	1.65 (0.27-2.73)	0.49 (0.02-2.13)	0.149
		2017	
Total Population (2017)	33,559 (16,300.5–303,146.5)	16,856.5 (11,870.75–30,222.25)	**0.006**
GDP (2017)	20,322.5 (16,487.8-26,809.5)	17,023.5 (14,144.8-20,923.9)	0.054
Gini Index (2010)	0.49 (0.47-0.53)	0.50 (0.49-0.53)	0.573
MHDI (2010)	0.69 (0.67-0.73)	0.68 (0.66-0.71)	0.225
% Piped Water (2010)	92.38 (88.00-98.63)	94.49 (90.80-96.93)	1.000
Child Mortality Rate (2017)	8.93 (5.93-10.81)	10.60 (5.10-15.69)	0.400
Hospitalization rates due to diarrhea (2017)	3.63 (0.63-10.55)	3.39 (0.00-17.80)	0.951
COHT (2017)	39.78 (19.79-59.86)	76.28 (51.86-95.33)	**0.002**
% of Tooth Extractions in relation to Dental Procedures (2017)	4.19 (2.57-6.39)	4.06 (2.67-6.31)	0.975
Average of Supervised Tooth Brushing (2017)	0.46 (0.02-1.64)	0.16 (0.00-1.21)	0.500

*Mann-Whitney Test: Bold indicates significance on the 95% confidence limit.
a- 2014: available (13), unavailable (65); b- 2015 and 2017: available (16), unavailable (62); c- 2016: available (15), Unavailable (63)

Table 4. Correlation between municipal indicators and the percentage of samples suitable for fluoride concentration (according to CECOL/USP classification criteria) in the state of ES, in the period from 2014 to 2017.

Municipal Indicators	2014 r (p-valor)	2015 r (p-valor)	2016 r (p-valor)	2017 r (p-valor)
Total Population	-.251 (0.408)	.213 (0.429)	-.302 (0.274)	-.252 (0.347)
GDP	-.017 (0.957)	.337 (0.202)	-.324 (0.240)	-.018 (0.948)
Gini Index	-.003 (0.993)	.310 (0.243)	.218 (0.435)	.231 (0.389)
MHDI	-.232 (0.446)	.170 (0.529)	-.369 (0.177)	.179 (0.507)
% Piped Water	-.344 (0.250)	.026 (0.923)	-.461 (0.084)	-.008 (0.976)
Child Mortality Rate	**-.900** **(< 0.001)**	.072 (0.799)	.026 (0.929)	0.339 (0.199)
Hospitalization rates due to diarrhea	.215 (0.502)	.024 (0.934)	.203 (0.527)	-.190 (0.535)
COHT	.493 (0.087)	-.133 (0.623)	.071 (0.800)	-.021 (0.940)
Percentage of Tooth Extractions in relation to Dental Procedures	-.218 (0.475)	-.379 (0.148)	-.057 (0.839)	-.208 (0.440)
Average of supervised tooth brushing	.276 (0.361)	.085 (0.756)	-.239 (0.390)	-.246 (0.357)

The child mortality rate is considered an important indicator in public health, being widely used to analyze the level of health and quality of life in different regions, due to the sensitivity of the child population to different pathologies and environmental factors. This rate could reflect the quality of water supply and sewage in health (Carvalho *et al.*, 2015). In this study, the correlation found between the child mortality rate and the quality of fluoridation, only in the year 2014, can be justified by the greater number of samples considered inadequate in the same year, when compared to the following years surveyed. It suggests that regions with higher values of this index have possible irregularities in the quality of public water supply. The relationship between the quality of fluoridation and the child mortality rate was also found in the study by Belotti *et al.* (2018), undertaken in the Grande Vitória Metropolitan Region.

The limitations relevant to this study correspond to the lack of data available by most municipalities in the surveillance system. During the bibliographic survey process, a small number of studies were identified with analysis of data generated specifically by Sisagua, not only in the state of Espirito Santo, but also in Brazil, revealing an important research gap regarding the analysis of the surveillance organization due to the external control of fluoridation of public water supply.

The absence of data regarding external control of water points to a major failure in the surveillance of some municipalities and the need for improvements in the water quality and control program, as a way to assist in the correct interpretation of the data generated and in the prioritization of strategies aimed at the surveillance of water, thus ensuring the achievement of the purpose for which Sisagua sets out. It should be noted that the methodology used in this research can be reproduced in all regions of the country and even in other countries, analyzing not only the fluoride parameter, but also taking into account other parameters recommended by sanitation programs around the world.

For fluoridation to be able to actually exercise its role as a social measure, greater investments are needed in technical, human and financial resources in the sector responsible for monitoring water for human consumption. However, for this to happen, the interest not only of

political representatives, public servants and managers of water supply companies, but also of the community itself is extremely important, guaranteeing better quality of life.

4. CONCLUSION

The state of Espirito Santo showed a significant improvement with regard to the registration of data generated by surveillance due to the monitoring of public water supply. However, the number of municipalities that performed analysis of the fluoride concentration is still small and is concentrated almost entirely in the metropolitan region of health. Considering the quality of fluoridation, the level remained high; however, no municipality complied with the sampling plan in all years. The results exhibited that the larger the total population and the coverage of the oral health team, the higher the record of the system data. On the other hand, regarding the quality of fluoridation, the municipalities with the higher infant mortality rate showed lowest quality. This reinforces the importance of directing public policies that ensure the correct execution of activities aimed at monitoring fluoridation, in addition to encouraging research that analyzes not only the implementation but the maintenance of the quality of the fluoride parameter through social determinants as a way to reduce inequalities and guarantee access and use of services in an egalitarian way.

5. ACKNOWLEDGMENTS

To the State for Health's Secretary of the state of Espírito Santo, for allowing access to information on heterocontrol of public water available in Sisagua. And to the Environmental Surveillance team of the state, for their collaboration with the research.

6. REFERENCES

ALVES, R. X. *et al.* Evolução do acesso à água fluoretada no Estado de São Paulo, Brasil: dos anos 1950 à primeira década do século XXI. **Cadernos de Saúde Pública**, v. 28, p. s69-s80, 2012. http://dx.doi.org/10.1590/S0102-311X2012001300008

BELOTTI, L. *et al.* Quality of the water fluoridation and municipal-level indicators in a Brazilian metropolitan region. **Revista Ambiente & Água**, v. 13, n. 6, p. 1-15, 2018. http://dx.doi.org/10.4136/ambi-agua.2270

BELOTTI, L. *et al.* Vigilância da qualidade da água para consumo humano: potencialidades e limitações com relação à fluoretação segundo os trabalhadores. **Saúde Debate**, v. 43, n. especial 3, p. 51-62, 2019. http://dx.doi.org/10.1590/0103-11042019s304

BELOTTI, L. *et al.* Municipality-Level Characteristics Associated with Very Low to Good Quality of Water Fluoridation in São Paulo State, Brazil, in 2015. **JDR Clinical & Translational Research**, v. 20, n. 10, p. 1-11, 2020. https://doi.org/10.1177/2380084420970867

BERGAMO, E. T. P.; BARBANA, M.; TERADA, R. S. S.; CURY, J. A.; FUJIMAKI, M. Fluoride concentrations in the water of Maringá, Brazil, considering the benefit/risk balance of caries and fluorosis. **Brazilian Oral Research**, v. 29, n. 1, p. 1-6, 2015. http://dx.doi.org/10.1590/1807-3107BOR-2015.vol29.0047

BRASIL. Ministério da Saúde. **Diretrizes da política nacional de saúde bucal**. Brasília, DF, 2004.

BRASIL. Ministério da Saúde. **Diretriz nacional do plano de amostragem da vigilância em saúde ambiental relacionada à qualidade da água para consumo humano**. Brasília, 2014.

BRASIL. Ministério da Saúde. **Indicadores institucionais do Programa Nacional de Vigilância da Qualidade da Água para Consumo Humano 2018**. Brasília, DF, 2018. Available at: http://bvsms.saude.gov.br/bvs/publicacoes/indicadores_programa_nacional_qualidade_agua_2018.pdf. Access: 19 jul. 2019.

BRITO, C. S. *et al.* Vigilância da concentração de flúor nas águas de abastecimento público na cidade de Passo Fundo - RS. **Cadernos Saúde Coletiva**, v. 24, n.4, p. 452-459, 2016. http://dx.doi.org/10.1590/1414-462x201600040240

BUZALAF, M. A. R. *et al.* Seven years of external control of fluoride levels in the public water supply in Bauru, São Paulo, Brazil. **Journal of Applied Oral Science**, v. 21, n. 1, p. 92-98, 2013. http://dx.doi.org/10.1590/S0034-89102006005000005

CAMPOS, M. A. *et al.* Análise do gerenciamento do heterocontrole da fluoretação das águas de abastecimento público de um município de médio porte no estado do Espírito Santo. **Revista Brasileira de Pesquisa em Saúde**, v. 17, n. 3, p. 89-97, 2015. https://doi.org/10.21722/rbps.v17i3.14140

CARVALHO, R. A. S. *et al.* Desigualdades em saúde: condições de vida e mortalidade infantil em regiões do nordeste do Brasil. **Revista de Saúde Pública**, v. 49, p. 5, 2015. http://10.1590/S0034-8910.2015049004794

CECOL/USP. Documento de consenso técnico: classificação de águas de abastecimento público segundo o teor de flúor. *In:* SEMINÁRIO VIGILÂNCIA DA FLUORETAÇÃO DE ÁGUAS, 2011, São Paulo. **Arquivos[...]** São Paulo: Faculdade de Saúde Pública, Universidade de São Paulo, 2011.

CESA, K.; ABEGG, C.; AERTS, D. R. G. C. A vigilância da fluoretação de águas nas capitais brasileiras. **Epidemiologia e Serviços de Saúde**, v. 20, n. 4, p. 547-555, 2011. http://dx.doi.org/10.5123/S1679-49742011000400014

FISCHER, T. K. *et al.* Indicadores de atenção básica em saúde bucal: associação com as condições socioeconômicas, provisão de serviços, fluoretação de águas e a estratégia de saúde da família no Sul do Brasil. **Revista Brasileira de Epidemiologia**, v. 13, n. 1, p. 126-138, 2010. https://doi.org/10.1590/S1415-790X2010000100012

FERNANDES, L. S.; PERES, M. A. Associação entre a atenção básica em saúde bucal e indicadores socioeconômicos municipais. **Revista de Saúde Pública**, v. 39, n. 6, p. 930-936, 2005. http://dx.doi.org/10.1590/S0034-89102005000600010

FRAZÃO, P.; NARVAI, P. C. **Cobertura e vigilância da fluoretação da água no Brasil:** municípios com mais de 50 mil habitantes. São Paulo: Faculdade de Saúde Pública da USP, 2017. https://doi.org/10.11606/9788588848252

FRAZÃO, P.; NARVAI, P. C. Fluoretação da água em cidades brasileiras na primeira década do século XXI. **Revista de Saúde Pública**, v. 51, n. 47, p. 1-11, 2017. http://dx.doi.org/10.1590/s1518-8787.2017051006372

FRAZÃO, P. *et al.* Fluoretação da água e insuficiências no sistema de informação da política de vigilância à saúde. **Revista da Associação Paulista de Cirurgiões Dentistas** [**on-line**], v. 67, n. 2, p. 94-100, 2013.

IHEOZOR-EJIOFOR, Z. *et al.* Water fluoridation fluoridation for the prevention of dental caries. **Cochrane Database of Systematic Reviews**, v. 6, p. 1 – 274, 2015. http://10.1002/14651858.CD010856.pub2

IBGE. **Pesquisa Nacional de Saneamento Básico**. Rio de Janeiro, 2017. Available at: https://cidades.ibge.gov.br/brasil/es/pesquisa/30/84366. Access: 20 jul. 2019.

MOIMAZ, S. A. S. *et al.* Dificuldades enfrentadas no processo de fluoretação das águas de abastecimento público. **Revista Brasileira de Pesquisa em Saúde**, v. 17, n. 1, p. 87-94, 2015. https://doi.org/10.21722/rbps.v17i1.12455

OLIVEIRA JUNIOR, A. *et al.* Sistema de Informação de Vigilância da Qualidade da Água para Consumo Humano (Sisagua): características, evolução e aplicabilidade. **Epidemiologia e Serviços de Saúde**, v. 28, n.1, p. e2018117, 2019. https://dx.doi.org/10.5123/S1679-49742019000100024

PELLETIER A. R. Maintenance of optimal fluoride levels in public water systems. **Journal of Public Health Dentistry**, v. 64, n. 4, p. 237-239, 2004. https://doi.org/10.1111/j.1752-7325.2004.tb02759.x

PETERSEN, P. E. The World Oral Health Report 2003: continuous improvement of oral health in the 21st century-the approach of the WHO Global Oral Health Programme. **Community Dent Oral Epidemiol**, v. 31, n. 1, p. 3-24, 2003. https://dx.doi.org/10.1046/j..2003.com122.x

PIORUNNECK, C. M. O; DITTERICH, R. G.; GOMES, E. C. Heterocontrole da fluoretação nos municípios da Região Metropolitana de Curitiba nos anos de 2014 e 2015. **Cadernos de Saúde Coletiva**, v. 25, n. 4, p. 414-422, 2017. http://dx.doi.org/10.1590/1414-462x201700040171

PNUD. **Atlas do Desenvolvimento humano no Brasil**. Brasília, 2010. Available at: http://www.atlasbrasil.org.br/2013/ Access: 20 abr. 2018.

QUEIROZ, A. C. L. *et al.* Programa Nacional de Vigilância em Saúde Ambiental Relacionada à Qualidade da Água para Consumo Humano (Vigiagua): lacunas entre a formulação do programa e sua implantação na instância municipal. **Saúde e Sociedade**, v. 21, n. 2, p. 465-478, 2012. http://doi.org/10.1590/S0104-12902012000200019

RONCALLI, A.G. *et al.* Fluoretação da água no Brasil: distribuição regional e acurácia das informações sobre vigilância em municípios com mais de 50 mil habitantes. **Cadernos de Saúde Pública**, v. 35, n. 6, p. e00250118, 2019. http://dx.doi.org/10.1590/0102-311x00250118

SCALIZE, P. S. *et al.* Heterocontrole da fluoretação da água de abastecimento público em cidades do estado de Goiás, Brasil. **Ciência & Saúde Coletiva**, v. 23, n. 11, p. 3849-3860, 2018. http://dx.doi.org/10.1590/1413-812320182311.24712016

SLADE, G. D. *et al.* Water fluoridation and dental caries in US children and adolescents. **Journal of Dental Research**, v. 97, n. 10, p. 1122-1128, 2018. https://doi.org/10.1177/0022034518774331

SPENCER, A. J.; DO, L. G.; HA, D. H. Contemporary evidence on the effectiveness of water fluoridation in the prevention of childhood caries. **Community Dent Oral Epidemiol**, v. 46, n. 4, p. 407-415, 2018. https://doi.org/10.1111/cdoe.12384

TUCCI C. *et al.* Scenarios of water management in Brazil: a contribution to the "World Water Vision". **Revista Brasileira de Recursos Hídricos**, v. 5, n. 3, p. 31-43, 2000. http://doi.org/10.21168/rbrh.v5n3.p31-43

VENTURINI, C. Q. *et al.* Vigilância e monitoramento de fluoretos em águas de abastecimento público: uma revisão sistemática. **Revista Ambiente & Água**, v. 11, n. 4, p. 972-988, 2016. http://dx.doi.org/10.4136/ambi-agua.1929.

WHO. **Diarrhoea**: why children are still dying and what can be done. 2009. Available at: https://www.who.int/maternal_child_adolescent/documents/9789241598415/en/. Access: 20 jul. 2019.

Ambiente & Água - An Interdisciplinary Journal of Applied Science
ISSN 1980-993X – doi:10.4136/1980-993X
www.ambi-agua.net
E-mail: ambi.agua@gmail.com

Application of the SWAT hydrological model in flow and solid discharge simulation as a management tool of the Indaia River Basin, Alto São Francisco, Minas Gerais

ARTICLES doi:10.4136/ambi-agua.2694

Received: 12 Jan. 2021; Accepted: 03 May 2021

Kauem Simões[1,2]; Rita de Cássia Cerqueira Condé[1,3]; Henrique Llacer Roig[1]; Rejane Ennes Cicerelli[1*]

[1]Instituto de Geociências. Programa de Pós-Graduação em Geociências Aplicadas e Geodinâmica. Universidade de Brasília (UnB), Campus Universitário Darcy Ribeiro, CEP: 70910-900, Brasília, DF, Brazil. E-mail: kauem2001@gmail.com, rita.piscoya@ana.gov.br, roig@unb.br
[2]Companhia de Desenvolvimento dos Vales do São Francisco e Parnaíba (CODEVASF/DF), SGAN 601, Módulo I, Edifício Deputado Manoel Novaes, CEP: 70830-019, Brasília, DF, Brazil. E-mail: kauem2001@gmail.com
[3]Agência Nacional de Águas e Saneamento Básico (ANA), Setor Policial, área 5, Quadra 3, s/n, CEP: 70610-200, Brasília, DF, Brazil. E-mail: rita.piscoya@ana.gov.br
[*]Corresponding author. E-mail: rejaneig@unb.br

ABSTRACT

Measurement and evaluation of soil erosion and consequent sediment yield are fundamental in the planning and management of watersheds, as they allow the identification of critical areas susceptible to erosive processes. This study analyzed the sediment yield generated by water erosion in the Indaia River Basin, Alto São Francisco, Minas Gerais, by using the SWAT hydrological model. From a regional/local scale, the initial simulation of the variables (flow and solid discharge) was performed on a monthly scale from 1988 to 2017. Then, parameter-sensitivity analysis, calibration, and validation of the model were executed. In the monthly calibration (1988 to 2007), the performance of the simulations for flow was R^2=0.92 and NSE=0.91 and for total solid discharge R^2=0.51 and NSE=0.50. In the monthly validation (2008 to 2017) for flow, R^2=0.85 and NSE=0.82 was obtained and for total solid discharge R^2=0.19 and NSE=0.16. Despite the unsatisfactory result in the validation stage, the model was able to analyze the distribution of sediment production by sub-basins or even by the Hydrologic Response Unit (HRU). Therefore, a sediment-yield map was generated which qualitatively indicated a tendency for greater erosive processes in the central portion of the basin. The results will support public policies mitigating environmental degradation of the Indaia River Basin.

Keywords: calibration and validation of models, sediment yield, sensitivity analysis, water erosion.

Aplicação do modelo hidrológico SWAT na simulação de vazão e descarga sólida como instrumento de gestão da bacia hidrográfica do rio Indaiá, Alto São Francisco, Minas Gerais

RESUMO

A mensuração e avaliação da erosão do solo e, consequentemente, da produção de sedimentos são fundamentais no planejamento e gestão de bacias hidrográficas, pois permitem

This is an Open Access article distributed under the terms of the Creative Commons Attribution License, which permits unrestricted use, distribution, and reproduction in any medium, provided the original work is properly cited.

a identificação de áreas críticas susceptíveis aos processos erosivos. Assim, o objetivo deste estudo foi analisar a produção de sedimentos gerada por erosão hídrica na bacia do rio Indaiá, Alto São Francisco, Minas Gerais, aplicando o modelo hidrológico SWAT. De posse de uma base de dados (espaciais e alfanuméricos), realizou-se a simulação inicial das variáveis (vazão e descarga sólida) em escala mensal no período de 1988 a 2017. Em seguida, executou-se a análise de sensibilidade dos parâmetros, a calibração e a verificação do modelo. Na calibração mensal (1988 a 2007), o desempenho das simulações para vazão foi R^2=0,92 e NSE=0,91, e para descarga sólida total R^2=0,51 e NSE=0,50. Já na verificação mensal (2008 a 2017) para vazão foi obtido R^2=0,85 e NSE=0,82, e para descarga sólida total R^2=0,19 e NSE=0,16. Apesar deste resultado insatisfatório na etapa de validação, foi possível analisar a distribuição da produção de sedimentos por sub-bacias ou mesmo por Unidade de Resposta Hidrológica. Dessa forma, gerou-se um mapa de produção de sedimentos que indicou, de forma qualitativa, uma tendência de ocorrência de maiores processos erosivos na porção central da bacia. Espera-se que os resultados gerados apoiem às políticas públicas mitigadoras da degradação ambiental da bacia do rio Indaiá.

Palavras-chave: análise de sensibilidade, calibração e verificação de modelos, erosão hídrica, produção de sedimentos.

1. INTRODUCTION

Characterization, measurement, and evaluation of soil erosion and consequent sediment yield are fundamental for effective planning and management of watersheds. Such analyses allow the identification of critical areas susceptible to erosive processes and the implementation of appropriate soil management and conservation practices known as Best Management Practices (BMPs), thus contributing to the control of environmental degradation by reducing sediment and nutrient losses (Briak *et al.*, 2019; Himanshu *et al.*, 2019).

Currently, the monitoring of sediment loads is carried out punctually through hydro sedimentological stations located in or near the basin, and generally only four measurements are taken per year of suspended solid discharge (Carvalho, 2008). However, it is expensive and impractical to monitor a watershed "in loco".

For this reason, since the 1940s mathematical simulation models have been developed to represent in a simplified way the physical phenomena of nature, whether they are empirical, conceptual, or physically based (Devia *et al.*, 2015). Among the various hydrological models that consider the physical processes occurring in the basin, the Soil and Water Assessment Tool (SWAT) is the most used because it is friendly and its interface is coupled to the geographic information system (SIG). It is also easily linked to sensitivity, calibration, and uncertainty analysis tools as SWATCUP (Van Griensven *et al.* 2012; Devia *et al.*, 2015). SWAT is a semi-distributed hydrological model drawing of continuous simulations in time (yearly, monthly, daily, and more recently in the sub-daily) (Boithias, *et al.*, 2017; Brighenti *et al.*, 2019b), mainly to simulate and predict the water discharge in a basin by generating scenarios (Neitsch *et al.*, 2011; Gassman and Yingkuan, 2015, Krysanova and White, 2015).

This tool was developed by the United States Department of Agriculture (USDA) in partnership with Texas A&M University (TAMU) (Arnold *et al.*, 2012a) to simulate various physical processes in the scale of watersheds, sub-basins, hydrological response units (HRUs), rivers (river reaches). It also has been frequently used to predict and evaluate the impacts caused by anthropic actions (changes in land use and coverage) and/or climate change on water balance, sediment yield, and water quality, and can be used in the assessments of land and agricultural management impacts (Francesconi *et al.*, 2016).

The SWAT hydrological model has been evaluated by several researchers worldwide for

runoff (Pandey *et al.*, 2015; Tiwari *et al.*, 2018; Upadhyay *et al.*, 2019), sediment load (Vigiak *et al.*, 2015; 2017; Himanshu *et al.*, 2017; 2019; Duru *et al.*, 2018; Brighenti *et al.*, 2019a) and nutrient simulations (Malagó *et al.*, 2017; Qiu *et al.*, 2018; Uribe *et al.*, 2018; Pulighe *et al.*, 2020), and satisfactory model performance was reported. SWAT was used in the identification of critical erosion-prone areas in watersheds (Himanshu *et al.*, 2019; Pulighe *et al.*, 2020) and to respond to total suspended solids (TSS) load affecting climate change scenarios (Tan *et al.*, 2019; Khoi *et al.*, 2020).

Specifically, in Brazil in the last 5 years, several studies have been developed using SWAT with a focus on soil erosion and sediment loads, including the studies of Bonumá *et al.* (2014), Creech *et al.* (2015), Dantas *et al.* (2015), Silva *et al.* (2016; 2017; 2018a; 2018b) and Condé (2021). Overall, all these previous investigations identified inconsistencies in the estimation of variables related to sedimentological processes (e.g. solid discharge, sediment yield, the concentration of suspended sediments), demonstrating the complexity in such modeling.

Therefore, in this study we analyzed the sediment yield generated by water erosion in the Indaia River Basin, Alto São Francisco, state of Minas Gerais (MG), from 1988 to 2017, applying the SWAT hydrological model. The Indaia River Basin is located in a very critical region concerning soil erosion and sediment production, the Alto São Francisco. It is an important contributor to the Três Marias Reservoir, which in turn has a significant regularization function of the São Francisco River flow. There are few studies on soil erosion and sediments developed in the basin, highlighting the following works: Macêdo (2009), Menezes (2013), and Pinto *et al.* (2014). However, none of these works used a physically based model to understand the sediment yield and the impact on the land use of this process. Thus, the main motivation of this work was to develop a calibrated model, based on a robust dataset that identified the areas most prone to erosive processes in the Indaia River Basin, supporting the decision-making of public policy to combat environmental degradation in the study area.

2. MATERIAL AND METHODS

2.1. Study Area

The Indaia River Basin is located in the São Francisco River Basin, state of Minas Gerais, southeastern Brazil, upstream of the Três Marias Hydroelectric Plant Reservoir. (Figure 1).

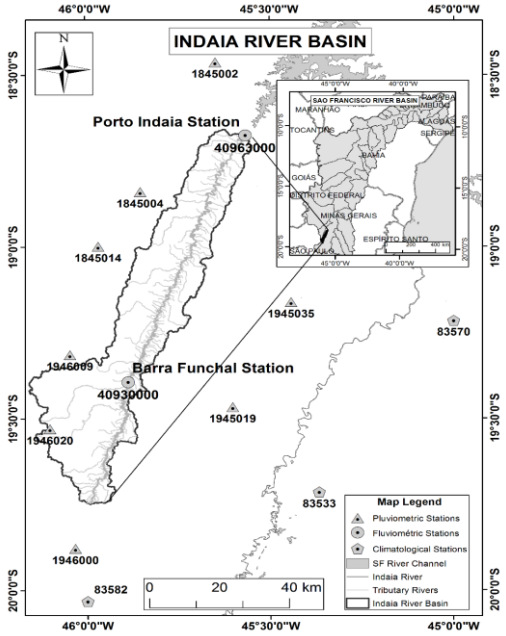

Figure 1. Study area with the localization of fluviometric, climatological and pluviometric stations.

The Indaia River is one of the main tributaries of the São Francisco River in Minas Gerais, which, together with the Abaete, Borrachudo, Para and Paraopeba Rivers, form the Upper São Francisco Basin. It is a 6th order basin, with an area of approximately 2,300 km^2 and a length of about 262 km, rising in the municipality of Corrego Danta-Minas Gerais at the elevation of 1170 m, and disemboguing into the Três Marias Reservoir, whose operation is under the control of "Companhia Energética de Minas Gerais" (CEMIG) (Macêdo, 2009).

Two climatic types are found in the region, according to the Köppen classification: Cwa - humid temperate climate with dry winter and hot summer; Aw - tropical climate with dry winter and rainy summer. The region has high rainfall rates, with values ranging between 1,000 and 2,000 mm annually, the average temperature around 23ºC, average annual sunshine of 2,400 hours, average annual evaporation of 1,000 mm, and average annual relative humidity around 70 to 80%, with the highest values occurring in the highest altitude areas (Brasil, 2006).

Cambisols (± 59%), red oxisols (± 21%), and litholic neossols (± 19%) predominate in the basin area, with a less significant occurrence of red yellow oxisol (<1%). The Indaia River Basin is a rural basin, located in the Cerrado biome (Brazilian Savanna), where the following classes of land use and cover stand out: Gallery Forest (± 37%); Savanna (± 13%), Field (± 11%), Agriculture and Pasture (± 39%), and presence of bodies of water (± 1%) (MapBiomas, 2018). In the Indaiá Basin, 34% of the area has flat to smooth wavy relief, 10% wavy relief, and 56% wavy, mountainous, or rugged relief.

2.2. Hydrological and Sedimentological Modeling

The methodological procedures started with the selection of the input data required by the SWAT. The spatial data were pre-processed in ArcGIS for compatibility and integration of these, transforming them into the raster format, with a spatial resolution of 30 meters, metric plane coordinates in the UTM projection system (Universal Transverse Mercator), Zone 23 South, datum SIRGAS 2000 (Geocentric Reference System for the Americas), and scale 1:250,000. The spatial database of the study area was composed of the following maps:

- Digital Elevation Model (DEM): SRTM / NASA, base year 2014 – spatial resolution of 30 meters;
- Solo Map: RadamBrasil / IBGE, base year 1987;
- Land Use and Coverage Map: MapBiomas, base year 2007 – spatial resolution of 30 meters (Mapbiomas, 2018).

Alphanumeric data (climate, precipitation, flow, sediments, soil parameters, parameters of land use and cover) were first edited, tabulated, and organized according to the ArcSWAT standard. The alphanumeric database was then composed of:

- Weather Data: Historical series of daily data of maximum/minimum surface temperature (degrees Celsius), solar radiation (MJ/m²), average wind speed (m/s), and relative air humidity (%), of 3 (three) conventional climatological stations of the "Instituto Nacional de Meteorologia" (INMET) located close to the Indaia River Basin (Figure 1), from 1988 to 2017.
- Pluviometric data: Historical series of daily rainfall data (mm), from 9 (nine) pluviometric stations of the "Agência Nacional de Águas" (ANA), located near the Indaia River Basin (Figure 1), from 1988 to 2017.
- Fluviometric data: Historical series of daily flow data (m^3/s), from 2 (two) fluviometric stations, Barra do Funchal (ANA) located in the central part of the basin and Porto Indaia (CEMIG) located in the basin outflow (Figure 1), from 1988 to 2017.

- Sedimentometric data: Daily sample data of suspended sediment concentration (mg/L) from the Porto Indaia sedimentometric station (CEMIG), from 1974 to 2013 (data available).

For parameterization of the SWAT, an adaptation of the original MDB was performed to the local reality of the study region, with new values of physical and chemical properties of soils and land use and cover. In addition to statistical weather parameters. The parameters were adapted on the following SWAT bases:

- UserSoil: parameters of the physical and chemical properties of the soil profiles.
- Crop: vegetation growth parameters for each type of use and land cover.
- Wgen: statistical climate parameters needed to use the SWAT climate generator.

Regarding the values of the parameters of the UserSoil and Crop databases, these were obtained from the literature according to Table 1. Meaning of each parameter see Neitsch *et al.* (2011).

The statistical parameters of the Wgen climate database were obtained with the tools available on the SWAT official website (WeatherDatabase and PcpSTAT), which use basic information from the climatological and pluviometric stations existing in the study region to calculate the climatic statistical data.

The first processing performed by ArcSWAT is related to watershed delineation by selecting the outlet point. In a watershed delineation, sub-basins are created by subdivision of the watershed from the DEM map. Watershed Delineation tools define multiple hydrologically connected sub-watersheds within a given study area.

After subdividing the basin into 14 sub-basins, the next step was the insertion of soil maps, land use and cover, and slope. The slope map was created through processing on the DEM after defining 3 (three) slope classes: from 0 to 8%, from 8 to 20%, and values above 20%.

Hydrologic Response Units (HRUs) were then created, which correspond to homogeneous polygons with the same characteristics of soil, land use and cover, and slope (Arnold *et al.*, 2012a). 471 HRUs were generated in this work.

Regarding the equations performed, the hydrological cycle simulated by the SWAT was based on the water balance equation (Neitsch *et al.*, 2011). The CN-SCS method (USDA, 1972) was used to calculate the runoff. The Penman-Monteith method (Penman, 1948; Monteith, 1965) was used to calculate evapotranspiration. The Muskingum Method (Brakensiek, 1967) was selected for the routing of water in the river channel, considering its degradation, and the Bagnold Simplified Equation (Bagnold, 1977) for the transport of sediments in a river.

According to guidelines by Arnold *et al.* (2012b), the model's warm-up period was 3 years, from 01/01/1985 to 12/31/1987. The simulation period, on the other hand, was based on 30 years of observations, from 01/01/1988 to 12/31/2017, defined based on climatological data existing in the study region. For calibration, the period of 20 years was considered, from 01/01/1988 to 12/31/2007, due to the pluviometric and fluviometric data being only in that period. For the validation, 10 years were considered, from 01/01/2008 to 12/31/2017.

After insertion of the input data (climatological and rainfall), was performed in the ArcSWAT the initial simulation of the flow and solid discharge variables on the monthly scale.

The sensitivity analysis and calibration were performed concurrently and semi-automatically in the SWAT-CUP software, which has several built-in optimization algorithms, such as SUFI2 (Sequential Uncertainty Fitting Algorithm Version 2), GLUE (Generalized Likelihood Uncertainty Estimation), PARASOL (Parameter Solution), PSO (Particle Swarm Optimization), MCMC (Markov Chain Monte Carlo).

Table 1. Parameters of the UserSoil and Crop databases.

Usersoil database parameters	
Parameter	**Reference**
SOL_ZMX SOL_CBN CLAY SILT SAND ROCK	Brasil (1987) for Cambisols, red oxisols and red yellow oxisol, and Baldissera (2005) for litolic neossol
SOL_ZMX SOL_CBN CLAY SILT ANION_EXCL SOL_CRK TEXTURE SOL_BD SOL_AWC SOL_K SOL_ALB USLE_K	Ferrigo (2014) for Cambisols, red oxisols and red-yellow oxisol, and Baldissera (2005) for litolic neossol.
Crop database parameters	
Parameter	**Reference**
BIO_E BLAI FRGRW1 LAIMX1 FRGRW2 LAIMX2 DLAI T_BASE GSI VPDFR CN ALAI_MIN	Strauch and Volk (2013) for classes of Gallery Forest (MATA), Savanna (CERR) e Field (CAMP), and default values for classes of Pasture (PAST), silviculture (EUCA), Annual Cultures (AGRL), Semi-Perennial Cultures (SUGC), and Bodies of Water (WATR).
HVSTI CHTMX RDMX T_OPT CNYLD CPYLD BN1 BN3 BP1 BP2 BP3 WSYF USLE_C FRGMAX WAVP CO2HI BIOEHI RSDCO_PL OV_N BIO_LEAF MAT_YRS BMX_TREES EXT_COEF BM_DIEOFF	Ferrigo (2014) for classes of Gallery Forest (MATA), Savanna (CERR) and Field (CAMP), and default values for classes of Pasture (PAST), silviculture (EUCA), Annual Cultures (AGRL), Semi-Perennial Cultures (SUGC), and Bodies of Water (WATR)

In this work, the optimization algorithm SUFI-2 was chosen, since it is the most-recommended algorithm, especially due to its computational efficiency and good performance (Wu and Chen, 2015). The SUFI-2 uses the Latin hypercube method to define the parameters, and the process starts with a range of values determined by the user (Abbaspour, 2015). As the SWAT-CUP provides a vast list of parameters (651 parameters) that the user can choose, and to rationalize the procedures, it was necessary to previously select a set of more sensitive parameters to be used in sensitivity analysis and calibration.

For this, a bibliographic review was performed that prioritized hydrological modeling works, whose study areas were in the Cerrado Biome, to indicate parameters with behavior similar to the study area of the present work (Baldissera, 2005; Strauch and Volk, 2013; Fernandes, 2015; Castro *et al.*, 2016; Nunes, 2016). In all, 26 parameters were selected to be used in the sensitivity analysis, calibration and validation of the model.

Hydrology (flow) and sediments (total solid discharges) were modeled together, and all steps of calibration and validation of the model were performed on a monthly scale.

In general, the results provided by the SWAT-CUP for sensitivity are given based on the generated values of t-stat and p-value. The t-stat provides the average sensitivity in which the higher the absolute value, the greater the sensitivity of the parameter. The p-value determines the significance of the sensitivity, in which values close to zero (p-value <0.05) indicate greater significance (Abbaspour, 2015b).

In the calibration step, to represent the effects of the uncertainties of the input parameters, SUFI2 quantifies the adjustment between the simulation result, expressed with a 95% uncertainty prediction (95PPU), and the observation, expressed as a single signal (with some error associated with it), by estimating two statistics: P-factor and R-factor. The P-factor is the percentage between the measured data and the 95% prediction uncertainty range (95PPU). The R-factor is the ratio between the width of this 95PPU range and the standard deviation of the observed data. The quality adjustment and calibration uncertainty are examined at each iteration by the balance between the P-factor and R-factor. There are no exact numbers that express the best value for both factors. For flow simulations, a P-factor greater than 70% and an R-factor close to 1 (one) is allowed. For sediment, a smaller P-factor and a larger R-factor could be acceptable (Abbaspour *et al.*, 2015b).

Objective functions were also used in calibration and validation, which are equations that determine the deviation between the output values of the model and observed data. These are the metrics used by the optimization algorithms to determine the quality and efficiency of the simulation, that is, how far the new simulation is from the original simulation or the observed data. The objective functions used in this work were: NSE (Nash-Sutcliffe Efficiency), R^2 (Coefficient of Determination) and PBIAS (Percent Bias).

The monthly simulated flows were calibrated (1988-2007) and validated (2008-2017) based on the values observed flows (monthly averages) of the two (2) fluviometric control stations: Barra do Funchal (ANA) located in the central part of the basin and Porto Indaia (CEMIG) located in the outlet of the watershed (Figure 1).

The monthly simulated total solid discharges were calibrated (1988-2007) and validated (2008-2017) based on the values of the total solid discharges obtained by applying a ratio of 10% of solid bottom discharge and 90% of solid suspended discharge, with the total solid discharge equaling the sum of the two discharges, as explained by Carvalho (2008).

Solid suspended discharges were determined using a potential equation generated by a sediment rating curve based on the suspended sediment concentration samples (mg/L) collected from the Porto Indaia sedimentometric station (1985-2013). The sediment rating curve was needed to fill the gap in the temporal sequence of sediment data.

In the calibration step, five iterations of 500 simulations were performed until a satisfactory result was obtained, each simulation being run monthly for 20 years (1988-2007).

In the validation step, one (1) iteration of 500 simulations was performed using the best parameter ranges obtained in the 3rd round of calibration (iteration 3), each simulation being run monthly for 10 years (2008-2017).

In the calibration and validation at the end of each iteration, the graphic output generated by SWAT-CUP was analyzed: graphs of the variables of interest (flow and total solid discharge) with the measured and simulated values versus time. The values of the objective functions (R^2, NSE and PBIAS) and the values of the statistics that measure the uncertainties of the parameters (P-factor and p-value) were also evaluated, as well as the amplitude of the new intervals generated for the parameters.

Through the calibrated hydrological and sedimentological model, the annual sediment yield values (ton/ha.year) of each sub-basin were obtained for the years 1988 and 2007, as well as the annual average of 20 years (1988 to 2017). A map of the distribution of the annual average sediment yield of the Indaia river basin by HRU was then drawn up and analyzed.

3. RESULTS AND DISCUSSION

The initial and final values of the parameters related to the monthly calibration (1988-2007) as well as the results of the sensitivity analysis are shown in Table 2.

Table 2. Parameter values and sensitivity analysis.

*Parameter	Initial Value	*Final Value	Sensitivity	
			t-stat	p-value
GW_REVAP	0.02	V:0.19	3.71	0.00
SOL_K	0.0	R:-0.56	-3.51	0.00
GWQMN	0.0	V:3223.47	3.18	0.00
USLE_P	0.0	R:+0.33	3.39	0.00
SHALLST	0.0	V:1341.90	-2.54	0.01
USLE_K	0.0	R:+0.37	1.97	0.04
CN2	69.0	R:-0.09	1.76	0.07
CH_K2	0.0	V:124.54	1.61	0.10
SLSUBBSN	10	R:-0.004	-1.61	0.10
SPCON	0.0001	V:0.004	1.33	0.18
CH_N2	0.0	V:0.17	-1.24	0.21
SURLAG	0.05	V:1.39	1.22	0.22
ADJ_PKR	0.5	V:0.67	-1.21	0.22
PRF	0.0	V:1.97	1.04	0.29
SOL_AWC	0.0	R:+0.11	-0.95	0.34
ALPHA_BF	0.0	V:0.70	-0.69	0.48
REVAPMN	0.0	V:435.95	0.63	0.52
RCHRG_DP	0.0	V:0.25	-0.60	0.54
LAT_SED	0.0	V:1.53	0.50	0.61
SPEXP	1.0	V:1.2421	-0.45	0.64
ESCO	0.0	V:0.21	0.39	0.69
CH_COV1	0.0	V:0.47	0.34	0.73
USLE_C	0.001	R:+0.09	0.32	0.74
CH_COV2	0.0	V:0.62	-0.09	0.92
GWHT	0.0	V:19.05	0.04	0.96
GW_DELAY	0.0	V:32.52	-0.02	0.97

*Meaning of each parameter see Neitsch *et al.* (2011). *R (relative): the value of the initial parameter is multiplied by 1 + (calibrated value); V (replace): the initial value is replaced by the given value.

Analyzing the t-stat and p-value values provided by SWAT-CUP (Table 2), it was found that the 5 (five) parameters that most influenced the flow estimate results were GW_REVAP, SOL_K, GWQMN, SHALLST, and CN2, with p-value values ranging from 0.00 to 0.07. It can be inferred from the results that the parameters associated with groundwater flow (GW_REVAP, GWQMN AND SHALLST) were significant in the model. These parameters are related to the amount of water that moves in the soil zone in response to water deficiencies and the depth of the water level in the shallow aquifer.

The five (5) parameters that most influenced the results of the estimate of the total solid discharge were USLE_P, USLE_K, SLSUBBSN, SPCON, and ADJ_PKR with p-value values ranging from 0.00 to 0.22. The first three (3) parameters are related to the Modified Soil Loss Universal Equation (MUSLE) used in the SWAT, specifically with the conservationist practices factor (P), soil erodibility factor (K), and topographic factor (LS). The other two (2) parameters are related to sediment transport in the main channel and the tributary channels.

3.1. Calibration and Validation

The hydrological and sedimentological calibrations were performed from 1988 to 2007 (20 years). The graphs of the historical series of the average monthly flows (simulated and observed), resulting from the best simulation obtained in the monthly calibration, can be seen in the following figures: Porto Indaia Station and Barra do Funchal Station (Figure 2).

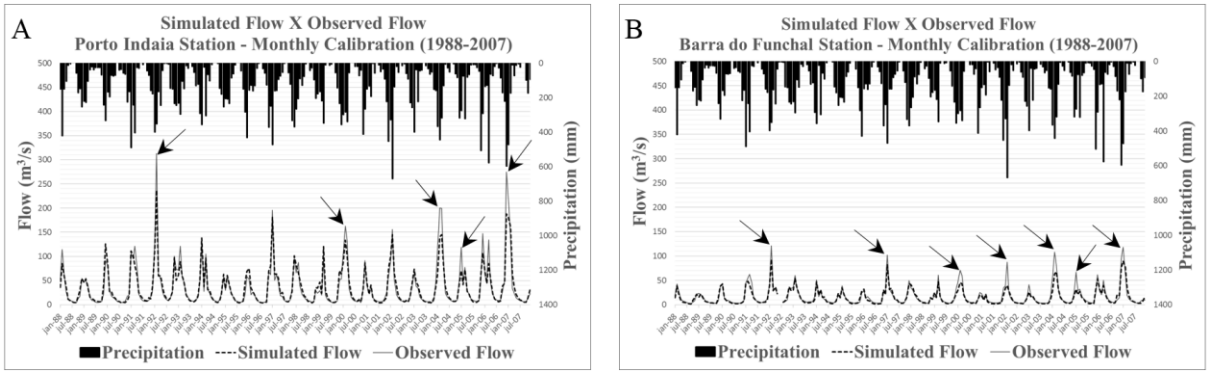

Figure 2. Better flow simulation in calibration – Porto Indaia Station (a) and Barra do Funchal Station (b).

It is observed in Figure 2 that the simulated flow results were represented satisfactorily along with the historical monitoring series, mainly in periods of drought, where the base flow was well adjusted, presenting values greater than zero during the recession period. However, in some periods of the series, such as the years 1992, 1997, 2000, 2002, 2004, 2005 and 2007, there is a tendency for simulation to underestimate the runoff in the rainy months (peaks), with simulated flow values lower than observed flows.

A better adjustment of the simulation is observed in the Porto Indaia fluviometric station (Figure 2-a) compared to the Barra do Funchal station (Figure 2-b), which can be explained in part by the climatic variability in the basin. The long period for calibration is used to balance the influences of the dry and humid periods caused by climate parameters (Choubin *et al.*, 2019). Thus, it is assumed that 20 years of monthly simulated flows (1988-2007) used in the calibration process were satisfactory for estimation. The graph of the historical series of the monthly total solid discharges (Qst simulated and observed) at the Porto Indaia Station, resulting from the best simulation obtained in the monthly calibration, can be seen in Figure 3.

It is observed in Figure 3 that in practically all periods of the series the observed data of total solid discharge were slightly smaller than the simulated data. In these years, solid discharge has been overestimated. However, there are exceptions where the solid discharge was

underestimated, such as the peaks of 1992, 1997, 2000, 2006 and 2007, corresponding to years of heavy rainfall.

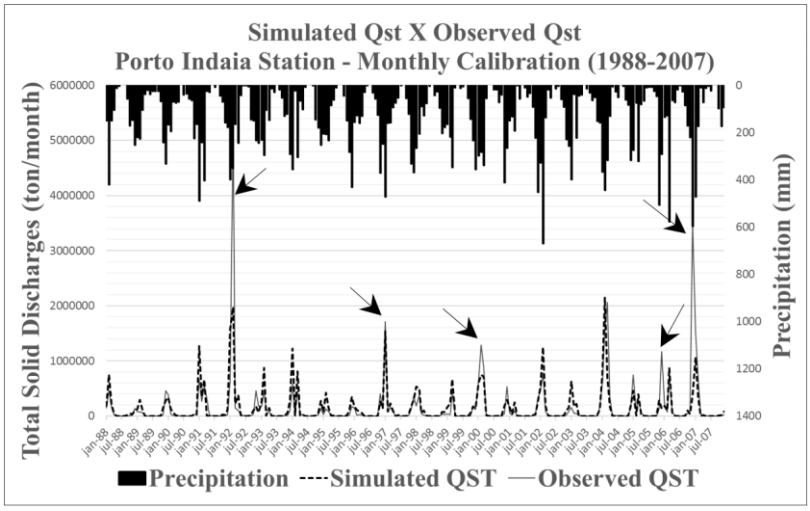

Figure 3. Better total solid discharge (QST) simulation in calibration – Porto Indaia Station.

Analyzing the results of the statistical analysis of the modeling in the step of monthly calibration for 5 iterations of 500 simulations, it was verified that the 3rd calibration iteration presented the best result. In this iteration, the following performance indexes for the simulation of the flow variable were obtained: Porto Indaia Station (P-factor = 0.96, R-factor = 0.98, R^2 = 0.92, NSE = 0.91 and PBIAS = 1.9) and Barra do Funchal Station (P-factor = 0.95, R-factor = 0.88, R^2 = 0.90, NSE = 0.87 and PBIAS = 12.5), and variable total solid discharge: Porto Indaia Station (P-factor = 0.78, R-factor = 0.74, R^2 = 0.51, NSE = 0.50 and PBIAS = 5.6).

It was observed that R^2 and NSE improved with the iterations, unlike the P-factor and R-factor. As a P-factor> 0.7 and a R-factor close to 1.00 (one) are recommended, the 3rd calibration iteration was defined as the best result.

According to Moriasi *et al.* (2007), the NSE values obtained in the monthly calibration indicate that the model satisfactorily simulates the flow and the total solid discharge.

The hydrological and sedimentological validation was performed from 2008 to 2017 (10 years). A validation of 500 simulations was performed using the parameter ranges obtained in the 3rd calibration iteration (best result).

The graphs of the historical series of monthly average flows (simulated and observed), resulting from the simulation obtained in the monthly validation, can be seen in the following figures: Porto Indaia Station (Figure 4-a) and Barra do Funchal Station (Figure 4-b).

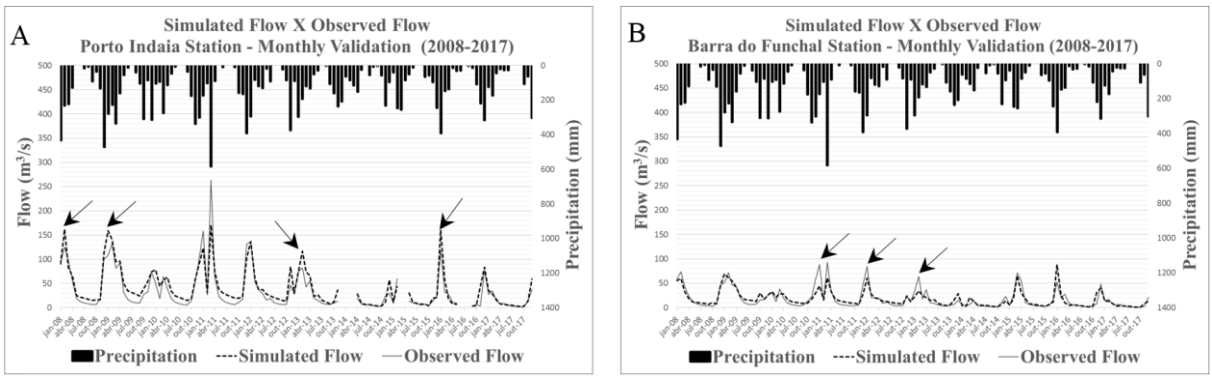

Figure 4. Flow simulation in validation – Porto Indaia Station (a) and Barra do Funchal Station (b).

It is observed in the two figures (Figure 4-a and Figure 4-b) that the results of the simulated flow were represented along with the historical monitoring series unsatisfactorily. In Figure 4-a, the flow simulations were overestimated in practically the entire series, mainly in the years 2008, 2009, 2013 and 2016. In Figure 4-b, the flow simulations were also overestimated, but in some rainy years the simulations were underestimated, as is the case for the years 2011, 2012 and 2013. As previously stated, rainfall and fluviometric data were not consistent in the validation period (2008 to 2017), which may partly explain these discrepancies. Hydrological behaviors of ungauged basins (for example, complex geological conditions and loss from the aquifer) may cause other problems which could lead to a reduction in model performance parameters (Choubin *et al.*, 2019).

The graph of the historical series of monthly total solid discharges (simulated and observed) at the Porto Indaia Station, resulting from the simulation obtained in the monthly validation, can be seen in Figure 5.

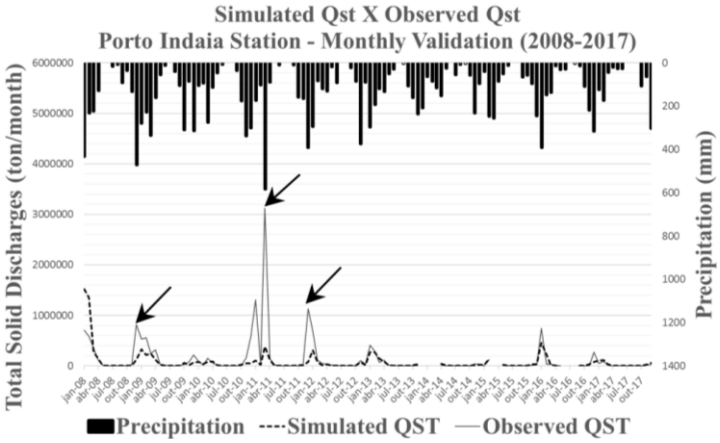

Figure 5. Total solid discharge (QST) simulation in validation – Porto Indaia Station.

The graph of the simulated results of total solid discharge in the validation stage (Figure 5) showed an inadequate adjustment, the value being underestimated in almost the entire series, mainly in the years 2009, 2011 and 2012. In the model validation, the following performance indexes for the simulation of the flow variable were obtained: Porto Indaia Station (P-factor= 0.91, R-factor = 1.07, R^2 = 0.85, NSE = 0.82 and PBIAS = -20.8) and Barra do Funchal Station (P-factor= 0.82, R-factor = 0.86, R^2 = 0.77, NSE = 0.77 and PBIAS = 0.5), and variable total solid discharge: Porto Indaia Station (P-factor= 0.76, R-factor = 1.04, R^2 = 0.19, NSE = 0.16 and PBIAS = 43.5).

Although the majority of research in the literature focusing on SWAT model concludes that this model can satisfactorily estimate sediments (Duru *et al.*, 2018), there are numerous studies on sediment modeling in which it was not possible to obtain satisfactory results (Zanin *et al.*, 2018; Ferrigo, 2014; Strauch *et al.*, 2013; Uzeika *et al.*, 2012). We assume that the origin of the inconsistencies in the solid discharge simulations is due in part to the data that generated the sediment rating curve (daily sampling of solid suspended discharge - Qss, and flow measurement -Q), which presented a high dispersion along with the historical series. A possible solution would be the temporal analysis of the rating curve. Analyzing the variability of the behavior of the data (dispersion) over the historical series, it is possible to detect trends in time variations that can alter the definition of the rating curves or even define some rating curves for each time interval.

The difficulty of SWAT in estimating sediments budget are mainly associated with the limitations of the MUSLE (Modified Universal Soil Loss Equation) equation (Uzeika *et al.*, 2012). The model's inability to capture the undulations of the landscape on slopes greater than

45% is considered one of these limitations (Bonumá *et al.*, 2014).

On the other hand, the deficiency in the measure of sediment transport in overflow conditions in the river is another inconsistency related to parametrization in the SWAT model (Santini, 2020; Neitsch *et al.*, 2011). The default method of SWAT (Bagnold method) does not guarantee the best results for the calculation of sediment transport (Yen *et al.*,2017); and the use of sediment rating curves elaborated with field measurements performed at low- and medium-flow rates are unable to represent the change in the behavior of the sediment flow occurring at high-flow rates (Condé, 2021).

In this study, three factors may have contributed to the overestimation of the sediment load in the Indaiá Basin: 1. The difficulty of SWAT in capturing the undulations of the landscape in the Indaiá Basin, which has a high slope in 66% of the Indaiá Basin (10% of the area with wavy relief and 56% with strong-wavy, mountainous or strong-mountainous relief), keeping the sediment influx instead of accounting for deposition in the relief depressions; 2. The sediment rating curve was elaborated in a range of flow rates (3 to 943 m^3s^{-1}) less than the flow occurring in the analysis period (2 to 1319 m^3s^{-1}), and is not mainly representative of the behavior of the sediment flow at higher flows, which are responsible for most of the sediment transport; 3. The use of Bagnold's simplified equation for sediment transport, instead of the equations with approaches in the laws of physics available in SWAT.

3.2. Distribution of Sediment Yield

The average annual sediment yield map (ton/ha.year) of the Indaia Basin by HRU is shown in Figure 6.

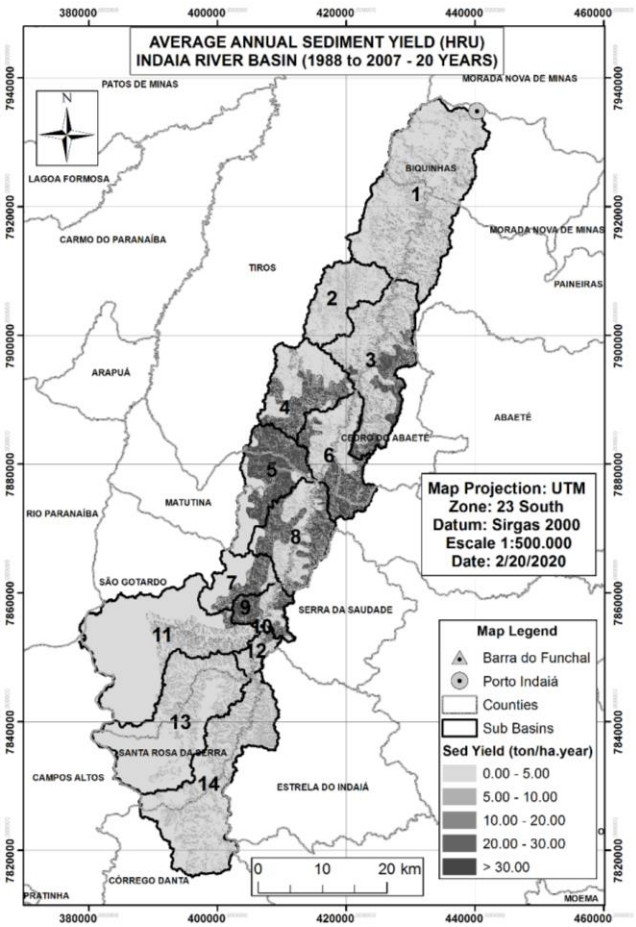

Figure 6. Average annual sediment yield in the Indaia River Basin (per HRU).

Analyzing the figure, it can be seen that the most critical sub-basins are numbers five (5) and nine (9), followed by sub-basins eight (8), six (6), four (4), seven (7), and three (3). When viewing the maps of soil, land use and cover and slope of the basin, it is observed that the soil of sub-basins 5 and 9 is mostly litolic neossol and the land use and cover is pasture with a high slope, which contributes to the formation of sediments carried by the tributaries and from these to the channel of the Indaia River.

The result obtained from the sediment yield for the Indaia River Basin corroborates the results achieved by Creech *et al.* (2015), which determined that the Upper São Francisco Basins are the main sources of sediment carried into the São Francisco River channel. As the Indaia River is the main contributor to the Três Marias Reservoir, which in turn has a significant regularization function of the São Francisco River flow, understanding the amount of sediment entering this reservoir allows the CEMIG Concessionaire to better manage the sedimentation rate.

Concerning the water-resource planning and management, the results of this work allow us to identify the areas that contribute most to the sediment yield in the basin, that is, the source areas. This is important for municipal and state agencies that are responsible for territorial planning and public policies to combat environmental degradation.

4. CONCLUSIONS

It is concluded that the calibrated hydrological and sedimentological model in this work allowed the estimation of the sediment yield generated by water erosion in the Indaia River Basin, despite the model not having been adjusted properly. Thus, it is understood that despite the result having generated values of tons per hectare per year, it is considered that the resulting map shows an indication of the places with the highest sediment yield.

The sensitivity analysis showed that parameters related to groundwater flow showed greater sensitivity in the flow simulation, while the parameters related to MUSLE showed greater sensitivity in the simulation of the solid discharge. It is important to note that additional tests could have been performed with the inclusion and removal of parameters to improve the results.

The SWAT was able to simulate the monthly flow (runoff and base flow) satisfactorily, both in the calibration and in the model validation, presenting good quality and efficiency of the hydrological simulation. However, it did not adequately simulate the total solid discharge, mainly in the validation of the model. It is assumed that the origin of the inconsistencies in the solid discharge simulations is partly due to the data that generated the sediment rating curve (daily sampling of suspended solid discharge and flow measurement), which presented high dispersion along with the historical series. It should be noted that the quality of the modeling is associated with the quality of the input data, the algorithms used, and the elaborated sediment rating curves.

Finally, the average annual sediment yield map (ton/ha.year), generated using the calibrated hydrological and sedimentological model, indicates, in a qualitative way, a tendency for greater erosion processes to occur in the central portion of the basin, in sub-basins with less extension and greater slope. This result can be used to support decision-making related to conservation planning in the Indaia River Basin, contributing to guide public policies that mitigate environmental degradation in the study area.

5. ACKNOWLEDGEMENT

CEMIG (Companhia Energética de Minas Gerais), ANA (Agência Nacional de Águas) and INMET (Instituto Nacional de Meteorologia), for providing sedimentological, fluviometric, pluviometric and climatological data. ESRI (Environmental Systems Research

Institute) for using the Toolkit that is comprised of the ArcGIS 10.x Family through Contract No. 2011 MLK 8733. CAPES (Coordenação de Aperfeiçoamento de Pessoal de Nível Superior) for promoting the Programa de Pós-graduação em Geociências Aplicadas e Geodinâmica do Instituto de Geociências (PPGGAG) of UnB (Universidade de Brasília).

6. REFERENCES

ABBASPOUR, K. C.; ROUHOLAHNEJAD, E.; VAGHEFI, S.; SRINIVASAN, R.; YANG, H.; KLØVE, B. A continental-scale hydrology and water quality model for Europe: Calibration and uncertainty of a high-resolution large scale SWAT model. **Journal of Hydrology**, v. 524, n. 5, p. 733-752, 2015. https://doi.org/10.1016/j.jhydrol.2015.03.027

ARNOLD, J. G.; KINITY, J. R.; SRINIVASAN, R.; WILLIAMS, J. R.; HANEY, E. B.; NEITSCH, S. L. **Input/Output Documentation Version 2012**. Texas Water Resources Institute, 2012a. Report n. 439, 650p.

ARNOLD, J. G. *et al.* SWAT: Model Use, Calibration, and Validation. **Transactions of the ASABE**, v. 55, n. 4, p. 1491-1508, 2012b.

BAGNOLD, R. A. Bedload transport in natural rivers. **Water Resources Research,** v. 13, n. 2, p. 303-312, 1977. https://doi.org/10.1029/WR013i002p00303

BALDISSERA, G. C. **Aplicabilidade do modelo de simulação hidrológica SWAT (Soil and Water Assessment Tool), para a bacia hidrográfica do Rio Cuiabá/MT**. 2005. 148f. Dissertação (Mestrado em Física e Meio Ambiente) – Instituto de Ciências Exatas e da Terra, Universidade Federal do Mato Grosso, Cuiabá, 2005.

BOITHIAS, L.; SAUVAGE, S.; LENICA, A.; ROUX, H.; ABBASPOUR, K.C.; LARNIER, K.; DARTUS, D.; SÁNCHEZ-PÉREZ, J. M. Simulating Flash Floods at Hourly Time-Step Using the SWAT Model. **Water,** v. 9, p. 929, 2017. https://doi.org/10.3390/w9120929

BONUMÁ, N. B. *et al.* Simulating landscape sediment transport capacity by using a modified SWAT model. **Journal of environmental quality**, v. 43, n. 1, p. 55-66, 2014. https://doi.org/10.2134/jeq2012.0217

BRAKENSIEK, D. L. Kinematic flood routing. **Transactions of the ASAE. American Society of Agricultural Engineers**, v. 10, n. 3, p. 340-343, 1967. http://dx.doi.org/10.13031/2013.39668

BRASIL. Ministério das Minas e Energia. Departamento Nacional de Produção Mineral. **Projeto RADAMBRASIL. Levantamento de Recursos Naturais**. Rio de Janeiro: MME, 1987.

BRASIL. Ministério do Meio Ambiente. Secretaria de Recursos Hídricos. **Caderno da Região Hidrográfica do São Francisco**. Brasília/DF: MMA, 2006. 148p. Available at: www.mma.gov.br/estruturas/161/_publicacao/161_publicacao03032011023538.pdf. Access: 18 Feb. 2020.

BRIAK, H.; MRABET, R.; MOUSSADEK, R.; ABOUMARIA, K. Use of a calibrated SWAT model to evaluate the effects of agricultural BMPs on sediments of the Kalaya river basin (North of Morocco). **International Soil and Water Conservation Research**, v. 7, n. 2, p. 176-183, 2019. https://doi.org/10.1016/j.iswcr.2019.02.002

BRIGHENTI, T. M.; BONUMÁ, N. B.; GRISON, F.; MOTA, A. A.; KOBIYAMA, M.; CHAFFE, P. L. B. Two calibration methods for modeling streamflow and suspended sediment with the swat model. **Ecological Engineering**, v. 127, p. 103-113, 2019a. https://doi.org/10.1016/j.ecoleng.2018.11.007

BRIGHENTI, T. M.; BONUMÁ, N. B.; SRINIVASAN, R.; CHAFFE, P. L. B. Simulating sub-daily hydrological process with SWAT: a review, **Hydrological Sciences Journal**, v. 64, n. 12, p. 1415-1423. 2019b. https://doi.org/10.1080/02626667.2019.1642477

CARVALHO, N. O. **Hidrossedimentologia Prática**. 2. ed. Rio de Janeiro: Interciência, 2008. 600p.

CASTRO, K. B.; ROIG, H. L.; LIMA, J. E. F. W.; FERRIGO, S. Aplicação de série temporal mínima para simulação de vazões em bacia experimental do cerrado. **Revista Brasileira de Cartografia**, v. 68, n. 8, p. 1497-1513, 2016.

CREECH, C. T.; SIQUEIRA, R. B.; SELEGEAN, J. P.; MILLER, C. Anthropogenic impacts to the sediment budget of São Francisco River navigation channel using SWAT. **International Journal of Agricultural & Biological Engineering**, v. 8, n. 3, p. 140-157, 2015. http://dx.doi.org/10.3965/j.ijabe.20150803.1372.

CHOUBIN, B. *et al.* Streamflow regionalization using a similarity approach in ungauged basins: Application of the geo-environmental signatures in the Karkheh River Basin, Iran. **Catena**, v. 182, p. 104128, 2019. https://doi.org/10.1016/j.catena.2019.104128

CONDÉ, R. de C. C. **Análise da integração das ferramentas de Hidrologia Espacial "cor das águas" para o monitoramento e a modelagem SWAT dos processos hidrossedimentológicos na Bacia do Rio São Francisco – Brasil**. 2021. 258p. Tese (Doutorado em Geociências Aplicadas) - Instituto de Geociências, Universidade de Brasília, Brasília, 2021. 258p.

DANTAS, J. C.; SILVA, M. A.; SILVA, R. M.; VIANNA P. C. G. Simulação vazão-erosão usando o modelo SWAT para uma grande bacia da região semiárida da Paraíba. **Geociências**, v. 34, n. 4, p. 816-827, 2015.

DEVIA, G. K.; GANASRI, B. P.; DWARAKISH, G. S. A review on hydrological models. **Aquatic Procedia**, v. 4, p. 1001-1007, 2015. https://doi.org/10.1016/j.aqpro.2015.02.126

DURU, U.; ARABI, M.; WOHL, E. E. Modeling stream flow and sediment yield using the SWAT model: a case study of Ankara River basin, Turkey. **Physical Geography**, v. 39, n. 3, p. 264-289, 2018. https://doi.org/10.1080/02723646.2017.1342199.

FERNANDES, G. F. **Estimativa de vazão e produção de sedimentos na bacia hidrográfica do rio São Francisco, utilizando o modelo SWAT**. 2015. 185f. Tese (Doutorado em Geografia) – Universidade Federal de Pernambuco, Recife, 2015.

FERRIGO, S. **Análise de consistência dos parâmetros do modelo SWAT obtidos por calibração automática – Estudo de caso da bacia do lago Descoberto – DF**. 2014. 164f. Dissertação (Mestrado em Tecnologia Ambiental e Recursos Hídricos) – Departamento de Engenharia Civil e Ambiental, Universidade de Brasília, Brasília, 2014.

FRANCESCONI, W. *et al.* Using the Soil and Water Assessment Tool (SWAT) to model ecosystem services: A systematic review. **Journal of Hydrology**, v. 535, p. 625-636, 2016. https://doi.org/10.1016/j.jhydrol.2016.01.034

GASSMAN, P. W.; YINGKUAN, W. IJABE SWAT Special Issue: Innovative modeling solutions for water resource problems. **International Journal of Agricultural and Biological Engineering**, v. 8, n. 3, p. 1-8, 2015. https://ijabe.org/index.php/ijabe/article/view/1763.

HIMANSHU, S. K., PANDEY, A.; YADAV, B.; GUPTA, A. Evaluation of best management practices for sediment and nutrient loss control using SWAT model. **Soil & Tillage Research**, v. 192, p. 42-58, 2019. https://doi.org/10.1016/j.still.2019.04.016.

HIMANSHU, S. K.; PANDEY, A.; SHRESTHA, P. Application of SWAT in an Indian river basin for modeling runoff, sediment and water balance. **Environmental Earth Sciences**, v. 76, n. 3, p. 1-18, 2017. https://doi.org/10.1007/s12665-016-6316-8.

KHOI, D. N. *et al.* Responses of river discharge and sediment load to climate change in the transboundary Mekong River Basin. **Water and Environment Journal**, v. 34, p. 367-380, 2020. https://doi.org/10.1111/wej.12534

KRYSANOVA, V.; WHITE, M. Advances in water resources assessment with SWAT – an overview. **Hydrological Sciences Journal**, v. 60, n. 5, p. 771-783, 2015. https://doi.org/10.1080/02626667.2015.1029482.

MACÊDO, Í. L. **Estudo de Modelos em Ambiente de Geoprocessamento para a Previsão de Erosão e Assoreamento de Reservatórios**: o Caso da Bacia do Rio Indaia-UHE Três Marias, MG. 2009. 312f. Tese (Doutorado em Geotecnia) – Departamento de Engenharia Civil e Ambiental, Faculdade de Tecnologia, Universidade de Brasília, Brasília, 2009.

MALAGÓ, A.; BOURAOUI, F.; VIGIAK, O.; GRIZZETTI, B.; PASTORI, M. Modelling water and nutrient fluxes in the Danube River Basin with SWAT. **Science of the Total Environment**, v. 603-604, p. 196-218, 2017. http://dx.doi.org/10.1016/j.scitotenv.2017.05.242.

MAPBIOMAS. **Collection 4 of the Annual Land Use Land Cover Maps of Brazil**. Available at: http://mapbiomas.org. Access: 10 Jan. 2018.

MENEZES, P. H. B. J. **Estudo da Dinâmica Espaço-Temporal do Fluxo de Sedimentos a partir das Propriedades Ópticas das Águas no Reservatório de Três Marias - MG. 2013**. 2013. 112f. Tese (Doutorado em Geociências Aplicadas) – Instituto de Geociências, Universidade de Brasília, Brasília/DF, 2013.

MONTEITH, J. L. Evaporation and Environment. **Symposia of the Society for Experimental Biology**, v. 19, p. 205-234, 1965.

MORIASI, D. N.; ARNOLD, J. G.; VAN LIEW, M. W; BINGNER, R. L.; HARMEL, R. D.; VEITH, T. L. Model evaluation guidelines for systematic quantification of accuracy in watershed simulations. **Transactions of the ASABE**, v. 50, n. 3, p. 885−900, 2007.

NEITSCH, S. L.; ARNOLD, J. G.; KINIRY, J. R.; WILLIAMS, J. R. **Soil and Water Assessment Tool, Theoretical documentation version 2009**. Temple: Blackland Research Center, 2011. Report nº 406, 618p.

NUNES, G. **Aplicação do modelo SWAT no estudo hidrológico e de qualidade de água da Bacia Hidrográfica do lago Paranoá - DF**. 2016. 148p. Dissertação (Mestrado em Tecnologia Ambiental e Recursos Hídricos) – Departamento de Engenharia Civil e Ambiental, Universidade de Brasília, Brasília, 2016.

PANDEY, A.; LALREMPUIA, D.; JAIN, S. K. Assessment of hydropower potential using spatial technology and SWAT modelling in the Mat River, southern Mizoram, India. **Hydrological Sciences Journal**, v. 60, n. 10, p. 1651-1665, 2015. https://doi.org/10.1080/02626667.2014.943669

PENMAN, H. L. Natural evaporation from open water, bare soil and grass. **Proceedings of the Royal Society of London**, v. 193, n. 1032, p. 120–145, 1948. https://doi.org/10.1098/rspa.1948.0037

PINTO, C. E. T.; MENEZES, P. H. B. J.; MARTINEZ, J. M.; ROIG, H. L.; VILLAR, R. A. E. Uso de imagens MODIS no monitoramento do fluxo de sedimentos no reservatório de Três Marias. **Revista Brasileira de Engenharia Agrícola e Ambiental**, v. 18, n. 5, p. 507-516, 2014. https://doi.org/10.1590/S1415-43662014000500007

PULIGHE, G.; BONATI, G.; COLANGELI, M.; TRAVERSO, L.; LUPIA, F.; ALTOBELLI, F.; DALLA MARTA, A.; NAPOLI, M. Predicting streamflow and nutrient loadings in a semi-arid mediterranean watershed with ephemeral streams using the SWAT model. **Agronomy**, v. 10, n. 2, 2020. https://doi.org/10.3390/agronomy10010002.

QIU, J.; SHEN, Z.; HUANG, M.; ZHANG, X. Exploring Effective Best Management Practices in the Miyun Reservoir Watershed, China. **Ecological Engineering**, v. 123, p. 30–42, 2018. https://doi.org/10.1016/j.ecoleng.2018.08.020

SANTINI, W. **Caractérisation de la dynamique hydro-sédimentaire du bassin de l'Ucayali (Pérou) par une approche intégrant réseau de mesures, télédétection, et modélisation hydrologique**. 2020. 471p. Tese (Doutorado) – Université Toulouse 3 – Paul Sabatier, Toulouse, 2020.

SILVA, A. K. L.; SOUZA, A. M. L.; SANTOS, J. T. S.; VILLELA, J. M.; MARTORANO, L. G.; CRESTANA, S. Estimation of sediment production in oil palm expansion areas in the Amazon. **Revista Brasileira Engenharia Agrícola e Ambiental**, v. 22, n. 5, p. 344-348, 2018a. http://dx.doi.org/10.1590/1807-1929/agriambi.v22n5p344-348.

SILVA, M. T.; AZEVEDO, P. V.; SILVA, V. P.; SILVA, B. K.; MARIANO, E. B.; AMORIM, M. R. B. Estimativa da produção de sedimentos na bacia hidrográfica do submédio Rio São Francisco. **Journal of Environmental Analysis and Progress**, v. 02, n. 03, p. 203-211, 2017. http://dx.doi.org/10.24221/jeap.2.3.2017.1430.203-211.

SILVA, R. M.; SANTOS, C. A. G.; SANTOS, J. Y. G. Evaluation and modeling of runoff and sediment yield for different land covers under simulated rain in a semiarid region of Brazil. **International Journal of Sediment Research**, v. 33, n. 2, p. 117-125, 2018b. https://doi.org/10.1016/j.ijsrc.2017.04.005.

SILVA, V. P. R.; SILVA, M. T.; SOUZA, E. P. Influence of land use change on sediment yield: a case study of the sub-middle of the São Francisco river basin. **Engenharia Agrícola,** v. 36, n. 06, p. 1005-1015, 2016. http://dx.doi.org/10.1590/1809-4430-eng.agric.v36n6p1005-1015/2016

STRAUCH, M.; VOLK, M. SWAT plant growth modification for improved modeling of perennial vegetation in the tropics. **Ecological Modelling**, v. 269, p. 98–112, 2013. https://doi.org/10.1016/j.ecolmodel.2013.08.013

STRAUCH, M. *et al.* The impact of Best Management Practices on simulated streamflow and sediment load in a Central Brazilian catchment. **Journal of Environmental Management**, v. 127, p. S24–S36, 2013. https://doi.org/10.1016/j.jenvman.2013.01.014

TAN, M. L. *et al.* A review of SWAT studies in Southeast Asia: applications, challenges and future directions. **Water**, v. 11, n. 5, p. 914, 2019. https://doi.org/10.3390/w11050914

TIWARI, D; TIWARI, H. L.; SAINI, R. Hydrological Modelling in Narmada Basin using Remote Sensing and GIS with SWAT model and Runoff Prediction in Patan Watershed. **International Journal of Advanced Research, Ideas and Innovations in Technology**, v. 4, n. 2, p. 344-352, 2018.

UPADHYAY, H.; MITTAL, H. K.; SINGH, M.; HIRAPARA, J. G. Application of SWAT Model for Estimation of Runoff in Pindwara Watershed and Assessment of its Feasibility. **International Journal of Current Microbiology and Applied Sciences**, v. 8, n. 6, p. 3056-3065, 2019. https://doi.org/10.20546/ijcmas.2019.806.364.

URIBE, N.; CORZO, G.; QUINTERO, M.; VAN GRIENSVEN, A.; SOLOMATINE, D. Impact of conservation tillage on nitrogen and phosphorus runoff losses in a potato crop system in Fuquene watershed, Colombia. **Agricultural Water Management**, v. 209, p. 62-72, 2018. https://doi.org/10.1016/j.agwat.2018.07.006.

USDA. **National Engineering Handbook**: section 4: hydrology. Washington: Soil Conservation Service, 1972. chap. 4-10.

UZEIKA, T. *et al.* Use of the SWAT model for hydro-sedimentologic simulation in a small rural watershed. **Revista Brasileira de Ciência do Solo**, v. 36, n. 2, p. 557-565, 2012. https://doi.org/10.1590/S0100-06832012000200025

VAN GRIENSVEN, A.; NDOMBA, P.; YALEW, S.; KILONZO, F. Critical review of SWAT applications in the upper Nile basin countries. **Hydroloy and Earth System Sciences**, v. 16, p. 3371–3381, 2012. https://doi.org/10.5194/hess-16-3371-2012

VIGIAK, O.; MALAGÓ, A.; BOURAOUI, F.; VANMAERCKE, M.; POESEN, J. Adapting SWAT hillslope erosion model to predict sediment concentrations and yields in large Basins. **Science of the Total Environment**, v. 538, p. 855–875, 2015. https://doi.org/10.1016/j.scitotenv.2015.08.095.

VIGIAK, O.; MALAGÓ, A.; BOURAOUI, F.; VANMAERCKE, M.; OBREJA, F.; POESEN, J.; HABERSACK, H.; FEHER, J.; GROSELJ, S. Modelling sediment fluxes in the Danube River Basin with SWAT. **Science of The Total Environment**, v. 599–600, n. 1, p. 992-1012, 2017. http://dx.doi.org/10.1016/j.scitotenv.2017.04.236.

WU, H.; CHEN, B. Evaluating uncertainty estimates in distributed hydrological modeling for the Wenjing River watershed in China by GLUE, SUFI-2, and ParaSol methods. **Ecological Engineering**, v. 76, p. 110–121, 2015. https://doi.org/10.1016/j.ecoleng.2014.05.014

YEN, H. *et al.* Assessment of optional sediment transport functions via the complex watershed simulation model SWAT. **Water**, v. 9, n. 2, p. 76, 2017. https://doi.org/10.3390/w9020076

ZANIN, P. R.; BONUMA, N. B.; CORSEUIL, C. W. Hydrosedimentological modeling with SWAT using multi-site calibration in nested basins with reservoirs. **RBRH**, v. 23, 2018. https://doi.org/10.1590/2318-0331.231820170153

Ambiente & Água - An Interdisciplinary Journal of Applied Science
ISSN 1980-993X – doi:10.4136/1980-993X
www.ambi-agua.net
E-mail: ambi.agua@gmail.com

Use of natural mucilage extracted from the *Stenocereus griseus* (Cardón Guajiro) plant as a coagulant in the treatment of domestic wastewater

ARTICLES doi:10.4136/ambi-agua.2705

Received: 04 Feb. 2021; Accepted: 03 May 2021

Arnulfo Antonio Tarón Dunoyer[1*]; Rafael Emilio González Cuello[1]; Fredy Colpas Castillo[2]

[1]Faculty of Engineering. Food Engineering Program. University of Cartagena, Street 30, n°48-152, 130014, Zaragocilla, Cartagena, Colombia. E-mail: rgonzalezc1@unicartagena.edu.co
[2]Exact and Natural Sciences Faculty. Chemistry program. University of Cartagena, Street 50, n°24120, 130014, Zaragocilla, Cartagena, Colombia. E-mail: fcolpasc1@unicartagena.edu.co
[*]Corresponding author. E-mail: atarond@unicartagena.edu.co

ABSTRACT

Coagulants can be extracted from vegetal material and applied in the treatment of wastewater. These coagulants are derived from seeds, leaves, bark, roots and fruits. This study focuses on the use of the mucilaginous extract of *Stenocereus griseus* (known as Cardón Guajiro) for removal of biochemical oxygen demand (BOD_5), chemical oxygen demand (COD), total solids, turbidity and color in domestic wastewater from a pumping station in the city of Cartagena (Colombia). The optimal dose of *S. griseus* extract was determined by a pitcher test employing an E&Q F6-300 digital flocculator. All physicochemical tests were carried out following the specifications of the standard methods for wastewater (APHA). When 1400 mgL^{-1} of natural coagulants were used in the sewage treatment, the turbidity obtained was 29.57 TNU, representing removal of 67.24%, considering the initial turbidity. This parameter decreases until 68.61 PCU, for a 72.12% removal at the same coagulant dosage regarding the color. It must be noted that significant statistical differences were found between all tested doses of the coagulant. The mucilaginous extract of *S. griseus* exhibited useful properties in the primary treatment of domestic wastewater.

Keywords: coagulation, color, removal, turbidity, water treatment.

Tratamento primário de águas residuais domésticas a partir da mucilagem natural extraída da fábrica de *Stenocereus griseus* (Cardón Guajiro) como coagulante

RESUMO

Os coagulantes podem ser extraídos de matéria vegetal e aplicados no tratamento de efluentes. Esses coagulantes são derivados de sementes, folhas, cascas, raízes e frutos. Este estudo enfoca o uso do extrato mucilaginoso de Stenocereus griseus (conhecido como Cardón Guajiro) para a remoção da demanda bioquímica de oxigênio (DBO_5), demanda química de oxigênio (COD), sólidos totais, turbidez e cor em águas residuais domésticas de uma estação de bombeamento na cidade de Cartagena (Colômbia). A dose ideal de extrato de *S. griseus* foi

This is an Open Access article distributed under the terms of the Creative Commons Attribution License, which permits unrestricted use, distribution, and reproduction in any medium, provided the original work is properly cited.

determinada por um teste de jarro empregando um floculador digital E & Q F6-300. Todas as determinações físico-químicas foram realizadas seguindo as especificações dos métodos padrão para efluentes da APHA (Standard Methods for Water and Wastewater). Quando foram utilizados 1400 mgL^{-1} de coagulante natural no tratamento de esgoto, a turbidez obtida foi de 29,57 TNU, representando remoção de 67,24% considerando a turbidez inicial. Este parâmetro diminui até 68,61 PCU para uma remoção de 72,12% na mesma dosagem de coagulante em relação à cor. Deve-se notar que diferenças estatísticas significativas foram encontradas entre todas as doses testadas do coagulante. O extrato mucilaginoso de *S. griseus*, teve propriedades valiosas no tratamento primário de águas residuais domésticas.

Palavras-chave: coagulação, cor, remoção, tratamento de água, turbidez.

1. INTRODUCTION

Domestic wastewater processes involve physicochemical treatment (coagulation and flocculation). Coagulation is defined as adding chemicals reagents to wastewater for agglutination of small particles into larger particles that can be removed by solids processes (Ang and Mohammad, 2020; Luo *et al*., 2020; Guzmán *et al*., 2013). A wide range of wastewater treatments has been developed over the last decades. These treatments can be classified into physical (sedimentation, filtration, adsorption and UV), chemical (coagulation, electrochemical, ion exchange, oxidation, catalytic reduction and disinfection) and biological (phytoremediation and biodegradation) (Kooijman *et al.,* 2020; Ang and Mohammad, 2019; Hamzah *et al.,* 2017; Kumar and Chowdhury, 2020; Hoong and Ismail, 2018).

Coagulation is an essential process for removing turbidity, color and organic matter in domestic and industrial wastewater. Some coagulants employed to remove impurities and colloidal particles from wastewater are ferric chlorides, aluminum sulfate, polyaluminum chloride, and calcium carbonate (Bergamasco *et al.,* 2009). Nevertheless, there are some disadvantages related to the use of coagulants, such as cost, production of large volumes of sludge and pH modifications of the treated water (Olivero *et al*., 2014; Yin, 2010). Bergamasco *et al.,* 2009). Several studies have reported the efficiency of some low-cost coagulants employed in wastewater treatments. For example, Jaafari *et al.* (2020) employed a magnetic chitosan to remove anionic dyes from polluted waters. Likewise, Naghipour *et al.* (2018) carried out studies to remove diclofenac from aqueous solutions using activated pine charcoal as adsorbent material.

Natural coagulants have been studied as an alternative to traditional chemical coagulants. Some natural coagulants studied are those obtained from vegetal species such as *Moringa oleifera* (Okuda *et al.,* 1999; Caldera *et al*., 2007) from *Cereus deficiens* (commonly known as cactus or cardon lefaria) (Martínez *et al*., 2003) and from *Opuntia cochinellifera* (Almendárez de Quezada, 2004). The genus *Stenocereus* (Berger) Riccob Comprises a heterogeneous group of cacti distributed from southern Arizona to northern Colombia and Venezuela (Anderson, 2001; Terrazas *et al*., 2005). The "cardón guajiro" or "yosú" (in Wayúu language), *Stenocereus griseus* (Haw.) Buxb, is a columnar cactus that can reach up to 11 m in height. In Colombia, it is present in the departments of Guajira, Cesar and Magdalena. This vegetal species has not been studied previously as a coagulant of wastewater.

However, the active compounds of cardon guajiro, such as polysaccharides and proteins, can be a useful alternative to coagulation and flocculation processes of various pollutants. It is also a plant that grows easily on the north coast of Colombia; it has low cost and does not generate a negative environmental impact, which makes this plant a very attractive source of coagulant material for the industry. This work therefore focuses on evaluating the use of mucilage extracted from *Stenocereus griseus* as a natural coagulant in domestic wastewater.

2. MATERIALS AND METHODS

2.1. Wastewater sample

The wastewater was obtained from a pumping station located in Cartagena de Indias, Colombia. The water sample was collected in the morning because, at that time, there was maximum discharge volume and the wastewater presents high levels of turbidity. The plants of *S. griseus* were obtained from the northern region of Colombia, at San Juan del Cesar in Guajira.

2.2. Physicochemical characterization of wastewater.

The wastewater sample was characterized following the Standard Methods for Water and Wastewater (APHA *et al.*, 2012). For color determination, a colorimeter (Lovibond PFX 195) was employed using the 2120B method; the results were expressed as platinum-cobalt units (PCU). Turbidity was determined by the nephelometric method (Method 2130B) using a turbidity meter (Turbiquant 3000 IR). The pH was assessed by potentiometry with a digital potentiometer (Bench pH/Conductivity meter PC 510). Alkalinity was calculated by titration (expressed in mg of $CaCO_3$/L). Hardness was measured by titration using an EDTA solution as the titrating agent; this parameter was expressed in mg of $CaCO_3$/L. Table 1 shows the values obtained for the wastewater characterization.

Table 1. Physicochemical characterization of domestic wastewater.

Parameters	Value	Unit
Total alkalinity	218.0±1.00	mg $CaCO_3$ L^{-1}
Biochemical Oxygen Demand (BOD_5)	128.1±0.81	mgL^{-1}
Chemical Oxygen Demand (COD)	219.4±0.76	mgL^{-1}
Total hardness	490.0±0.57	mg $CaCO_3$ L^{-1}
Conductivity	1210.2±0.8	μScm^{-1}
Turbidity	90.28±1.00	NTU
Color	246.1±0.60	UPC
Total solids	610.0±0.22	mgL^{-1}

2.3. Preparation of the coagulant

The mucilage (coagulant) was extracted from plants of *S. griseus*, especially the section between the bark and the woody tubular medulla (stem pulp). The epidermis was removed from fragments of *S. griseus* stems and the parenchymatous tissue. This parenchyma was liquefied for one (1) minute. Then, the solid phase was separated from the aqueous phase and the aqueous phase mass was determined by gravimetry. Finally, distilled water was added to obtain a mucilaginous heterogeneous mixture (Fuentes *et al.*, 2011).

2.4. Coagulation process

The standard jar test described by Satterfield (2005) was used to determine the optimum coagulant dosage. The mucilaginous mixture described in Section 2.3 500 mL of coagulant-wastewater solutions at different concentrations (800, 1000, 1200, 1400 and 1600 mg L^{-1}) was prepared employing wastewater without coagulant and another containing $Al_2(SO_4)_3$ as control. Then, both wastewaters (with and without coagulant) were subjected to agitation at 100 rpm during 1 minute, followed by slow agitation at 40 rpm for 30 minutes. Finally, all samples were left for 60 minutes to allow sedimentation (Tarón *et al.*, 2017). The assays were performed at room temperature in an E&Q F6-300 Digital Flocculator.

The turbidity removal percentage was determined using Equation 1.

$$Turbidity\ removal\ (\%) = \frac{T_0 - T_f}{T_0} * 100 \quad (1)$$

Where: T_o is the initial value of turbidity and y T_f is the final value of turbidity.

The percentage of color removal was determined using Equation 2.

$$color\ removal\ (\%) = \frac{Co - Cf}{Co} * 100 \quad (2)$$

Where, C_o is the initial value of color and C_f is the final value of color.

2.5. Statistical analysis

The results were analyzed by means of ANOVA (one way) to determine statistically significant differences (P<0.05) among the samples. The software SPSS (Version 17.0 for Windows) was used. All tests were done in triplicate.

3. RESULTS AND DISCUSSION

3.1. Physicochemical characterization of the effluent after treatment with coagulants

Table 2 shows the physicochemical parameters evaluated in wastewater subjected to coagulant at different dosages. Statistical differences can be seen (P<0.05) between initial and final values of alkalinity at doses 800, 100 and 1200 mgL^{-1} of the mucilaginous extract of *S. griseus* (ME*S. g*). These removal percentages are lower than those found for (Al2(SO4)3 at all doses tested. At 1400, 1600 and 1800 mgL-1 of ME*S. g*, no significant differences (P>0.05) were found. The results are similar to those reported by Dearmas Duarte and Ramírez Hernández (2015), that achieve efficient nutrient removal through the use of natural and chemical coagulants in a wastewater treatment plant.

As doses of ME*S. g increase*, the percentages of total solids removed also increase. The highest percentage of removal was 70.49%, which was reached employing a coagulant dosage of 1400 mgL^{-1}. When high doses (>1600mgL^{-1}) of coagulant were used, a slight increase in solid content was observed due to the load that can produce a re-stabilization of the system. This behavior also could be associated with the increase of coagulant requirement when the suspended solids rise, since the polymers can present an optimum coagulant concentration that depends on the molecular weight and ion concentration solids in suspension (Sánchez and Untiveros, 2004).

Regarding the chemical coagulant employed ($Al_2(SO_4)_3$, a similar behavior was seen. However, it must be noted that solids-removal levels are higher using low doses of coagulant (25 mgL^{-1}). The highest percentage of solid removal was 74.95; this is in accordance with the observations of Dearmas Duarte and Ramírez Hernández (2015). Statistical differences were appreciated among the percentages of solids removal using different dosages of coagulant. Presently, no investigations have been conducted pertaining to the use of coagulants extracted from *S. griseus* for water purification. Nevertheless, the effect of various suspensions of *Stenocereus griseus*, *Cereus deficiens*, *Opuntia ficus-indica* and polyacrylamide on physical properties of the soil of Quibor (Lara State, Venezuela) has been evaluated, with Stenocereus griseus being considered the best flocculants (Henríquez *et al*., 2000).

The findings seen in Table 2 demonstrate that mucilaginous extract of *S. griseus* can be employed to decrease levels of biological and chemical degradation of organic matter. A higher percentage of chemical degradation of organic matter was reached when 1400 mgL^{-1} of dosage of coagulant was used in the process. Statistical differences were observed among all coagulant dosages. Similar behavior was found for BOD_5; the best degradation result is obtained when high doses of coagulant (>1400 mgL^{-1}) are used. Statistical differences were noted between all values of BOD_5 obtained, as can be seen in Figure 1.

Table 2. Physicochemical characterization of domestic wastewater using different dosages of coagulants.

Parametros	Dosages of mucilaginous extract of *S. griseus* [mgL^{-1}]							
	C_i	800	1000	1200	1400	1600	1800	Unidades
Total alkalinity	218.0±1.0[a]	222±05[b]	230±2[c]	237±2[d]	240±1[d]	241±09[d]	242±2[d]	mg $CaCO_3$ L^{-1}
BOD_5	128.1±0.81[a]	114±02[b]	102.1±08[c]	96.8±01[d]	57.64±1[e]	59.8±08[e]	60.6±01[e]	mgL^{-1}
COD	219.4±0.76[a]	137±07[b]	104.7±04[c]	100±09[d]	70.5±03[e]	82.6±1.5[f]	84.2±1.3[f]	mgL^{-1}
Total hardness	490.0±2.5[a]	450±2.1[b]	445±1.1[c]	409±1.5[d]	400±1.0[e]	402±1.9[e]	406±1.8[d]	mg $CaCO_3$ L^{-1}
Conductivity	1210.2±1.3[a]	1220±1[ab]	1226±1.2[b]	1252±3[c]	1250±4[c]	1251±2[c]	1260±3.1[d]	μScm^{-1}
Turbidity	90.28±1.00[a]	54.7±05[b]	46.66±02[c]	33.8±01[d]	29.57±05[e]	32.4±02[e]	35.90±09[f]	NTU
Color	246.1±1.1[a]	180±1[b]	115.2±2[c]	80.50±2[d]	68.61±09[f]	70.6±05[f]	72.30±1[g]	UPC
Total solids	610.0±1.5[a]	335±08[b]	261.2±01[c]	219.±02[d]	180.4±08[e]	204±0.3[f]	211,1±07[f]	mgL^{-1}
	Dosages of $Al_{2(}SO_4)_3$ [mgL^{-1}]							
	C_i	10	15	20	25	30	35	
Total alkalinity	218.0±1.0[a]	219±02[a]	226±1.2[b]	230±2.3[c]	233±1.1[c]	239±2.2[d]	240±1.9[d]	mg $CaCO_3$ L^{-1}
BOD_5	128.1±0.81[a]	105±0.8[b]	91.2±1.2[c]	82.9±1.6[d]	44.30±05[e]	47.8±1.1[f]	50.05±0.9[f]	mgL^{-1}
COD	219.4±0.76[a]	123±2[b]	96.5±1[c]	82.4±09[d]	60.27±03[e]	68.4±09[f]	70.9±1.3[f]	mgL^{-1}
Total hardness	490.0±2.5[a]	431±2.5[b]	430±1.5[b]	394±1.1[c]	381±2.1[d]	383±1.9[d]	389±1.2[e]	mg $CaCO_3$ L^{-1}
Conductivity	1210.2±1.3[a]	1213±4[a]	1220±2.3[c]	1239±2[d]	1248±3.1[c]	1252±1[c]	1256±2.5[c]	μScm^{-1}
Turbidity	90.28±1.0[a]	42.4±09[b]	37.26±1[c]	28.7±09[d]	25.67±1.2[e]	26.9±1[ed]	27.5±1.1[d]	NTU
Color	246.1±1.1[a]	150±1.3[b]	100.5±2.2[c]	62.4±1.8[d]	51.11±1-4[f]	55.4±09[g]	59.90±1.6[h]	UPC
Total solids	610.0±1.5[a]	290±2.1[b]	246.1±2.2[c]	201.±1.9[d]	152.8±1.3[e]	180±1.6[f]	183.4±1.9[f]	mgL^{-1}

***rows with different letters are significantly different ($p < 0.05$); mean ± standard deviation of 3 repetitions.*

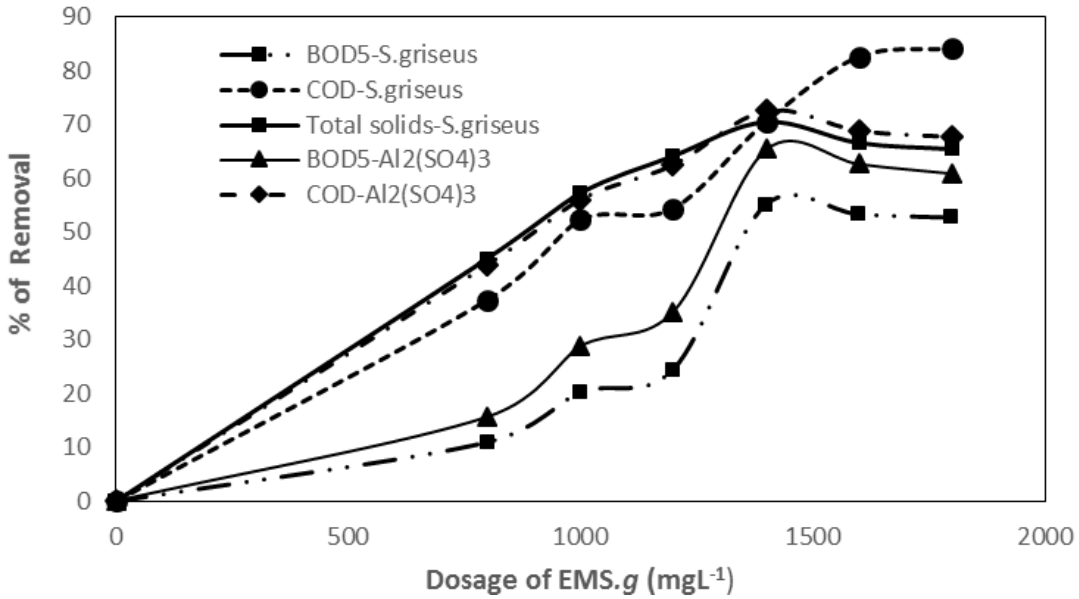

Figure 1. Removal of BOD_5, COD and total solids employing mucilaginous extract of *S. griseus* and the chemical coagulant $Al_2(SO_4)_3$. *Dosages of $Al_2(SO_4)_3$: 10, 15, 20, 25, 30 and 35 mgL^{-1}.

It is observed that $Al_2(SO_4)_3$ had better results than ME*S. g*. with respect to the removal of COD and BOD_5. When 25 mgL^{-1} of coagulant was used in the treatment, a BOD_5 removal of 65.41% was reached. However, it must be highlighted that the percentage of BOD_5 removal decreased at higher dosages, likely due to system restabilization. Regarding chemical oxygen demand, a similar behavior was obtained. Its mean, the highest removal percentage was 67.86, which was significantly different from the other values obtained with various coagulants. These findings are similar to those reported by Dearmas Duarte and Ramírez Hernández (2015), who reduced wastewater BOD to 62.63%.

As shown in Figure 1, chemical coagulant $Al_2(SO_4)_3$ presents better coagulation properties than natural coagulant (ME*S. g*). It can be concluded that ME*S. g* could be an effective alternative to decrease BOD_5 and COD values in domestic wastewater treatment; these results corroborate the studies of Tarón *et al*. (2017) and Guzmán *et al*. (2013). It is important to mention that both industrial and domestic wastewater have key characteristics regarding the composition and structure of organic matter. Hence, a better understanding of organic matter's characteristics is important to improve treatment (Liu *et al*., 2016).

Color and turbidity are descending functions of ME*S. g* concentration; the highest values of color and turbidity were 72.12 and 67.24%, respectively. These values were obtained using a coagulant concentration of 1400 mgL^{-1}. Similar findings were published by Dearmas Duarte and Ramírez Hernández (2015). At low doses of natural coagulant, the removal of color and turbidity was not significant, possibly due to the slowness of the coagulation process, a product of the low doses (ME*S. g*). On the contrary, the use of high doses of ME*S. g* is not adequate, since the system restabilizes and presents a stationary behavior, where there is little variation in color and turbidity removal.

In the case of $Al_2(SO_4)_3$, the higher removal percentage was obtained for both turbidity (71.56%) and color (79.23%); these values were obtained using a concentration of 25 mgL^{-1} of $Al_2(SO_4)_3$. Comparing the turbidity removal percentages, significant statistical differences at $p<0.05$ between the two coagulants studied were observed. These results of BOD and COD are lower than those published by Tarón *et al.* (2017) in aqueous extract of Cassia fistula seed in the primary treatment of domestic wastewater (Figure 2).

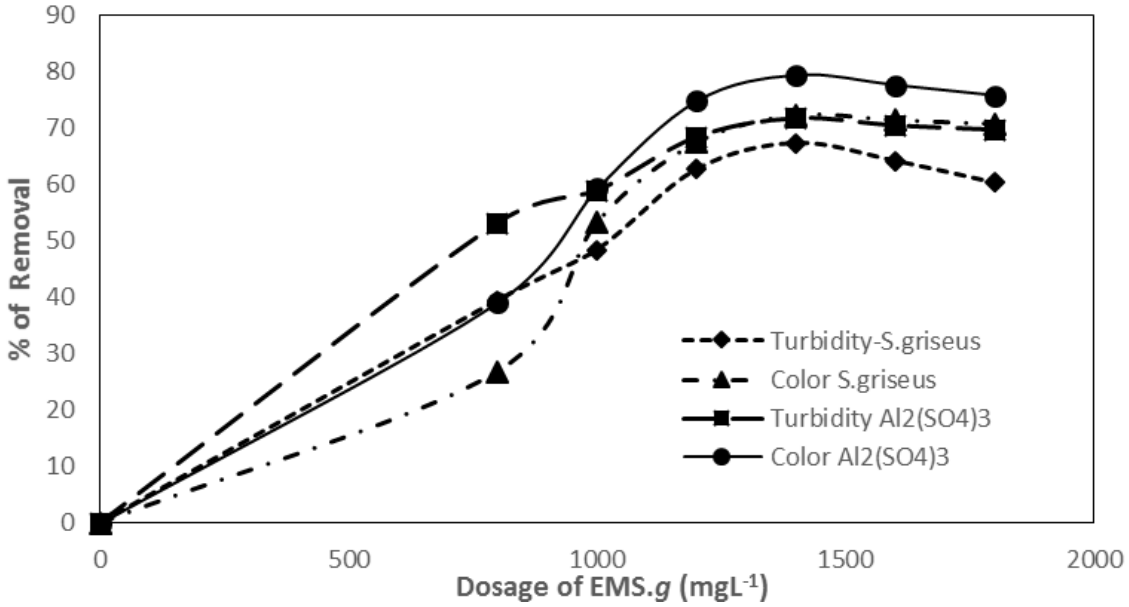

Figure 2. Turbidity and color removal using mucilaginous extract of *S. griseus* (ME*S. g*) and $Al_2(SO_4)_3$. *Dosages of $Al_2(SO_4)_3$: 10,15,20,25,30 y 35 mgL^{-1}.

Although the coagulation mechanism of mucilage of *S. griseus* in wastewater is unknown, it is presumed that pectins (mucilage) act as coagulant-flocculants. Mucilage is a polymer with high molecular weight, which can remain long and flexible, adsorbing various particles (Sánchez and Untiveros, 2004). Likewise, Gardiner *et al.* (1999) indicate no clear hypothesis for the mechanism of action of cactus extracts. However, these authors suggest that the mucilage synthesized are polysaccharides structured with functional groups such as -NH2, -COOH and –OH, which leave charges that promote hydrogen bond formation.

4. CONCLUSIONS

The mucilaginous extract of *S. griseus* (ME*S. g*) can be used as a coagulant in domestic wastewater treatment due to its properties to remove color, turbidity, BOD_5, COD and total solids. These properties are similar to some coagulants employed in primary treatment of domestic wastewater. The percentages of removal of both turbidity and color are promising and the dosages of inorganic chemical coagulants could be reduced. The highest removal percentages (70.42% for total solids, 72.12% color, 67.24% turbidity, 55% BOD5, and 67.86% COD) were obtained using a dosage of 1400 mgL^{-1} of coagulant. These findings therefore could have interesting implications in the industry for the reduction of effluent contaminants.

5. ACKNOWLEDGMENT

The authors are especially grateful to the University of Cartagena for all their collaboration during the development of the research.

6. REFERENCES

ALMENDÁREZ DE QUEZADA, N. Comprobación de la efectividad del coagulante (Cochifloc) en aguas del lago de Managua Piedras Azules. **Revista Iberoamericana de Polímeros,** v. 5, n. 1, p. 46-54, 2004.

ANDERSON, E. **The cactus family**. Portland: Timber Press, 2001.

ANG, W. L.; MOHAMMAD, A. W. Integrated and Hybrid Process Technology. **Sustainable Water and Wastewater Processing**, v. 9, p. 279-329, 2019. https://doi.org/10.1016/b978-0-12-816170-8.00009-0

ANG, W. L.; MOHAMMAD, A. W. State of the art and sustainability of natural coagulants in water and wastewater treatment. **Journal of Cleaner Production**, v. 262, n. 121267, 2020. https://doi.org/10.1016/j.jclepro.2020.121267

APHA; AWWA; WEF. **Standard Methods for the examination of water and wastewater**. 22nd ed. Washington, 2012. 1496 p.

BERGAMASCO, R.; BOUCHARD, C.; VIEIRA DA SILVA, F.; HESPANHOLD, M.; REIS, M.; FAGUNDES, M.R. An application of chitosan as a coagulant/flocculant in a microfiltration process of natural water. **Desalination**, v. 245, p. 205-213, 2009. https://doi.org/10.1016/j.desal.2008.04.049

CALDERA, Y.; MENDOZA, I.; BRICEÑO, L.; GARCÍA, J., FUENTES, L. Eficiencia de las semillas de *Moringa oleifera* como coagulante alternativo en la potabilización del agua. **Boletín del Centro de Investigaciones Biológicas**, v. 41, n. 2, p. 244-254, 2007.

DEARMAS DUARTE, D.; RAMÍREZ HERNÁNDEZ, L. F. Remoción de nutrientes mediante coagulantes naturales y químicos en planta de tratamiento de aguas residuales, Valledupar Colombia. **Revista De Investigación Agraria Y Ambiental**, v. 6, n. 2, 183–196, 2015. https://doi.org/10.22490/21456453.1415

FUENTES, L.; MENDOZA, IVÁN.; LÓPEZ, A.; CASTRO, M.; URDANETA, C. Efectividad de un coagulante extraído de *Stenocereus griseus* (Haw.) Buxb. en la potabilización del agua. **Revista Técnica de la Facultad de Ingemiería Univídad del Zulia**, v.34. n. 1, p. 39-47, 2011.

GARDINER, D.; PETER, F.; CARR, Y. Cactus extract increases water infiltration rates in two soils. **Communications in Soil Science and Plant Analysis,** n. 30, p. 1713-1719, 1999. https://doi.org/10.1080/00103629909370323

GUZMÁN, J.; VILLABONA, A.; TEJADA, C.; GARCÍA, R. Reduction of water turbidity using natural coagulants: a review. **Revista UDCA Actualidad & Divulgación Científica**, v. 16, n. 1, p. 253–262, 2013. https://doi.org/10.31910/rudca.v16.n1.2013.881

HAMZAH, A.; MANIKAN, V.; ABD AZIZ, N.A.F. Biodegradation of tapis crude oil using consortium of bacteria and fungi: optimization of crude oil concentration and duration of incubation by response surface methodology. **Sains Malaysiana**, v. 46. n. 1, p. 43-50, 2017. https://doi.org/10.17576/jsm-2017-4601-06

HENRÍQUEZ, M.; MONTERO, F.; RODRÍGUEZ, O.; HERNÁNDEZ, A. Efecto de diferentes suspensiones de cardón dato, cactus lefaria, tuna española y PAM sobre algunas propiedades físicas de un suelo de Quibor-Lara. **Revista de la Faculdad de Agronomia,** v. 17, p. 295-306, 2000.

HOONG, H. N. J.; ISMAIL, N. Removal of dye in wastewater by adsorption coagulation combined system with Hibiscus sabdariffa as the coagulant. **MATEC Web of Conferences**, v. 152. n. 01008, p. 1-14, 2018. https://doi.org/10.1051/matecconf/201815201008

JAAFARI, J.; BARZANOUNI, H.; MAZLOOMI, S.; ABADI FARAHANI, N.; SHARAFI, K.; SOLEIMANI, P.; HAGHIGHAT, G. Effective adsorptive removal of reactive dyes by magnetic chitosan nanoparticles: Kinetic, isothermal studies and response surface methodology**. International Journal of Biological Macromolecules,** v. 164, p. 344–355, 2020. https://doi.org/10.1016/j.ijbiomac.2020.07.042

KOOIJMAN, G.; DE KREUK, M. K.; HOUTMAN, C.; VAN LIER, J. B. (2020). Perspectives of coagulation/flocculation for the removal of pharmaceuticals from domestic wastewater: A critical view at experimental procedures. **Journal of Water Process Engineering**, v. 34, p. 101161, 2020. https://doi.org/10.1016/j.jwpe.2020.101161

KUMAR, K.; CHOWDHURY, A. Use of Novel Nanostructured Photocatalysts for the Environmental Sustainability of Wastewater Treatments, Reference Module in Mater. **Encyclopedia of Renewable and Sustainable Materials**, v. 1, p. 949-964, 2020. https://doi.org/10.1016/b978-0-12-803581-8.11149-x

LIU, X.; CHEN, Q.; ZHU, L. Improving biodegradation potential of domestic wastewater by manipulating the size distribution of organic matter. **Journal of Environmental Sciences,** v. 47, p. 174–182, 2016. https://doi.org/10.1016/j.jes.2016.02.004

LUO, X.; SHE, M.; HUANG, Z.; CHEN, Z.; CHEN, Z.; LIN, B.; CUI, L. Efficient removal of Pb(II) through recycled biochar-mineral composite from the coagulation sludge of swine wastewater. **Environmental Research**, v. 190, n. 110014, 2020. https://doi.org/10.1016/j.envres.2020.110014

MARTÍNEZ, D.; CHÁVEZ, M.; DÍAZ, A.; CHACÍN, E.; FERNÁNDEZ, N. Eficiencia del cactus lefaria para su uso como coagulante en la clarificación de las aguas. **Revista Técnica de la Facultad de Ingeniería, Universidad del Zulia,** v. 26. n. 1, p. 27-33, 2003.

NAGHIPOUR, D.; HOSEINZADEH, L.; TAGHAVI, T.; JAAFARI, J. Characterization, kinetic, thermodynamic and isotherm data for diclofenac removal from aqueous solution by activated carbon derived from pine tree. **Data in Brief,** v. 8, p. 1082–1087, 2018. https://doi.org/10.1016/j.dib.2018.03.068

OKUDA, T.; BAES, A.; NISHIJIMA, W.; OKADA, M. Improvement of extraction method of coagulation active components from *Moringa oleifera* seed. **Water Research**, v. 33, n. 15, p. 3373-3378, 1999. https://doi.org/10.1016/S0043-1354(99)00046-9

OLIVERO, R.; AGUAS, Y.; MERCADO, I.; CASAS, D.; MONTES, L. Utilización de Tuna (*Opuntia ficus-indica*) como coagulante natural en la clarificación de aguas crudas. **AVANCES Investigación en Ingeniería,** v. 11, n. 1, p. 70-76, 2014. https://doi.org/10.18041/1794-4953/avances.1.302

SÁNCHEZ, S.; UNTIVEROS, G. Determinación de la actividad floculante de la pectina en soluciones de hierro (III) y cromo (III). **Revista de la Sociedad Química del Perú**, v. 70. n. 4, p. 201-208, 2004.

SATTERFIELD, Z. Jar testing. **Tech Brief**, v. 5, n. 1, p. 1-4, 2005.

TARÓN, A.; GUZMAN, L.; PORTNOY, I. Evaluación de la *Cassia fistula* como coagulante natural en el tratamiento primario de aguas residuales. **Revista Orinoquia**, v. 21, n. 1, p. 73-78, 2017. https://doi.org/10.22579/20112629.396

TERRAZAS, T.; LOZA, S.E.; ARREOLA, H. J. Anatomía caulinar de las especies del género Stenocereus (Cactaceae). **Acta Botánica Venezuellica**, v. 28. n. 2, p. 321-336, 2005.

YIN, C-Y. Emerging usage of plant-based coagulants for water and wastewater treatment. **Process Biochem**, v.45, p.1437-144, 2010. https://doi.org/10.1016/j.procbio.2010.05.030

Ambiente & Água - An Interdisciplinary Journal of Applied Science
ISSN 1980-993X – doi:10.4136/1980-993X
www.ambi-agua.net
E-mail: ambi.agua@gmail.com

Analysis of fire risk in the Amazon: a systematic review

ARTICLES doi:10.4136/ambi-agua.2706

Received: 05 Feb. 2021; Accepted: 03 May 2021

Natasha Sousa Araujo Lemos*; José Mauricio Cunha

Instituto de Educação, Agricultura e Ambiente. Programa de Pós Graduação em Ciências Ambientais. Universidade Federal do Amazonas (UFAM), Rua 29 de agosto, n°786, CEP: 69800-000, Humaitá, AM, Brazil.
E-mail: maujmc@gmail.com
*Corresponding author. E-mail: geo.natashalemos@gmail.com

ABSTRACT

Fires such as those that occurred in 2019 in the Amazon are examples of the intensification of these events in recent years and contradict the claim that forest fires only reach great proportions in years of extreme drought. This is a worrying scenario, as the Amazon Rainforest plays an important role in regional and global climate regulation. This study therefore sought to identify the methodologies used to describe and predict fire events in the Brazilian Amazon. For this, a systematic literature review was carried out in the open access databases Scientific Electronic Library Online (SciELO) and Directory of Open Access Journals (DOAJ) using the descriptors "fire risk" and "Amazon", and their variants in the Portuguese language and the logical operator "AND" in the search. From the resulting search materia we identified the use of predictive models based on projections for climate change developed by the Intergovernmental Panel on Climate Change (IPCC), which indicate a substantial increase in the probability of fires. Another technique used is the crossing of heat foci data with the forms of land use, evidencing the areas that burn the most and when, as well as the most susceptible areas. There were also studies analyzing the performance of fire risk indexes, demonstrating those that could be used after adaptations to local characteristics. These results allow an understanding of the behavior of fire in the Amazon, since they provide a broad view of how studies on fires have been conducted and what techniques have been used.

Keywords: Amazon biome, climate change, fire behavior, fire hazard, forest fires.

Análise de risco de fogo na Amazônia: uma revisão sistemática

RESUMO

Incêndios como os ocorridos no ano de 2019 na Amazônia representam um exemplo da intensificação destes eventos nos últimos anos e contradizem a afirmação de que incêndios florestais só atingem grandes proporções em anos de seca extrema. Este é um cenário preocupante, uma vez que a Floresta Amazônica executa um importante papel na regulação climática regional e global. Assim, este estudo tem por objetivo identificar quais são as metodologias utilizadas para descrever e prever os eventos de incêndios na Amazônia brasileira. Para isso, realizou-se uma revisão sistemática de literatura nas bases de dados de acesso aberto Scientific Eletronic Library Online (SciELO) e Directory of Open Access Journals (DOAJ) utilizando-se os descritores fire risk e Amazon, suas variantes em Língua Portuguesa e o operador lógico AND na busca. Do material resultante da busca, identificou-se o uso de

This is an Open Access article distributed under the terms of the Creative Commons Attribution License, which permits unrestricted use, distribution, and reproduction in any medium, provided the original work is properly cited.

modelos preditivos baseados nas projeções para as mudanças climáticas desenvolvidas pelo Intergovernmental Panel on Climate Change (IPCC), os quais indicam aumento substancial na probabilidade de incêndios. Outra técnica utilizada é o cruzamento dos dados de focos de calor com as formas de uso do solo, evidenciando as áreas que mais queimam e quando, como também as áreas mais suscetíveis. Houve ainda, estudos analisando o desempenho de índices de risco de incêndio, demonstrando aqueles que poderiam ser utilizados após adequações às características locais. Tais resultados permitem uma compreensão sobre o comportamento do fogo na Amazônia, visto fornecer uma visão ampla sobre como os estudos sobre incêndios vem sendo conduzidos e quais técnicas têm sido utilizadas.

Palavras-chave: bioma Amazônia, comportamento de incêndio, incêndios florestais, mudanças climáticas, perigo de incêndio.

1. INTRODUCTION

Forest fires are complex phenomena dependent on several factors, such as weather conditions, topographic conditions, fuel availability and ignition potential (Matin *et al.*, 2017). In order to mitigate their damage, different fire risk indexes were developed to measure the probability of fire ignition, either due to natural or anthropic causes, in forest areas (Antunes *et al.*, 2011).

In tropical forests such as the Amazon, natural combustion events are rare (Cochrane, 2003; Cammelli *et al.*, 2020). This is explained by the great humidity in these forests from their own trees (Fearnside, 2009; Nobre and Borma, 2009). The maintenance of its always green canopy and moisture comes from the ability of its trees to establish deep roots, preserving these characteristics even in conditions of severe drought and water stress (Cochrane, 2003; Nobre and Borma, 2009).

With the rare episodes of natural fires over the last millennium, the Amazon Forest did not need to develop adaptation mechanisms against fire, such as Cerrado vegetation (Fearnside, 2009). Although it has some resistance to drought, natural dysfunctions and anthropic causes have modified the ability of the tropical forest to maintain its moisture, making it susceptible to burning (Cochrane, 2003; Aragão and Shimabukuro, 2010).

Among these dysfunctions, we highlight the transformations in its landscape promoted by government policies to encourage the occupation of the region, the expansion of agricultural activity and the construction of major infrastructure works such as highways and hydroelectric dams; actions that have historically promoted deforestation in the Amazon (Cochrane, 2003; Becker, 2005; Fearnside, 2006; Ferrante and Fearnside, 2020; Libonati *et al.*, 2021).

The selective extraction of trees carried out by timber trees also contributes to this process, promoting forest fragmentation (Carvalho Junior *et al.*, 2020). The use of fire is also a recurrent practice of soil management in agricultural activities, generating aerosols that interfere in photosynthetic, radioactive processes and cloud formation (Bowman *et al.*, 2008; Armenteras *et al.*, 2009; Nobre and Borma, 2009; Cammelli *et al.*, 2020; Silva *et al.*, 2020).

All these events promote changes in land use and cover and act synergistically in reducing the forest resilience of the Amazon, causing interference in its biogeochemical cycles, reducing evapotranspiration and modifying the microclimate, thus compromising its existence (Bowman *et al.*, 2008; Nobre and Borma, 2009; Silva *et al.*, 2020). Given the gap in knowledge about the inflection point of the forest, as a precautionary measure strong efforts should be made to conserve the Amazon Forest yet standing (Fearnside, 2009; Nobre and Borma, 2009).

However, the number of fires in the Amazon has intensified in recent years, driven by the increase in deforestation (Silveira *et al.*, 2020; Libonati *et al.*, 2021). About 1/3 of the fire occurrences between 2003 and 2019 occurred up to 1 km away from deforested areas in the same year and up to 500 m from deforested areas in the previous year; in 2019, fires occurred

in 45% of the total deforested areas in the Amazon (Silveira *et al.*, 2020). As explained by Barlow *et al.* (2019) and Silveira *et al.* (2020), fire is used to remove the remaining biomass from deforestation, a technique commonly called "cutting and burning". Subsequently, fire is used as a management tool for deforested areas to be converted into agricultural land (Barlow *et al.*, 2019).

Thus, part of the forest fires in the Brazilian Amazon are linked to two distinct and intrinsically related activities: deforestation and the management of soils destined to agricultural activities (Morello *et al.*, 2020; Oliveira *et al.*, 2020; Penha *et al.*, 2020). Due to poor management in the use of fire, fires get out of control and commonly reach nearby forested areas (Morello *et al.*, 2020; Oliveira *et al.*, 2020).

In 2019, approximately 906,000 hectares of the Amazon Rainforest were lost in fires (Kelley *et al.*, 2021). This year, the fires were devastating both in scale and duration of the burning and were not potentiated by meteorological factors, suggesting that these are linked to changes in land use and cover (Kelley *et al.*, 2021; Li *et al.*, 2020).

Given this scenario of changes and intensification of fire records in the Amazon, this study involved a literature review on the rates of fire risks used in studies of fire in the Brazilian Amazon and was motivated by two questions: i) what methodologies are used to measure the risk of fire in the Brazilian Amazon? and ii) what are the prospects in the current scenario of intense occurrence of fires? Thus, the objective of this research was to identify the methodologies used to describe and predict the occurence of fires in the Amazon.

2. MATERIAL AND METHOD

This study comprised a qualitative research with secondary data collection, analyzed according to the methodological contribution of the systematic literature review. The bibliographic survey was carried out in the scientific databases of open access: the Scientific Electronic Library Online (SciELO) and the Directory of Open Access Journals (DOAJ).

The articles were searched on August 30, 2020, and the descriptors "fire risk" and "Amazon" and their variants in Portuguese were used, applying the use of the logical operator "AND". The time frame encompassed articles published in the last ten years (2010-2020) and available entirely by electronic means, thus capturing what is most recent in the literature on the subject.

The inclusion criterion of the articles consisted of verifying whether they addressed the theme of forest fire risk in the Amazon and contained the descriptors in their title, abstract or keywords. All articles that did not meet the parameters described were excluded.

3. RESULTS

Fifteen articles were found in the initial search. When applying the temporal filter composed of the period of years between 2010 and 2020 and the inclusion criteria previously established, nine publications remained. Of these, four publications were in the SciELO database and five in the DOAJ database. The articles analyzed in this study are presented in Table 1, organized by source database and year of publication.

Based on the above, it is noted that at the beginning of the decade the theme on the risk of forest fires in the Amazon was addressed in a very incipient way with a study published in each year of 2010, 2011 and 2012. Then there was a lack of indexed publications in the databases consulted, SciELO and DOAJ, comprising the years 2013, 2014, 2015. From 2016, there was the resumption of publications, with one published article, two articles in 2017, two in 2018 and one in 2019.

The methodology and results of these studies are summarized in Table 2 below, according to the date of publication.

Table 1. Articles collected in the DOAJ and SciELO databases on the risk of fires in the Amazon, analyzed in this study.

Data base	Year Publication	Authors	Title	Journal
DOAJ	2010	LIBERATO, A. M.; BRITO, J. I. B.	Influence of changes in the water balance of the Western Amazon	Revista Brasileira de Geografia v. 3, p. 170-180, 2010.
DOAJ	2011	MÉLO, A. S.; JUSTINO, F.; LEMOS, C. F.; SEDIYAMA, G.; RIBEIRO, G.	Susceptibility of the environment to occurrences of fires under current climatic conditions and future global warming	Revista Brasileira de Meteorologia v. 26, n. 3, p. 401-418, 2011.
DOAJ	2017	ANDERSON, L. O.; YAMAMOTO, M.; CUNNINGHAM, C.; FONSECA, M. G.; FERNANDES, L. K.; PIMENTEL, A.; BROWN, F.; SILVA JR, C. H. L.; LOPES, E. S. S.; MOREIRA, D. S.; SALAZAR, N.; ANDERE, L.; ROSAN, T. M.; REIS, V.; ARAGÃO, L. E. O. C.	Use of orbital data from heat sources to characterize forest fire risks and prioritize areas for decision making	Revista Brasileira de Cartografia v. 1, n. 69, p. 163-177, 2017.
DOAJ	2017	PAGE, Y. L.; MORTON, D.; HARTIN, C.; BOND-LAMBERTY, B.; PEREIRA, J. M. C.; HURTT, G.; ASRAR, G.	Synergy between land use and climate change increases future fire risk in Amazon forests	Earth System Dynamics v. 8, p. 1237-1246, 2017.

Continue...

Continued...

DOAJ	2018	SODRÉ, G. R. C.; SOUZA, E. B.; OLIVEIRA, J. V.; MORAES, B. C.	Risk calculation and fire detection: an analysis in the Eastern Amazon	Revista Brasileira de Ciências Ambientais v. 49, p. 1-14, 2018.
SciELO	2012	RIBEIRO, L.; SOARES, R. V.; BEPLLER, M.	Mapping the risk of forest fires in the municipality of Mundo Novo, Mato Grosso, Brazil	CERNE v. 18, n. 1, p. 117-126, 2012.
SciELO	2016	SILVA, P. R. S.; IGNOTTI, E.; OLIVEIRA, B. F. A.; JUNGER, W. L.; MORAIS, F.; ARTAXO, P.; HACON, S.	High risk of respiratory diseases in children in the fire period in Western Amazon	Revista de Saúde Pública v. 50, n. 29, p. 1-11, 2016.
SciELO	2018	WHITE, B. L. A.	Spatiotemporal variation in fire occurrence in the state of Amazonas, Brazil, between 2003 and 2016	Acta Amazonica v. 48, n. 4, p. 358-367, 2018.
SciELO	2019	CASAVECCHIA, B. H.; SOUZA, A. P.; STANGERLIN, D. M.; ULIANA, E. M.; MELO, R. R.	Fire hazard indices in a Cerrado-Amazon transition area	Revista da Sociedade de Ciências Agrárias de Portugal v. 42, n. 3, p. 842-854, 2019.

Table 2. Methodology used and results described in the studies analyzed in this study.

Year Publication	Title of the article	Methodology	Result found
2010	Influence of changes in the water balance of the Western Amazon	Calculation of water balance and estimation of climatic indices using the methodology proposed by Thornthwaite & Mather (1957) and modified by Krishan (1980) with the calculation of potential evapotranspiration estimated by the Thornthwaite method (1948). The input variables of the model were average air temperature and monthly rainfall totals from 1961 to 2005, coming from INMET weather stations.	In the projections made in two scenarios (A2 and B2) of the IPCC, with an increase in temperature in the order of 3.8ºC and 1.3ºC, respectively, there was a trend of drier climate, reduction of humidity, and reduction of river flow, which will lead to an increase in the risk of fire in the Western Amazon.
2011	Susceptibility of the environment to occurrences of fires under current climatic conditions and future global warming	Evaluation of atmospheric conditions favorable to the occurrence of fire by Haines Index. The calculation of the Haines Index has as input data the differences in air temperature and temperature of the dew point according to altitude. Simulations are generated in the current scenario and in a global warming circumstance (IPCC scenario A1B) using the ECHAM5/MPI-OM model of the MaxPlanck Institute of Meteorology.	The risks of fires in Brazil were found in the current situation and future scenario for the months of June to October. Currently, the risk of fire is concentrated in the Midwest and North, mainly in august; in the projection (2080-2100), in a global warming scenario, there is an increase in the size of areas exposed to fire risks, especially in the Amazon.
2012	Mapping the risk of forest fires in the municipality of Novo Mundo, Mato Grosso, Brazil	Generation of maps of land use and cover classification and digital elevation model of the terrain and used as input variables the slope of the terrain, hydrographic network and road network. From the overlay of the maps (overlay technique), weights from 0 to 5 were assigned according to their risk potential and the degree of fire risk was categorized as null, low, moderate, high, very high and extreme.	A forest fire risk map was generated for the municipality of Novo Mundo-MT, which indicates that 95% of the municipality area is at high risk and very high risk of fire incidence. It was found that forests near pasture areas and roads are the most susceptible to fires.
2016	High risk of respiratory diseases in children in the fire period in Western Amazon	Continuous monitoring of air performed hourly for measurement of fine particulate matter and ozone. The 2B Tech meter was installed near the public school unit in order to monitor the quantitative pollutants present in the air to which children aged 6 to 14 years are exposed.	There was high exposure of school-age children to ozone (O_3) and fine particulate matter with toxicological risk during the dry season in the city of Rio Branco-AC, where 19% of the children presented asthma. The pollutants present in the air come from the burning of forest biomass and their high concentration occurs mainly during the dry season, when the volume of fires increases.
2017	Use of orbital data from heat foci to characterize forest fire risk and prioritize areas for decision making	Crossing the records of heat foci captured from 2000 to 2014 by different satellites with data of land structure of the State of Acre. With this, they obtained information about areas that burn the most and when they burn, categorized by land structure of occurrence.	A fire risk map was generated for the State of Acre, based on the spatial-temporal analysis of fire outbreaks recorded by different orbital sensors, in order to spatialize the risk of fire. It was found that the highest volume of heat foci was in Settlement Projects and the lowest volume occurred in Indigenous Lands.

Continue...

Continued...			
2017	Synergy between land use and climate change increases future fire risk in Amazon forests	Use of the HESFIRE model parameterized for fires in the understory, in which interactions between anthropic activity and current (1990-2010) and future (scenario 2080-2100) were tested. THE HESFIRE consists of three modules: ignition, propagation and finalization and each module is adjusted according to values described in the literature and field data. The input data of the model consist of frequency of anthropic ignition of fire, land use, GDP, weather conditions, soil moisture, fuel type, fuel availability, fire suppression effort.	Projection was carried out in two scenarios: in a scenario of low effort of change in land use and mitigation of climate change, fires in the understory of the Amazon Forest would increase by 4 to 28 times, while in a scenario of active mitigation against climate change and containment of changes in land use, the increased risk of fire would be 0.9 to 5.4 times higher than the current one.
2018	Risk calculation and detection of fires: an analysis in the Eastern Amazon	The calculation of the Fire Risk used in the study is that developed by INPE and is based on meteorological data. The input data of the index are precipitation, temperature of the relative humidity, use and cover of the soil in three categories (forest, agriculture and pasture) and heat foci. The risk of fire is categorized into five classes: minimal, low, medium, high and critical. The study carried out an analysis from 2000 to 2017 and considered the occurrence of the meteorological phenomena El Niño and La Niña.	The areas with pasture concentrated 47.3% of the fire records. On the other hand, the agriculture areas centralized 32.8% of the records, while the forested areas presented 19.9% of the heat foci. It was found that the Fire Risk Index based so only on meteorological data is not suitable for use as a fire prediction index, limited to an environmental indicator.
2018	Spatiotemporal variation in fire occurrence in the state of Amazonas, Brazil, between 2003 and 2016	Crossing the data of heat foci provided by INPE, recorded between 2003 and 2016 in the State of Amazonas, with data on temperature, precipitation, population density, deforested area, agricultural area and pasture areas. The data were quantified monthly and individualized by municipality of occurrence.	The year with the lowest incidence was 2008 and the highest was in 2015. The month that registers the most outbreaks of fire is the month of September. Lábrea is the municipality with the most registered outbreaks and Japurá with the lowest record. The municipalities with a high number of heat foci also showed higher deforestation. The most affected areas are the South and East region of the State of Amazonas.
2019	Fire hazard indices in a Cerrado-Amazon transition area	The performance of seven fire risk indexes was evaluated: Monte Alegre Formula (FMA) and Modified Monte Alegre (FMA+), Nesterov, Telitsyn, Ängstrom, P-EVAP and EVAP/P in an Amazon-Cerrado transition area by the Skill Score method. The input data used were air temperature, humidity, rain and wind speed provided by INMET.	Regarding the prediction of heat foci, the Telitsyn index presented 94.8% of correct answers. The Ängstrom index showed 74.7% of correct answers for non-occurrences of fires. In the general evaluation, it was found that the Ängstrom Index was the one that presented the best suitability for the Sinop-MT region, with a performance of 84.9% in the evaluation by the Skill Score.

The study by Liberato and Brito (2010) presents projections based on the report released by the Intergovernmental Panel on Climate Change (IPCC) on climate change and global warming. In this, the risk of fire in the Western Amazon rises considerably in these conditions. The authors used the Thornthwaite & Mather Method (1975) adapted by Krishan (1980) to elaborate the water balance.

With this, the authors do not use a fire risk index to verify the increase in the probability of fires in the Amazon. They infer the possibility of increased fires from the intensification of the consequences caused by climate change, such as reduction of soil moisture, surface and subsurface runoff, which decreases the flow of rivers and makes the forest less humid, favorable conditions for the occurrence of fires (Liberato and Brito, 2010).

The study by Mélo *et al.* (2011) is also based on the projections disclosed in the IPCC report and uses the Haines Index to calculate the risk of fire. The authors consider the months of June to October, because these are those that present favorable atmospheric conditions for the occurrence of fires. According to the authors, certain atmospheric conditions and the amount of water vapor in the atmosphere would be related to the spread of the fire.

The Haines Index would be an indicator of the potential condition for the occurrence of fires from vertical temperature and air humidity calculated in the low, medium and high atmosphere. The study by Mélo *et al.* (2011) is based on the monthly climatology of two periods: a current scenario (1980-2000) and a future scenario (IPCC projection A1B, 2080-2100), and the projected results indicate a substantial increase in the area at risk of fire in the Amazon.

An important factor highlighted by the authors regards the ignition of fire in the Amazon being of anthropic cause, mainly linked to agropastoral activities. In this context, in future scenario projections, even if atmospheric conditions are conducive to the occurrence of burning, human behavior may differ and the number of fires may be lower (Mélo *et al.*, 2011).

On the other hand, the research conducted by Ribeiro *et al.* (2012) considers the anthropic aspect in fire ignition and resulted in a map outlining the zoning of the risk of fires for the municipality of Novo Mundo-MT. The authors based their estimates on the characterization of land use and cover from orbital image classification and considered as input variables the slope of the terrain, hydrographic and road network.

In this sense, the authors emphasize the openness and proximity to highways as a factor of intensification of the risk of fire due to the accumulation of combustible material on their margins, increased human occupation and ease of access to forested areas, which may contribute to wood extraction and forest fragmentation (Ribeiro *et al.*, 2012).

While water bodies can influence both the negative aspect (attraction of people for recreation and consequent inappropriate use of fire) and the positive aspect (such as fire-containment barrier). The slope of the terrain acts on the speed of fire propagation, where in sloped areas the fire propagates faster than in non-sloped areas. In relation to soil cover, agropastoral areas are very close to forested areas and the use of fire as a soil management tool considerably increases the risk of forest fire (Ribeiro *et al.*, 2012).

The study conducted by Silva *et al.* (2016) presented the results of a research conducted in the health area on the exposure of children to pollutants present in the air from biomass burning, in the city of Rio Branco-AC, part of the "deforestation arc". The burning of volatile organic compounds (VOC) present in forest biomass generates Ozone (O_3) and this has a high degree of toxicity causing respiratory problems to the exposed population.

Although the research of Silva *et al.* (2016) does not explore the risk of fire in the Amazon, the study exposes the impacts to public health caused by fire. As reported by the authors, even if a particular municipality or state area is not the place of occurrence of the fire, air currents transport pollutants from the fires and reach distant areas, thereby affecting more people (Silva *et al.*, 2016).

The work of Anderson *et al.* (2017) was also conducted in the State of Acre and resulted in a map presenting the spatialization of fire risk to the State, based on the State's land organization. Data from heat foci captured by several satellites between 2000 and 2014 were used. Based on the historical-spatial analysis of the heat foci register, the authors produced a map showing the fire-risk classification categorized into eight levels: no risk, very low risk, low risk, observation, attention 1, attention 2, alert, maximum alert.

As stated by the authors, the technique of crossing historical data with the land structure is simple but efficient for analyzing fires of anthropic cause. The data generated can also be incorporated into models based on climate data, optimizing the analysis of fire risk (Anderson *et al.*, 2017).

The research of Page *et al.* (2017) also correlates fire data with forms of land use and presents projections in climate change scenarios, considering the scenarios contained in the IPCC. These projections consider scenarios of mitigation and not mitigation of climate change. In both scenarios, the risk of fires in the Amazon increases; however, when there is no control regarding the form of land use, the risks increase substantially (Page *et al.*, 2017).

The authors point out that fires in the Amazon are anthropically ignited, and that their origin may be deforestation or agricultural practices. In this context, the study considers in its analysis the human factor regarding fire ignition and climate change mitigation. In case of continued intensive use of natural resources, the Amazon would be at risk both for the consequences of climate change and for the severity and volume of fires (Page *et al.*, 2017).

Looking at the impact of the anthropic aspect on the occurrence of fires in Amazonia, the study presented by Sodré *et al.* (2018), held in Paragominas/PA, emphasizes that about 80% of heat foci in the region originate in areas modified by human action. Thus, the authors perform a space-time analysis of fires detected via satellite in contrast to the Fire Risk developed by the National Institute of Space Research (INPE) that considers only environmental variables.

The Fire Risk developed by INPE measures the susceptibility of the environment to combustion, regardless of the form of fire ignition (whether natural or anthropic). By contrasting the record of heat foci with the Fire Risk alert, the authors found the occurrence of fires even when the risk was considered minimal. The authors also found that, when there is an increase in the number of fires in agricultural areas, there is also an increase in forested areas, demonstrating the close connection between anthropic activities and the registration of forest fires. This is due to the proximity between these two forms of cover and land use, aggravated by the effects of edge and forest fragmentation (Sodré *et al.*, 2018).

The research developed by White (2018) performed a spatial and temporal analysis of the record of heat foci in the State of Amazonas between the years 2003 and 2016, categorizing the municipalities into five classes (very low, low, medium, high and very high) according to the number of heat foci recorded per km^2 of area of the municipality. The study performed statistical analyses seeking the correlation of the variable heat foci with variables that can influence the occurrence of fires, such as: air temperature, precipitation, population density, deforestation, agricultural areas and pastures.

Like the study by Anderson *et al.* (2017), White's study (2018) does not analyze the applicability of a given fire risk, but part of the analysis regards the temporal and spatial history of the heat foci register, correlating it with forms of land use and environmental variables. From this, information is generated about the areas that burn the most and when they burn, a condition that allows us to infer about behavior in the near future, if there are no circumstantial changes.

In addition, the analysis of historical recurrences favors the understanding of fire behavior in years of occurrence of climatic events such as El Niño and La Niña as proposed by Sodré *et al.* (2018), also pointed out by White (2018), when identifying interannual changes in his temporal analysis. Using geoprocessing techniques, White (2018) highlights that these results can be crossed with different thematic maps, expanding the scope of analysis and understanding of the phenomenon.

Finally, the work developed by Casavecchia *et al.* (2019) evaluates the performance of fire risk indexes in an Amazon-Cerrado transition area. The Monte Alegre Formula (FMA) and Modified Monte Alegre (FMA+), Nesterov, Telitsyn, Ängstrom, P-EVAP and EVAP/P are evaluated by the Skill Score method. All indexes have weather information input data. The standard indices used in Brazil are FMA and FMA+, which are used in the calibration of indexes not developed for Brazilian climatic conditions (Casavecchia *et al.*, 2019).

According to the authors, changes in rainfall regimes and relative humidity are the factors that most interfere in the performance of the indices. In this sense, Casavecchia *et al.* (2019) highlight the importance of adjusting the indices for local climatic conditions, aiming to mitigate mistaken results, as well as the need for daily calculation and maintenance of records to control fire occurrences.

4. DISCUSSION

In the Brazilian Amazon, the use of fire is a common practice for soil cleaning for agricultural use (Cammelli *et al.*, 2020). However, its indiscriminate use goes beyond the intended areas and reaches forested areas in the surroundings (Campanharo *et al.*, 2019; Barlow *et al.*, 2019). These occurrences tend to be aggravated by climatic events that cause an increase in temperature and low air humidity,as well as forest fragmentation promoted by selective logging and by deforestation promoted by illegal land ownership (Campanharo *et al.*, 2019; Azevedo-Ramos *et al.*, 2020; Carvalho Junior *et al.*, 2020).

Considering climate change as a threat factor to the Amazon Forest, three studies (Liberato and Brito, 2010; Mélo *et al.*, 2011; Page *et al.*, 2017) analyzed in this study made projections with different methodologies, and all scenarios indicated an increase in the occurrence of forest fires in the region. The increase in temperature and the reduction of air humidity that has made tropical forests less humid and susceptible to fires (Barlow *et al.*, 2019).

Barlow *et al.* (2019) highlight that the number of fires in 2019 was three times higher than in 2018 and is the highest recorded since 2010, although 2019 has not had an extreme weather event record this year. The increase in the number of fires was accompanied by a high increase in deforestation, in which it is estimated that more than 10,000 km^2 of forest is lost between 2018-2019, constituting the largest deforestation/year recorded since 2008 (Barlow *et al.*, 2019).

Even recognizing that climatic projections are imprecise and that they are also dependent on human behavior (Mélo *et al.*, 2011), it is possible to identify certain results by direct experience (Fearnside, 2009). In this sense, each year new scars caused by fires and fragmentation points in the forest are identified (Campanharo *et al.*, 2019; Carvalho *et al.*, 2020).

Considering the scenario of intensification of land use and changes in land cover, with and without behaviors to mitigate climate change, Page *et al.* (2017) projected an increased risk of fires in the understory of the Amazon Rainforest. Forest fires of this type, even low intensity, kill approximately 50% of the trees (Barlow *et al.*, 2019).

Since the ignition of forest fires in the Brazilian Amazon is of anthropic causes, fire risk indexes that consider only climatic factors tend to be inappropriate (Silva *et al.*, 2020), reaffirming what was determined by Sodré *et al.* (2018). According to the authors, the calculation of fire risk (RF) created by INPE and used in the study was developed to monitor rainfall indices, so the fire risks did not efficiently represent the occurrence of fires (Sodré *et al.*, 2018).

In the seventeen years of analysis that comprised the study (2000-2017), Sodré *et al.* (2018) found that 47.3% of the fires occurred in pasture areas, followed by agriculture areas with 32.8% and forest with 19.9%. In the years in which the occurrence of the La Niña phenomenon was identified, which generates more precipitation in the Amazon, heat foci are concentrated

in the second half, when the influence of the climatic event decreases in intensity. However, in years of El Niño occurrence, which decreases precipitation, fire outbreaks were recorded in the first and second semester (Sodré *et al.*, 2018).

The largest forest fires recorded in the Amazon in the last twenty years coincided with years of more intense drought associated with the El Niño phenomenon, which provides high temperatures and lower humidity (Campanharo *et al.*, 2019). In this context, it is urgent to use reliable fire risk indices that can be applied in the development of policies for planning, prevention and combating forest fires (Silva *et al.*, 2020).

Among the studies analyzed in this study, the research conducted by Casavecchia *et al.* (2019) analyzed seven fire-risk indexes: Monte Alegre Formula (FMA) and Modified Monte Alegre (FMA+), Nesterov, Telitsyn, Ängstrom, P-EVAP and EVAP/P. The one that presented the best performance was the Ängstrom index, followed by FMA and FMA+ for the Sinop-MT region, an Amazon-Cerrado transition area.

Regarding FMA, Silva *et al.* (2020) highlight that the human factor is not explicitly considered and that it was created based on the characteristics of a region with humid subtropical climate. In the Amazon, the climate is hot equatorial super humid (Silva *et al.*, 2020). Pertinently, Casavecchia *et al.* (2019) reinforced the need for regional adjustments in indices based on local characteristics.

The FMA was the first fire risk index developed in Brazil in the 1970s (Silva *et al.*, 2020). The FMA and FMA+ are the standard indices used in Brazil; from them, the calibration of indexes not developed for the Brazilian climatic characteristics was performed. The Ängstrom Index, which does not present fire risk classes, was therefore adapted from the classes contained in the FMA+ index and the literature (Casavecchia *et al.*, 2019).

Spatialization in maps of areas susceptible to fires are important and necessary to the fire risk index, and in this sense, three studies analyzed herein objectively addressed this goal: those of Ribeiro *et al.* (2012), Anderson *et al.* (2017) and White (2018). Ribeiro *et al.* (2012) worked on a municipal scale, while Anderson *et al.* (2017) and White (2018) dedicated themselves to the state scale to present their results.

Addressing the risk of fire in the state land organization, Anderson *et al.* (2017) identified that indigenous lands are the areas least prone to fire risk. According to Paiva *et al.* (2020), the designation of protected areas (Conservation Units and Indigenous Lands) is an effective measure for biodiversity conservation, deforestation prevention and forest fragmentation.

White (2018) classified municipalities according to the heat foci quantified in relation to the total area of the municipality, and thus found that the area that most records fires is located in the south of the State of Amazonas. This region coincides with the location of the "Deforestation Arc" and concentrates a high percentage of deforestation along the southern and eastern edges of the Amazon Forest (Fearnside, 2009; Nobre and Borma, 2009).

Contemplating a local scale, the municipality of Novo Mundo-MT, Ribeiro *et al.* (2012) developed thematic fire risk maps considering a certain degree of risk according to terrain slope, hydrography, road network and soil cover. The authors found that the road network and the form of land use are the variables that most generate fire risks, where forests near roads and pastures would be more susceptible to burning (Ribeiro *et al.*, 2012). The areas of the forest edge are hotter and drier than the interior of the forest, being more sensitive to fire (Fearnside, 2006; 2009; Aragão and Shimabukuro, 2010).

The recognition of vulnerable areas allows the elaboration of more precise prevention and relocation plans for human and financial efforts in the fight against forest fires (Ribeiro *et al.*, 2012; Anderson *et al.*, 2017). The identification of the population living in these areas would allow community training on fire prevention and correct management, since small farmers are the main actors involved in fighting fires that occur (Cammelli *et al.*, 2019).

Since the use of fire is a culturally consolidated practice essential to the guarantee of

subsistence of economically disadvantaged populations living in the Amazon (White, 2018; Barlow *et al.*, 2019), control and management policies are more likely to achieve positive results than prohibitions (Cammelli *et al.*, 2019). Understanding the use and control of fire is essential for the preservation of the Amazon Forest, which requires the execution of complementary public policies (Cammelli and Angelsen, 2019).

In addition to environmental damage, forest fires expose the populations of affected areas to a large amount of pollutants, characterized by plumes of smoke from the burning of plant biomass (Barlow *et al.*, 2019). In this sense, burning would become a public health problem, as evidenced in the study developed by Silva *et al.* (2016), analyzed in this work.

In this study, the authors evaluated the toxicological risk of exposure to ozone (O_3) and fine particulate matter present in the air during the dry season – a circumstance in which there is an increase in the number of fires in the Amazon – and identified a high incidence of respiratory infections (Silva *et al.*, 2016).

It is emphasized that forest degradation is also a source of pollutants, such as carbon dioxide, methane and nitrous oxide, into the atmosphere (Fearnside, 2009; Celentano *et al.*, 2018). In addition to this, the emission of pollutants generated in fires would cancel the carbon sink consumed by untouched forests, invalidating compensation mechanisms such as those proposed by the Reducing Emissions from Deforestation and Forest Degradation (REDD) (Nobre and Borma, 2009; Aragão and Shimabukuro, 2010). Of course, government action and the engagement of actors involved in the ignition of fires are essential to prevent this scenario (Cammelli *et al.*, 2019; Cammelli and Angelsen, 2019).

5. FINAL CONSIDERATIONS

Several studies have proposed methodologies for the measurement and analysis of fire risk, using the application of remote-sensing techniques; geoprocessing; climate modelling; measurement of economic costs; space-time analysis of heat foci; verification of the adequacy of risk indices; analysis of health impacts, among others.

Given the different possibilities of analysis and the current Amazonian scenario, the questions emerged about what methodologies would be used to study the risks of fire in the Brazilian Amazon and what are the future perspectives in the current scenario of intense fire occurrence.This work answers these questions by analyzing nine studies published in the last ten years and indexed in the databases of free access DOAJ and SciELO. These studies examined forest fires in the Brazilian Amazon using different methodologies, which allows a broad perspective of the solutions developed on the subject, which synthesized herein.

Three studies analyzed presented results of climatic modeling, the projections of which indicate marked increase in the risk of Amazonian fires. This would be due to the intensification of land use and changes in land cover, increased temperature and decreased rainfall in the Amazon. These results show the risks that climate change imposes on the Amazon and how these are intensified by anthropic actions, in a circular dynamic.

The analysis of the historical information of the fire registry along with forms of land use were the object of study in three other studies, which returned information about the areas that suffer the most from the incidence of fires and when they occur, in addition to providing relevant data on the behavior of the fire in years of recording climatic extremes. The results of these studies also demonstrated the upward trend of increase in the recording of heat foci over the years.

Regarding the analysis of fire-risk indexes, two studies addressed the issue and used indexes whose input data are meteorological data. It is recognized in the literature that the ignition of fires in the Amazon is of anthropic origin. Due to the specificities of the environment, the analyzed indexes required adjustment and adaptation in order to be applied to other regions or proved inappropriate to predict the risk of burning.

Given the above, an immediate improvement in the management and use of natural resources is required, and urgent action on the part of all involved. Fire control deserves special attention, due to the historic roots of its use in local culture. It is noted that the use of fire contributes greatly to the degradation of the Amazonian environment, producing negative impacts in all spheres: environmental, economic and social.

Due to the relevance of the theme, we believe that this work contributes to the existing literature in that it provides a systematized and comprehensive view of recent studies on fires in the Amazon, which highlight areas that deserve attention. The work also provides a future perspective of the scenario. An understanding of the behavior of fire provided by the studies favors its control and management through the precise targeting of human and economic resources in the fight against Amazonian forest fires.

6. REFERENCES

ANDERSON, L. O.; YAMAMOTO, M.; CUNNINGHAM, C.; FONSECA, M. G.; FERNANDES, L. K.; PIMENTEL, A. *et al.* Utilização de dados orbitais de focos de calor para caracterização de riscos de incêndios florestais e priorização de áreas para a tomada de decisão. **Revista Brasileira de Cartografia,** v. 69, n. 1, p. 163-177, 2017.

ANTUNES, C. C.; VIEGAS, D. X.; MENDES, J. M. Avaliação do Risco de Incêndio Florestal no Concelho de Arganil. **Silva Lusitana,** v. 19, n. 2, p. 165-179, 2011.

ARAGÃO, L. E. O. C.; SHIMABUKURO, Y. E. The incidence of fire in Amazonian Forests with implications for REDD. **Science,** v. 328, p. 1275-1278, 2010. https://doi.org/10.1126/science.1186925

ARMENTERAS, D.; GONZÁLEZ-ALONSO, F.; AGUILERA, C. F. Distribución geográfica y temporal de incendios en Colombia utilizando datos de anomalías térmicas. **Caldasia,** v. 31, n. 2, p. 303-318, 2009. https://doi.org/10.15446/caldasia

AZEVEDO-RAMOS, C.; MOUTINHO, P.; ARRUDA, V. L. S.; STABILE, M. C. C.; ALENCAR, A.; CASTRO, I.; RIBEIRO, J. P. Lawless land in no man's land: The undesignated public forests in the Brazilian Amazon. **Land use Policy,** v. 99, p. 1-4, 2020. https://doi.org/10.1016/j.landusepol.2020.104863

BARLOW, J.; BERENGUER, E.; CARMENTA, R.; FRANÇA, F. Clarifying Amazonia's burning crisis. **Global Change Biology,** v. 26, n. 2, p. 319-321, 2019. https://doi.org/10.1111/gcb.14872

BECKER, B. K. Geopolítica da Amazônia. **Estudos Avançados,** vol. 19, n. 53, p. 71-86, 2005. https://doi.org/10.1590/S0103-40142005000100005

BOWMAN, M. S.; AMACHER, G. S.; MERRY, F. D. Fire use and prevention by traditional households in the Brazilian Amazon. **Ecological Economics,** v. 67, p. 117-130, 2008. https://doi.org/10.1016/j.ecolecon.2007.12.003

CAMMELLI, F.; COUDEL, E.; ALVES, L. F. N. Smallholders' perceptions of fire in the Brazilian Amazon: exploring implications for governance arrangements. **Human Ecology,** v. 47, p. 601-612, 2019. https://doi.org/10.1007/s10745-019-00096-6

CAMMELLI, F.; ANGELSEN, A. Amazonian farmers' response to fire policies and climate change. **Ecological Economics,** v. 165, p. 1-10, 2019. https://doi.org/10.1016/j.ecolecon.2019.106359

CAMMELLI, F.; GARRETT, R. D.; BARLOW, J.; PARRY, L. Fire risk perpetuates poverty and fire use among Amazonian smallholders. **Global Environmental Change,** v. 63, p. 1-10, 2020. https://doi.org/10.1016/j.gloenvcha.2020.102096

CAMPANHARO, W. A.; LOPES, A. P.; ANDERSON, L. O.; SILVA, T. F. M. R.; ARAGÃO, L. E. O. C. Translating fire impacts in Southwestern Amazonia into economic costs. **Remote Sensing,** v. 11, n. 764, p. 1-24, 2019. https://doi.org/10.3390/rs11070764

CARVALHO JUNIOR, E. A. R.; MENDONÇA, E. N.; MARTINS, A.; HAUGAASEN, T. Effects of illegal logging on Amazonian medium and large-sized terrestrial vertebrates. **Forest Ecology and Management,** v. 466, p. 1-9, 2020. https://doi.org/10.1016/j.foreco.2020.118105

CASAVECCHIA, B. H.; SOUZA, A. P.; STANGERLIN, D. M.; ULIANA, E. M.; MELO, R. R. Índices de perigo de incêndios em uma área de transição Cerrado-Amazônia. **Revista de Ciências Agrárias,** v. 42, n. 3, p. 842-854, 2019. https://doi.org/10.19084/rca.17756

CELENTANO, D.; MIRANDA, M. V. C.; MENDONÇA, E. N.; ROUSSEUA, G. X.; MUNIZ, F. H.; LOCH, V. C. *et al*. Desmatamento, degradação e violência no "Mosaico Gurupi" – A região mais ameaçada da Amazônia. **Estudos Avançados,** v. 32, n. 92, p. 315-339, 2018. https://doi.org/10.5935/0103-4014.20180021

COCHRANE, M. A. Fire science for rainforests. **Nature,** v. 421, p. 913-919, 2003. https://doi.org/10.1038/nature01437

FEARNSIDE, P. M. Desmatamento na Amazônia: dinâmica, impactos e controle. **Acta Amazonica,** v. 36, n. 3, p. 395-400, 2006. http://dx.doi.org/10.1590/S0044-59672006000300018

FEARNSIDE, P. M. Global warming in Amazonia: impacts and mitigation. **Acta Amazonica,** v. 39, n. 4, p. 1003-1012, 2009. http://dx.doi.org/10.1590/S0044-59672009000400030

FERRANTE, L.; FEARNSIDE, P. M. The Amazon's road to deforestation. **Science,** v. 369, p. 634, 2020. https://doi.org/10.1126/science.abd6977

KELLEY, D. I.; BURTON, C.; HUNTINGFORD, C.; BROWN, M. A. J.; WHITLEY, R.; DONG, N. Technical note: Low meteorological influence found in 2019 Amazonia fires. **Biogeosciences,** v. 18, p. 787-804, 2021. https://doi.org/10.5194/bg-18-787-2021

LI, X.; SONG, K.; LIU, G. Wetland Fire Scar Monitoring and Its Response to Changes of the Pantanal Wetland. **Sensor,** v. 20, p. 1-17, 2020. https://doi.org/10.3390/s20154268

LIBERATO, A. M.; BRITO, J. I. B. Influência de mudanças climáticas no balanço hídrico da Amazônia Ocidental. **Revista Brasileira de Geografia Física,** v. 03, p. 170-180, 2010. https://doi.org/10.26848/rbgf.v3.3.p170-180

LIBONATI, R.; PEREIRA, J. M. C.; DA CAMARA, C. C.; PERES, L. F.; OOM, D.; RODRIGUES, J. A. *et al.* Twenty‑first century droughts have not increasingly exacerbated fire season severity in the Brazilian Amazon. **Scientific Reports,** v. 11, p. 1-13, 2021. https://doi.org/10.1038/s41598-021-82158-8

MATIN, M. A.; CHITALE, V. S.; MURTHY, M. S. R.; UDDIN, K.; BAJRACHARYA, B.; PRADHAN, S. Understanding forest fire patterns and risk in Nepal using remote sensing, geographic information system and historical fire data. **International Journal of Wildland Fire,** v. 26, p. 276-286, 2017. http://dx.doi.org/10.1071/WF16056

MÉLO, A. S.; JUSTINO, F.; LEMOS, C. F.; SEDIYAMA, G.; RIBEIRO, G. Suscetibilidade do ambiente a ocorrências de queimadas sob condições climáticas atuais e de futuro aquecimento global. **Revista Brasileira de Meteorologia,** v. 26, n. 3, p. 401-418, 2011. https://doi.org/10.1590/S0102-77862011000300007

MORELLO, T. F.; RAMOS, R. M.; ANDERSON, L. O.; OWEN, N.; ROSAN, T. M.; STEIL, L. Predicting fires for policy making: Improving accuracy of fire brigade allocation in the Brazilian Amazon. **Ecological Economics,** v. 169, p. 1-14, 2020. https://doi.org/10.1016/j.ecolecon.2019.106501

NOBRE, C. A.; BORMA, L. S. 'Tipping points' for the Amazon forest. **Environmental Sustainability,** v. 1, p. 28-36, 2009. https://doi.org/10.1016/j.cosust.2009.07.00

OLIVEIRA, G.; CHEN, J. M.; STARK, S. C.; BERENGUER, E.; MOUTINHO, P.; ARTAXO, P. *et al.* Smoke pollution's impacts in Amazonia. **Science,** v. 369, p. 634-635, 2020. https://doi.org/10.1126/science.abd5942

PAGE, Y. L.; MORTON, D.; HARTIN, C.; BOND-LAMBERTY, B.; PEREIRA, J. M. C.; HURTT, G.; ASRAR, G. Synergy between land use and climate change increases future fire risk in Amazon forests. **Earth System Dynamics,** v. 8, p. 1237-1246, 2017. https://doi.org/10.5194/esd-8-1237-2017

PAIVA, P. F. P. R.; RUIVO, M. L. P.; SILVA JUNIOR, O. M.; MACIEL, M. N. M.; BRAGA, T. G. M.; ANDRADE, M. M. N. *et al.* Deforestation in protected areas in the Amazon: a threat to biodiversity. **Biodiversity and Conservation,** v. 29, p. 19-38, 2020. https://doi.org/10.1007/s10531-019-01867-9

PENHA, T. V.; KORTING, T. S.; FONSECA, L. M. G.; SILVA JUNIOR, C. H. L.; PLETSCH, M. A. J. S.; ANDERSON, L. O.; MORELLI, F. Burned Area Detection in the Brazilian Amazon using Spectral Indices and GEOBIA. **Revista Brasileira de Cartografia,** v. 72, n. 2, p. 253-269, 2020. http://dx.doi.org/10.14393/rbcv72n2-48726

RIBEIRO, L.; SOARES, R. V.; BEPLLER, M. Mapeamento do risco de incêndios florestais no município de Novo Mundo, Mato Grosso, Brasil. **Cerne,** v. 18, n. 1, p. 117-126, 2012. https://doi.org/10.1590/S0104-77602012000100014

SILVA, P. R. S.; IGNOTTI, E.; OLIVEIRA, B. F. A.; JUNGER, W. L.; MORAIS, F.; ARTAXO, P.; HACON, S. High risk of respiratory diseases in children in the fire period in Western Amazon. **Revista de Saúde Pública,** v. 50, n. 29, p. 1-11, 2016. https://doi.org/10.1590/S1518-8787.2016050005667

SILVA, I. D. B.; VALLE, M. E.; BARROS, L. C.; MEYER, J. F. C. A. A wildfire warning system applied to the state of Acre in the Brazilian Amazon. **Applied Soft Computing Journal,** v. 89, p. 1-15, 2020. https://doi.org/10.1016/j.asoc.2020.106075

SILVEIRA, M. V. F.; PETRI, C. A.; BROGGIO, I. S.; CHAGAS, G. O.; MACUL, M. S.; LEITE, C. C. S. S. *et al.* Drivers of Fire Anomalies in the Brazilian Amazon: Lessons Learned from the 2019 Fire Crisis. **Land,** v. 9, n. 516, p. 1-24, 2020. https://doi.org/10.3390/land9120516

SODRÉ, G. R. C.; SOUZA, E. B.; OLIVEIRA, J. V.; MORAES, B. C. Cálculo de risco e detecção de queimadas: uma análise na Amazônia Oriental. **Revista Brasileira de Ciências Ambientais,** v. 49, p. 1-14, 2018. https://doi.org/10.5327/Z2176-947820180345

WHITE, B. L. A. Spatiotemporal variation in fire occurrence in the state of Amazonas, Brazil, between 2003 and 2016. **Acta Amazonica,** v. 48, n. 4, p. 358-367, 2018. http://dx.doi.org/10.1590/1809-4392201704522